Scattering Amplitudes in effective gravitational theories

Stavros Mougiakakos

université PARIS-SACLAY

Scattering Amplitudes in effective gravitational theories

Amplitudes de diffusion en théorie de gravité effective

Thèse de doctorat de l'université Paris-Saclay

École doctorale n° 564, Physique en Ile-de-France (PIF)
Spécialité de doctorat: Physique
Unité de recherche: Université Paris-Saclay, CNRS, CEA, Institut de physique théorique, 91191, Gif-sur-Yvette, France.
Graduate school: Physique. Référent: Faculté des sciences d'Orsay

Thèse présentée et soutenue à Paris-Saclay, le 9 décembre 2021, par

Stavros MOUGIAKAKOS

Composition du jury:

Mariana C. GRAÑA Directrice de recherche CEA, Université Paris-Saclay	Présidente
N. Emil J. BJERRUM-BOHR Maître de conférences (HDR), Niels Bohr Institute, Niels Bohr International Academy	Rapporteur et Examinateur
Rodolfo RUSSO Maître de conférences (HDR), Queen Mary University of London: London, GB	Rapporteur et Examinateur
Constantin P. BACHAS Directeur de recherche, Ecole Normale Supérieure, PSL	Examinateur
Philippe BRAX Directeur de recherche CEA, Université Paris-Saclay	Examinateur
Donal O'CONNELL Maître de conférences, Higgs Centre for Theoretical Physics, University of Edinburgh	Examinateur
Justin E. VINES Maître de recherche, Max Planck Institute for Gravitational Physics (Albert Einstein Institute)	Examinateur

Direction de thèse:

Pierre VANHOVE Directeur de recherche CEA, Université Paris-Saclay	Directeur de thèse

Thèse de doctorat
NNT: 2021UPASP122

Declaration of Authorship

I, Stavros Mougiakakos, declare that this thesis titled, "Scattering Amplitudes in Effective Gravitational Theories" and the work presented in it are my own. I confirm that:

- This work was done wholly in candidature for the degree of Doctor of Philosophy at the Université Paris-Saclay.
- Where any part of this thesis has previously been submitted for a degree or any other qualification at this University or any other institution, this has been clearly stated.
- Where I have consulted the published work of others, this is always clearly attributed.
- Where I have quoted from the work of others, the source is always given. With the exception of such quotations, this thesis is entirely my own work.
- I have acknowledged all main sources of help.
- Where the thesis is based on work done by myself jointly with others, I have made clear exactly what was done by others and what I have contributed myself.

Signed:

_____

Date:

_____

UNIVERSITÉ PARIS SACLAY

Abstract

Ecole doctorale 564: Physique en l'Île-de-France

Doctor of Philosophy

Scattering Amplitudes in Effective Gravitational Theories

by Stavros MOUGIAKAKOS

In this thesis we study gravitational dynamics described via an Effective Field Theory exploiting Scattering Amplitudes methods. In the first chapter, we provide a discussion regarding the different approaches on the binary problem in gravity and give some of the latest results in the field. In the second chapter, we discuss in detail the Non-Relativistic General Relativity (NRGR) formalism and derive the complete conservative gravitational cubic-in spin effective action at the next-to-leading order in the post-Newtonian (PN) expansion for the interaction of generic compact binaries entering at the fourth and a half PN (4.5PN) order. In the third chapter, we derive the static Schwarzschild-Tangherlini metric by extracting the classical contributions from the multi-loop vertex functions of a graviton emitted from a massive scalar field. By computing the scattering amplitudes up to three-loop order in general dimension, we explicitly derive the expansion of the metric up to the fourth post-Minkowskian order $\mathcal{O}(G_N^4)$ in four, five and six dimensions. Gauge issues and induced non-physical non-minimal couplings as well as their subsequent treatment are discussed in detail. In the fourth chapter, we study the gravitational radiation emitted during the scattering of two spinless bodies in the post-Minkowskian Effective Field Theory approach. We derive the conserved stress-energy tensor linearly coupled to gravity and the classical probability amplitude of graviton emission at leading and next-to-leading order in G_N. We use it to recover the leading-order in G_N angular momentum and total four-momentum radiated into gravitational waves finding agreement with what was recently computed using scattering amplitude methods. Our results also allow us to investigate the zero frequency limit of the emitted energy spectrum.

This thesis is based on the works [1–3].

Acknowledgements

Firstly, I would like to thank my supervisor Pierre Vanhove for these three years of guidance and interesting discussions. I would also like to thank all my collaborators: Michele Levi, Mariana Vieira, Filippo Vernizzi and Massimiliano Maria Riva. Without you, all the scientific work in this thesis would not be possible. A special mention to Massimiliano and Filippo for the last fruitful year of collaboration and stimulating talks.

Furthermore, I would like to thank all the fellow participants of the Amsterdam-Brussels-Geneva-Paris Doctoral School on "Quantum Field Theory, Strings and Gravity" 2018 and the GGI Lectures on the Theory of Fundamental Interactions 2019 for exchanging experiences and knowledge in this journey. In addition, I would like to thank all the people from IPhT and EDPIF for making my PhD life easier and especially Laure Sauboy, Camille Flouret and Sylvie Zaffanella for putting up with my struggles of handling administrative issues.

A huge thank to all my beloved friends in Paris for the beautiful moments we spent together. A special thank to Mary and the rest of the Couronnes family Maria, Anna, Stelios, Manos, Sofia and Nefeli without whom the whole journey would be deficit. I would like to thank all my friends in Greece and Copenhagen as well, for always supporting me and motivating me even from far away. Lastly, I would like to thank my parents Petros and Chrysa and my siblings Antonis and Marilena for all the things they have taught me and always being there for me.

Contents

Chapter 1

Introduction

Modern physics as we know it is based on two basic pillars: Quantum Mechanics and General Relativity (GR). Quantum Field Theory (QFT) is the basic framework we have to reconcile Quantum Mechanics and Special Relativity. QFT has enjoyed a series of successful predictions, being at the heart of the Standard Model of Particle Physics, and at the same time is a mathematically elegant framework to describe physical phenomena. Therefore, QFT acquires a strong claim in being the correct guideline to describe nature. On the other hand, GR provides an extremely accurate framework to describe gravitational phenomena, being the protagonist of cosmology, in the classical regime and verified experimentally in several different cases as well. A natural reasoning would lead to the statement that gravity should be quantized. Even though this is not proven, the fact that all interactions at low-distance exhibit a quantum behavior, which for gravity is concluded to be $E_{\text{Planck}} \approx 10^{19} GeV$, provides a strong argument in favor of the above claim. In addition, recent developments connecting quantum entanglement and black holes [4] and the so called AdS/CFT correspondence [5], which have seen a huge progress in the recent years, suggest that gravity and quantum mechanics are closer than we thought. A natural approach to quantize gravity would be to directly proceed to canonical quantization, as we have done with the rest of the interactions, by considering the deviations from the flat metric as the quantum field and quantize the Einstein-Hilbert action

$$\mathcal{L}_{\text{EH}} = \int d^4x \sqrt{g} \frac{R}{16\pi G_N}. \tag{1.1}$$

Unfortunately, the above procedure is not straightforward, as it is for QED, QCD etc., since GR is a non-renormalizable theory due to its dimensionful coupling. In other words, in order to make sense of GR as a QFT we need to augment the theory with an infinite number of counterterms which render the theory not predictive in general. From the above, it seems that there is an

incompatibility between gravity and quantum mechanics which poses a paradox considering the previous claims. Many potential candidate theories resolve this paradox, such as String Theory, Loop Quantum Gravity etc., but all of these theories are beyond our current experimental limits. Therefore, we do not have, a foreseeable, direct experimental proof of their validity. Nevertheless, the approach of directly unifying gravity with quantum mechanics has offered tremendous insights and mathematical structures which are exploited in other approaches, as we shall see below.

In this thesis, we adopt a more "humble" approach to the problem of describing gravity as a QFT. One can consider the Einstein-Hilbert term as the first term of a low-energy effective action , describing the gravitational force as the exchange of a quantized massless spin-2 graviton field [6–10], augmented by an infinite number of higher derivative operators [11]. Thus, the problem of non-renormalizability arises naturally since the theory we are considering is a low-energy Effective Field Theory (EFT) valid up to a specific energy scale, as it happens with all EFTs. Equipped with the EFT approach, one can compute and make predictions relevant for gravitational dynamics exploiting mathematical tools inherited from particle physics and QFT. In the framework of General Relativity as a QFT (GRQFT), Scattering Amplitudes are fundamental quantities for understanding the physics of elementary interactions. A precise understanding of their properties is necessary to make contact with the experiments and predict new physical phenomena. The analysis of their mathematical properties makes it possible to update new physical principles underlying the organization of quantum physics governing the fundamental interactions. It has long been known that using the path integral formulation of GRQFT, it is very involved to compute Scattering Amplitudes even for simple processes due to the complicated form of the Feynman rules. Nevertheless, recent developments in the field of Scattering Amplitudes have enabled us to effectively tackle multiloop computations in gravity, rendering the theory a practical tool for actual computations.

The basic idea of the on-shell methods for Scattering Amplitudes program (see [12–14] for review) is to construct the Amplitude directly using symmetry arguments (locality, unitarity, Lorentz invariance) without deriving it from the action as we traditionally do via the path integral formalism. Namely, one can bootstrap the form of the Amplitude by imposing symmetry conditions to the result which is applicable to physical on-shell external states. Thus, we do not need to introduce the redundant degrees of freedom which are introduced in

the action to keep the symmetries manifest through the calculation, simplifying immensely the computation. Spinor helicity formalism, BCFW relations, generalized unitarity [15–17] and other techniques have proven extremely valuable in the program and are used throughout the literature enabling us to calculate a large number of physical processes at high orders in loops and with high multiplicity of interacting particles. This progress opens new theoretical investigations, and the discovery of new properties. The application of these methods to the theories of GRQFT is of paramount importance in understanding the nature of the gravitational force at the classical and quantum level. A milestone in the application of the on-shell methods in gravity are the BCJ relations (double copy) [18–20], motivated from string theory through the KLT relations [21], which relate straightforwardly a gauge theory amplitude with a gravitational amplitude making such computations significantly simpler and at the same time revealing a previously unknown relation between gauge and gravitational theories. Now that we can analytically calculate gravitational scattering processes, it is possible to quantify more precisely the experimental predictions of gravity theories generalizing, and going beyond, the ones introduced by Einstein 106 years ago [22]. In particular it is now possible to extract contributions of quantum gravity impossible to calculate a few years ago. In addition, it is now clear how one can extract higher G_N order contributions in classical gravity from quantum multi-loop Scattering Amplitudes in GRQFT [23–29], thus enabling us to make precise predictions in Classical Gravity exploiting the above techniques.

A strong motivation for studying gravitational dynamics is related to the recent discoveries by the LIGO collaboration [30,31]. Since the first detection of gravitational waves (GW) from a binary black hole coalescence was announced in 2016, it has been an exciting period for research in gravity. It is the first time we have observational data, with much more to come, for gravity in the strong regime. The binary coalescence contains three phases: inspiral, merger, ringdown (see Fig.1.1). It is important to stress, that while numerical simulations currently exclusively treat the strong field regime in full detai, they are inherently not suitable for tackling the inspiral phase. The long inspiral phase makes up the major portion of the GW signal if observed in its entirety, and depending on the masses in the binary, it can be the only observed signal falling within the frequency band of the detectors, yet it can not be treated numerically due to the intrinsic long timescale. The quest for analytic solution of the inspiral phase of the binary, the weak coupling regime of the process, being of paramount importance both for phenomenology and theory, has brought together researchers

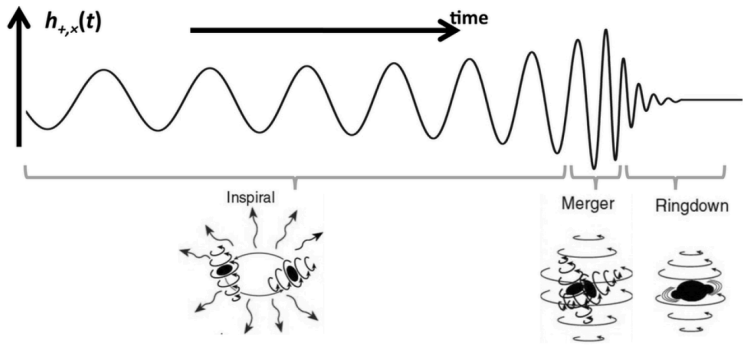

FIGURE 1.1: An illustration of the various phases of a black hole merger and the corresponding gravitational wave signal. The inspiral and the ringdown phase can be treated analytically, while the merger phase is treated solely numerically.

from General Relativity and Particle physics. GR community has produced a plethora of results within the so-called Post-Newtonian (PN) approximation, an expansion both in G_N and velocity, suitable for slow rotating objects during the inspiral phase (see [32,33] and references therein). Most recently, there have been many results in the Post-Minkowskian (PM) approximation within GR as well.

In particle physics, there has already been a huge amount of work accompanied with the development of efficient tools for particle scatterings. Therefore, it has been a natural step to apply these methods to the binary problem. With the seminal work of [34], the introduction of Post-Newtonian Effective Field Theory (PNEFT), or Non-Relativistic General Relativity (NRGR) (see Fig.1.2), formalism enabled us to apply particle physics tools to the binary problem, giving rise to many new results compensating the huge progress that has already been made from the GR community. For a detailed introduction to the PNEFT formalism and the state of the art results, go to Chapter 2.

Most recently, the so-called Post-Minkowskian (PM) framework [36–45], which consists in expanding the gravitational dynamics in the Newton's constant G_N while keeping the velocities fully relativistic, has received a renewed

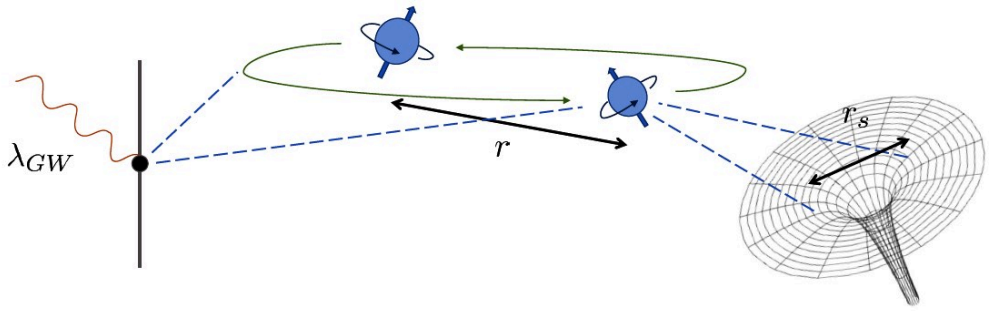

FIGURE 1.2: A graphic representation of the conceptual pipeline of the PNEFT formalism. Similarly, one works in the PMEFT framework. r_S is the radius of the compact object, r is the distance between the components of the binary and $\lambda_{\rm GW}$ is the characteristic wavelength of the emitted gravitational wave. Image reproduced from [35].

interest. This is complementary to the post-Newtonian approach, where one expands in both velocity and G_N, since in a bound state these two are related by the virial theorem (see Fig.1.3). Many progresses have been made within the PM approximation thanks to the application of several complementary approaches: in particular the effective one-body method [43, 44, 46, 47], the use of scattering amplitude techniques, such as the double copy, generalized unitarity and effective field theory (EFT) [27, 28, 48–55] (see [2, 7–10, 23, 56–58] for the quantum field theoretic description of gravity), the eikonal approximation [59–68] and worldline EFT approaches [3,69–73]. These developments concern the scattering of unbound states, but results can be extended to bound states by applying an analytic continuation between hyperbolic and elliptic motion [74,75]. Progresses have addressed the conservative binary dynamics up to 4PM order [76–81], as well as tidal [82–88], spin [89–97] and radiation effects [3, 98–105], and have spurred other new interesting results (see e.g. [106–110] for an incomplete list).

Evidently, the quest for analytic solutions of the dissipative two body problem in gravity is far from over. The field is highly motivated by the plethora of the forthcoming observational data and the need for higher precision in order to both investigate the validity of our current understanding and the discovery of

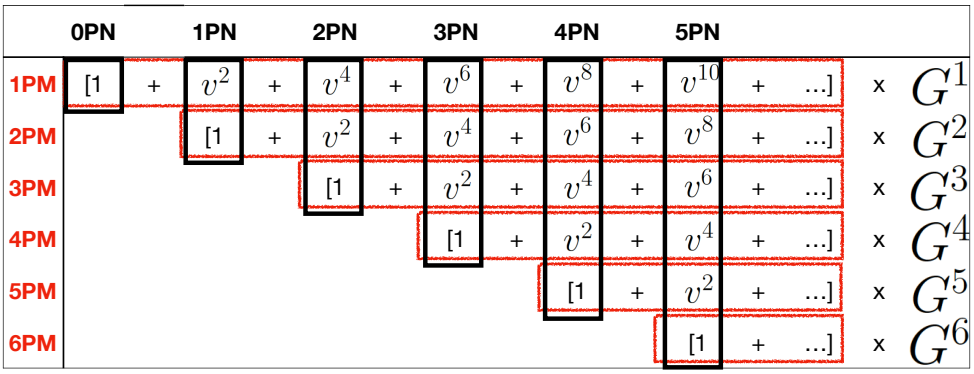

FIGURE 1.3: A depiction of the relative comparison between Post-Newtonian (PN) and Post-Minkowskian (PM) approximation.

new physics. The amount of the cited research work in the recent years suggests that much more progress is on the way. In the heart of the recent advances lies the complementarity of the many different approaches to the problem as it has already been exhibited. In addition, highly sophisticated integration techniques have been employed lately to push the precision frontier of the state of the art results. Furthermore, investigations of GR extensions and quantum signatures in the observational data is a pathway that could be of interest in the coming years. At the same time, the search for the fundamental nature of quantum gravity and the relation between the other forces is pursued in the same direction. All in all, the dialectic dynamic between observational data and new ideas, on the theoretical side, promises exciting advances in the future.

Adopting the significance of approaching a problem from different angles, this thesis is devoted in this direction. The rest of the dissertation is organized as follows: In Chapter 2 we introduce the NRGR formalism, which serves as a conceptual guideline of the different effects appearing in the dissipative binary problem, and explicitly compute the gravitational cubic in spin conservative interaction at NLO entering at 4.5PN order being of importance for rapidly rotating compact objects and their internal structure. In Chapter 3, we derive the Schwarzschild-Tangherlini metric in general dimensions via a GRQFT approach using quantum off-shell Scattering Amplitudes, for the first time up to 3-loop

order, providing a systematic way to extract consistently classical physics from quantum amplitudes, albeit the formalism is suitable for considering quantum effects as well. In chapter 4, we devote ourselves in the study of radiation emission in the PMEFT framework which serves both as a tool to compute actual waveforms relevant for the gravitational wave detectors and also unveil radiation reaction effects affecting the conservative dynamics of the system.

1.1 Présentation en français

La physique moderne telle que nous la connaissons repose sur deux piliers fondamentaux : la Mécanique Quantique et la Relativité Générale (RG). La théorie Quantique des Champs (QFT) est le cadre de base dont nous disposons pour réconcilier la Mécanique Quantique et la Relativité Restreinte. QFT a bénéficié d'une série de prédictions réussies, étant au cœur du modèle standard de physique des particules, et en même temps est un cadre mathématiquement élégant pour décrire les phénomènes physiques. Par conséquent, QFT acquiert une forte prétention à être la ligne directrice correcte pour décrire la nature. D'autre part, GR fournit un cadre extrêmement précis pour décrire les phénomènes gravitationnels, étant le protagoniste de la cosmologie, dans le régime classique et vérifié expérimentalement dans plusieurs cas différents également. Un raisonnement naturel conduirait à affirmer que la gravité doit être quantifiée. Même si cela n'est pas prouvé, le fait que toutes les interactions à faible distance présentent un comportement quantique, qui pour la gravité est conclu à $E_{\text{Planck}} \approx 10^{19} GeV$, fournit une forte argument en faveur de l'allégation ci-dessus. De plus, les développements récents reliant l'intrication quantique et les trous noirs [4] et la correspondance AdS/CFT [5], qui ont connu d'énormes progrès ces dernières années, suggèrent que la gravité et le quantum la mécanique est plus proche qu'on ne le pensait. Une approche naturelle pour quantifier la gravité serait de procéder directement à la quantification canonique, comme nous l'avons fait avec le reste des interactions, en considérant les écarts par rapport à la métrique plate comme le champ quantique et de quantifier l'action d'Einstein-Hilbert

$$\mathcal{L}_{\text{EH}} = \int d^4x \sqrt{g} \frac{R}{16\pi G_N}. \tag{1.2}$$

Malheureusement, la procédure ci-dessus n'est pas simple, comme c'est le cas pour QED, QCD, etc., car GR est une théorie non renormalisable en raison de son couplage dimensionnel. En d'autres termes, pour donner un sens à GR en tant que QFT, nous devons augmenter la théorie avec un nombre infini de contre-termes qui rendent la théorie non prédictive en général. D'après ce qui précède, il semble qu'il existe une incompatibilité entre la gravité et la mécanique quantique qui pose un paradoxe compte tenu des revendications précédentes. De nombreuses théories candidates potentielles résolvent ce paradoxe, telles que la théorie des cordes, la gravité quantique à boucle, etc., mais toutes ces théories dépassent nos limites expérimentales actuelles. Par conséquent, nous n'avons pas de preuve expérimentale directe et prévisible de leur

validité. Néanmoins, l'approche consistant à unifier directement la gravité avec la mécanique quantique a offert d'énormes connaissances et structures mathématiques qui sont exploitées dans d'autres approches, comme nous le verrons ci-dessous.

Dans cette thèse, nous adoptons une approche plus « humble » du problème de la description de la gravité comme un QFT. On peut considérer le terme d'Einstein-Hilbert comme le premier terme d'une action efficace à basse énergie, décrivant la force gravitationnelle comme l'échange d'un champ de graviton quantifié de spin-2 sans masse [6–10], augmenté d'un nombre infini d'opérateurs dérivés supérieurs [11]. Ainsi, le problème de la non-renormalisabilité se pose naturellement puisque la théorie que nous considérons est une théorie des champs effectifs à basse énergie (EFT) valable jusqu'à une échelle d'énergie spécifique, comme c'est le cas avec tous les EFT. Equipé de l'approche EFT, on peut calculer et faire des prédictions pertinentes pour la dynamique gravitationnelle en exploitant des outils mathématiques hérités de la physique des particules et du QFT. Dans le cadre de la relativité générale en tant que QFT (GRQFT), les amplitudes de diffusion sont des grandeurs fondamentales pour comprendre la physique des interactions élémentaires. Une compréhension précise de leurs propriétés est nécessaire pour prendre contact avec les expériences et prédire de nouveaux phénomènes physiques. L'analyse de leurs propriétés mathématiques permet de mettre à jour de nouveaux principes physiques sous-tendant l'organisation de la physique quantique régissant les interactions fondamentales. On sait depuis longtemps qu'en utilisant la formulation intégrale de chemin de GRQFT, il est très compliqué de calculer les amplitudes de diffusion même pour des processus simples en raison de la forme compliquée des règles de Feynman. Néanmoins, les développements récents dans le domaine des amplitudes de diffusion nous ont permis d'aborder efficacement les calculs multi-boucles en gravité, faisant de la théorie un outil pratique pour les calculs réels.

L'idée de base des méthodes sur shell pour le programme Scattering Amplitudes (voir [12–14] pour examen) est de construire l'amplitude directement en utilisant des arguments de symétrie (localité, unitarité, invariance de Lorentz) sans la dériver de l'action comme on le fait traditionnellement par le chemin du formalisme intégral. A savoir, on peut amorcer la forme de l'amplitude en imposant des conditions de symétrie au résultat qui est applicable aux états externes physiques sur la coque. Ainsi, nous n'avons pas besoin d'introduire les degrés de liberté redondants qui sont introduits dans l'action pour garder

les symétries manifestes à travers le calcul, simplifiant énormément le calcul. Le formalisme de l'hélicité de spinor, les relations BCFW, l'unitarité généralisée [15–17] et d'autres techniques se sont avérées extrêmement précieuses dans le programme et sont utilisées dans toute la littérature nous permettant de calculer un grand nombre de processus physiques à des ordres élevés dans les boucles et avec une multiplicité élevée de particules en interaction. Ces progrès ouvrent de nouvelles investigations théoriques, et la découverte de nouvelles propriétés. L'application de ces méthodes aux théories de GRQFT est d'une importance primordiale pour comprendre la nature de la force gravitationnelle au niveau classique et quantique. Les relations BCJ (double copie) [18–20], motivées de la théorie des cordes à travers les relations KLT [21], qui relient directement une amplitude de théorie de jauge à une amplitude gravitationnelle, ce qui simplifie considérablement ces calculs et révèle en même temps une relation jusqu'alors inconnue entre les théories de jauge et la théorie gravitationnelle. Maintenant que nous pouvons calculer analytiquement les processus de diffusion gravitationnelle, il est possible de quantifier plus précisément les prédictions expérimentales des théories de la gravité généralisant, et allant au-delà, celles introduites par Einstein il y a 106 ans [22]. En particulier, il est désormais possible d'extraire des contributions de la gravité quantique impossibles à calculer il y a quelques années. De plus, il est maintenant clair comment on peut extraire des contributions d'ordre G_N plus élevées en gravité classique à partir d'amplitudes de diffusion multi-boucles quantiques dans GRQFT [23–29], nous permettant ainsi de faire des prédictions précises en gravité classique en exploitant les techniques ci-dessus.

Une forte motivation pour étudier la dynamique gravitationnelle est liée aux récentes découvertes de la collaboration LIGO [30, 31]. Depuis que la première détection d'ondes gravitationnelles (GW) à partir d'une coalescence binaire de trous noirs a été annoncée en 2016, cela a été une période passionnante pour la recherche en gravité. C'est la première fois que nous avons des données d'observation, avec beaucoup plus à venir, pour la gravité en régime fort. La coalescence binaire contient trois phases : inspirale, fusion, ringdown (voir Fig.1.4). Il est important de souligner que si les simulations numériques traitent actuellement exclusivement le régime de champ fort en détail, elles ne sont intrinsèquement pas adaptées pour aborder la phase inspiratoire. La longue phase inspiratoire constitue la majeure partie du signal GW si elle est observée dans son intégralité, et en fonction des masses dans le binaire, elle peut être le seul signal observé entrant dans la bande de fréquence des détecteurs, mais elle

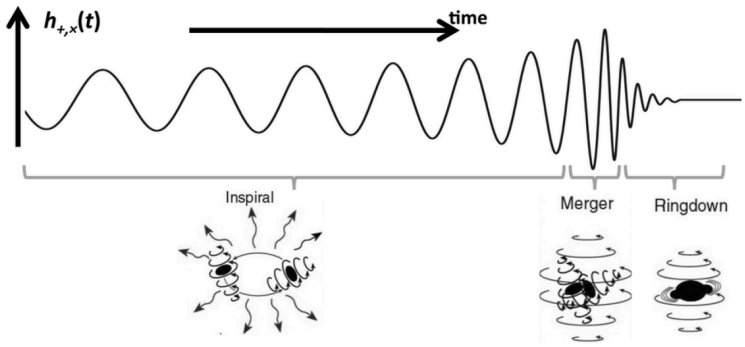

FIGURE 1.4: Une illustration des différentes phases d'une fusion de trous noirs et le signal d'onde gravitationnelle correspondant. La phase inspirale et la phase de ringdown peuvent être traitées analytiquement, tandis que la phase de fusion est traitée uniquement numériquement.

ne peut pas être traitée. numériquement en raison de la longue échelle de temps intrinsèque. La recherche d'une solution analytique de la phase inspiratoire du binaire, le régime de couplage faible du processus, étant d'une importance capitale tant pour la phénoménologie que pour la théorie, a réuni des chercheurs de la Relativité Générale et de la Physique des Particules. La communauté GR a produit une pléthore de résultats dans l'approximation dite post-newtonienne (PN), une expansion à la fois en G_N et en vitesse, adaptée aux objets à rotation lente pendant la phase d'inspiration (voir [32, 33] et références). Plus récemment, il y a eu de nombreux résultats dans l'approximation post-minkowskienne (PM) au sein de la RG également.

En physique des particules, il y a déjà eu un énorme travail accompagné du développement d'outils efficaces pour la diffusion des particules. Par conséquent, il a été naturel d'appliquer ces méthodes au problème binaire. Avec les travaux fondateurs de [34], l'introduction de la théorie des champs effectifs post-newtoniens (PNEFT), ou de la relativité générale non relativiste (NRGR) (voir Fig.1.5), le formalisme nous a permis de appliquer des outils de physique des particules au problème binaire, donnant lieu à de nombreux nouveaux résultats compensant les énormes progrès déjà réalisés par la communauté des RG. Pour une introduction détaillée au formalisme PNEFT et à l'état de l'art

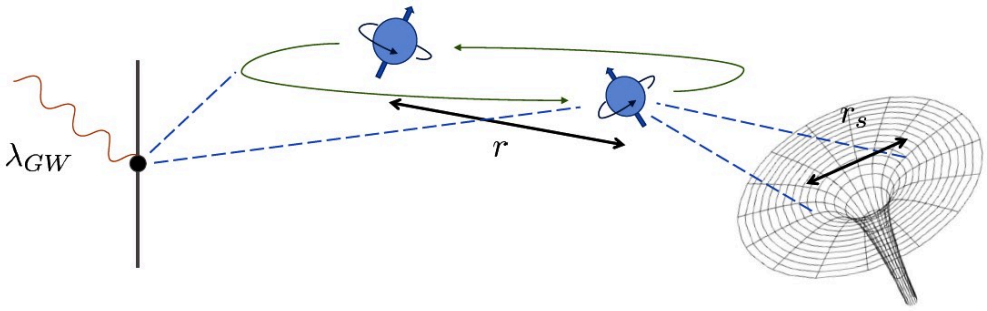

FIGURE 1.5: Une représentation graphique du pipeline conceptuel du formalisme PNEFT. De même, on travaille dans le cadre PMEFT. r_S est le rayon de l'objet compact, r est la distance entre les composantes du binaire et $\lambda_{\rm GW}$ est la longueur d'onde caractéristique de l'onde gravitationnelle émise. Image reproduite de [35].

des résultats, reportez-vous au chapitre 2.

Plus récemment, le cadre dit post-minkowskien (PM) [36–45], qui consiste en l'expansion de la dynamique gravitationnelle dans la constante de Newton G_N tout en gardant les vitesses totalement relativistes, a suscité un regain d'intérêt. Ceci est complémentaire à l'approche post-newtonienne, où l'on développe à la fois la vitesse et G_N, puisque dans un état lié ces deux sont liés par le théorème du viriel (voir Fig.1.6). De nombreux progrès ont été réalisés au sein de l'approximation PM grâce à l'application de plusieurs approches complémentaires : en particulier la méthode efficace à un seul corps [43, 44, 46, 47], l'utilisation de techniques d'amplitude de diffusion, telles que la double copie, l'unitarité généralisée et la théorie des champs effectifs (EFT) [27, 28, 48–55] (voir [2, 7–10, 23, 56–58] pour la description de la théorie quantique des champs de la gravité), l'approximation eikonale [59–68] et les approches EFT worldline [3, 69–73]. Ces développements concernent la diffusion des états non liés, mais les résultats peuvent être étendus aux états liés en appliquant une continuation analytique entre le mouvement hyperbolique et elliptique [74, 75]. Les progrès ont abordé la dynamique binaire conservatrice jusqu'à l'ordre de 16

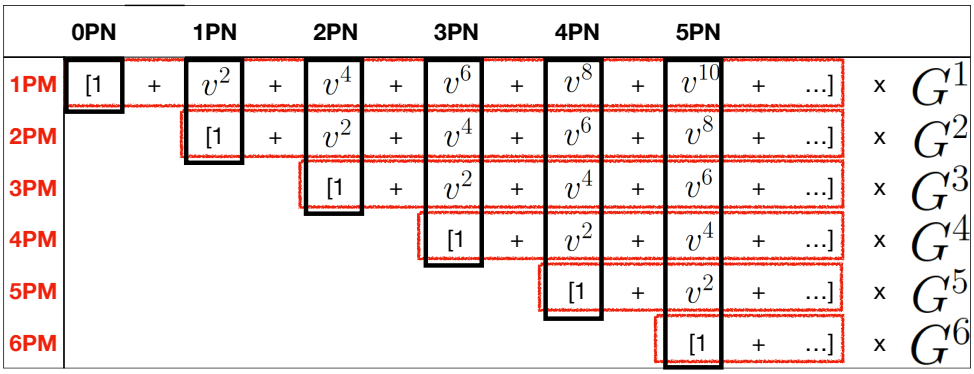

FIGURE 1.6: Une représentation de la comparaison relative entre l'approximation post-newtonienne (PN) et post-minkowskienne (PM).

heures [76–81], ainsi que la marée [82–88], spin [89–97] et les effets des radiations [3, 98–105], et ont suscité d'autres nouveaux résultats intéressants (voir par exemple [106–110] pour une liste incomplète).

De toute évidence, la quête de solutions analytiques du problème dissipatif à deux corps en gravité est loin d'être terminée. Le domaine est fortement motivé par la pléthore de données d'observation à venir et le besoin d'une plus grande précision afin d'étudier à la fois la validité de notre compréhension actuelle et la découverte de nouvelles physiques. La quantité de travaux de recherche cités au cours des dernières années suggère que beaucoup plus de progrès sont en cours. Au cœur des avancées récentes se trouve la complémentarité des nombreuses approches différentes du problème tel qu'il a déjà été exposé. De plus, des techniques d'intégration très sophistiquées ont été utilisées ces derniers temps pour repousser la frontière de la précision des résultats de pointe. De plus, les investigations sur les extensions GR et les signatures quantiques dans les données d'observation sont une voie qui pourrait être intéressante dans les années à venir. En même temps, la recherche de la nature fondamentale de la gravité quantique et de la relation entre les autres forces est poursuivie dans la même direction. Au total, la dynamique dialectique entre données d'observation et idées nouvelles, du côté théorique, promet des avancées passionnantes dans le futur.

Adoptant l'importance d'aborder un problème sous différents angles, cette thèse est consacrée dans cette direction. Le reste de la thèse est organisé comme suit : Dans le chapitre 2 nous introduisons le formalisme NRGR, qui sert de guide conceptuel des différents effets apparaissant dans le problème binaire dissipatif, et calculons explicitement la cubique gravitationnelle en interaction conservatrice de spin à NLO, l'entrée à l'ordre de 4,5PN est importante pour les objets compacts à rotation rapide et leur structure interne. Dans le chapitre 3, nous dérivons la métrique de Schwarzschild-Tangherlini en dimensions générales via une approche GRQFT utilisant des amplitudes de diffusion quantiques hors coque, pour la première fois jusqu'à l'ordre de 3 boucles, fournissant un moyen systématique d'extraire systématiquement la physique classique à partir des amplitudes quantiques, bien que le formalisme soit adapté pour considérer également les effets quantiques. Dans le chapitre 4, nous nous consacrons à l'étude de l'émission de rayonnement dans le cadre PMEFT qui sert à la fois d'outil pour calculer les formes d'onde réelles pertinentes pour les détecteurs d'ondes gravitationnelles et dévoile également les effets de réaction de rayonnement affectant la dynamique conservatrice du système .

Chapter 2

Effective Field Theory of Post-Newtonian Gravity

In this chapter we will introduce the basics of the Effective Field Theory of Post-Newtonian Gravity (EFT of PNG), also known as Non-Relativistic General Relativity (NRGR). The formalism was firstly developed in [34] and further expanded by several authors. Our aim is to familiarize the reader with the systematics of the NRGR formalism (see refs. [111, 112] for extensive reviews), which will prove useful as a conceptual guideline for the rest of this thesis, and finally focus on the contribution of the author [1] on the conservative sector of the cubic-in-spin effective action at the next-to-leading order.

In this work [1] we derive for the first time the complete gravitational cubic-in-spin effective action at the next-to-leading order in the post-Newtonian (PN) expansion for the interaction of generic compact binaries via the effective field theory for gravitating spinning objects, which we extend in this work. This sector, which enters at the fourth and a half PN (4.5PN) order for rapidly-rotating compact objects, completes finite-size effects up to this PN order, and is the first sector completed beyond the current state of the art for generic compact binary dynamics at the 4PN order. At this order in spins with gravitational nonlinearities we have to take into account additional terms, which arise from a new type of worldline couplings, due to the fact that at this order the Tulczyjew gauge for the rotational degrees of freedom, which involves the linear momentum, can no longer be approximated only in terms of the four-velocity. One of the main motivations for us to tackle this sector is also to see what happens when we go to a sector, which corresponds to the gravitational Compton scattering with quantum spins larger than one, and maybe possibly also get an insight on the inability to uniquely fix its amplitude from factorization when spins larger than two are involved. A general observation that we can clearly make already is that even-parity sectors in the order of the spin are easier to handle than odd ones. In the quantum context this corresponds to the greater

ease of dealing with bosons compared to fermions.

2.1 Basics of Non-Relativstic General-Relativity

In this section we will provide the basic background of the Non-Relativistic General Relativity (NRGR) formalism [111, 112] for studying the inspiral phase of the binary problem in gravity. The general considerations below serve as a conceptual guideline beyond the specific formulation of the NRGR formalism. Namely, the tower of EFTs and the method of regions are schemes that are used also in a PM approximation of the problem.

2.1.1 Basics of EFTs

Let us first consider a general interacting scalar theory in 4 dimensions $\mathcal{S}(\phi)$ as a toy model and suppose that we are interested in investigating an energy regime $E \ll \Lambda$ where Λ is an ultraviolet (UV) energy cutoff. For this purpose, it is convenient to split the field as $\phi = \Phi + \psi$, such that:

- ψ are light Degrees of Freedom (DOF) with an energy scale E
- Φ are heavy DOFs with an energy scale Λ.

Thus, Φ don't propagate as a physical DOF, in the energies that we are interested, but only off-shell. This fact is in the heart of the EFT approach. One can integrate out Φ and acquire an effective description of the theory in terms of the light field ψ, as long as we are interested in energies of order $E \ll \Lambda$.

$$e^{i\mathcal{S}_{\text{eff}}(\psi)} \equiv \int \mathcal{D}\Phi \; e^{i\mathcal{S}(\psi,\Phi)}. \tag{2.1}$$

The procedure of integrating out Φ can be done via standard QFT methods perturbatively, considering the heavy field Φ propagating only off-shell. By doing so, one ends up with

$$\mathcal{S}_{\text{eff}}(\psi) = \int d^4x \Big(\frac{1}{2}(\partial_\mu \psi)^2 + \sum_n C_n \mathcal{O}_n(\psi) \Big) \ , \tag{2.2}$$

where $\mathcal{O}_n(\psi)$ are local operators with mass dimension n. This is the *Top-Down* approach, first developed by Wilson [113, 114]. The coefficients C_n are called Wilson coefficients and they encode all the information of the UV theory, the effects of the heavy field Φ, on the low-energy effective theory.

Another way to build an EFT is the *Bottom-Up* approach. One employs this approach when there is no knowledge of the UV theory from the beginning. In this case, symmetries and other properties of the low-energy theory can be applied in order to construct an effective theory of the form 2.2. Since we don't have knowledge of the UV complete theory, the Wilson coefficients, C_n, in this case are unfixed and one requires a matching procedure either by comparing with experimental data or performing *Top-Down* computation and adjusting the coefficients by matching.

In both approaches, power counting is an extremely powerful tool since it enables us to organize and identify the contributions of the operators $\mathcal{O}_n(\psi)$ at any given order. From power counting arguments, we can deduce that the scaling of the Wilson coefficients is

$$C_n \sim \frac{1}{\Lambda^{n-4}}. \tag{2.3}$$

Thus, the contributions from the operators are suppressed as $\left(\frac{E}{\Lambda}\right)^n \ll 1$, enabling us to identify the relevance of each operator at any given order.

One last important remark concerns the identification of the classical and the quantum contributions. As in all perturbative QFT treatments, loop diagrams contribute to quantum contributions while tree diagrams give classical contributions. In theories with both massive and massless degrees of freedom, the situation is more subtle [25, 26] and will be discussed further in Chapter 3. Nevertheless, for the scalar case the above holds true. In addition, in the rest of this chapter as we will see we will use a worldline description of the sources, thus the only propagating degrees of freedom will be the gravitons. Therefore, again for worldline theories the identification of trees=classical and closed loops=quantum holds true.

To sum up, EFT is an extremely powerful framework, both conceptually and practically, allowing us to decouple the UV physics from the low-energy scales that we are interested in. The large separation of scales plus the identification of the low-energy DOFs and the symmetries of a theory enables us to approach almost any problem from a low-energy point of view. These general considerations will be our guidelines for the rest of this chapter and, adjusted properly, for the rest of this thesis as well.

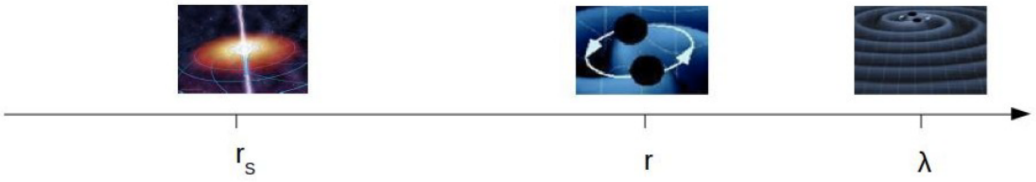

FIGURE 2.1: The hierarchy of scales in the binary inspiral problem: r_s, the scale of the single compact object; r, the scale of the orbital separation between the components of the binary; λ_{rad}, the wavelength of radiation, emitted from the inspiraling binary; it holds that $r_s \ll r \ll \lambda_{rad}$. Reproduced from [112]

2.1.2 Tower of EFTs

Having established the general considerations of the EFT approach, we are ready to confront the binary problem in gravity. As we have already said, the crucial starting point of constructing the EFT is the identification of the scales of the problem. Fortunately, the binary problem can be viewed as an (interacting) tower of EFTs separated by three largely separated scales, $r_s \ll r \ll \lambda_{rad}$ as shown in 2.1. Thus, we can split the problem in zones:

- *internal zone*: In this zone we work at the scale r_s, which for compact neutron stars or black holes is the Schwarzschild radius $r_s \approx 2G_N m$. The effective description at this scale will be of the point-particle EFT, as we will see below, where the finite size effects (dissipation and tidal deformations) can be generally parametrized upon integrating out the short scale degrees of freedom.

- *potential zone*: At this intermediate zone, we are working at the orbit scale r which is the typical separation between the point-particles consisting the binary. In the inspiral phase, where $v \ll 1$, it is guaranteed via the virial theorem that $\frac{G_N m}{r} \sim v^2$ and therefore the expansion parameter $\frac{r_s}{r} \sim v^2 \ll 1$. In this zone, we analyze the conservative dynamics of the binary system by describing point particles interacting via the exchange of off-shell potential graviton modes. These potential modes, typically scaling as $|\vec{k}| \sim 1/r$, probe the internal structure of the objects which affect the conservative dynamics. Furthermore, the conservative dynamics are also influenced by the radiation zone via radiation back-reaction effects.

- *radiation zone*: In this outer zone, the orbital scale r becomes part of the internal zone and the binary system is treated as a point-like source equipped with a series of multipole moments I^L, J^L, emitting on-shell

graviton modes of momentum $\vec{p}$. At this stage, both *Top-Down* and *Bottom-Up* approaches are used to compute the multipole moments of the binary system. The scale we are working is $\lambda_{rad} \sim r/v$ and the expansion parameter is $|\vec{p}|r \sim \frac{r}{\lambda_{rad}} \sim v \ll 1$. In addition, we observe hereditary effects coming from the interaction of the emitted radiation with the static potential and also radiation-reaction effects whose origin comes from the back-reaction of the gravitational wave to the dynamics of the binary.

To summarize, we split the metric as

$$g_{\mu\nu} = g^s_{\mu\nu} + \eta_{\mu\nu} + H_{\mu\nu} + h_{\mu\nu} \ , \tag{2.4}$$

where $g^s_{\mu\nu}$ is the strong modes at scale $\sim r_s$, $H_{\mu\nu}$ is the potential off-shell graviton modes at scale r and $h_{\mu\nu}$ are the radiation on-shell graviton modes at scale λ_{rad}. In order to compute the effective action, we integrate out scale by scale the "shorter" degrees of freedom within the saddle-point approximation (classical physics) via standard QFT methods perturbatively as

$$e^{i\mathcal{S}_{\text{eff}}} = \int \mathcal{D}h \ \mathcal{D}H \ \mathcal{D}g^s \ e^{i\mathcal{S}}. \tag{2.5}$$

Then, by extremizing the real part,

$$\frac{\delta}{\delta x_a(t)} \text{Re} \ \mathcal{S}_{\text{eff}} = 0 \tag{2.6}$$

one obtains the equations of motion for the binary constituents, while from the optical theorem,

$$\frac{1}{T} \text{Im} \ \mathcal{S}_{\text{eff}} = \frac{1}{2} \int \frac{d^2\Gamma}{dEd\Omega} dEd\Omega \tag{2.7}$$

we get the radiated power, with $dP = Ed\Gamma$.

2.1.3 Internal zone

As we have already proclaimed, the NRGR formalism starts from integrating out the strong gravitational field at the level of the single body in order to acquire an effective description of an extended object as a point particle. Namely, we are considering the gravitational action

$$\mathcal{S} = -\frac{1}{16\pi G_N} \int d^4x \sqrt{g} R[g_{\mu\nu}] + ... \ , \tag{2.8}$$

where ... stands for higher derivative corrections to Einstein gravity and matter couplings (e.g. in the case of neutron stars). It is beyond the purpose of this thesis to consider GR extensions, thus we will contain ourselves in the Einstein-Hilbert action. Furthermore, the matter couplings at the scale r_s will be encoded, as we will see, in the Wilson coefficients of the one-particle EFT that we will arrive. Therefore, the Wilson coefficients will distinguish between different extended objects at the level of the EFT and can be computed via a matching procedure. Next, we split the metric as

$$g_{\mu\nu} \equiv g^s_{\mu\nu} + \tilde{g}_{\mu\nu} \ , \tag{2.9}$$

where $g^s_{\mu\nu}$ denotes the strong field (short distance) modes that are to be integrated out from the theory and $\tilde{g}_{\mu\nu}$ describes the metric outside the radius r_s. At this point, we employ a *Bottom-Up* approach to describe the single body. We identify the relevant DOFs at this scale as the worldline of the particle and we introduce an infinite series of worldline operators which respect the known symmetries of the system, namely diffeomorphism and reparameterization invariance. Our goal is to keep the discussion as general as possible, therefore we will include also the spinning case on which we will focus mainly later on. So, when including spinning bodies in the description we have more independent DOFs beyond the worldline coordinates. The spinning case is not that trivial due to the fundamental conflict between an actual rotating gravitating object, which must have an extended finite size for its rotational velocity to not surpass the speed of light, and its view in the EFT as a point particle. Below, we list the relevant DOFs and the associated symmetries for the general case of a spinning object including finite size and spin effects.

Degrees of Freedom

- *The gravitational field.* The metric $\tilde{g}_{\mu\nu}$ and the gravitational tetrad field satisfying $\tilde{g}^{\mu\nu} = \tilde{e}^\mu_a \tilde{e}^\nu_b \eta^{ab}$.

- *The particle worldline coordinate.* $x_\mu(\sigma)$ is a function of an arbitrary affine parameter σ. The time coordinate is used to fix the gauge of the affine parameter, and we have the 3 DOFs, giving the position of the particle

- *The particle worldline rotating DOFs.* We consider the worldline tetrad, an orthonormal frame $\tilde{g}^{\mu\nu} = e^\mu_A(\sigma) e^\nu_B(\sigma) \eta^{AB}$, localized on the particle worldline connecting the body fixed and general coordinate frames. The

gravitational field DOFs satisfy $\tilde{e}^{\mu}_{a}(x(\sigma)) = \Lambda^{A}_{a}(\sigma)e^{\mu}_{A}$, where $\Lambda^{A}_{a}(\sigma)$ is the worldline Lorentz matrix.

Symmetries

- *General coordinate invariance.*
- *Worldline reparametrization invariance.*
- *Internal Lorentz invariance of the local frame field.*
- *SO*(3) *invariance of the body fixed spatial triad.*
- *Spin gauge invariance*, that is an invariance under the choice of a completion of the body-fixed spatial triad through a timelike vector. This is a gauge of the rotational variables.

Finally, upon integrating out the short distance modes $g^{s}_{\mu\nu}$ following a *Bottom-Up* approach, identifying the relevant degrees of freedom and invoking the symmetries of the problem, the one-particle EFT takes the form

$$\mathcal{S}_{\text{eff}}[x(\sigma),\tilde{g}] = -\frac{1}{16\pi G_N}\int d^4x\sqrt{\tilde{g}}\tilde{R}[\tilde{g}_{\mu\nu}] + \mathcal{S}_{\text{p.p.}}\ , \tag{2.10}$$

where $\mathcal{S}_{\text{p.p.}}$ is

$$\begin{aligned}
\mathcal{S}_{\text{p.p.}} =& -\int d\sigma\big[m\sqrt{u^2} + \frac{1}{2}S_{\mu\nu}\Omega^{\mu\nu}\big] \\
&+ c_R\int d\sigma\ \tilde{R}\sqrt{u^2} + c_V\int d\sigma\ \tilde{R}_{\mu\nu}\frac{u^\mu u^\nu}{\sqrt{u^2}} + ... \\
&+ \int d\tau\ Q^{ij}_{E}(\tau)E_{ij}(x) + ... + (E\to B) \\
&+ \sum_{n=1}^{\infty}\int d\sigma\frac{(-1)^n C_{ES^{2n}}}{(2n)!m^{2n-1}}D_{\mu_{2n}}...D_{\mu_3}E_{\mu_1\mu_2}\frac{S^{\mu_1}...S^{\mu_{2n}}}{\sqrt{u^2}} \\
&+ \sum_{n=1}^{\infty}\int d\sigma\frac{(-1)^n C_{BS^{2n}}}{(2n+1)!m^{2n}}D_{\mu_{2n+1}}...D_{\mu_3}B_{\mu_1\mu_2}\frac{S^{\mu_1}...S^{\mu_{2n+1}}}{\sqrt{u^2}}\ ,
\end{aligned} \tag{2.11}$$

where τ is the proper time, σ is the coordinate time, $x(\sigma)$ is the worldline coordinate, $e^{\mu}_{A}(\sigma)$ is the worldline tetrad defined as $\tilde{g}^{\mu\nu} \equiv \eta^{AB}e^{\mu}_{A}e^{\nu}_{B}$, $u^{\mu}(\sigma) \equiv \frac{dx^{\mu}(\sigma)}{d\sigma}$ is the coordinate velocity, $\Omega^{\mu\nu} \equiv e^{\mu}_{A}\frac{De^{A\nu}}{D\sigma}$ is the worldline angular velocity, $S^{\mu\nu}$ is the antisymmetric worldline spin tensor (conjugate to the angular velocity) and the dual is defined as $*S_{\alpha\beta} \equiv \frac{1}{2}\epsilon_{\alpha\beta\mu\nu}S^{\mu\nu}$, $S^{\mu} \equiv *S^{\mu\nu}\frac{p_\nu}{\sqrt{p^2}}$ is the spin vector, $E_{\mu\nu}(x) = C_{\mu\nu\alpha\beta}u^\alpha u^\beta$ and $B_{\mu\nu}(x) = \frac{1}{2}\epsilon_{\alpha\beta\gamma\mu}C^{\alpha\beta}{}_{\delta\nu}u^\gamma u^\delta$ are the electric and

magnetic components of the Weyl tensor, $Q^{ij}_{E,B}$ are the trace-free electric (and magnetic) quadrupole moments DOFs, $E(B)_{ij}$ are the spatial components of the projected to the locally flat comoving frame $e^{\mu}_{A}(x)$ (with $e^{\mu}_{0}(x) = u^{\mu}$) electric and magnetic components of the Weyl tensor and ... stands for higher derivative contributions.

The first line describes the minimal coupling of the worldline DOFs for a general spinning object.

The second line describes the first non-minimal coupling terms of the worldline DOFs for the non-spinning case incorporating finite size effects. Nevertheless, a consequence of the Birkhoff's theorem is that these operators are, what is called in EFT terminology, *redundant*. Essentially, for on-shell quantities these operators can be set to zero since they can be canceled when one replaces the leading order equations of motion back to the action. Equivalently, one can perform a field redefinition and drop them. Even though, these operators can be effectively ignored for our purposes, and subsequently in the definition of $E_{\mu\nu}, B_{\mu\nu}$ we can replace the Weyl with the Riemann tensor, this is not the case when considering off-shell quantites such as the metric as we will see in detail in Chapter 3, although in a different setup but along the same physical arguments.

The third line gives us the physical finite size effects for non-spinning objects in the EFT description of the extended compact object. Several comments are in order here. Firstly, we introduced a new set of DOFs to describe finite size effects, which we will see below that are relevant for describing dissipative effects, where we have used the $SO(3)$ symmetry of a static spacetime in order to write down the operators. Secondly, even though the gravitational interaction is local the quadrupole moments may depend on time. Thus, we can split them in different components $Q^{E,B}_{i_1,..,i_n} = \langle Q^{E,B}_{i_1,..,i_n}\rangle_S + (Q^{E,B}_{i_1,..,i_n})_R$, where $\langle\rangle_S$ is computed in the background of short modes and $()_R$ is in general the induced multipole moment in the presence of long wavelength perturbations. Furthermore, we know that for spherically symmetric non-spinning isolated objects, $\langle Q^{E}_{ij}\rangle_S = 0$, so for simplicity we will focus only on this term for what follows. Using linear response theory, we can write

$$(Q^{E}_{ij})_R(\tau) = \frac{1}{2}\int d\tau' \big(iG^{ij,kl}_{ret}(\tau,\tau')\big) E_{kl}(x) + \dots \,, \tag{2.12}$$

where $G^{ij,kl}_{ret}(\tau,\tau') = \langle[Q^E_{ij}(\tau), Q^E_{kl}(\tau')\rangle]\theta(\tau-\tau')$ and similarly for the magnetic-type components. The crucial identification is that the real part of $iG^{ij,kl}_{ret}(\tau,\tau')$ is associated with the tidal effects while the imaginary part is associated with dissipation effects, e.g. absorption from the BH's horizons or the dissipative tidal deformations of NSs. One can write, in the frequency domain, $iG^{ij,kl}_{ret}(\omega) = f(\omega)(\delta_{ik}\delta_{jl} + \delta_{il}\delta_{jk} + \delta_{ij}\delta_{kl})$. For the imaginary, dissipative, contribution one can compute via the optical theorem the absorption cross section in the EFT in terms of $Im\ f(\omega)$, match with the GR result [115] and deduce that this contribution enters at 6.5PN order. On the other side, for the real, tidal, contribution we can expand $Re\ f(\omega)$ in powers of $\omega r_s \ll 1$, since we are considering the long wavelength perturbations, and using the time reversal symmetry of the real part of the response we can write $Re\ f(\omega) = c_E + c_{\ddot{E}}(\omega r_s)^2 + ...$. Replacing back into the action and writing in terms of the coordinate time, σ, we get that the second line can be written, up to 6.5PN order neglecting dissipation, as

$$c_E \int d\sigma \frac{E^2_{\mu\nu}}{\sqrt{u}^3} + c_B \int d\sigma \frac{B^2_{\mu\nu}}{\sqrt{u}^3} + ... \tag{2.13}$$

Note that as long as we are neglecting dissipative finite size effects, we don't need to introduce a new DOF to describe the compact object. Furthermore, the first operators stand for the mass-induced quadrupolar tidal deformation of the extended object by the gravitational field. Each added derivative in an operator scales as $1/r$, and is preceded by a Wilson coefficient with the proper power of r_s, so that overall each term scales as powers of $r_s/r \sim v^2$. Thus, from dimensional analysis one easily finds that the leading Wilson coefficients $c_{E,B}$, which are equivalent to the 'Love numbers' originally defined in Newtonian gravity, scale as r_s^5 at LO, and that these finite size operators enter at the 5PN order. It has also been proven that for non-spinning BHs in $d = 4$, the 'Love numbers' vanish. Note that these coefficients are gauge invariant, because they appear multiplying gauge invariant terms in the effective action, and even though their matching is always done in some specific gauge, when they vanish they do at all scales, and there is no RG running of this coupling.

The final lines give the generalised non-minimal coupling of the worldline for a spinning compact object, describing finite size effects due to spin, that we will discuss in more detail in the rest of this chapter.

2.1.4 Potential zone

In the potential zone, we want to obtain the EFT of the composite particle via the *Top-Down* procedure using standard perturbative QFT methods, involving a diagrammatic expansion and Feynman calculus. This EFT removes the scale of orbital separation between the components of the binary. It is then matched onto the effective action constructed bottom-up, as we will see in the next section, with the point-particle action now being that of the composite particle, in terms of multipole moments. Equipped with the point-particle EFT from (2.10),(2.11), one can proceed to consider the binary system in the potential zone using the action

$$\mathcal{S}_{\text{cons.}} = \mathcal{S}_{\text{EH}} + \mathcal{S}_{\text{GF}} + \mathcal{S}_{\text{p.p.1}} + \mathcal{S}_{\text{p.p.2}} \ , \tag{2.14}$$

where $\mathcal{S}_{\text{GF}}$ is the gauge-fixing term we have to add to the action in order to integrate out the gravitational field.

Furthermore, at this stage we will decompose the metric as

$$\tilde{g}_{\mu\nu} = \eta_{\mu\nu} + H_{\mu\nu} + h_{\mu\nu} \ , \tag{2.15}$$

where $H_{\mu\nu}$ is the off-shell potential modes and $h_{\mu\nu}$ is the emitted on-shell radiation modes. We will work in the fully harmonic gauge, thus

$$\mathcal{S}_{\text{GF}}[H] = \frac{1}{32\pi G_N} \int d^4x \sqrt{\tilde{g}} \tilde{g}_{\mu\nu} \Gamma^{\mu}_{(h)}[H] \Gamma^{\nu}_{(h)}[H] \ , \tag{2.16}$$

where $\Gamma^{\mu}_{(h)}[H] = \Gamma^{\mu}_{\nu\sigma(h)}[H]\tilde{g}^{\nu\sigma} = \nabla^{\nu}_{(h)} H^{\mu}_{\nu} - \frac{1}{2}\nabla^{\mu}_{(h)} H^{\nu}_{\nu}$. Working within the background field method, covariant derivatives are taken with respect to the background field. However, in the conservative sector that we are now considering, no background radiation modes are present, and so the covariant derivative is just the standard one. In addition, when including spin one needs to fix the gauge of the rotational DOFs in order to integrate out completely the orbital modes. This discussion will be held in the spinning EFT of the next sections in detail.

Finally, we know that for the orbital modes we have $k_0 \sim v/r$ while $|\vec{k}| \sim 1/r$, so that we can expand the propagator in momentum space as

$$\frac{1}{k_0^2 - \vec{k}^2} = -\frac{1}{\vec{k}^2}(1 + \frac{k_0^2}{\vec{k}^2} + ...) = -\frac{1}{\vec{k}^2}(1 + \mathcal{O}(v^2)) \ , \tag{2.17}$$

so that the propagator is instantaneous, and the relativistic time corrections to the propagator are considered as PN perturbations. Therefore it makes sense, and indeed it has proven very useful in practice, to reduce over the time coordinate in the metric in a *Kaluza-Klein* (KK) fashion, so that the metric is rewritten as follows:

$$ds^2 = \tilde{g}_{\mu\nu}dx^\mu dx^\nu \equiv e^{2\phi}(dt - A_i dx^i)^2 - e^{-2\phi}\gamma_{ij}dx^i dx^j \ , \tag{2.18}$$

which defines the KK fields: ϕ, A_i, and $\gamma_{ij} = \delta_{ij} + \sigma_{ij}$, identified as the Newtonian scalar, the gravito-magnetic vector, and the tensor fields, respectively, where $\gamma^{ij}\gamma_{jk} \equiv \delta^i_k$ and $A^i \equiv \gamma^{ij}A_j$. What is left is to derive the Feynman rules and using standard QFT diagrammatic techniques, integrate out the orbital modes (see Fig. 2.2) and obtain the effective action for the composite particle. In doing so, one derives a Hamiltonian containing only physical DOFs an higher order time derivatives which can be eliminated either by replacing the EOMs, obtained via a variation of the action, back to the action or via appropriate field redefinitions. Thus, the *Top-Down* approach to construct the EFT of the composite particle in the potential zone for the conservative sector is concluded at a given order. One will encounter UV divergencies, coming from the point particle approximation, which are regularized in dimensional regularization. After renormalization of the theory through counter-terms, the couplings will depend on a scale μ and obey renormalization group equations whose boundary conditions are obtained via a matching procedure. Furthermore, as we will se below in the radiation zone, one encounters an IR/UV mixing originating from a double counting of the potential (IR) and the radiation (UV) zone and thus is taken care of in the EFT by means of the zero-bin subtraction [116]. The current state of the art in the conservative sector is at the 4PN order [117] while partial results have been obtained at 5PN as well [106, 118]. Spin effects have also been computed at high PN order and the current state of the art has been computed in [1, 119–121].

2.1.5 Radiation zone

In the previous section, we described how one can derive the conservative dynamics by neglecting the radiation modes from the effective action. However, in order to compute physical quantities for the gravitational wave emission we need to consider also the physical on-shell radiation modes. Thus, in this section we will restore the radiation modes which will induce interactions both

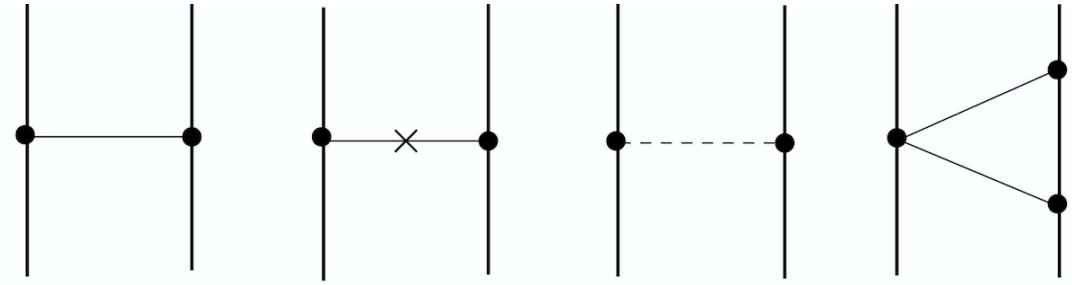

FIGURE 2.2: Sample diagrams needed for the conservative sector.

with the worldlines and the potential graviton modes. We will see several features coming from the subtle interplay between the conservative and the radiation regions such as hereditary effects(tails, memory) and dissipative (radiation back-reaction) which influence the conservative dynamics. Furthermore, the following discussion will be connected with the content of Chapter 4, albeit in a Post-Minkowskian approximation.

The general logic is that we will construct an EFT for a radiating source via a *Bottom-Up* approach and we will match to the EFT of the composite particle that we obtained via explicitly integrating out the potential modes in the previous section, considering also radiation modes. Namely, we consider a general effective action of a single composite object coupled to the gravitational field $\bar{g}_{\mu\nu} \equiv \eta_{\mu\nu} + h_{\mu\nu}$

$$\mathcal{S} = -\frac{1}{16\pi G_N}\int d^4x\sqrt{\bar{g}}\bar{R} + \mathcal{S}_{\rm GF}[h] + \mathcal{S}_{\rm p.p.(comp.)} \ , \tag{2.19}$$

where $\mathcal{S}_{\rm GF}[h]$ is the gauge fixing term for the radiation modes on flat background and $\mathcal{S}_{\rm p.p.(comp.)}$ is the effective worldline action at the radiation scale describing a composite object which, by employing reparametrization and diffeomorphism invariance, takes the following form

$$\begin{aligned}\mathcal{S}_{\rm p.p.(comp.)} = -\int dt\sqrt{\bar{g}}\Big(M(t) + \frac{1}{2}\epsilon_{ijk}L^k(t)(\Omega^{ij}_{\rm LF} + \omega^{ij}_{\mu}u^{\mu}) \\ - \sum_{l=2}^{\infty}\big(\frac{1}{l!}I^L(t)\nabla_{L-2}E_{i_{l-1}i_l} - \frac{2l}{(l+1)!}J^L(t)\nabla_{L-2}B_{i_{l-1}i_l}\big)\Big) \ ,\end{aligned} \tag{2.20}$$

where M is the total mass of the composite object, $\Omega^{ij}_{\rm LF}$ is the locally flat angular velocity and the spin connection, ω^{ij}_{μ}, couple to the total angular momentum,

$L^{ij} = \epsilon_{ijk}L^k$, of the composite object. The $SO(3)$ tensors I^L, J^L, with the superscript L as an abbreviated notation for $i_1...i_l (l \geq 2)$, which are symmetric and trace free (STF) with respect to the spatial Euclidean metric, are commonly referred to as the mass and current multipoles, and are of even and odd parity, respectively. Along the worldline, latin indices are defined with respect to a (comoving) locally-flat vierbein, $e^\mu_A(x)$ with $e^\mu_0 = u^\mu$, such that $\bar{g}^{\mu\nu} = e^\mu_0 e^\nu_0 - \delta^{ij} e^\mu_i e^\nu_j$, and $\nabla \equiv e^\mu_i \nabla_\mu$, where ∇_μ is the covariant derivative with respect to $\bar{g}_{\mu\nu}$.

From the above action we can compute the radiated power, by integrating out $h_{\mu\nu}$ using Feynman's boundary conditions and taking the imaginary part of the final effective action, as a function of the mass and current multipoles. Furthermore, we can directly compute the graviton emission amplitude $\mathcal{A}_h(\omega, \mathbf{k})$, in terms of the multipoles, which is again very useful for the computations of the gravitational waveforms and the radiation back-reaction contribution. To do so, ones needs a matching procedure in order to extract the mass and current multipoles in terms of the short distance physics, that we can in principle derive in a *Top-Down* approach from the potential zone. Essentially, we need to compute the stress-energy pseudotensor, which includes all the potential zone "microphysics" but not non-linear effects in the wave's propagation, these effects will be included when considering the tails and extend the definition of the stress-tensor, which couples to the radiation field to leading order, as

$$\int d^4x \; \mathcal{T}^{\mu\nu}(x) h_{\mu\nu}(x). \tag{2.21}$$

In order to restore the PN power counting and perform the matching, we first expand the radiation mode, assuming that the center of mass of the binary is defined as $x^i_{\rm cm} \equiv \int d^3x \; \mathcal{T}^{00}(t,x) x^i$ and $\dot{x}^i_{\rm cm} = 0$, as

$$h_{\mu\nu}(x) = \sum_{n=0}^{\infty} \frac{1}{n!} x^{i_1} ... x^{i_n} \partial_{i_1} ... \partial_{i_n} h^{\mu\nu}(t,0) \; , \tag{2.22}$$

where each $x^i \partial_i \sim v$, thus restoring the PN power counting. In the end, one can compute the graviton emission amplitude $\mathcal{A}_h(\omega, \mathbf{k}) = -\frac{\epsilon^*_{ij}(\mathbf{k},h)}{2M_{\rm Pl}} \mathcal{T}^{ij}(\omega, \mathbf{k})$ from the *Top-Down* approach in the transverse-traceless gauge, suited for physical modes, and match with the amplitude computed in the *Bottom-Up* $\mathcal{A}_h(\omega, \mathbf{k}) = \frac{\epsilon^*_{ij}(\mathbf{k},h)}{4M_{\rm Pl}} [\omega^2 I^{ij}(\omega) + \frac{4}{3} \omega \mathbf{k}^l \epsilon^{ikl} J^{jk}(\omega) + ...]$. Note that since we do not neglect the radiation modes in the potential zone when integrating out the potential modes H, the radiation modes will induce also worldline couplings that contain both H, h and we will also have purely graviton couplings of the form HHh etc. The

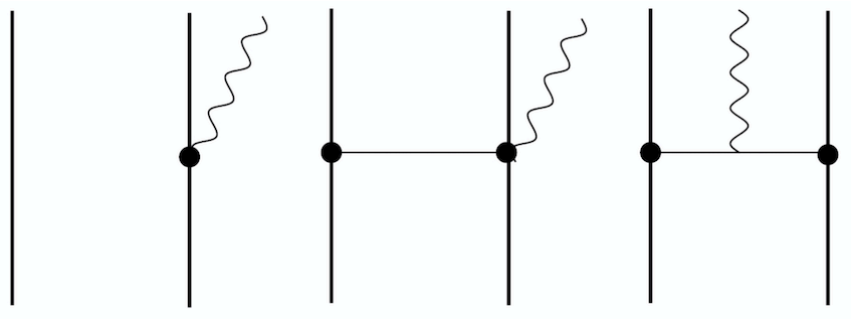

FIGURE 2.3: Sample diagrams needed for the graviton emission.

associated Feynman rules and the relevant diagrams must be included in the computation of the graviton emission amplitude (see Fig. 2.3).

Some last remarks concern several non-trivial effects that one observes when working in the radiation zone. Firstly, there are *Tail effects* appearing. These effects originate from the fact that the gravitational wave interacts with the background geometry which is sourced from the binary system in the radiation zone far away from the binary system. These effects are corrections to the multipole moments and induce both UV and IR singularities. The IR singularities exponentiate to an overall phase and can be absorbed into a time redefinition. The UV singularities are handled by renormalization of the theory, thus the multipole moments exhibit a classical Renormalization Group (RG) flow. Tail effects contribute logarithmic contributions to the multipole moments which are independent of the short distance physics of the composite particle. In addition, one obtains *Memory effects*, which originate from the self interactions of the radiation modes and are treated in a similar manner as the *tails* (See Fig. 2.4).

Finally, a very intriguing effect is the *Radiation Backreaction* effect. As it has already been noted, the radiating binary system is dissipative since there is no incoming radiation at the asymptotic past. Thus, one should impose boundary conditions which are not symmetric in time in order to obtain physical observables such as the gravitational waveform or the radiation reaction effect. Up to now, we have been working with standard Feynman propagators in an "in-out" formalism, for which we assume time symmetry. It has been shown that in order to consistently impose retarded boundary conditions, breaking time symmetry, when integrating out the radiation modes one may use the "in-in" (or Schwinger Keldysh) formalism. Using the "in-in" formalism and computing the real part of the effective action by integrating out the radiation modes,

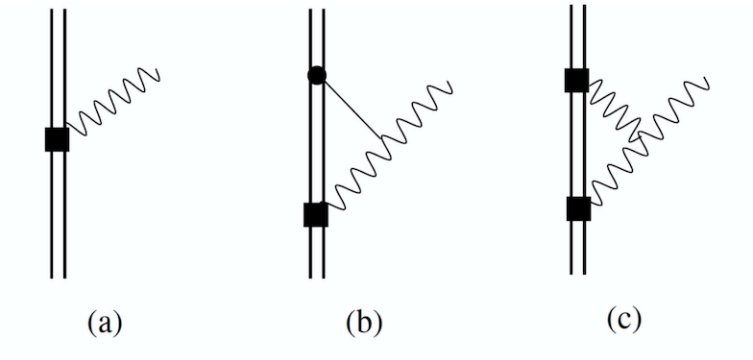

FIGURE 2.4: Sample Feynman diagrams needed for the hereditary effects. (a) depicts the quadrupole radiation in the effective theory of the composite particle derived via matching with the diagrams of Fig.2.3, (b) is the leading *tail* effect (relative 1.5PN correction) and (c) represents the leading *memory* effect (relative 2.5PN correction) related to the *radiation backreaction* in Fig. 2.5 (a).

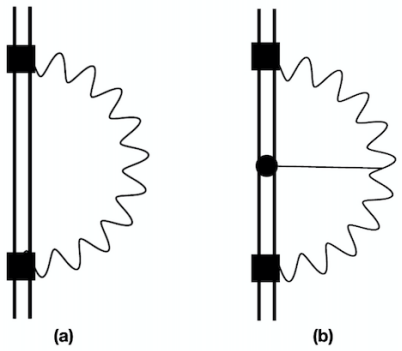

FIGURE 2.5: Sample Feynman diagrams needed for the *radiation backreaction* effects. (a) is the LO effect at 2.5PN related to Fig. 2.4(c) and (b) is the leading non-linear effect entering at 4PN and contributes to the conservative potential.

one gets a contribution to the conservative potential due to radiation reaction. Furthermore, by including hereditary effects, we get UV/IR divergences as we discussed in the previous paragraph. The origin of these divergences comes from a double counting between the potential and the radiation zone. Specifically, it has been shown that the IR divergencies in the potential zone are associated with UV singularities in the radiation zone coming from the point particle approximation of the binary (See Fig. 2.5). Nevertheless, within an EFT formalism the overlapping is avoided by implementing the 'zero-bin subtraction' (see [122]) and we can consistently treat these divergencies and renormalize the theory. Radiative corrections have been tackled in [123]. The current state of the art results including radiation reaction effects were derived in [124–126] for the non-spinning case while for spinning objects in [127, 128].

l \ n	$(\mathrm{N}^{\mathbf{0}})$LO	$\mathrm{N}^{(\mathbf{1})}$LO	$\mathrm{N}^{\mathbf{2}}$LO	$\mathrm{N}^{\mathbf{3}}$LO	$\mathrm{N}^{\mathbf{4}}$LO
$\mathrm{S}^{\mathbf{0}}$	1	0	3	0	25
$\mathrm{S}^{\mathbf{1}}$	2	7	32	174	
$\mathrm{S}^{\mathbf{2}}$	2	2	18	52	
$\mathrm{S}^{\mathbf{3}}$	4	24			
$\mathrm{S}^{\mathbf{4}}$	3	5			

TABLE 2.1: The complete state of the art of PN gravity theory for the orbital dynamics of generic compact binaries. Each PN correction enters at the order $n + l + \mathrm{Parity}(l)/2$, where the parity is 0 or 1 for even or odd l, respectively. We elaborate on the meaning of the numerical entries and the gray area in the text.

2.2 Gravitational S^3 interaction at the NLO PN order

2.2.1 Introduction

In recent years we have made a remarkable progress in pushing the precision frontier for the orbital dynamics of compact binaries, i.e. whose components are generic compact objects, such as black holes or neutron stars. The complete state of the art to date for the orbital dynamics of a generic compact binary is shown in table 2.1.

As a measure for the loop computational scale we show in table 2.1 the number of n-loop graphs that enter at the $\mathrm{N}^n\mathrm{LO}$ in l powers of the spin, i.e. up to the lth spin-induced multipole moment, in the sectors approached to date. The count is based on computations carried out with the effective field theory (EFT) of PN Gravity [34], which use the Kaluza-Klein decomposition of the field from [129], that has considerably facilitated high-precision computations within the EFT approach [106, 117–121, 129–139]. As can be seen the current complete state of the art is at the 4PN order, whereas the next-to-leading order (NLO) cubic-in-spin sector that enters at the 4.5PN order for maximally-rotating objects is evaluated in this work. We note that recently the static piece of the non-rotating sector at the 5PN order was also obtained in [106, 118].

Let us stress that in order to attain a certain level of PN accuracy, the various sectors should be tackled across the diagonals of table 2.1, rather than along the axes, namely progress must be made by going in parallel to higher loops and to higher orders of the spin. In general, the former involves more computational

challenges of loop technology and tackling associated divergences, whereas the latter necessitates an improvement of the fundamental understanding of spin in gravity, and tackling finite-size effects with spin [112]. The latter enter first at the 2PN order [140] from the LO spin-induced quadrupole. Within the EFT approach, whose extension to the spinning case was first approached in [141], finite-size effects include as additional parameters the Wilson coefficients, that correspond, e.g., to the multipole deformations of the object due to its spin, as in [142] for the spin-induced quadrupole.

With a considerable time gap from the LO result, the NLO spin-squared interaction was treated in a series of works [136, 143–146], where in [136] it was derived within the formulation of the EFT for gravitating spinning objects, that provided the leading non-minimal couplings to all orders in spin. The LO cubic- and quartic-in-spin interactions were first tackled in [145, 147] for black holes. In [135], based on the formulation presented in [136], these were derived for generic compact objects, where also the quartic-in-spin interaction was completed. Only specific pieces of the latter were recovered in [148] via S-matrix combined with EFT techniques, whereas [149], which treated only cubic-in-spin effects, also provided the LO effects in the energy flux. Following the work in [135, 136], the case of black holes was then also completed for the LO sectors to all orders in spin [150]. Finally, the NNLO spin-squared interaction was derived in [138]. Notably the latter results together with the complete quartic-in-spin results for generic compact objects in [135], both at the 4PN order, were derived exclusively within the EFT formulation of spinning gravitating objects [136]. Building on the latter, recent works further pushed at the 4.5PN [119] and 5PN [120, 121] orders for maximally-spinning objects.

Recently, there has also been a surge of interest in harnessing modern advances in scattering amplitudes to the problem of a coalescence of a compact binary. Notably, a new implementation for the non-rotating case to the derivation of classical potentials was carried out in [76, 77]. Further, based on a new spinor-helicity formalism introduced in [89] for massive particles of any spin, new approaches to the computation of spin effects of black holes in the classical potential were put forward in [151, 152] and then in [90, 93]. In these approaches classical effects with spin to the lth order correspond to scattering amplitudes involving a quantum spin of $s = l/2$. In particular as of the one-loop level the gravitational Compton amplitude in figure 2.6 is required, where factorization constraints can not uniquely determine the amplitude for $s > 2$ [89]. The gray area in table 2.1 then corresponds in the quantum context to where the gravitational Compton scattering with a spin $s > 1$ is required.

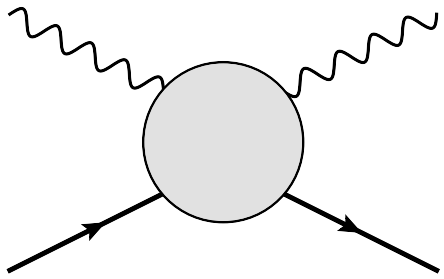

FIGURE 2.6: The gravitational Compton scattering relevant as of the one-loop level. The gravitational Compton amplitude involves two massive spinning particles and two gravitons, where factorization constraints do not uniquely determine the amplitude for $s > 2$ [89].

Notably, the gray area in table 2.1 also corresponds to, as was already pointed out in [136], where we can no longer take the linear momentum p_μ, with which the generic formulation in [136] was made, to be its leading approximation given by $m\frac{u^\mu}{\sqrt{u^2}}$, as in all previously tackled spin sectors, but we have to take into account corrections to the linear momentum from the non-minimal coupling part of the spinning particle action. Can we then get a well-defined result? Can we get an insight from examining this new feature at the classical level on the non-uniqueness of the graviton Compton amplitude with $s > 2$?

This work builds on the formalism of the EFT for gravitating spinning objects introduced in [136] and the implementation on [135], to compute the cubic-in-spin interaction at the NLO, that enters at the 4.5PN order for maximally-rotating compact objects, pushing the current state of the art of PN theory in general and with spins in particular [153], and that is the leading sector in the intriguing gray area of table 2.1. We compute the complete sector, taking into account all interactions that include all possible spin multipoles terms up to and including the octupole. Thus beyond pushing the state of the art in PN theory, there are two conceptual objectives that we get to address in this work: 1. To learn how the spin dependence of the linear momentum affects the results in the interaction; 2. To see whether this new feature is related with the non-uniqueness of the gravitational Compton amplitude of higher-spin states, or get any possible insight on this non-uniqueness.

The section is organized as follows. In section 2.2.2 we go over the formulation from [136], and the necessary ingredients to evaluate the more familiar part of the sector. In section 2.2.3 we present the essential computation, where the linear momentum assumes its leading approximation in terms of the four-velocity, as in all past evaluations of spin sectors. In section 2.2.4 we find the new contributions arising from the spin-dependent correction to the linear

momentum, which matters as of this sector, and gives rise to a new type of worldline-graviton coupling. In section 2.2.5 we assemble the final action of this sector, and finally we conclude in section 2.2.6 with some observations and questions.

2.2.2 The EFT of gravitating spinning objects

Let us consider the ingredients of the theory that are required in order to carry out the evaluation of this sector, that contains spins up to cubic order along with first gravitational nonlinearities. This evaluation will build on the EFT of gravitating spinning objects formulated in [136], and its implementation from LO up to the state of the art at the 4PN order in [135–138,153]. We will also use here the Kaluza-Klein decomposition of the field [129,154], which was adopted in all high-order PN computations both with and without spins for its facilitating virtues [112], and follow conventions consistent with the abovementioned works. Further, we keep similar gauge choices, notational and pictorial conventions as presented in [136].

The effective action we start from is that of a two-particle system [112], with each of the particles described by the effective point-particle action of a spinning particle, that was provided in [136]. This effective action contains a purely gravitational piece, from which the propagators and self-interacting vertices are derived. The Feynman rules for the propagator and the time insertions on the propagators are given, e.g. in eqs. (5)-(10) of [134], and for the cubic gravitational vertices in eqs. (2.10)-(2.13), and (2.15) of [137]. Further, for each of the two particles, the worldline action of a spinning particle is considered from [136], where its non-minimal coupling spin-induced part was constructed to all orders in spin, and then gauge freedom of the rotational DOFs is incorporated into the action.

We recall that this action has the form

$$S_{\rm pp}(\sigma) = \int d\sigma \left[-m\sqrt{u^2} - \frac{1}{2}\hat{S}_{\mu\nu}\hat{\Omega}^{\mu\nu} - \frac{\hat{S}^{\mu\nu}p_\nu}{p^2}\frac{Dp_\mu}{D\sigma} + L_{\rm SI} \right], \tag{2.23}$$

given in terms of the four-velocity u^μ, the linear momentum p_μ, and the rotational DOFs in a generic gauge, denoted with a hat, e.g. $\hat{S}_{\mu\nu}$, and the label "SI" stands for the spin-induced non-minimal coupling part of the action. For the sector evaluated here the latter part will consist of its two leading terms given

by

$$L_{\rm SI} = -\frac{C_{ES^2}}{2m}\frac{E_{\mu\nu}}{\sqrt{u^2}}S^\mu S^\nu - \frac{C_{BS^3}}{6m^2}D_\lambda\frac{B_{\mu\nu}}{\sqrt{u^2}}S^\mu S^\nu S^\lambda, \tag{2.24}$$

in which we use the definite-parity curvature components defined as

$$E_{\mu\nu} \equiv R_{\mu\alpha\nu\beta}u^\alpha u^\beta, \tag{2.25}$$

$$B_{\mu\nu} \equiv \frac{1}{2}\epsilon_{\alpha\beta\gamma\mu}R^{\alpha\beta}{}_{\delta\nu}u^\gamma u^\delta, \tag{2.26}$$

for the electric and magnetic components of even and odd parity, respectively. Notice also that here we need to use the Levi-Civita tensor density in curved spacetime, $\epsilon_{\alpha\beta\gamma\lambda} = \sqrt{-g}\,e_{\alpha\beta\gamma\lambda}$, in which g is the determinant of $g_{\mu\nu}$, and $e_{\alpha\beta\gamma\lambda}$ is the totally antisymmetric Levi-Civita symbol with $e_{0123} = +1$. We note also that we use here a classical version of the Pauli-Lubanski pseudovector, S^μ, as first defined in [135]

$$S_\mu = \frac{1}{2}\epsilon_{\alpha\beta\gamma\mu}S^{\alpha\beta}\frac{p^\gamma}{p}, \tag{2.27}$$

which is with a reverse sign with respect to the definition in [136], that was applied up to the quadratic-in-spin order, where this sign choice does not matter. The spin tensor that is used in eq. (2.27) is related to the spin in the generic gauge $\hat{S}_{\mu\nu}$ via the projection of the latter onto the spatial hypersurface of the rest frame according to eq. (3.29) in [136].

We recall that in eq. (2.23) there is an extra term, which appears in the action from the restoration of gauge freedom of the rotational DOFs. This term, which is essentially the Thomas precession, as discussed in detail in [136] (and recovered recently as "Hilbert space matching" in [92, 93]), contributes to all orders in the spin as of the LO spin-orbit sector, and in particular also to finite-size spin effects, though it does not encode any UV physics, but rather in the context of an effective action, just accounts for the fact that a relativistic gravitating object has an extended measure.

Since we compute here the *complete* NLO cubic-in-spin sector our graphs will contain all multipoles in the presence of spin up to the spin-induced octupole, i.e. also including the mass, spin and spin-induced quadrupole. For this reason we need to use Feynman rules of worldline-graviton coupling to NLO for all of these multipoles, where in this work we need to derive further new rules for the octupole couplings. The Feynman rules required for the mass couplings are given in eqs. (64), (67), (68), (79), (81), (93), (95) of [132]. Next, we

approach the Feynman rules linear in spin, noting that first we have kinematic contributions as noted in eq. (5.28) of [136], that are linear in the spin but have no field coupling, which we will take into account in section 2.2.5. The Feynman rules required for the linear-in-spin couplings are given in eqs. (5.29)-(5.31) of [136], and eqs. (2.31)-(2.34) of [137]. For the spin quadrupole couplings the rules are given in eqs. (2.18)-(2.24) of [138], and for the LO spin octupole couplings they are found in eqs. (2.19),(2.20) of [135].

As we noted in addition to the abovementioned Feynman rules, further rules are required here for the spin-induced octupole worldline-graviton coupling. The two Feynman rules of the scalar and vector components of the KK decomposition, which appeared already at LO in [135] should be extended to a higher PN order, and further we will have new rules that enter for the one-graviton coupling of the tensor component of the KK fields, and a couple of two-graviton couplings, involving again the scalar and the vector components of the KK fields.

The extended rules for the one-graviton couplings are then given as follows:

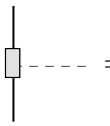

$$= \int dt \left[\frac{C_{\mathrm{BS}^3}}{12m^2} S_i S_j \epsilon_{klm} \Big[A_{k,ijl} \Big(S_m \Big(1 + \frac{1}{2} v^2 \Big) - \frac{1}{2} v^m S_n v^n \Big) + S_m \Big(v^l v^n \big(A_{i,njk} - A_{n,ijk} \big) + v^l \big(\partial_t A_{k,ij} + \partial_t A_{i,jk} \big) + v^i \partial_t A_{k,jl} \Big) \Big] \right], \tag{2.28}$$

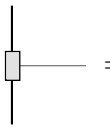

$$= \int dt \left[\frac{C_{\mathrm{BS}^3}}{3m^2} S_i S_j \epsilon_{klm} S_m v^l \Big(\phi_{,ijk} \Big(1 + \frac{v^2}{2} \Big) + v^i \partial_t \phi_{,jk} \Big) \right], \tag{2.29}$$

in which the rectangular boxes represent the spin-induced octupole.

The new Feynman rules required here are given as follows:

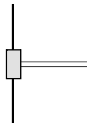

$$= \int dt \left[\frac{C_{\mathrm{BS}^3}}{12m^2} S_i S_j \epsilon_{klm} S_m \partial_i \partial_l \Big(\big(\partial_j \sigma_{kn} - \partial_n \sigma_{jk} \big) v^n - \partial_t \sigma_{jk} \Big) \right], \tag{2.30}$$

for the one-graviton coupling, whereas for the two-graviton couplings we get:

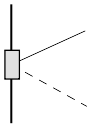

$$= \int dt \left[\frac{C_{\mathrm{BS}^3}}{12m^2} S_i S_j \epsilon_{klm} S_m \Big(6\phi A_{k,ijl} + 9\phi_{,i} A_{k,jl} + 3\phi_{,k} \partial_j \big(A_{i,l} - A_{l,i} \big) + 4\phi_{,ij} A_{k,l} + 4\phi_{,jk} \big(A_{i,l} - A_{l,i} \big) + \delta_{ij} \phi_{,n} A_{l,kn} \Big) \right], \tag{2.31}$$

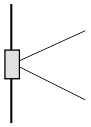

$$= \int dt \left[\frac{C_{\mathrm{BS}^3}}{3m^2} S_i S_j \epsilon_{klm} S_m \Big[v^l \Big(2\phi_{,ijk}\phi + 3\phi_{,ij}\phi_{,k} + 5\phi_{,i}\phi_{,jk} - \delta_{ij}\phi_{,n}\phi_{,kn} \Big) + v^i \phi_{,lj} \phi_{,k} \Big] \right]. \tag{2.32}$$

We note that in these rules the spin is already fixed to the canonical gauge in the local frame, and all indices are Euclidean. Notice the complexity of these couplings with respect to other worldline couplings at the NLO level, and notice also the dominant role that the gravitomagnetic vector plays in the coupling to the odd-parity octupole, similar to the situation in the coupling to the spin dipole. This is the first sector which necessitates to actually take the curved Levi-Civita tensor and the covariant derivative into account.

For this sector there is no need to extend the non-minimal coupling part of the spinning particle action and add higher dimensional operators beyond what was provided in [136], but we need to pay special attention to the new feature that differentiates this specific sector from all the spin sectors which were tackled in the past. In this sector it is no longer sufficient to use the leading approximation for the linear momentum p_μ in terms of the four-velocity u_ν all throughout, rather one has to take into account the subleading term in the linear momentum, which is linear in Riemann and quadratic in the spin, and becomes relevant first once we get to the level that is cubic in the spins and non-linear in gravity, i.e. at this sector, as was already explicitly noted in [136]. We will address in detail the particular contributions coming from this new feature in section 2.2.4 below, after we have done in the following section the essential computation, which requires only the leading approximation to the linear momentum that is independent of spin, similar to what was considered in all past PN computations in spin sectors.

2.2.3 The essential computation

In this section we carry out the perturbative expansion of the effective action in terms of Feynman graphs, and provide the value of each diagram, while using the leading approximation of the linear momentum. At the NLO level, i.e. up to the G^2 order, all of the three relevant topologies are realized with spins, even when the beneficial KK decomposition of the field is used, as discussed in [112, 130, 132, 136]. As shown in figures 2.7-2.9 below (drawn using Jaxodraw [155, 156] based on [157]) there is a total of $49 = 10 + 15 + 24$ graphs making up this part of the sector, distributed among the relevant topologies of one- and two-graviton exchanges and cubic self-interaction, respectively. As shown in table 2.1 about half of the total graphs require a one-loop evaluation (the highest loop in this sector). We note that as we go into the nonlinear part of the sector, the options for the make-up of the interaction become more intricate.

At the one-graviton exchange level we only have two kinds of interaction contributing, similar to the LO in [135], namely either an octupole-monopole or a quadrupole-dipole interaction. As noted in [135] there are nice analogies among these interactions according to the parity of the multipole moments involved. Following these analogies the relevant graphs of one-graviton exchange are easily constructed. Yet, once we proceed to the level nonlinear in the gravitons further types of interactions emerge. In particular, there are also interactions involving various multipoles on two different points of the worldline, which add up to interactions that are cubic in the spin, such as a spin and a spin-induced quadrupole or two spin dipoles, on the same worldline, which can already be seen as of the NLO spin-squared sector [136, 138].

We note that all the graphs in this sector should be included together with their mirror images, i.e. with the worldline labels $1 \leftrightarrow 2$ exchanged. For more specific details on the generation of the Feynman graphs, and their evaluation, including the conventions and notations used here, we refer the reader to [112] and references therein. We note that the generation and the evaluation of the graphs was crosschecked using the publicly-available `EFTofPNG` code [158].

2.2.3.1 One-graviton exchange

As can be seen in figure 2.7 we have 10 graphs of one-graviton exchange in this sector, the majority of which already involve time derivatives to be applied. Consistent with former works by one of the authors we keep all of the higher order time derivative terms that emerge in the evaluations of the graphs, and they will be treated properly via redefinitions of the position and the rotational

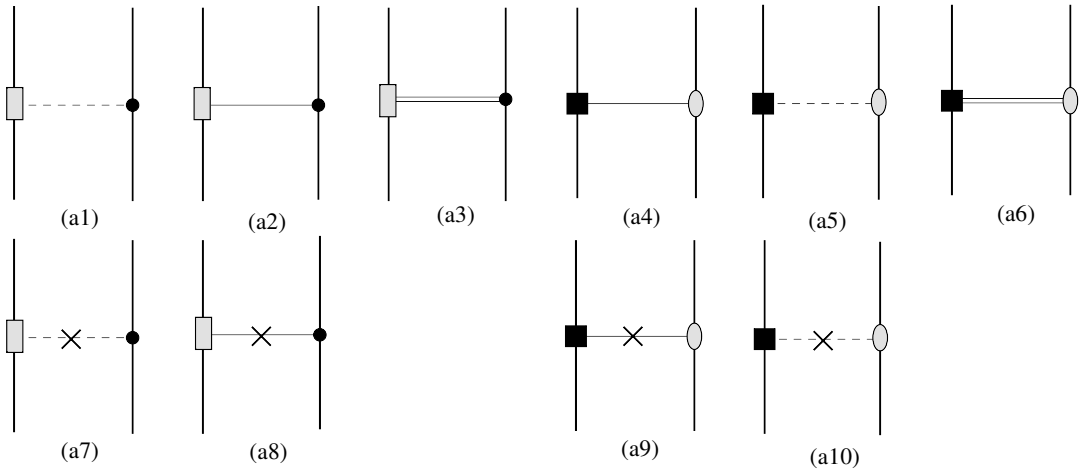

FIGURE 2.7: The Feynman graphs of one-graviton exchange, which contribute to the NLO cubic-in-spin interaction at the 4.5PN order for maximally rotating compact objects. The graphs should be included together with their mirror images, i.e. with the worldline labels $1 \leftrightarrow 2$ exchanged. At the linear level of one-graviton exchange we only have two kinds of interactions contributing, similar to the LO in [135], namely either a quadrupole-dipole or an octupole-monopole interaction. As noted in [135] there are nice analogies among these interactions according to the parity of the multipole moments involved. Following these analogies the relevant graphs here are easily constructed. Notice that we have here the four graphs that appeared at the LO with the quadratic time insertions on the propagators at graphs (a7)-(a10), and a new octupole coupling involving the KK tensor field at graph (a3).

variables as shown in [159]. Notice that we have here the 4 graphs that appeared at the LO with the quadratic time insertions on the propagators at graphs 1(a7)-(a10), and a new octupole coupling involving the KK tensor field at graph 1(a3).

The graphs in figure 2.7 are evaluated as follows:

$$\begin{aligned}
\text{Fig. 2(a1)} &= -C_{1(BS^3)}\frac{G}{r^4}\frac{m_2}{m_1^2}\Big[\vec{S}_1\cdot\vec{v}_1\times\vec{v}_2\big(2\vec{S}_1\cdot\vec{v}_2\ \vec{S}_1\cdot\vec{n}+\vec{v}_2\cdot\vec{n}\big(S_1^2-5\big(S_1\cdot\vec{n}\big)^2\big)\\
&\qquad -\vec{S}_1\cdot\vec{v}_1\ \vec{S}_1\cdot\vec{n}\big)\\
&+\vec{S}_1\cdot\vec{v}_1\times\vec{n}\Big(\big(S_1^2-5\big(\vec{S}_1\cdot\vec{n}\big)^2\big)\vec{v}_1\cdot\vec{v}_2+\vec{S}_1\cdot\vec{v}_2\big(\vec{S}_1\cdot\vec{v}_2-5\vec{S}_1\cdot\vec{n}\ \vec{v}_2\cdot\vec{n}\big)\\
&-\vec{S}_1\cdot\vec{v}_2\big(\vec{S}_1\cdot\vec{v}_1-5\vec{S}_1\cdot\vec{n}\ \vec{v}_1\cdot\vec{n}\big)\Big)+\vec{S}_1\cdot\vec{v}_2\times\vec{n}\Big(\frac{1}{2}S_1^2\big(v_1^2+v_2^2\big)\\
&-\vec{S}_1\cdot\vec{v}_1\big(\vec{S}_1\cdot\vec{v}_2-5\vec{S}_1\cdot\vec{n}\ \vec{v}_2\cdot\vec{n}\big)-\frac{5}{2}\big(\vec{S}_1\cdot\vec{n}\big)^2\big(v_1^2+v_2^2\big)\Big)\\
&-\frac{1}{2}\vec{v}_1\cdot\vec{v}_2\times\vec{n}\ \vec{S}_1\cdot\vec{v}_1\big(S_1^2-5\big(\vec{S}_1\cdot\vec{n}\big)^2\big)\Big]\\
&-\frac{1}{3}C_{1(BS^3)}\frac{G}{r^3}\frac{m_2}{m_1^2}\ \Big[\vec{S}_1\cdot\vec{v}_1\times\vec{a}_2\big(S_1^2-3\big(\vec{S}_1\cdot\vec{n}\big)^2\big)-3\vec{S}_1\cdot\vec{v}_1\times\vec{n}\vec{S}_1\cdot\vec{a}_2\ \vec{S}_1\cdot\vec{n}
\end{aligned} \tag{2.33}$$

$$+3\vec{S}_1\cdot\vec{a}_2\times\vec{n}\vec{S}_1\cdot\vec{v}_1\ \vec{S}_1\cdot\vec{n}\Big], \tag{2.34}$$

$$\begin{aligned}
\text{Fig. 2(a2)} &= \frac{1}{2}C_{1(BS^3)}\frac{G}{r^4}\frac{m_2}{m_1^2}\ \Big[\vec{S}_1\cdot\vec{v}_1\times\vec{n}\Big(S_1^2\big(v_1^2+3v_2^2\big)-2\vec{S}_1\cdot\vec{n}\big(\vec{S}_1\cdot\vec{v}_2-5\ \vec{S}_1\cdot\vec{n}\ \vec{v}_2\cdot\vec{n}\big)\\
&-5(\vec{S}_1\cdot\vec{n})^2\big(v_1^2+3v_2^2\big)\Big)-2\vec{S}_1\cdot\vec{v}_1\times\vec{v}_2\ \vec{S}_1\cdot\vec{v}_1\ \vec{S}_1\cdot\vec{n}\Big],
\end{aligned} \tag{2.35}$$

$$\begin{aligned}
\text{Fig. 2(a3)} &= -C_{1(BS^3)}\frac{G}{r^4}\frac{m_2}{m_1^2}\Big[\big(\vec{S}_1\cdot\vec{v}_1\times\vec{n}\ v_2^2-\vec{S}_1\cdot\vec{v}_2\times\vec{n}\ \vec{v}_1\cdot\vec{v}_2\big)\big(S_1^2-5(\vec{S}_1\cdot\vec{n})^2\big)\Big]\\
&+C_{1(BS^3)}\frac{G}{r^3}\frac{m_2}{m_1^2}\Big[\vec{S}_1\cdot\vec{v}_2\times\vec{n}\big(\vec{S}_1\cdot\vec{v}_2\dot{\vec{S}}_1\cdot\vec{n}+\dot{\vec{S}}_1\cdot\vec{v}_2\vec{S}_1\cdot\vec{n}\big)\\
&+\dot{\vec{S}}_1\cdot\vec{v}_2\times\vec{n}\ \vec{S}_1\cdot\vec{v}_2\ \vec{S}_1\cdot\vec{n}\Big],
\end{aligned} \tag{2.36}$$

$$\begin{aligned}
\text{Fig. 2(a4)} &= \frac{3}{2}C_{1(ES^2)}\frac{G}{r^4}\frac{1}{m_1}\Big[2\vec{S}_1\cdot\vec{S}_2\times\vec{v}_2\Big(\vec{S}_1\cdot\vec{v}_1\ \vec{v}_1\cdot\vec{n}-\vec{S}_1\cdot\vec{n}\big(3v_1^2+v_2^2\big)\ \Big)\\
&+2\vec{S}_2\cdot\vec{v}_1\times\vec{v}_2\Big(2S_1^2\ \vec{v}_1\cdot\vec{n}-\vec{S}_1\cdot\vec{v}_1\ \vec{S}_1\cdot\vec{n}\Big)\\
&-\vec{S}_2\cdot\vec{v}_2\times\vec{n}\Big(S_1^2\big(5v_1^2+v_2^2-10\big(\vec{v}_1\cdot\vec{n}\big)^2\big)-2\vec{S}_1\cdot\vec{v}_1\big(\vec{S}_1\cdot\vec{v}_1-5\vec{S}_1\cdot\vec{n}\ \vec{v}_1\cdot\vec{n}\big)\\
&-5\big(\vec{S}_1\cdot\vec{n}\big)^2\big(3v_1^2+v_2^2\big)\Big)\Big]\\
&+C_{1(ES^2)}\frac{G}{r^3}\frac{1}{m_1}\Big[2\ \vec{S}_1\cdot\vec{S}_2\times\vec{v}_2\ \big(\vec{S}_1\cdot\vec{a}_1+\dot{\vec{S}}_1\cdot\vec{v}_1\big)+2\dot{\vec{S}}_1\cdot\vec{S}_2\times\vec{v}_2\ \vec{S}_1\cdot\vec{v}_1\\
&+4\vec{S}_2\cdot\vec{v}_1\times\vec{v}_2\ \dot{\vec{S}}_1\cdot\vec{S}_1\ +2\vec{S}_2\cdot\vec{v}_2\times\vec{a}_1\ S_1^2\ +\vec{S}_2\cdot\vec{v}_2\times\vec{a}_2\big(S_1^2-3\big(\vec{S}_1\cdot\vec{n}\big)^2\big)\\
&-6\vec{S}_2\cdot\vec{v}_2\times\vec{n}\Big(S_1^2\ \vec{a}_1\cdot\vec{n}-2\dot{\vec{S}}_1\cdot\vec{S}_1\ \vec{v}_1\cdot\vec{n}+\vec{S}_1\cdot\vec{v}_1\ \dot{\vec{S}}_1\cdot\vec{n}+\dot{\vec{S}}_1\cdot\vec{v}_1\ \vec{S}_1\cdot\vec{n}\\
&+\vec{S}_1\cdot\vec{a}_1\ \vec{S}_1\cdot\vec{n}\Big)\Big]\\
&-4C_{1(ES^2)}\frac{G}{r^2}\frac{1}{m_1}\vec{S}_2\cdot\vec{v}_2\times\vec{n}\Big(\dot{S}_1^2+\ddot{\vec{S}}_1\cdot\vec{S}_1\Big),
\end{aligned} \tag{2.37}$$

$$
\begin{aligned}
\text{Fig. 2(a5)} = &-\frac{3}{2}C_{1(ES^2)}\frac{G}{r^4}\frac{1}{m_1}\Big[2\vec{S}_1\cdot\vec{S}_2\times\vec{v}_1\big(\vec{S}_1\cdot\vec{v}_1\ \vec{v}_1\cdot\vec{n}-\vec{S}_1\cdot\vec{n}\,v_1^2\big)\\
&-6\vec{S}_1\cdot\vec{S}_2\times\vec{v}_2\ \vec{S}_1\cdot\vec{n}\ \vec{v}_1\cdot\vec{v}_2+\vec{S}_2\cdot\vec{v}_1\times\vec{v}_2\Big(S_1^2\vec{v}_2\cdot\vec{n}+2\vec{S}_1\cdot\vec{v}_2\ \vec{S}_1\cdot\vec{n}\\
&-5\big(\vec{S}_1\cdot\vec{n}\big)^2\vec{v}_2\cdot\vec{n}\Big)-\vec{S}_2\cdot\vec{v}_1\times\vec{n}\Big(S_1^2\ \big(3v_1^2-10\big(\vec{v}_1\cdot\vec{n}\big)^2\big)-2\big(\vec{S}_1\cdot\vec{v}_1\big)^2\\
&+10\vec{S}_1\cdot\vec{v}_1\ \vec{S}_1\cdot\vec{n}\ \vec{v}_1\cdot\vec{n}-5\big(\vec{S}_1\cdot\vec{n}\big)^2\ \vec{v}_1^2\Big)\\
&-3\vec{S}_2\cdot\vec{v}_2\times\vec{n}\ \Big(S_1^2-5\big(\vec{S}_1\cdot\vec{n}\big)^2\Big)\vec{v}_1\cdot\vec{v}_2\ \Big]\\
&-\frac{1}{2}C_{1(ES^2)}\frac{G}{r^3}\frac{1}{m_1}\Big[\vec{S}_1\cdot\vec{S}_2\times\vec{v}_2\big(4\ \dot{\vec{S}}_1\cdot\vec{v}_2-3\dot{\vec{S}}_1\cdot\vec{n}\ \vec{v}_2\cdot\vec{n}\big)\\
&+\dot{\vec{S}}_1\cdot\vec{S}_2\times\vec{v}_2\big(4\ \vec{S}_1\cdot\vec{v}_2-3\vec{S}_1\cdot\vec{n}\ \vec{v}_2\cdot\vec{n}\big)-3\vec{S}_1\cdot\vec{S}_2\times\vec{n}\Big(\vec{S}_1\cdot\vec{v}_1\ \vec{a}_1\cdot\vec{n}\\
&+\dot{\vec{S}}_1\cdot\vec{v}_1\ \vec{v}_1\cdot\vec{n}+\vec{S}_1\cdot\vec{a}_1\ \vec{v}_1\cdot\vec{n}-2\vec{S}_1\cdot\vec{n}\ \vec{v}_1\cdot\vec{a}_1-\ \dot{\vec{S}}_1\cdot\vec{n}\,v_1^2\Big)\\
&-3\dot{\vec{S}}_1\cdot\vec{S}_2\times\vec{n}\big(\vec{S}_1\cdot\vec{v}_1\ \vec{v}_1\cdot\vec{n}-\vec{S}_1\cdot\vec{n}\,v_1^2\big)\\
&+4\big(\vec{S}_2\cdot\vec{v}_1\times\vec{a}_2+\dot{\vec{S}}_2\cdot\vec{v}_1\times\vec{v}_2\big)\Big(S_1^2-3\big(\vec{S}_1\cdot\vec{n}\big)^2\Big)\\
&-3\vec{S}_2\cdot\vec{v}_1\times\vec{n}\Big(2S_1^2\ \vec{a}_1\cdot\vec{n}+4\dot{\vec{S}}_1\cdot\vec{S}_1\ \vec{v}_1\cdot\vec{n}-\vec{S}_1\cdot\vec{v}_1\ \dot{\vec{S}}_1\cdot\vec{n}-\dot{\vec{S}}_1\cdot\vec{v}_1\ \vec{S}_1\cdot\vec{n}\\
&-\vec{S}_1\cdot\vec{a}_1\ \vec{S}_1\cdot\vec{n}\Big)-3\vec{S}_2\cdot\vec{a}_1\times\vec{n}\big(2S_1^2\ \vec{v}_1\cdot\vec{n}-\vec{S}_1\cdot\vec{v}_1\ \vec{S}_1\cdot\vec{n}\big)\\
&+3\vec{S}_2\cdot\vec{v}_2\times\vec{n}\big(8\dot{\vec{S}}_1\cdot\vec{S}_1\ \vec{v}_2\cdot\vec{n}-3\vec{S}_1\cdot\vec{v}_2\dot{\vec{S}}_1\cdot\vec{n}-3\dot{\vec{S}}_1\cdot\vec{v}_2\ \vec{S}_1\cdot\vec{n}\big)\Big]\\
&+2C_{1(ES^2)}\frac{G}{r^2}\frac{1}{m_1}\Big[\big(\vec{S}_1\cdot\vec{S}_2\times\vec{a}_2+\vec{S}_1\cdot\dot{\vec{S}}_2\times\vec{v}_2\big)\dot{\vec{S}}_1\cdot\vec{n}\\
&+\big(\dot{\vec{S}}_1\cdot\dot{\vec{S}}_2\times\vec{v}_2+\dot{\vec{S}}_1\cdot\vec{S}_2\times\vec{a}_2\big)\vec{S}_1\cdot\vec{n}-2\big(\dot{\vec{S}}_2\cdot\vec{v}_2\times\vec{n}+\vec{S}_2\cdot\vec{a}_2\times\vec{n}\big)\dot{\vec{S}}_1\cdot\vec{S}_1\Big],
\end{aligned}
\tag{2.38}
$$

$$
\begin{aligned}
\text{Fig. 2(a6)} = &-3C_{1(ES^2)}\frac{G}{r^4}\frac{1}{m_1}\Big[2\vec{S}_1\cdot\vec{S}_2\times\vec{v}_1\ \vec{S}_1\cdot\vec{n}\ \vec{v}_1\cdot\vec{v}_2-2\vec{S}_1\cdot\vec{S}_2\times\vec{v}_2\ \vec{S}_1\cdot\vec{n}\,v_1^2\\
&+\Big(\vec{S}_2\cdot\vec{v}_1\times\vec{n}\ \vec{v}_1\cdot\vec{v}_2-\vec{S}_2\cdot\vec{v}_2\times\vec{n}\ v_1^2\Big)\Big(S_1^2-5\big(\vec{S}_1\cdot\vec{n}\big)^2\Big)\Big]\\
&+C_{1(ES^2)}\frac{G}{m_1r^3}\Big[\vec{S}_1\cdot\vec{S}_2\times\vec{v}_1\dot{\vec{S}}_1\cdot\vec{v}_2+\dot{\vec{S}}_1\cdot\vec{S}_2\times\vec{v}_1\vec{S}_1\cdot\vec{v}_2+2\vec{S}_1\cdot\vec{S}_2\times\vec{a}_1\vec{S}_1\cdot\vec{v}_2\\
&-2\vec{S}_1\cdot\vec{S}_2\times\vec{v}_2\big(\dot{\vec{S}}_1\cdot\vec{v}_1+\vec{S}_1\cdot\vec{a}_1\big)-2\dot{\vec{S}}_1\cdot\vec{S}_2\times\vec{v}_2\ \vec{S}_1\cdot\vec{v}_1\\
&+3\vec{S}_1\cdot\vec{S}_2\times\vec{n}\Big(\vec{S}_1\cdot\vec{n}\ \vec{a}_1\cdot\vec{v}_2-\vec{S}_1\cdot\vec{v}_2\ \vec{a}_1\cdot\vec{n}+\dot{\vec{S}}_1\cdot\vec{n}\ \vec{v}_1\cdot\vec{v}_2\Big)\\
&+3\dot{\vec{S}}_1\cdot\vec{S}_2\times\vec{n}\ \vec{S}_1\cdot\vec{n}\ \vec{v}_1\cdot\vec{v}_2-6\vec{S}_2\cdot\vec{v}_1\times\vec{v}_2\dot{\vec{S}}_1\cdot\vec{S}_1+2\vec{S}_2\cdot\vec{v}_2\times\vec{a}_1S_1^2\\
&+3\vec{S}_2\cdot\vec{v}_1\times\vec{n}\Big(2\dot{\vec{S}}_1\cdot\vec{S}_1\ \vec{v}_2\cdot\vec{n}-\vec{S}_1\cdot\vec{v}_2\ \dot{\vec{S}}_1\cdot\vec{n}-\dot{\vec{S}}_1\cdot\vec{v}_2\ \vec{S}_1\cdot\vec{n}\Big)\\
&-3\vec{S}_2\cdot\vec{v}_2\times\vec{n}\Big(S_1^2\ \vec{a}_1\cdot\vec{n}+4\dot{\vec{S}}_1\cdot\vec{S}_1\ \vec{v}_1\cdot\vec{n}\\
&-2\vec{S}_1\cdot\vec{v}_1\ \dot{\vec{S}}_1\cdot\vec{n}-2\dot{\vec{S}}_1\cdot\vec{v}_1\ \vec{S}_1\cdot\vec{n}-2\vec{S}_1\cdot\vec{n}\ \vec{S}_1\cdot\vec{a}_1\Big)\\
&+3\vec{S}_2\cdot\vec{a}_1\times\vec{n}\big(S_1^2\vec{v}_2\cdot\vec{n}-\vec{S}_1\cdot\vec{v}_2\ \vec{S}_1\cdot\vec{n}\big)\Big]\\
&-C_{1(ES^2)}\frac{G}{r^2}\frac{1}{m_1}\Big[\vec{S}_1\cdot\vec{S}_2\times\vec{n}\ \ddot{\vec{S}}_1\cdot\vec{v}_2+2\dot{\vec{S}}_1\cdot\vec{S}_2\times\vec{n}\ \dot{\vec{S}}_1\cdot\vec{v}_2+\ddot{\vec{S}}_1\cdot\vec{S}_2\times\vec{n}\ \vec{S}_1\cdot\vec{v}_2\\
&-2\vec{S}_2\cdot\vec{v}_2\times\vec{n}\ \big(\dot{S}_1^2+\ddot{\vec{S}}_1\cdot\vec{S}_1\big)\Big],
\end{aligned}
\tag{2.39}
$$

$$
\begin{aligned}
\text{Fig. 2(a7)} = \frac{1}{2}C_{1(BS^3)}\frac{G}{r^4}\frac{m_2}{m_1^2}\Big[&\vec{S}_1\cdot\vec{v}_1\times\vec{v}_2\Big(S_1^2\vec{v}_2\cdot\vec{n}+2\vec{S}_1\cdot\vec{v}_2\ \vec{S}_1\cdot\vec{n}-5\big(\vec{S}_1\cdot\vec{n}\big)^2\vec{v}_2\cdot\vec{n}\Big)\\
&-\vec{S}_1\cdot\vec{v}_2\times\vec{n}\Big(S_1^2\big(\vec{v}_1\cdot\vec{v}_2-5\vec{v}_1\cdot\vec{n}\ \vec{v}_2\cdot\vec{n}\big)+2\vec{S}_1\cdot\vec{v}_1\ \vec{S}_1\cdot\vec{v}_2\\
&-10\vec{S}_1\cdot\vec{v}_1\ \vec{S}_1\cdot\vec{n}\ \vec{v}_2\cdot\vec{n}-10\vec{S}_1\cdot\vec{v}_2\ \vec{S}_1\cdot\vec{n}\ \vec{v}_1\cdot\vec{n}\\
&-5\big(\vec{S}_1\cdot\vec{n}\big)^2\big(\vec{v}_1\cdot\vec{v}_2-7\vec{v}_1\cdot\vec{n}\ \vec{v}_2\cdot\vec{n}\big)\Big)\Big]\\
&+\frac{1}{6}C_{1(BS^3)}\frac{G}{r^3}\frac{m_2}{m_1^2}\Big[\vec{S}_1\cdot\vec{v}_1\times\vec{a}_2\big(S_1^2-3\big(\vec{S}_1\cdot\vec{n}\big)^2\big)\\
&-6\vec{S}_1\cdot\vec{v}_2\times\vec{n}\big(\dot{\vec{S}}_1\cdot\vec{S}_1\vec{v}_2\cdot\vec{n}+\dot{\vec{S}}_1\cdot\vec{v}_2\vec{S}_1\cdot\vec{n}+\vec{S}_1\cdot\vec{v}_2\dot{\vec{S}}_1\cdot\vec{n}-5\dot{\vec{S}}_1\cdot\vec{n}\ \vec{S}_1\cdot\vec{n}\ \vec{v}_2\cdot\vec{n}\big)\\
&+3\vec{S}_1\cdot\vec{a}_2\times\vec{n}\big(S_1^2\vec{v}_1\cdot\vec{n}+2\vec{S}_1\cdot\vec{v}_1\ \vec{S}_1\cdot\vec{n}-5\big(\vec{S}_1\cdot\vec{n}\big)^2\vec{v}_1\cdot\vec{n}\big)\\
&-3\dot{\vec{S}}_1\cdot\vec{v}_2\times\vec{n}\big(S_1^2\vec{v}_2\cdot\vec{n}+2\vec{S}_1\cdot\vec{v}_2\ \vec{S}_1\cdot\vec{n}-5\big(\vec{S}_1\cdot\vec{n}\big)^2\vec{v}_2\cdot\vec{n}\big)\Big]\\
&-\frac{1}{6}C_{1(BS^3)}\frac{G}{r^2}\frac{m_2}{m_1^2}\Big[2\vec{S}_1\cdot\vec{a}_2\times\vec{n}\big(\dot{\vec{S}}_1\cdot\vec{S}_1-3\dot{\vec{S}}_1\cdot\vec{n}\ \vec{S}_1\cdot\vec{n}\big)\\
&+\dot{\vec{S}}_1\cdot\vec{a}_2\times\vec{n}\big(S_1^2-3(\vec{S}_1\cdot\vec{n})^2\big)\Big],
\end{aligned}
\tag{2.40}
$$

$$
\begin{aligned}
\text{Fig. 2(a8)} = \frac{1}{2}C_{1(BS^3)}\frac{G}{r^4}\frac{m_2}{m_1^2}\Big[&\vec{S}_1\cdot\vec{v}_1\times\vec{v}_2\Big(S_1^2\vec{v}_1\cdot\vec{n}+2\vec{S}_1\cdot\vec{v}_1\ \vec{S}_1\cdot\vec{n}\ -5(\vec{S}_1\cdot\vec{n})^2\vec{v}_1\cdot\vec{n}\Big)\\
&+\vec{S}_1\cdot\vec{v}_1\times\vec{n}\Big(S_1^2\big(\vec{v}_1\cdot\vec{v}_2-5\ \vec{v}_1\cdot\vec{n}\ \vec{v}_2\cdot\vec{n}\big)+2\vec{S}_1\cdot\vec{v}_1\ \vec{S}_1\cdot\vec{v}_2\\
&-10\vec{S}_1\cdot\vec{v}_1\ \vec{S}_1\cdot\vec{n}\ \vec{v}_2\cdot\vec{n}-10\vec{S}_1\cdot\vec{v}_2\ \vec{S}_1\cdot\vec{n}\ \vec{v}_1\cdot\vec{n}\\
&-5(\vec{S}_1\cdot\vec{n})^2\big(\vec{v}_1\cdot\vec{v}_2-7\vec{v}_1\cdot\vec{n}\ \vec{v}_2\cdot\vec{n}\big)\Big)\Big]\\
&-\frac{1}{6}C_{1(BS^3)}\frac{G}{r^3}\frac{m_2}{m_1^2}\Big[2\vec{S}_1\cdot\vec{v}_1\times\vec{v}_2\big(\dot{\vec{S}}_1\cdot\vec{S}_1-3\dot{\vec{S}}_1\cdot\vec{n}\ \vec{S}_1\cdot\vec{n}\big)\\
&-\big(\vec{S}_1\cdot\vec{v}_2\times\vec{a}_1-\dot{\vec{S}}_1\cdot\vec{v}_1\times\vec{v}_2\big)\big(S_1^2-3\big(\vec{S}_1\cdot\vec{n}\big)^2\big)-6\vec{S}_1\cdot\vec{v}_1\times\vec{n}\big(\dot{\vec{S}}_1\cdot\vec{S}_1\ \vec{v}_2\cdot\vec{n}\\
&+\dot{\vec{S}}_1\cdot\vec{v}_2\ \vec{S}_1\cdot\vec{n}+\vec{S}_1\cdot\vec{v}_2\ \dot{\vec{S}}_1\cdot\vec{n}-5\dot{\vec{S}}_1\cdot\vec{n}\ \vec{S}_1\cdot\vec{n}\ \vec{v}_2\cdot\vec{n}\big)\\
&-3\big(\vec{S}_1\cdot\vec{a}_1\times\vec{n}+\dot{\vec{S}}_1\cdot\vec{v}_1\times\vec{n}\big)\big(S_1^2\ \vec{v}_2\cdot\vec{n}+2\vec{S}_1\cdot\vec{v}_2\ \vec{S}_1\cdot\vec{n}-5(\vec{S}_1\cdot\vec{n})^2\vec{v}_2\cdot\vec{n}\big)\Big],
\end{aligned}
\tag{2.41}
$$

$$
\begin{aligned}
\text{Fig. 2(a9)} = &-\frac{3}{2}C_{1(ES^2)}\frac{G}{r^4}\frac{1}{m_1}\Big[2\vec{S}_1\cdot\vec{S}_2\times\vec{v}_2\Big(\vec{S}_1\cdot\vec{v}_1\ \vec{v}_2\cdot\vec{n}\ +\vec{S}_1\cdot\vec{v}_2\ \vec{v}_1\cdot\vec{n}\\
&+\vec{S}_1\cdot\vec{n}\ \vec{v}_1\cdot\vec{v}_2\ -5\vec{S}_1\cdot\vec{n}\ \vec{v}_1\cdot\vec{n}\ \vec{v}_2\cdot\vec{n}\ \Big)-\vec{S}_2\cdot\vec{v}_1\times\vec{v}_2\Big(S_1^2\vec{v}_2\cdot\vec{n}+2\vec{S}_1\cdot\vec{v}_2\ \vec{S}_1\cdot\vec{n}\\
&-5\big(\vec{S}_1\cdot\vec{n}\big)^2\vec{v}_2\cdot\vec{n}\Big)-\vec{S}_2\cdot\vec{v}_2\times\vec{n}\ \Big(S_1^2\big(\vec{v}_1\cdot\vec{v}_2\ -5\ \vec{v}_1\cdot\vec{n}\ \vec{v}_2\cdot\vec{n}\big)-2\vec{S}_1\cdot\vec{v}_1\ \vec{S}_1\cdot\vec{v}_2\\
&+10\vec{S}_1\cdot\vec{v}_1\ \vec{S}_1\cdot\vec{n}\ \vec{v}_2\cdot\vec{n}+10\vec{S}_1\cdot\vec{v}_2\ \vec{S}_1\cdot\vec{n}\ \vec{v}_1\cdot\vec{n}\Big)\\
&+5\big(\vec{S}_1\cdot\vec{n}\big)^2\big(\vec{v}_1\cdot\vec{v}_2\ -7\ \vec{v}_1\cdot\vec{n}\ \vec{v}_2\cdot\vec{n}\big)\Big)\Big]\\
&+\frac{1}{2}C_{1(ES^2)}\frac{G}{r^3}\frac{1}{m_1}\Big[2\vec{S}_1\cdot\vec{S}_2\times\vec{v}_2\big(\dot{\vec{S}}_1\cdot\vec{v}_2-3\dot{\vec{S}}_1\cdot\vec{n}\ \vec{v}_2\cdot\vec{n}\big)\\
&-2\Big(\vec{S}_1\cdot\vec{S}_2\times\vec{a}_2+\vec{S}_1\cdot\dot{\vec{S}}_2\times\vec{v}_2\Big)\Big(\vec{S}_1\cdot\vec{v}_1-3\ \vec{S}_1\cdot\vec{n}\ \vec{v}_1\cdot\vec{n}\Big)\\
&+2\dot{\vec{S}}_1\cdot\vec{S}_2\times\vec{v}_2\big(\vec{S}_1\cdot\vec{v}_2-3\vec{S}_1\cdot\vec{n}\ \vec{v}_2\cdot\vec{n}\big)\\
&-\Big(\vec{S}_2\cdot\vec{v}_1\times\vec{a}_2+\dot{\vec{S}}_2\cdot\vec{v}_1\times\vec{v}_2\Big)\Big(S_1^2+3\big(\vec{S}_1\cdot\vec{n}\big)^2\Big)+6\vec{S}_2\cdot\vec{v}_2\times\vec{n}\Big(\dot{\vec{S}}_1\cdot\vec{S}_1\ \vec{v}_2\cdot\vec{n}\\
&-\dot{\vec{S}}_1\cdot\vec{v}_2\ \vec{S}_1\cdot\vec{n}-\vec{S}_1\cdot\vec{v}_2\ \dot{\vec{S}}_1\cdot\vec{n}+5\dot{\vec{S}}_1\cdot\vec{n}\ \vec{S}_1\cdot\vec{n}\ \vec{v}_2\cdot\vec{n}\Big)\\
&-3\Big(\dot{\vec{S}}_2\cdot\vec{v}_2\times\vec{n}+\vec{S}_2\cdot\vec{a}_2\times\vec{n}\Big)\Big(S_1^2\ \vec{v}_1\cdot\vec{n}-2\vec{S}_1\cdot\vec{v}_1\ \vec{S}_1\cdot\vec{n}+5\big(\vec{S}_1\cdot\vec{n}\big)^2\ \vec{v}_1\cdot\vec{n}\Big)\Big]\\
&-C_{1(ES^2)}\frac{G}{r^2}\frac{1}{m_1}\Big[\vec{S}_1\cdot\vec{S}_2\times\vec{a}_2\ \dot{\vec{S}}_1\cdot\vec{n}+\vec{S}_1\cdot\dot{\vec{S}}_2\times\vec{v}_2\ \dot{\vec{S}}_1\cdot\vec{n}+\dot{\vec{S}}_1\cdot\vec{S}_2\times\vec{a}_2\ \vec{S}_1\cdot\vec{n}\\
&+\dot{\vec{S}}_1\cdot\dot{\vec{S}}_2\times\vec{v}_2\ \vec{S}_1\cdot\vec{n}-\Big(\dot{\vec{S}}_2\cdot\vec{v}_2\times\vec{n}+\vec{S}_2\cdot\vec{a}_2\times\vec{n}\Big)\Big(\dot{\vec{S}}_1\cdot\vec{S}_1+3\dot{\vec{S}}_1\cdot\vec{n}\ \vec{S}_1\cdot\vec{n}\Big)\Big],
\end{aligned}
\tag{2.42}
$$

$$
\begin{aligned}
\text{Fig. 2(a10)} = \frac{3}{2}C_{1(ES^2)}\frac{G}{r^4}\frac{1}{m_1}\Big[&2\vec{S}_1\cdot\vec{S}_2\times\vec{v}_1\Big(\vec{S}_1\cdot\vec{v}_1\ \vec{v}_2\cdot\vec{n}+\vec{S}_1\cdot\vec{v}_2\ \vec{v}_1\cdot\vec{n}+\vec{S}_1\cdot\vec{n}\vec{v}_1\cdot\vec{v}_2\\
&-5\vec{S}_1\cdot\vec{n}\ \vec{v}_1\cdot\vec{n}\ \vec{v}_2\cdot\vec{n}\Big)-\vec{S}_2\cdot\vec{v}_1\times\vec{v}_2\Big(S_1^2\vec{v}_1\cdot\vec{n}-2\vec{S}_1\cdot\vec{v}_1\ \vec{S}_1\cdot\vec{n}\\
&+5\big(\vec{S}_1\cdot\vec{n}\big)^2\vec{v}_1\cdot\vec{n}\Big)-\vec{S}_2\cdot\vec{v}_1\times\vec{n}\Big(S_1^2\big(\vec{v}_1\cdot\vec{v}_2-5\ \vec{v}_1\cdot\vec{n}\ \vec{v}_2\cdot\vec{n}\big)\\
&-2\vec{S}_1\cdot\vec{v}_1\ \vec{S}_1\cdot\vec{v}_2+10\vec{S}_1\cdot\vec{v}_1\ \vec{S}_1\cdot\vec{n}\vec{v}_2\cdot\vec{n}+10\vec{S}_1\cdot\vec{v}_2\ \vec{S}_1\cdot\vec{n}\vec{v}_1\cdot\vec{n}\\
&+5\big(\vec{S}_1\cdot\vec{n}\big)^2\big(\vec{v}_1\cdot\vec{v}_2-7\vec{v}_1\cdot\vec{n}\ \vec{v}_2\cdot\vec{n}\big)\Big)\Big]\\
&-\frac{1}{2}C_{1(ES^2)}\frac{G}{r^3}\frac{1}{m_1}\Big[\vec{S}_1\cdot\vec{S}_2\times\vec{v}_1\big(\dot{\vec{S}}_1\cdot\vec{v}_2-3\dot{\vec{S}}_1\cdot\vec{n}\ \vec{v}_2\cdot\vec{n}\big)\\
&+2\vec{S}_1\cdot\vec{S}_2\times\vec{a}_1\big(\vec{S}_1\cdot\vec{v}_2-3\vec{S}_1\cdot\vec{n}\ \vec{v}_2\cdot\vec{n}\big)+\dot{\vec{S}}_1\cdot\vec{S}_2\times\vec{v}_1\big(\vec{S}_1\cdot\vec{v}_2-3\vec{S}_1\cdot\vec{n}\ \vec{v}_2\cdot\vec{n}\big)\\
&-2\vec{S}_1\cdot\dot{\vec{S}}_2\times\vec{v}_1\Big(\vec{S}_1\cdot\vec{v}_1-3\vec{S}_1\cdot\vec{n}\ \vec{v}_1\cdot\vec{n}\Big)-\vec{S}_1\cdot\vec{S}_2\times\vec{v}_2\big(\dot{\vec{S}}_1\cdot\vec{v}_1-3\dot{\vec{S}}_1\cdot\vec{n}\ \vec{v}_1\cdot\vec{n}\big)\\
&-\dot{\vec{S}}_1\cdot\vec{S}_2\times\vec{v}_2\Big(\vec{S}_1\cdot\vec{v}_1-3\vec{S}_1\cdot\vec{n}\ \vec{v}_1\cdot\vec{n}\Big)+3\vec{S}_1\cdot\vec{S}_2\times\vec{n}\Big(\dot{\vec{S}}_1\cdot\vec{v}_1\ \vec{v}_2\cdot\vec{n}\\
&+\dot{\vec{S}}_1\cdot\vec{v}_2\ \vec{v}_1\cdot\vec{n}+\dot{\vec{S}}_1\cdot\vec{n}\ \vec{v}_1\cdot\vec{v}_2-5\dot{\vec{S}}_1\cdot\vec{n}\ \vec{v}_1\cdot\vec{n}\ \vec{v}_2\cdot\vec{n}\Big)\\
&+3\dot{\vec{S}}_1\cdot\vec{S}_2\times\vec{n}\Big(\vec{S}_1\cdot\vec{v}_1\ \vec{v}_2\cdot\vec{n}+\vec{S}_1\cdot\vec{v}_2\ \vec{v}_1\cdot\vec{n}+\vec{S}_1\cdot\vec{n}\ \vec{v}_1\cdot\vec{v}_2\\
&-5\vec{S}_1\cdot\vec{n}\ \vec{v}_1\cdot\vec{n}\ \vec{v}_2\cdot\vec{n}\Big)-2\vec{S}_2\cdot\vec{v}_1\times\vec{v}_2\big(\dot{\vec{S}}_1\cdot\vec{S}_1+3\dot{\vec{S}}_1\cdot\vec{n}\ \vec{S}_1\cdot\vec{n}\big)\\
&-\vec{S}_2\cdot\vec{a}_1\times\vec{v}_2\Big(S_1^2+3\big(\vec{S}_1\cdot\vec{n}\big)^2\Big)+6\vec{S}_2\cdot\vec{v}_1\times\vec{n}\Big(\dot{\vec{S}}_1\cdot\vec{S}_1\ \vec{v}_2\cdot\vec{n}-\vec{S}_1\cdot\vec{v}_2\dot{\vec{S}}_1\cdot\vec{n}\\
&-\dot{\vec{S}}_1\cdot\vec{v}_2\ \vec{S}_1\cdot\vec{n}+5\dot{\vec{S}}_1\cdot\vec{n}\ \vec{S}_1\cdot\vec{n}\ \vec{v}_2\cdot\vec{n}\Big)+3\vec{S}_2\cdot\vec{a}_1\times\vec{n}\Big(S_1^2\vec{v}_2\cdot\vec{n}-2\vec{S}_1\cdot\vec{v}_2\ \vec{S}_1\cdot\vec{n}\\
&+5\big(\vec{S}_1\cdot\vec{n}\big)^2\vec{v}_2\cdot\vec{n}\Big)-3\dot{\vec{S}}_2\cdot\vec{v}_1\times\vec{n}\big(S_1^2\ \vec{v}_1\cdot\vec{n}-2\vec{S}_1\cdot\vec{v}_1\ \vec{S}_1\cdot\vec{n}+5(\vec{S}_1\cdot\vec{n})^2\vec{v}_1\cdot\vec{n}\big)\Big]\\
&+\frac{1}{2}C_{1(ES^2)}\frac{G}{r^2}\frac{1}{m_1}\Big[\vec{S}_1\cdot\dot{\vec{S}}_2\times\vec{v}_1\ \dot{\vec{S}}_1\cdot\vec{n}+\dot{\vec{S}}_1\cdot\dot{\vec{S}}_2\times\vec{v}_1\ \vec{S}_1\cdot\vec{n}\\
&+\vec{S}_1\cdot\vec{S}_2\times\vec{v}_2\ \ddot{\vec{S}}_1\cdot\vec{n}+2\dot{\vec{S}}_1\cdot\vec{S}_2\times\vec{v}_2\ \dot{\vec{S}}_1\cdot\vec{n}+\ddot{\vec{S}}_1\cdot\vec{S}_2\times\vec{v}_2\ \vec{S}_1\cdot\vec{n}\\
&+\vec{S}_1\cdot\vec{S}_2\times\vec{n}\big(\ddot{\vec{S}}_1\cdot\vec{v}_2-3\ddot{\vec{S}}_1\cdot\vec{n}\ \vec{v}_2\cdot\vec{n}\big)-\vec{S}_1\cdot\dot{\vec{S}}_2\times\vec{n}\Big(\dot{\vec{S}}_1\cdot\vec{v}_1-3\dot{\vec{S}}_1\cdot\vec{n}\ \vec{v}_1\cdot\vec{n}\Big)\\
&+2\dot{\vec{S}}_1\cdot\vec{S}_2\times\vec{n}\big(\dot{\vec{S}}_1\cdot\vec{v}_2-3\dot{\vec{S}}_1\cdot\vec{n}\ \vec{v}_2\cdot\vec{n}\big)-\dot{\vec{S}}_1\cdot\dot{\vec{S}}_2\times\vec{n}\Big(\vec{S}_1\cdot\vec{v}_1-3\vec{S}_1\cdot\vec{n}\ \vec{v}_1\cdot\vec{n}\Big)\\
&+\ddot{\vec{S}}_1\cdot\vec{S}_2\times\vec{n}\big(\vec{S}_1\cdot\vec{v}_2-3\vec{S}_1\cdot\vec{n}\ \vec{v}_2\cdot\vec{n}\big)+2\vec{S}_1\cdot\dot{\vec{S}}_2\times\vec{a}_1\ \vec{S}_1\cdot\vec{n}\\
&-2\ \dot{\vec{S}}_2\cdot\vec{v}_1\times\vec{n}\Big(\dot{\vec{S}}_1\cdot\vec{S}_1+3\dot{\vec{S}}_1\cdot\vec{n}\ \vec{S}_1\cdot\vec{n}\Big)-\dot{\vec{S}}_2\cdot\vec{a}_1\times\vec{n}\Big(S_1^2+3\big(\vec{S}_1\cdot\vec{n}\big)^2\Big)\Big]\\
&-\frac{1}{2}C_{1(ES^2)}\frac{G}{r}\frac{1}{m_1}\Big[\vec{S}_1\cdot\dot{\vec{S}}_2\times\vec{n}\ \ddot{\vec{S}}_1\cdot\vec{n}+2\dot{\vec{S}}_1\cdot\dot{\vec{S}}_2\times\vec{n}\ \dot{\vec{S}}_1\cdot\vec{n}+\ddot{\vec{S}}_1\cdot\dot{\vec{S}}_2\times\vec{n}\ \vec{S}_1\cdot\vec{n}\Big].
\end{aligned}
\tag{2.43}
$$

Note that almost all these graphs contain higher order time derivatives terms, notably second order time derivatives, where graph 1(a10) even contains third order ones. Notice also that the value of graph 1(a5) will have to be supplemented with a piece that contains time derivatives of the spin, that

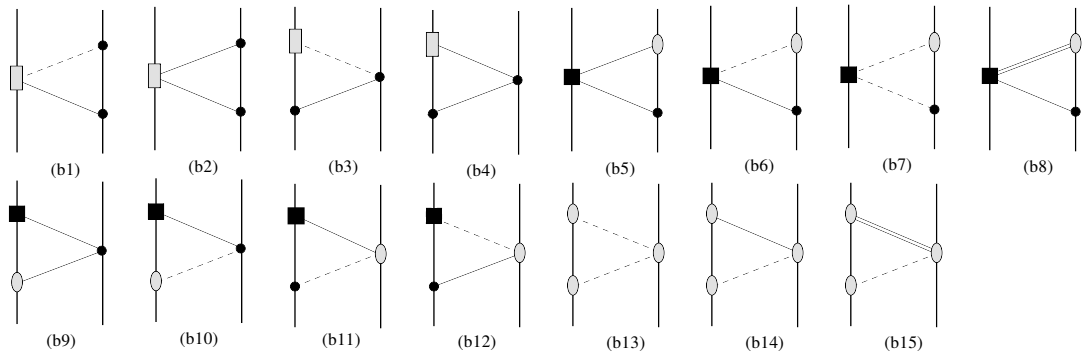

FIGURE 2.8: The Feynman graphs of two-graviton exchange, which contribute to the NLO cubic-in-spin interaction at the 4.5PN order for maximally-rotating compact objects. The graphs should be included together with their mirror images, i.e. with the worldline labels $1 \leftrightarrow 2$ exchanged. These graphs include all relevant interactions among the spin-induced quadrupole, octupole, and the mass and spin, in particular here at the nonlinear level there are also interactions involving the various multipoles on two different points of the worldline, which add up to interactions that are cubic in the spin, such as a spin dipole and a spin-induced quadrupole or two spin dipoles, on the same worldline, which can already be seen as of the NLO spin-squared sector [136, 138]. Consequently notice that there are nonlinearities originating from gravitons sourced strictly from minimal coupling to the worldline as shown in graphs (b13)-(b15). We also have here two new two-graviton octupole couplings in graphs (b1), (b2).

appeared already in graph 2(a) of the LO in [135], but eventually did not contribute at the LO. At this order, as we will see here in section 2.2.5 these terms actually contribute.

2.2.3.2 Two-graviton exchange

As can be seen in figure 2.8 we have 15 graphs of two-graviton exchange in this sector. Here the majority of the graphs do not involve time derivatives. We have here two new two-graviton octupole couplings in graphs 1(b1), 1(b2), and on the other hand we have here nonlinearities originating from gravitons sourced strictly from minimal coupling to the worldline as in graphs 1(b13)-1(b15).

The graphs in figure 2.8 are evaluated as follows:

$$\text{Fig. 3(b1)} = C_{1(BS^3)}\frac{G^2}{r^5}\frac{m_2^2}{m_1^2}\,\vec{S}_1\cdot\vec{v}_2\times\vec{n}\,\Big[9S_1^2-50(\vec{S}_1\cdot\vec{n})^2\Big], \tag{2.44}$$

$$\text{Fig. 3(b2)} = -\frac{1}{3}C_{1(BS^3)}\frac{G^2}{r^5}\frac{m_2^2}{m_1^2}\,\vec{S}_1\cdot\vec{v}_1\times\vec{n}\,\Big[11S_1^2-54(\vec{S}_1\cdot\vec{n})^2\Big], \tag{2.45}$$

$$\text{Fig. 3(b3)} = C_{1(BS^3)}\frac{G^2}{r^5}\frac{m_2}{m_1}\,\vec{S}_1\cdot\vec{v}_2\times\vec{n}\,\Big[S_1^2-5(\vec{S}_1\cdot\vec{n})^2\Big], \tag{2.46}$$

$$\text{Fig. 3(b4)} = -C_{1(BS^3)}\frac{G^2}{r^5}\frac{m_2}{m_1}\,\vec{S}_1\cdot\vec{v}_1\times\vec{n}\,\Big[S_1^2-5(\vec{S}_1\cdot\vec{n})^2\Big], \tag{2.47}$$

$$\text{Fig. 3(b5)} = 8C_{1(ES^2)}\frac{G^2}{r^5}\frac{m_2}{m_1}\,\Big[3\,\vec{S}_1\cdot\vec{S}_2\times\vec{v}_2\,\vec{S}_1\cdot\vec{n}+\vec{S}_2\cdot\vec{v}_2\times\vec{n}\,\Big[2S_1^2-9(\vec{S}_1\cdot\vec{n})^2\Big]\Big], \tag{2.48}$$

$$\begin{aligned}\text{Fig. 3(b6)} = {}& C_{1(ES^2)}\frac{G^2}{r^5}\frac{m_2}{m_1}\Big[-23\vec{S}_1\cdot\vec{S}_2\times\vec{v}_1\,\vec{S}_1\cdot\vec{n}+13\vec{S}_1\cdot\vec{S}_2\times\vec{v}_2\,\vec{S}_1\cdot\vec{n}\\ &-\vec{S}_2\cdot\vec{v}_1\times\vec{n}\big(31S_1^2-66\big(\vec{S}_1\cdot\vec{n}\big)^2\big)-\vec{S}_1\cdot\vec{S}_2\times\vec{n}\,\Big(10\vec{S}_1\cdot\vec{v}_1-51\vec{S}_1\cdot\vec{n}\,\vec{v}_1\cdot\vec{n}\Big)\\ &+\vec{S}_1\cdot\vec{S}_2\times\vec{n}\,\Big(11\vec{S}_1\cdot\vec{v}_2-54\vec{S}_1\cdot\vec{n}\,\vec{v}_2\cdot\vec{n}\Big)\Big]\\ &-13C_{1(ES^2)}\frac{G^2}{r^4}\frac{m_2}{m_1}\,\Big[\vec{S}_1\cdot\dot{\vec{S}}_2\times\vec{n}\;\vec{S}_1\cdot\vec{n}\Big],\end{aligned} \tag{2.49}$$

$$\begin{aligned}\text{Fig. 3(b7)} = {}& 2C_{1(ES^2)}\frac{G^2}{r^5}\frac{m_2}{m_1}\Big[2\,\vec{S}_1\cdot\vec{S}_2\times\vec{v}_2\,\vec{S}_1\cdot\vec{n}+\vec{S}_1\cdot\vec{S}_2\times\vec{n}\,\Big(\vec{S}_1\cdot\vec{v}_2-3\vec{S}_1\cdot\vec{n}\,\vec{v}_2\cdot\vec{n}\Big)\\ &+\vec{S}_2\cdot\vec{v}_2\times\vec{n}\,\Big(2S_1^2-3(\vec{S}_1\cdot\vec{n})^2\Big)\Big],\end{aligned} \tag{2.50}$$

$$\begin{aligned}\text{Fig. 3(b8)} = {}& -C_{1(ES^2)}\frac{G^2}{r^5}\frac{m_2}{m_1}\Big[2\,\vec{S}_1\cdot\vec{S}_2\times\vec{v}_2\,\vec{S}_1\cdot\vec{n}+3\vec{S}_1\cdot\vec{S}_2\times\vec{n}\,\Big(\vec{S}_1\cdot\vec{v}_2-2\vec{S}_1\cdot\vec{n}\,\vec{v}_2\cdot\vec{n}\Big)\\ &+\vec{S}_2\cdot\vec{v}_2\times\vec{n}\,\Big(5S_1^2-12(\vec{S}_1\cdot\vec{n})^2\Big)\Big],\end{aligned} \tag{2.51}$$

$$\text{Fig. 3(b9)} = -C_{1(ES^2)}\frac{G^2}{r^5}\frac{m_2}{m_1}\,\vec{S}_1\cdot\vec{v}_1\times\vec{n}\,\Big[S_1^2-3(\vec{S}_1\cdot\vec{n})^2\Big], \tag{2.52}$$

$$\text{Fig. 3(b10)} = C_{1(ES^2)}\frac{G^2}{r^5}\frac{m_2}{m_1}\,\vec{S}_1\cdot\vec{v}_2\times\vec{n}\,\Big[S_1^2-3(\vec{S}_1\cdot\vec{n})^2\Big], \tag{2.53}$$

$$\text{Fig. 3(b11)} = -4C_{1(ES^2)}\frac{G^2}{r^5}\,\vec{S}_2\cdot\vec{v}_1\times\vec{n}\,\Big[S_1^2-3(\vec{S}_1\cdot\vec{n})^2\Big], \tag{2.54}$$

$$\begin{aligned}\text{Fig. 3(b12)} = {}& -12C_{1(ES^2)}\frac{G^2}{r^5}\Big[2\,\vec{S}_1\cdot\vec{S}_2\times\vec{v}_1\,\vec{S}_1\cdot\vec{n}+\vec{S}_2\cdot\vec{v}_1\times\vec{n}\,\Big(S_1^2-5(\vec{S}_1\cdot\vec{n})^2\Big)\Big]\\ &+12C_{1(ES^2)}\frac{G^2}{r^4}\,\Big[\vec{S}_1\cdot\vec{S}_2\times\vec{n}\,\dot{\vec{S}}_1\cdot\vec{n}+\dot{\vec{S}}_1\cdot\vec{S}_2\times\vec{n}\,\vec{S}_1\cdot\vec{n}\Big],\end{aligned} \tag{2.55}$$

$$\begin{aligned}\text{Fig. 3(b13)} = {}& 2\frac{G^2}{r^5}\,\Big[\vec{S}_1\cdot\vec{v}_2\times\vec{n}\,\Big(\vec{S}_1\cdot\vec{S}_2-3\vec{S}_1\cdot\vec{n}\vec{S}_2\cdot\vec{n}\Big)-\vec{S}_1\cdot\vec{S}_2\;\vec{S}_1\cdot\vec{v}_1\times\vec{n}\Big]\\ &+2\frac{G^2}{r^4}\,\Big[\dot{\vec{S}}_1\cdot\vec{n}\;\vec{S}_1\cdot\vec{S}_2\times\vec{n}-\vec{S}_1\cdot\vec{n}\;\dot{\vec{S}}_1\cdot\vec{S}_2\times\vec{n}-\dot{\vec{S}}_1\cdot\vec{S}_1\times\vec{S}_2\Big],\end{aligned} \tag{2.56}$$

$$\text{Fig. 3(b14)} = -8\frac{G^2}{r^5}\,\vec{S}_1\cdot\vec{v}_1\times\vec{n}\,\Big[\vec{S}_1\cdot\vec{S}_2-3\vec{S}_1\cdot\vec{n}\vec{S}_2\cdot\vec{n}\Big], \tag{2.57}$$

$$\begin{aligned}\text{Fig. 3(b15)} = {}& -\frac{G^2}{r^5}\Big[2\,\vec{S}_1\cdot\vec{S}_2\times\vec{n}\,\vec{S}_1\cdot\vec{v}_1-\vec{S}_1\cdot\vec{v}_1\times\vec{n}\,\Big(5\,\vec{S}_1\cdot\vec{S}_2-9\vec{S}_1\cdot\vec{n}\,\vec{S}_2\cdot\vec{n}\Big)\\ &+3\,\vec{S}_2\cdot\vec{v}_1\times\vec{n}\,\Big(S_1^2-(\vec{S}_1\cdot\vec{n})^2\Big)\Big].\end{aligned} \tag{2.58}$$

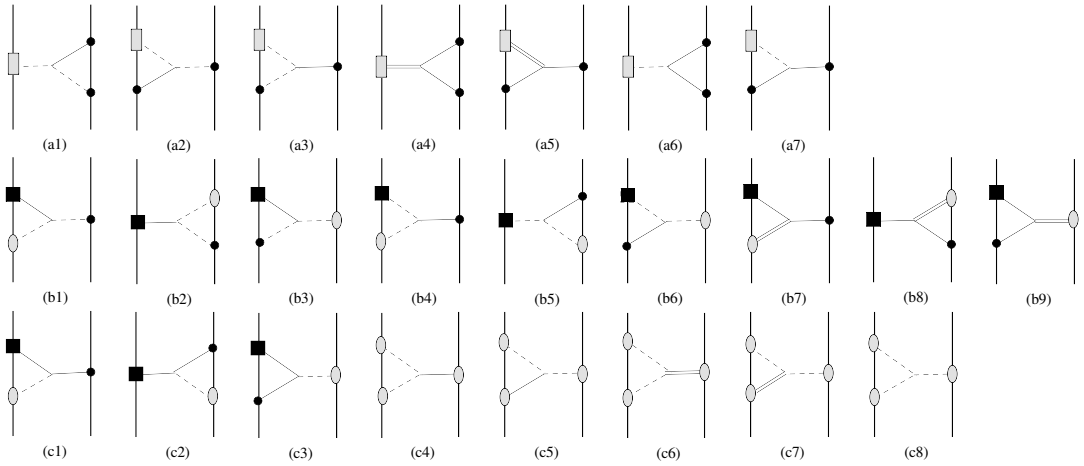

FIGURE 2.9: The Feynman graphs at one-loop level, i.e. with cubic self-gravitational interaction, which contribute to the NLO cubic-in-spin interaction at the 4.5PN order for maximally-rotating compact objects. The graphs should be included together with their mirror images, i.e. with the worldline labels $1 \leftrightarrow 2$ exchanged. Similar to the nonlinear graphs of two-graviton exchange, these graphs include all relevant interactions among the spin-induced quadrupole, octupole, and the mass and spin, and we have here nonlinearities originating from gravitons sourced strictly from minimal coupling to the worldline, as shown in graphs (c4)-(c8). We also have here cubic vertices containing time derivatives, similar to what we have in the NLO odd-parity spin-orbit sector [132, 136, 137].

2.2.3.3 Cubic self-interaction

As can be seen in figure 2.9 we have 24 graphs of cubic self-interaction in this sector, 6 of which contain time-dependent self-interaction, similar to what we have in the odd-parity spin-orbit sector [132, 136, 137]. Similar to the nonlinear graphs of two-graviton exchange, these graphs include all relevant interactions among the spin-induced quadrupole, octupole, and the mass and spin, and we have here nonlinearities originating from gravitons sourced strictly from minimal coupling to the worldline, as shown in graphs (c4)-(c8). This sector required using tensor one-loop integrals of up to order 5.

The graphs in figure 2.9 are evaluated as follows:

$$\text{Fig. 4(a1)} = -\frac{16}{3}C_{1(BS^3)}\frac{G^2}{r^5}\frac{m_2^2}{m_1^2}\,\vec{S}_1\cdot\vec{v}_2\times\vec{n}\left[S_1^2-6(\vec{S}_1\cdot\vec{n})^2\right], \tag{2.59}$$

$$\text{Fig. 4(a2)} = -\frac{3}{2}C_{1(BS^3)}\frac{G^2}{r^5}\frac{m_2}{m_1}\,\vec{S}_1\cdot\vec{v}_2\times\vec{n}\left[S_1^2-5(\vec{S}_1\cdot\vec{n})^2\right], \tag{2.60}$$

$$\text{Fig. 4(a3)} = \frac{3}{2}C_{1(BS^3)}\frac{G^2}{r^5}\frac{m_2}{m_1}\,\vec{S}_1\cdot\vec{v}_1\times\vec{n}\left[S_1^2-5(\vec{S}_1\cdot\vec{n})^2\right], \tag{2.61}$$

$$\text{Fig. 4(a4)} = -\frac{1}{3}C_{1(BS^3)}\frac{G^2}{r^5}\frac{m_2^2}{m_1^2}\,\vec{S}_1\cdot\vec{v}_1\times\vec{n}\left[S_1^2-6(\vec{S}_1\cdot\vec{n})^2\right], \tag{2.62}$$

$$\text{Fig. 4(a5)} = -\frac{1}{8}C_{1(BS^3)}\frac{G^2}{r^5}\frac{m_2}{m_1}\,\vec{S}_1\cdot\vec{v}_1\times\vec{n}\left[S_1^2-5(\vec{S}_1\cdot\vec{n})^2\right], \tag{2.63}$$

$$\text{Fig. 4(a6)} = \frac{1}{3}C_{1(BS^3)}\frac{G^2}{r^5}\frac{m_2^2}{m_1^2}\,\vec{S}_1\cdot\vec{v}_2\times\vec{n}\left[S_1^2-6(\vec{S}_1\cdot\vec{n})^2\right], \tag{2.64}$$

$$\text{Fig. 4(a7)} = \frac{1}{8}C_{1(BS^3)}\frac{G^2}{r^5}\frac{m_2}{m_1}\,\vec{S}_1\cdot\vec{v}_1\times\vec{n}\left[S_1^2-5(\vec{S}_1\cdot\vec{n})^2\right], \tag{2.65}$$

$$\text{Fig. 4(b1)} = -\frac{1}{2}C_{1(ES^2)}\frac{G^2}{r^5}\frac{m_2}{m_1}\,\vec{S}_1\cdot\vec{v}_2\times\vec{n}\left[S_1^2+3(\vec{S}_1\cdot\vec{n})^2\right], \tag{2.66}$$

$$\text{Fig. 4(b2)} = -8C_{1(ES^2)}\frac{G^2}{r^5}\frac{m_2}{m_1}\left[\vec{S}_1\cdot\vec{S}_2\times\vec{v}_2\;\vec{S}_1\cdot\vec{n}+\;\vec{S}_2\cdot\vec{v}_2\times\vec{n}\big(S_1^2-3(\vec{S}_1\cdot\vec{n})^2\big)\right], \tag{2.67}$$

$$\begin{aligned}\text{Fig. 4(b3)} = {}& 4C_{1(ES^2)}\frac{G^2}{r^5}\Big[4\;\vec{S}_1\cdot\vec{S}_2\times\vec{v}_1\;\vec{S}_1\cdot\vec{n}+\;\vec{S}_1\cdot\vec{S}_2\times\vec{n}\big(\vec{S}_1\cdot\vec{v}_1-6\vec{S}_1\cdot\vec{n}\;\vec{v}_1\cdot\vec{n}\big)\\ &+\vec{S}_2\cdot\vec{v}_1\times\vec{n}\big(2S_1^2-9(\vec{S}_1\cdot\vec{n})^2\big)\Big],\end{aligned} \tag{2.68}$$

$$\begin{aligned}\text{Fig. 4(b4)} = {}& \frac{1}{2}C_{1(ES^2)}\frac{G^2}{r^5}\frac{m_2}{m_1}\,\vec{S}_1\cdot\vec{v}_1\times\vec{n}\left[S_1^2+3(\vec{S}_1\cdot\vec{n})^2\right]\\ &-2C_{1(ES^2)}\frac{G^2}{r^4}\frac{m_2}{m_1}\,\dot{\vec{S}}_1\cdot\vec{S}_1\times\vec{n}\;\vec{S}_1\cdot\vec{n},\end{aligned} \tag{2.69}$$

$$\begin{aligned}\text{Fig. 4(b5)} = {}& 8C_{1(ES^2)}\frac{G^2}{r^5}\frac{m_2}{m_1}\Big[\vec{S}_1\cdot\vec{S}_2\times\vec{v}_1\;\vec{S}_1\cdot\vec{n}+\vec{S}_2\cdot\vec{v}_1\times\vec{n}\big(S_1^2-3(\vec{S}_1\cdot\vec{n})^2\big)\Big]\\ &-4C_{1(ES^2)}\frac{G^2}{r^4}\frac{m_2}{m_1}\left[\vec{S}_1\cdot\vec{S}_2\times\vec{n}\;\dot{\vec{S}}_1\cdot\vec{n}+\dot{\vec{S}}_1\cdot\vec{S}_2\times\vec{n}\;\vec{S}_1\cdot\vec{n}\right],\end{aligned} \tag{2.70}$$

$$\begin{aligned}\text{Fig. 4(b6)} = {}& 4C_{1(ES^2)}\frac{G^2}{r^5}\Big[2\vec{S}_1\cdot\vec{S}_2\times\vec{v}_1\;\vec{S}_1\cdot\vec{n}-\vec{S}_1\cdot\vec{S}_2\times\vec{n}\big(\vec{S}_1\cdot\vec{v}_1-6\vec{S}_1\cdot\vec{n}\;\vec{v}_1\cdot\vec{n}\big)\\ &+\vec{S}_2\cdot\vec{v}_1\times\vec{n}\big(2S_1^2-9(\vec{S}_1\cdot\vec{n})^2\big)\Big]\\ &-12C_{1(ES^2)}\frac{G^2}{r^4}\left[\vec{S}_1\cdot\vec{S}_2\times\vec{n}\;\dot{\vec{S}}_1\cdot\vec{n}+\dot{\vec{S}}_1\cdot\vec{S}_2\times\vec{n}\;\vec{S}_1\cdot\vec{n}\right],\end{aligned} \tag{2.71}$$

$$\text{Fig. 4(b7)} = -\frac{3}{8}C_{1(ES^2)}\frac{G^2}{r^5}\frac{m_2}{m_1}\,\vec{S}_1\cdot\vec{v}_1\times\vec{n}\left[S_1^2-5(\vec{S}_1\cdot\vec{n})^2\right], \tag{2.72}$$

$$\text{Fig. 4(b8)} = 2C_{1(ES^2)}\frac{G^2}{r^5}\frac{m_2}{m_1}\left[\vec{S}_1\cdot\vec{S}_2\times\vec{v}_2\,\vec{S}_1\cdot\vec{n}+\vec{S}_2\cdot\vec{v}_2\times\vec{n}\big(S_1^2-3(\vec{S}_1\cdot\vec{n})^2\big)\right], \tag{2.73}$$

$$\begin{aligned}\text{Fig. 4(b9)} = {}& \frac{1}{4}C_{1(ES^2)}\frac{G^2}{r^5}\Big[4\vec{S}_1\cdot\vec{S}_2\times\vec{v}_2\;\vec{S}_1\cdot\vec{n}-2\vec{S}_1\cdot\vec{S}_2\times\vec{n}\big(\vec{S}_1\cdot\vec{v}_2-3\vec{S}_1\cdot\vec{n}\;\vec{v}_2\cdot\vec{n}\big)\\ &+3\vec{S}_2\cdot\vec{v}_2\times\vec{n}\big(S_1^2-5(\vec{S}_1\cdot\vec{n})^2\big)\Big],\end{aligned} \tag{2.74}$$

$$\text{Fig. 4(c1)} = \frac{3}{8}C_{1(ES^2)}\frac{G^2}{r^5}\frac{m_2}{m_1}\Big[\,\vec{S}_1\cdot\vec{v}_1\times\vec{n}\big(S_1^2-5(\vec{S}_1\cdot\vec{n})^2\big)\Big] - C_{1(ES^2)}\frac{G^2}{r^4}\frac{m_2}{m_1}\Big[\,\dot{\vec{S}}_1\cdot\vec{S}_1\times\vec{n}\;\vec{S}_1\cdot\vec{n}\Big], \tag{2.75}$$

$$\text{Fig. 4(c2)} = -2C_{1(ES^2)}\frac{G^2}{r^5}\frac{m_2}{m_1}\Big[\vec{S}_1\cdot\vec{S}_2\times\vec{v}_2\,\vec{S}_1\cdot\vec{n}+\vec{S}_2\cdot\vec{v}_2\times\vec{n}\big(S_1^2-3(\vec{S}_1\cdot\vec{n})^2\big)\Big], \tag{2.76}$$

$$\text{Fig. 4(c3)} = -\frac{1}{4}C_{1(ES^2)}\frac{G^2}{r^5}\Big[4\vec{S}_1\cdot\vec{S}_2\times\vec{v}_1\;\vec{S}_1\cdot\vec{n}-2\vec{S}_1\cdot\vec{S}_2\times\vec{n}\big(\vec{S}_1\cdot\vec{v}_1-3\vec{S}_1\cdot\vec{n}\vec{v}_1\cdot\vec{n}\big) + 3\;\vec{S}_2\cdot\vec{v}_1\times\vec{n}\big(S_1^2-5(\vec{S}_1\cdot\vec{n})^2\big)\Big] + C_{1(ES^2)}\frac{G^2}{r^4}\Big[\,\vec{S}_1\cdot\vec{S}_2\times\vec{n}\;\dot{\vec{S}}_1\cdot\vec{n}+\dot{\vec{S}}_1\cdot\vec{S}_2\times\vec{n}\;\vec{S}_1\cdot\vec{n}\Big], \tag{2.77}$$

$$\text{Fig. 4(c4)} = 4\frac{G^2}{r^5}\Big[\,\vec{S}_1\cdot\vec{S}_2\times\vec{v}_2\;\vec{S}_1\cdot\vec{n}-3\vec{S}_2\cdot\vec{v}_2\times\vec{n}\;(\vec{S}_1\cdot\vec{n})^2\Big], \tag{2.78}$$

$$\text{Fig. 4(c5)} = 4\frac{G^2}{r^5}\Big[\,\vec{S}_1\cdot\vec{S}_2\times\vec{v}_1\;\vec{S}_1\cdot\vec{n}+\vec{S}_1\cdot\vec{v}_1\times\vec{n}\;\vec{S}_1\cdot\vec{S}_2\Big], \tag{2.79}$$

$$\text{Fig. 4(c6)} = -\frac{1}{2}\frac{G^2}{r^5}\Big[\,15\vec{S}_1\cdot\vec{S}_2\times\vec{n}\big(\vec{S}_1\cdot\vec{v}_2-\vec{S}_1\cdot\vec{n}\;\vec{v}_2\cdot\vec{n}\big) - \vec{S}_1\cdot\vec{v}_2\times\vec{n}\big(14\vec{S}_1\cdot\vec{S}_2-12\vec{S}_1\cdot\vec{n}\;\vec{S}_2\cdot\vec{n}\big)+\frac{1}{2}\vec{S}_2\cdot\vec{v}_2\times\vec{n}\big(29S_1^2-33(\vec{S}_1\cdot\vec{n})^2\big)\Big], \tag{2.80}$$

$$\text{Fig. 4(c7)} = -\frac{G^2}{r^5}\Big[4\vec{S}_1\cdot\vec{S}_2\times\vec{v}_1\;\vec{S}_1\cdot\vec{n}+3\vec{S}_1\cdot\vec{S}_2\times\vec{n}\big(\vec{S}_1\cdot\vec{v}_1-4\vec{S}_1\cdot\vec{n}\;\vec{v}_1\cdot\vec{n}\big) + \vec{S}_2\cdot\vec{v}_1\times\vec{n}\big(S_1^2-6(\vec{S}_1\cdot\vec{n})^2\big)\Big], \tag{2.81}$$

$$\text{Fig. 4(c8)} = \frac{1}{4}\frac{G^2}{r^5}\Big[\,4\vec{S}_1\cdot\vec{S}_2\times\vec{v}_1\;\vec{S}_1\cdot\vec{n}+8\vec{S}_1\cdot\vec{S}_2\times\vec{v}_2\;\vec{S}_1\cdot\vec{n} + 6\vec{S}_1\cdot\vec{S}_2\times\vec{n}\big(\vec{S}_1\cdot\vec{v}_1-5\vec{S}_1\cdot\vec{n}\;\vec{v}_1\cdot\vec{n}\big)+8\vec{S}_1\cdot\vec{S}_2\times\vec{n}\big(\vec{S}_1\cdot\vec{v}_2-6\vec{S}_1\cdot\vec{n}\;\vec{v}_2\cdot\vec{n}\big) + 8\vec{S}_1\cdot\vec{v}_1\times\vec{n}\big(\vec{S}_1\cdot\vec{S}_2-3\vec{S}_1\cdot\vec{n}\;\vec{S}_2\cdot\vec{n}\big)+\vec{S}_2\cdot\vec{v}_1\times\vec{n}\big(5S_1^2-9(\vec{S}_1\cdot\vec{n})^2\big)\Big] + \frac{G^2}{r^4}\Big[\vec{S}_1\cdot\vec{S}_2\times\vec{n}\;\dot{\vec{S}}_1\cdot\vec{n}-2\vec{S}_1\cdot\dot{\vec{S}}_2\times\vec{n}\;\vec{S}_1\cdot\vec{n}+\dot{\vec{S}}_1\cdot\vec{S}_2\times\vec{n}\;\vec{S}_1\cdot\vec{n}\Big]. \tag{2.82}$$

2.2.4 New features from spin dependence of linear momentum

The formulation of the EFT of a spinning gravitating particle in [136] consisted of an action initially taken in the covariant gauge as introduced by Tulczyjew in [160] (later extended to higher-multipoles by Dixon [161]). Tulczyjew put forward the spin supplementary condition (SSC) given by $S_{\mu\nu}p^\nu = 0$, which as noted in [136], corresponds to the choice $e_0^\mu = p^\mu/\sqrt{p^2}$ for the timelike component of the worldline tetrad in terms of the linear momentum p^μ. This

gauge is distinguished among possible covariant gauges, in particular with the four-velocity u^μ (as in $S_{\mu\nu}u^\nu = 0$) as the only gauge of rotational DOFs for which the existence and uniqueness of a corresponding "center" for the spinning particle were proven rigorously in General Relativity [162, 163].

For this reason the formulation in [136] was made in terms of the linear momentum p^μ, rather than the four-velocity u^μ, e.g., as in general the former is given by

$$p_\mu = -\frac{\partial L}{\partial u^\mu} = m\frac{u_\mu}{\sqrt{u^2}} + \mathcal{O}(RS^2), \tag{2.83}$$

where we recall that the Lagrangian is first constructed with the 'spin gauge-invariant' variable, as explained in [136]. Therefore the spin-dependent difference between p_μ and u_μ would show up, as was pointed out in [136], as of the NLO of the sector cubic in the spins, namely the sector that we are studying in this work.

Let us then find how this new feature transpires in this sector. Since we are working to cubic order in the spin in this sector, we should take into account in the linear momentum beyond the leading term only the first correction, that is we now consider also

$$\Delta p_\kappa[S] \equiv p_\kappa - \bar{p}_\kappa \simeq \frac{C_{ES^2}}{2m} S^\mu S^\nu \left(\frac{2}{u} R_{\mu\alpha\nu\kappa} u^\alpha - \frac{1}{u^3} R_{\mu\alpha\nu\beta} u^\alpha u^\beta u_\kappa\right), \tag{2.84}$$

where we denoted the leading approximation to the linear momentum as $\bar{p}_\kappa \equiv \frac{m}{u} u_\kappa$. Let us also note that due to eq. (4.8) of [136] at this order the expression with spin vectors can be used interchangeably as that with the spin tensors. The appearance of u^μ in p^μ itself thus requires further inquiry only as of the NLO quartic-in-spin sector [121], where it was in fact found that this subtlety is still irrelevant until even higher PN orders.

Hence, the part that is linear in the spin in the action of the spinning particle actually gives rise to a new type of worldline-graviton couplings that are cubic in the spin, due to its dependence in the linear momentum. We recall that the relevant part of the Lagrangian is given as follows [136]:

$$L_S = -\frac{1}{2}\hat{S}_{ab}\hat{\Omega}^{ab}_{\text{flat}} - \frac{1}{2}\hat{S}_{ab}\omega^{ab}_\mu u^\mu - \frac{\hat{S}_{ab}p^b}{p^2}\frac{Dp^a}{D\sigma}, \tag{2.85}$$

where the hatted DOFs represent the generic rotational DOFs. Therefore the new contributions arise from substituting in the linear-in-spin couplings the

gauge, which we choose here as the canonical gauge, formulated in [136] as

$$\hat{\Lambda}^{a}_{[0]} = \delta^{a}_{0}, \quad \hat{S}^{ab}\left(p_b + p\delta_{0b}\right) = 0, \tag{2.86}$$

as well as from the extra term that enters from minimal coupling, appearing last in eq. (2.85), which was found in [136] to be related with the gauge of the rotational DOFs, and stands for the Thomas precession as noted in section 2.2.2. Let us stress again that the subtlety here is not about switching from the covariant gauge, but rather about advancing from using u_ν in the basic covariant gauge, to using in it the spin-dependent p_ν, which is necessary as of this cubic order in spins and nonlinear order in gravity.

Working out explicitly this part of the action in terms of the local spin variable in the canonical gauge similarly to the derivations in [136], and keeping only terms that lead to new cubic-in-spin terms, we obtain here the following contribution:

$$L_{S\to S^3} = \omega^{ij}_{\mu} u^{\mu} \frac{\hat{S}_{ik} p^k p_j}{p\left(p + p^0\right)} - \omega^{0i}_{\mu} u^{\mu} \frac{\hat{S}_{ij} p^j}{p} + \frac{\hat{S}_{ij} p^i \dot{p}^j}{p\left(p + p^0\right)}, \tag{2.87}$$

where in principle all the temporal and spatial indices that are specified here are in the locally flat frame. In order to obtain the new cubic-in-spin couplings we only need to substitute in the correction to the linear momentum from eq. (2.84) to linear order, keeping in mind that all of the contributions at the zeroth order are taken into account in the Feynman rules from past sectors, e.g. [136, 137], and from section 2.2.2 above. At this point it becomes clear that the first two terms in eq. (2.87) give rise to new two-graviton couplings, and that the last term gives rise to new one-graviton couplings containing higher-order time derivatives.

The resulting new Feynman rules for the one-graviton couplings are then:

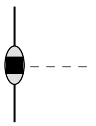

$$= \int dt \left[\frac{C_{\mathrm{ES}^2}}{4m^2} S_i S_j \epsilon_{klm} \left[\left(2S_m a^k + \dot{S}_m v^k\right)\left(A_{l,ij} - A_{j,il}\right)\right]\right], \tag{2.88}$$

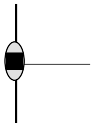

$$= \int dt \left[- \frac{C_{\mathrm{ES}^2}}{2m^2} S_i S_j \epsilon_{klm} \left[2S_m a^k \left(2\left(\phi_{,ij} v^l - \phi_{,il} v^j\right) + \delta_{ij}\left(\partial_t \phi_{,l} + \phi_{,ln} v^n\right)\right)\right.\right.$$
$$\left.\left. - \dot{S}_m v^k \left(2\phi_{,il} v^j - \delta_{ij}\left(\partial_t \phi_{,l} + \phi_{,ln} v^n\right) + \delta_{il}\left(\partial_t \phi_{,j} + \phi_{,jn} v^n\right)\right)\right]\right], \tag{2.89}$$

where a black square mounted on a gray oval blob represents this new type of

FIGURE 2.10: The extra Feynman graphs of one- and two-graviton exchange, which appear at the NLO cubic-in-spin interaction at the 4.5PN order for maximally-rotating compact objects. The graphs should be included together with their mirror images, i.e. with the worldline labels $1 \leftrightarrow 2$ exchanged. These graphs contain a new type of worldline-graviton couplings, which we refer to as "composite" octupole ones, and obviously yield similar graphs to the corresponding ones with the "elementary" spin-induced octupole couplings in figure 2.7(a1),(a2) and in figure 2.8(b1),(b2).

"composite" cubic-in-spin worldline couplings. Notice that all these rules contain accelerations and even time derivatives of spins, similar to the acceleration terms that appear first in the rules for the spin-orbit sector [136]. Note also that at this level the new couplings depend linearly on a single Wilson coefficient.

For the new two-graviton couplings we get the following rules:

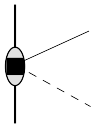

$$= \int dt \, \left[\frac{C_{\mathrm{ES}^2}}{2m^2} S_i S_j \epsilon_{klm} S_m \phi_{,k} \left(A_{l,ij} - A_{j,il} \right) \right], \tag{2.90}$$

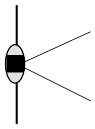

$$= \int dt \, \left[-\frac{C_{\mathrm{ES}^2}}{m^2} S_i S_j \epsilon_{klm} S_m \phi_{,k} \Big(2\big(\phi_{,ij} v^l - \phi_{,il} v^j \big) + \delta_{ij} \left(\partial_t \phi_{,l} + \phi_{,ln} v^n \right) \Big) \right]. \tag{2.91}$$

Note that the mass ratio together with the Wilson coefficient in these new rules for cubic-in-spin couplings indicate that these are truly new couplings that cannot be absorbed in the existing "elementary" octupole operator.

These new couplings give rise to 4 additional graphs as shown in figure 2.10, similar to those in figure 2.7 (a1), (a2), and in figure 2.8 (b1), (b2). The graphs

in figure 2.10 are evaluated as follows:

$$\text{Fig. 5(a1)} = -C_{1(ES^2)}\frac{G}{r^3}\frac{m_2}{m_1^2}\Bigg[2\vec{S}_1\cdot\vec{v}_2\times\vec{a}_1\left(S_1^2-3\left(\vec{S}_1\cdot\vec{n}\right)^2\right)-6\vec{S}_1\cdot\vec{a}_1\times\vec{n}\vec{S}_1\cdot\vec{v}_2\vec{S}_1\cdot\vec{n}$$
$$-\dot{\vec{S}}_1\cdot\vec{S}_1\times\vec{v}_1\vec{S}_1\cdot\vec{v}_2-\dot{\vec{S}}_1\cdot\vec{v}_1\times\vec{v}_2\left(S_1^2-3\left(\vec{S}_1\cdot\vec{n}\right)^2\right)$$
$$-3\dot{\vec{S}}_1\cdot\vec{v}_1\times\vec{n}\vec{S}_1\cdot\vec{v}_2\vec{S}_1\cdot\vec{n}\Bigg], \tag{2.92}$$

$$\text{Fig. 5(a2)} = \frac{1}{2}C_{1(ES^2)}\frac{G}{r^3}\frac{m_2}{m_1^2}\Bigg[6\vec{S}_1\cdot\vec{v}_1\times\vec{a}_1\left(S_1^2-2\left(\vec{S}_1\cdot\vec{n}\right)^2\right)-2\vec{S}_1\cdot\vec{v}_2\times\vec{a}_1S_1^2$$
$$+6\vec{S}_1\cdot\vec{a}_1\times\vec{n}\left(S_1^2(\vec{v}_1\cdot\vec{n}-\vec{v}_2\cdot\vec{n})-2\vec{S}_1\cdot\vec{v}_1\vec{S}_1\cdot\vec{n}\right)$$
$$-\dot{\vec{S}}_1\cdot\vec{S}_1\times\vec{v}_1\left(3\vec{S}_1\cdot\vec{v}_1-\vec{S}_1\cdot\vec{v}_2-3\vec{S}_1\cdot\vec{n}\,(\vec{v}_1\cdot\vec{n}-\vec{v}_2\cdot\vec{n})\right)$$
$$+\dot{\vec{S}}_1\cdot\vec{v}_1\times\vec{v}_2\,S_1^2+3\dot{\vec{S}}_1\cdot\vec{v}_1\times\vec{n}\left(S_1^2\,(\vec{v}_1\cdot\vec{n}-\vec{v}_2\cdot\vec{n})-2\vec{S}_1\cdot\vec{v}_1\vec{S}_1\cdot\vec{n}\right)\Bigg], \tag{2.93}$$

$$\text{Fig. 5(b1)} = -2C_{1(ES^2)}\frac{G^2}{r^5}\frac{m_2^2}{m_1^2}\,\vec{S}_1\cdot\vec{v}_2\times\vec{n}\left[S_1^2-3(\vec{S}_1\cdot\vec{n})^2\right], \tag{2.94}$$

$$\text{Fig. 5(b2)} = C_{1(ES^2)}\frac{G^2}{r^5}\frac{m_2^2}{m_1^2}\left[3\vec{S}_1\cdot\vec{v}_1\times\vec{n}\big(S_1^2-2(\vec{S}_1\cdot\vec{n})^2\big)-\vec{S}_1\cdot\vec{v}_2\times\vec{n}\,S_1^2\right]. \tag{2.95}$$

2.2.5 The gravitational cubic-in-spin action at the next-to-leading order

Let us then put together all the results from sections 2.2.3 and 2.2.4 to get the final effective action for this sector. This summation includes the values presented above plus similar results under the exchange of particle labels $1 \leftrightarrow 2$, where $\vec{n} \to -\vec{n}$. Next, we apply the 4-vectors identity for 3 dimensions presented in eq. (3.14) of [135], to further simplify and compress the results. As was already noted these results contain higher-order time derivatives of both the velocity and the spin, which will be treated rigorously at the level of the action, following the procedure shown in [159], by making variable redefinitions that will remove the higher-order terms (in complete analogy to the removal of redundant/on-shell operators by field redefinitions in effective field theories, as was pointed out by one of the authors in [159]).

The final result of these steps is then given as follows:

$$L_{\rm S^3}^{\rm NLO} = L_{\rm S_1^2S_2}^{\rm NLO} + L_{\rm S_1^3}^{\rm NLO} + (1 \leftrightarrow 2), \tag{2.96}$$

where we have:

$$\begin{aligned}L^{\rm NLO}_{\rm S_1^2S_2} =& + \frac{G^2}{r^5}L_{(1)} + C_{1(ES^2)}\frac{G}{r^4}\frac{1}{m_1}L_{(2)} + C_{1(ES^2)}\frac{G^2}{r^5}L_{(3)} + C_{1(ES^2)}\frac{G^2m_2}{r^5m_1}L_{(4)}\\ &+ \frac{G^2}{r^4}L_{(5)} + C_{1(ES^2)}\frac{G}{r^3}\frac{1}{m_1}L_{(6)} + C_{1(ES^2)}\frac{G^2}{r^4}L_{(7)} + C_{1(ES^2)}\frac{G^2m_2}{r^4m_1}L_{(8)}\\ &+ C_{1(ES^2)}\frac{G}{r^2}\frac{1}{m_1}L_{(9)} + C_{1(ES^2)}\frac{G}{r}\frac{1}{m_1}L_{(10)},\end{aligned} \tag{2.97}$$

with the following pieces:

$$\begin{aligned}L_{(1)} =& \frac{1}{2}\,\vec{S}_1\cdot\vec{S}_2\times\vec{n}\Big(-5\,\vec{S}_1\cdot\vec{v}_1+\,\vec{S}_1\cdot\vec{v}_2+9\,\vec{S}_1\cdot\vec{n}\,\vec{v}_1\cdot\vec{n}-9\,\vec{S}_1\cdot\vec{n}\,\vec{v}_2\cdot\vec{n}\Big)\\ &+9\,\vec{S}_1\cdot\vec{v}_1\times\vec{n}\,\vec{S}_1\cdot\vec{n}\,\vec{S}_2\cdot\vec{n}-\frac{5}{4}\,\vec{S}_2\cdot\vec{v}_2\times\vec{n}\big(S_1^2+3\big(\vec{S}_1\cdot\vec{n}\big)^2\big)\\ &+\vec{S}_1\cdot\vec{v}_2\times\vec{n}\big(3\,\vec{S}_1\cdot\vec{S}_2-12\,\vec{S}_1\cdot\vec{n}\,\vec{S}_2\cdot\vec{n}\big)-\frac{1}{4}\,\vec{S}_2\cdot\vec{v}_1\times\vec{n}\,\big(7S_1^2-27\big(\vec{S}_1\cdot\vec{n}\big)^2\big),\end{aligned} \tag{2.98}$$

$$\begin{aligned}L_{(2)} =& -3\,\vec{S}_1\cdot\vec{S}_2\times\vec{v}_1\Big(4\,\vec{S}_1\cdot\vec{v}_1\,\vec{v}_2\cdot\vec{n}+\vec{S}_1\cdot\vec{v}_2\,\vec{v}_2\cdot\vec{n}\Big)+\frac{9}{2}\,\vec{S}_2\cdot\vec{v}_1\times\vec{v}_2\,S_1^2\,\vec{v}_1\cdot\vec{n}\\ &+3\,\vec{S}_1\cdot\vec{S}_2\times\vec{v}_2\Big(4\,\vec{S}_1\cdot\vec{v}_2\,\vec{v}_1\cdot\vec{n}+\vec{S}_1\cdot\vec{n}\big(2\,\vec{v}_1\cdot\vec{v}_2-v_2^2\big)\Big)\\ &-3\,\vec{S}_1\cdot\vec{v}_1\times\vec{v}_2\,\vec{S}_1\cdot\vec{S}_2\,\vec{v}_2\cdot\vec{n}-\frac{15}{2}\,\vec{v}_1\cdot\vec{v}_2\times\vec{n}\,\vec{S}_2\cdot\vec{v}_1\big(\vec{S}_1\cdot\vec{n}\big)^2\\ &+\vec{S}_2\cdot\vec{v}_1\times\vec{n}\Big(\frac{15}{2}S_1^2\,\big(v_1^2-\vec{v}_1\cdot\vec{v}_2-2(\vec{v}_1\cdot\vec{n})^2-\vec{v}_1\cdot\vec{n}\,\vec{v}_2\cdot\vec{n}\big)\\ &+3\,\vec{S}_1\cdot\vec{v}_1\big(-2\,\vec{S}_1\cdot\vec{v}_1+2\,\vec{S}_1\cdot\vec{v}_2+5\,\vec{S}_1\cdot\vec{n}\,\vec{v}_1\cdot\vec{n}\big)-15\,\vec{S}_1\cdot\vec{v}_2\,\vec{S}_1\cdot\vec{n}\,\vec{v}_1\cdot\vec{n}\\ &+\frac{15}{2}\big(\vec{S}_1\cdot\vec{n}\big)^2\,\big(-v_1^2+7\,\vec{v}_1\cdot\vec{n}\,\vec{v}_2\cdot\vec{n}\big)\Big)+\vec{S}_2\cdot\vec{v}_2\times\vec{n}\Big(\frac{3}{2}\,S_1^2\big(-5v_1^2+4\,\vec{v}_1\cdot\vec{v}_2-v_2^2\\ &+10(\vec{v}_1\cdot\vec{n})^2+5\,\vec{v}_1\cdot\vec{n}\,\vec{v}_2\cdot\vec{n}\big)+\frac{15}{2}\big(\vec{S}_1\cdot\vec{n}\big)^2\big(2v_1^2-2\,\vec{v}_1\cdot\vec{v}_2+v_2^2-7\,\vec{v}_1\cdot\vec{n}\,\vec{v}_2\cdot\vec{n}\big)\\ &+3\,\vec{S}_1\cdot\vec{v}_1\big(2\,\vec{S}_1\cdot\vec{v}_1-\vec{S}_1\cdot\vec{v}_2-5\,\vec{S}_1\cdot\vec{n}\,\vec{v}_1\cdot\vec{n}+5\,\vec{S}_1\cdot\vec{n}\,\vec{v}_2\cdot\vec{n}\big)\Big)\\ &-3\,\vec{S}_1\cdot\vec{v}_1\times\vec{n}\Big(\vec{S}_1\cdot\vec{S}_2\,\big(v_1^2-\vec{v}_1\cdot\vec{v}_2-5\,\vec{v}_1\cdot\vec{n}\,\vec{v}_2\cdot\vec{n}\big)+\vec{S}_1\cdot\vec{v}_2\,\vec{S}_2\cdot\vec{v}_1\\ &+\vec{S}_1\cdot\vec{v}_1\big(-\vec{S}_2\cdot\vec{v}_1+5\,\vec{S}_2\cdot\vec{n}\,\vec{v}_2\cdot\vec{n}\big)\Big)+3\,\vec{S}_1\cdot\vec{v}_2\times\vec{n}\Big(\vec{S}_1\cdot\vec{S}_2\,\big(v_1^2-5\,\vec{v}_1\cdot\vec{n}\,\vec{v}_2\cdot\vec{n}\big)\\ &-\vec{S}_1\cdot\vec{v}_1\,\vec{S}_2\cdot\vec{v}_1+15\,\vec{S}_1\cdot\vec{v}_2\,\vec{S}_2\cdot\vec{n}\,\vec{v}_1\cdot\vec{n}\Big),\end{aligned} \tag{2.99}$$

$$\begin{aligned}L_{(3)} =& \frac{1}{2}\,\vec{S}_1\cdot\vec{S}_2\times\vec{v}_1\,\vec{S}_1\cdot\vec{n}-\frac{1}{2}\,\vec{S}_1\cdot\vec{S}_2\times\vec{v}_2\,\vec{S}_1\cdot\vec{n}+\frac{3}{2}\,\vec{S}_1\cdot\vec{S}_2\big(\vec{S}_1\cdot\vec{v}_1\times\vec{n}-\vec{S}_1\cdot\vec{v}_2\times\vec{n}\big)\\ &+\,\vec{S}_1\cdot\vec{S}_2\times\vec{n}\big(-\vec{S}_1\cdot\vec{v}_1+\vec{S}_1\cdot\vec{v}_2-\frac{3}{2}\,\vec{S}_1\cdot\vec{n}\,\vec{v}_1\cdot\vec{n}+\frac{3}{2}\,\vec{S}_1\cdot\vec{n}\,\vec{v}_2\cdot\vec{n}\big)\\ &-\frac{3}{4}\,\big(\vec{S}_2\cdot\vec{v}_1\times\vec{n}-\vec{S}_2\cdot\vec{v}_2\times\vec{n}\big)\big(3S_1^2-5(\vec{S}_1\cdot\vec{n})^2\big),\end{aligned} \tag{2.100}$$

$$
\begin{aligned}
L_{(4)} = {} & 31\ \vec{S}_1 \cdot \vec{S}_2 \big(\vec{S}_1 \cdot \vec{v}_1 \times \vec{n} - \vec{S}_1 \cdot \vec{v}_2 \times \vec{n}\big) \\
& - 2\Big(\vec{S}_2 \cdot \vec{v}_1 \times \vec{n} - \vec{S}_2 \cdot \vec{v}_2 \times \vec{n}\Big)\big(19 S_1^2 - 21 \big(\vec{S}_1 \cdot \vec{n}\big)^2\big) \\
& + \vec{S}_1 \cdot \vec{S}_2 \times \vec{n} \big(- 41\ \vec{S}_1 \cdot \vec{v}_1 + 41\ \vec{S}_1 \cdot \vec{v}_2 + 63\ \vec{S}_1 \cdot \vec{n}\ \vec{v}_1 \cdot \vec{n} - 66\ \vec{S}_1 \cdot \vec{n}\ \vec{v}_2 \cdot \vec{n}\big),
\end{aligned}
\tag{2.101}
$$

$$
L_{(5)} = 3\ \vec{S}_1 \cdot \vec{S}_2 \times \vec{n}\ \dot{\vec{S}}_1 \cdot \vec{n} - \dot{\vec{S}}_1 \cdot \vec{S}_2 \times \vec{n}\ \vec{S}_1 \cdot \vec{n} - 2\ \vec{S}_1 \cdot \dot{\vec{S}}_2 \times \vec{n}\ \vec{S}_1 \cdot \vec{n} + 2\ \vec{S}_1 \cdot \dot{\vec{S}}_1 \times \vec{S}_2,
\tag{2.102}
$$

$$
\begin{aligned}
L_{(6)} = {} & \frac{1}{2}\,\vec{S}_1\cdot\vec{S}_2\times\vec{v}_1\;\dot{\vec{S}}_1\cdot\vec{v}_2+\frac{1}{2}\,\dot{\vec{S}}_1\cdot\vec{S}_2\times\vec{v}_1\;\vec{S}_1\cdot\vec{v}_2\\
& +\frac{1}{2}\,\vec{S}_1\cdot\vec{S}_2\times\vec{v}_2\Big(\dot{\vec{S}}_1\cdot\vec{v}_1-2\,\dot{\vec{S}}_1\cdot\vec{v}_2-3\,\dot{\vec{S}}_1\cdot\vec{n}\;\vec{v}_1\cdot\vec{n}-3\,\dot{\vec{S}}_1\cdot\vec{n}\;\vec{v}_2\cdot\vec{n}\Big)\\
& +\vec{S}_1\cdot\vec{S}_2\times\vec{a}_1\;\vec{S}_1\cdot\vec{v}_2+\big(\vec{S}_1\cdot\vec{S}_2\times\vec{a}_2+\vec{S}_1\cdot\dot{\vec{S}}_2\times\vec{v}_2\big)\big(-\vec{S}_1\cdot\vec{v}_1+3\;\vec{S}_1\cdot\vec{n}\;\vec{v}_1\cdot\vec{n}\big)\\
& -2\;\vec{S}_1\cdot\dot{\vec{S}}_2\times\vec{v}_1\;\vec{S}_1\cdot\vec{v}_1+3\;\vec{S}_1\cdot\vec{v}_2\times\vec{a}_1\;\vec{S}_1\cdot\vec{n}\;\vec{S}_2\cdot\vec{n}\\
& +\frac{1}{2}\,\dot{\vec{S}}_1\cdot\vec{S}_2\times\vec{v}_2\Big(\vec{S}_1\cdot\vec{v}_1-\vec{S}_1\cdot\vec{v}_2-3\;\vec{S}_1\cdot\vec{n}\;\vec{v}_1\cdot\vec{n}-3\;\vec{S}_1\cdot\vec{n}\;\vec{v}_2\cdot\vec{n}\Big)\\
& -\vec{S}_2\cdot\vec{v}_1\times\vec{v}_2\big(\dot{\vec{S}}_1\cdot\vec{S}_1-3\;\dot{\vec{S}}_1\cdot\vec{n}\;\vec{S}_1\cdot\vec{n}\big)\\
& +\big(\vec{S}_2\cdot\vec{v}_2\times\vec{a}_2+\frac{3}{2}\;\vec{S}_2\cdot\vec{v}_2\times\vec{a}_1\big)\big(S_1^2-3(\vec{S}_1\cdot\vec{n})^2\big)\\
& +\frac{3}{2}\;\vec{S}_1\cdot\vec{S}_2\times\vec{n}\Big(2\;\vec{S}_1\cdot\vec{n}\;\vec{a}_1\cdot\vec{v}_2+\;\dot{\vec{S}}_1\cdot\vec{n}\;\vec{v}_1\cdot\vec{v}_2-\dot{\vec{S}}_1\cdot\vec{v}_2\;\vec{v}_1\cdot\vec{n}\\
& +5\;\dot{\vec{S}}_1\cdot\vec{n}\;\vec{v}_1\cdot\vec{n}\;\vec{v}_2\cdot\vec{n}\Big)-\frac{1}{2}\big(\vec{S}_2\cdot\vec{v}_1\times\vec{a}_2+\dot{\vec{S}}_2\cdot\vec{v}_1\times\vec{v}_2\big)\big(5S_1^2-9(\vec{S}_1\cdot\vec{n})^2\big)\\
& +\frac{3}{2}\;\dot{\vec{S}}_1\cdot\vec{S}_2\times\vec{n}\Big(-\vec{S}_1\cdot\vec{v}_2\;\vec{v}_1\cdot\vec{n}+\vec{S}_1\cdot\vec{n}\;\vec{v}_1\cdot\vec{v}_2+5\;\vec{S}_1\cdot\vec{n}\;\vec{v}_1\cdot\vec{n}\;\vec{v}_2\cdot\vec{n}\Big)\\
& +\frac{3}{2}\;\vec{S}_2\cdot\vec{v}_1\times\vec{n}\Big(S_1^2\;\vec{a}_1\cdot\vec{n}+\dot{\vec{S}}_1\cdot\vec{S}_1\;(2\vec{v}_1\cdot\vec{n}+4\vec{v}_2\cdot\vec{n})-10\;\dot{\vec{S}}_1\cdot\vec{n}\;\vec{S}_1\cdot\vec{n}\;\vec{v}_2\cdot\vec{n}\Big)\\
& +\frac{3}{2}\;\vec{S}_2\cdot\vec{a}_1\times\vec{n}\Big(S_1^2\;\vec{v}_1\cdot\vec{n}+S_1^2\;\vec{v}_2\cdot\vec{n}-5\;(\vec{S}_1\cdot\vec{n})^2\vec{v}_2\cdot\vec{n}\Big)\\
& +\frac{3}{2}\;\vec{S}_1\cdot\vec{v}_1\times\vec{n}\big(\vec{S}_1\cdot\vec{S}_2\;\vec{a}_1\cdot\vec{n}+2\vec{S}_1\cdot\dot{\vec{S}}_2\;\vec{v}_1\cdot\vec{n}+\dot{\vec{S}}_1\cdot\vec{S}_2\;\vec{v}_1\cdot\vec{n}-\dot{\vec{S}}_1\cdot\vec{S}_2\;\vec{v}_2\cdot\vec{n}\\
& -2\;\dot{\vec{S}}_2\cdot\vec{n}\;\vec{S}_1\cdot\vec{v}_1-\vec{S}_1\cdot\vec{n}\;\vec{S}_2\cdot\vec{a}_1-\dot{\vec{S}}_1\cdot\vec{n}\;\vec{S}_2\cdot\vec{v}_1\big)\\
& -3\;\vec{S}_1\cdot\vec{v}_2\times\vec{n}\;\vec{S}_1\cdot\vec{S}_2\;\vec{a}_1\cdot\vec{n}\\
& +\vec{S}_2\cdot\vec{v}_2\times\vec{n}\Big(\frac{3}{2}(\dot{\vec{S}}_1\cdot\vec{v}_2\;\vec{S}_1\cdot\vec{n}+\vec{S}_1\cdot\vec{v}_2\;\dot{\vec{S}}_1\cdot\vec{n})\\
& -3\;\vec{v}_2\cdot\vec{n}\;\big(3\;\dot{\vec{S}}_1\cdot\vec{S}_1-5\;\dot{\vec{S}}_1\cdot\vec{n}\;\vec{S}_1\cdot\vec{n}\big)\Big)\\
& -\frac{3}{2}\;\dot{\vec{S}}_2\cdot\vec{v}_1\times\vec{n}\Big(S_1^2\;\vec{v}_1\cdot\vec{n}-5(\vec{S}_1\cdot\vec{n})^2\vec{v}_1\cdot\vec{n}\Big)\\
& +\frac{3}{2}\;\dot{\vec{S}}_1\cdot\vec{v}_1\times\vec{n}\Big(\big(\vec{v}_1\cdot\vec{n}-\vec{v}_2\cdot\vec{n}\big)\vec{S}_1\cdot\vec{S}_2-\vec{S}_1\cdot\vec{n}\;\vec{S}_2\cdot\vec{v}_1\Big)\\
& +\frac{3}{2}\big(\vec{S}_2\cdot\vec{a}_2\times\vec{n}+\dot{\vec{S}}_2\cdot\vec{v}_2\times\vec{n}\big)\big(-S_1^2\;\vec{v}_1\cdot\vec{n}+2\;\vec{S}_1\cdot\vec{v}_1\;\vec{S}_1\cdot\vec{n}-5(\vec{S}_1\cdot\vec{n})^2\vec{v}_1\cdot\vec{n}\big)\\
& +\frac{3}{2}\;\vec{S}_1\cdot\vec{a}_1\times\vec{n}\big(-\vec{S}_1\cdot\vec{n}\;\vec{S}_2\cdot\vec{v}_1+\vec{S}_1\cdot\vec{S}_2\;\vec{v}_1\cdot\vec{n}\big),
\end{aligned}
\tag{2.103}
$$

$$
L_{(7)} = \vec{S}_1\cdot\vec{S}_2\times\vec{n}\;\dot{\vec{S}}_1\cdot\vec{n}+\dot{\vec{S}}_1\cdot\vec{S}_2\times\vec{n}\;\vec{S}_1\cdot\vec{n},
\tag{2.104}
$$

$$
L_{(8)} = -4\vec{S}_1\cdot\vec{S}_2\times\vec{n}\;\dot{\vec{S}}_1\cdot\vec{n}-13\vec{S}_1\cdot\dot{\vec{S}}_2\times\vec{n}\;\vec{S}_1\cdot\vec{n}-4\dot{\vec{S}}_1\cdot\vec{S}_2\times\vec{n}\;\vec{S}_1\cdot\vec{n},
\tag{2.105}
$$

$$
\begin{aligned}
L_{(9)} = {} & \vec{S}_1 \cdot \dot{\vec{S}}_2 \times \vec{v}_2 \; \dot{\vec{S}}_1 \cdot \vec{n} + \dot{\vec{S}}_1 \cdot \dot{\vec{S}}_2 \times \vec{v}_2 \; \vec{S}_1 \cdot \vec{n} + \vec{S}_1 \cdot \dot{\vec{S}}_2 \times \vec{a}_1 \; \vec{S}_1 \cdot \vec{n} \\
& + \vec{S}_1 \cdot \vec{S}_2 \times \vec{a}_2 \; \dot{\vec{S}}_1 \cdot \vec{n} + \dot{\vec{S}}_1 \cdot \vec{S}_2 \times \vec{a}_2 \; \vec{S}_1 \cdot \vec{n} - \frac{1}{2} \; \vec{S}_1 \cdot \vec{v}_2 \times \vec{n} \; \ddot{\vec{S}}_1 \cdot \vec{S}_2 \\
& - \frac{1}{2} \; \dot{\vec{S}}_1 \cdot \vec{v}_1 \times \vec{n} \; \vec{S}_1 \cdot \dot{\vec{S}}_2 - \frac{1}{2} \; \ddot{\vec{S}}_1 \cdot \vec{v}_2 \times \vec{n} \; \vec{S}_1 \cdot \vec{S}_2 - \dot{\vec{S}}_1 \cdot \vec{v}_2 \times \vec{n} \; \dot{\vec{S}}_1 \cdot \vec{S}_2 \\
& - \frac{1}{2} \; \vec{S}_1 \cdot \vec{v}_1 \times \vec{n} \; \dot{\vec{S}}_1 \cdot \dot{\vec{S}}_2 - \vec{S}_2 \cdot \vec{v}_2 \times \vec{n} \big(\ddot{\vec{S}}_1 \cdot \vec{S}_1 + \dot{\vec{S}}_1 \cdot \dot{\vec{S}}_1 \big) \\
& - 3 \Big(\vec{S}_2 \cdot \vec{a}_2 \times \vec{n} + \dot{\vec{S}}_2 \cdot \vec{v}_2 \times \vec{n} \Big) \big(\dot{\vec{S}}_1 \cdot \vec{S}_1 - \dot{\vec{S}}_1 \cdot \vec{n} \; \vec{S}_1 \cdot \vec{n} \big) \\
& - 3 \; \dot{\vec{S}}_2 \cdot \vec{v}_1 \times \vec{n} \; \dot{\vec{S}}_1 \cdot \vec{n} \; \vec{S}_1 \cdot \vec{n} - \frac{1}{2} \; \dot{\vec{S}}_2 \cdot \vec{a}_1 \times \vec{n} \Big(3 \big(\vec{S}_1 \cdot \vec{n} \big)^2 + S_1^2 \Big) \\
& - \frac{3}{2} \; \vec{S}_1 \cdot \vec{S}_2 \times \vec{n} \; \ddot{\vec{S}}_1 \cdot \vec{n} \; \vec{v}_2 \cdot \vec{n} + \frac{3}{2} \; \vec{S}_1 \cdot \dot{\vec{S}}_2 \times \vec{n} \; \dot{\vec{S}}_1 \cdot \vec{n} \; \vec{v}_1 \cdot \vec{n} \\
& - 3 \; \dot{\vec{S}}_1 \cdot \vec{S}_2 \times \vec{n} \; \dot{\vec{S}}_1 \cdot \vec{n} \; \vec{v}_2 \cdot \vec{n} - \frac{3}{2} \; \ddot{\vec{S}}_1 \cdot \vec{S}_2 \times \vec{n} \; \vec{S}_1 \cdot \vec{n} \; \vec{v}_2 \cdot \vec{n} \\
& + \frac{3}{2} \; \dot{\vec{S}}_1 \cdot \dot{\vec{S}}_2 \times \vec{n} \; \vec{S}_1 \cdot \vec{n} \; \vec{v}_1 \cdot \vec{n}, \qquad (2.106)
\end{aligned}
$$

$$
L_{(10)} = \; - \frac{1}{2} \vec{S}_1 \cdot \dot{\vec{S}}_2 \times \vec{n} \; \ddot{\vec{S}}_1 \cdot \vec{n} - \dot{\vec{S}}_1 \cdot \dot{\vec{S}}_2 \times \vec{n} \; \dot{\vec{S}}_1 \cdot \vec{n} - \frac{1}{2} \ddot{\vec{S}}_1 \cdot \dot{\vec{S}}_2 \times \vec{n} \; \vec{S}_1 \cdot \vec{n}, \qquad (2.107)
$$

and also:

$$
\begin{aligned}
L_{\mathrm{S}_1^3}^{\mathrm{NLO}} = {} & C_{1(ES^2)} \frac{G^2 m_2}{r^5 m_1} L_{[1]} + C_{1(ES^2)} \frac{G^2 m_2^2}{r^5 m_1^2} L_{[2]} + C_{1(BS^3)} \frac{G m_2}{r^4 m_1^2} L_{[3]} \\
& + C_{1(BS^3)} \frac{G^2 m_2}{r^5 m_1} L_{[4]} + C_{1(BS^3)} \frac{G^2 m_2^2}{r^5 m_1^2} L_{[5]} + C_{1(ES^2)} \frac{G m_2}{r^3 m_1^2} L_{[6]} \\
& + C_{1(ES^2)} \frac{G^2 m_2}{r^4 m_1} L_{[7]} + C_{1(BS^3)} \frac{G m_2}{r^3 m_1^2} L_{[8]} + C_{1(BS^3)} \frac{G m_2}{r^2 m_1^2} L_{[9]}, \qquad (2.108)
\end{aligned}
$$

with the pieces:

$$
L_{[1]} = \frac{1}{2} (-\vec{S}_1 \cdot \vec{v}_1 \times \vec{n} + \vec{S}_1 \cdot \vec{v}_2 \times \vec{n}) \big(S_1^2 - 9 \big(\vec{S}_1 \cdot \vec{n} \big)^2 \big), \qquad (2.109)
$$

$$
L_{[2]} = 3 \Big(\vec{S}_1 \cdot \vec{v}_1 \times \vec{n} - \vec{S}_1 \cdot \vec{v}_2 \times \vec{n} \Big) \left(S_1^2 - 2 (\vec{S}_1 \cdot \vec{n})^2 \right), \qquad (2.110)
$$

$$
\begin{aligned}
L_{[3]} = {} & \vec{S}_1\cdot\vec{v}_1\times\vec{v}_2\ \vec{S}_1\cdot\vec{v}_2\ \vec{S}_1\cdot\vec{n} \\
& + \vec{S}_1\cdot\vec{v}_1\times\vec{n}\Big(\ \frac{1}{2}\ S_1^2\big(v_1^2 - 2\ \vec{v}_1\cdot\vec{v}_2 + 2v_2^2 - 5\ \vec{v}_1\cdot\vec{n}\ \vec{v}_2\cdot\vec{n}\big) \\
& + \vec{S}_1\cdot\vec{v}_1\big(-\vec{S}_1\cdot\vec{v}_1 + \vec{S}_1\cdot\vec{v}_2 + \vec{S}_1\cdot\vec{n}\ \ (5\ \vec{v}_1\cdot\vec{n} - 6\ \vec{v}_2\cdot\vec{n})\ \big) - 5\ \vec{S}_1\cdot\vec{v}_2\ \vec{S}_1\cdot\vec{n}\ \vec{v}_1\cdot\vec{n} \\
& - \frac{5}{2}(\vec{S}_1\cdot\vec{n})^2\big(v_1^2 - 2\ \vec{v}_1\cdot\vec{v}_2 + 2v_2^2 - 7\ \vec{v}_1\cdot\vec{n}\ \vec{v}_2\cdot\vec{n}\big)\Big) \\
& + \vec{S}_1\cdot\vec{v}_2\times\vec{n}\Big(-\frac{1}{2}S_1^2\big(v_2^2 - 5\ \vec{v}_1\cdot\vec{n}\ \vec{v}_2\cdot\vec{n}\big) + \frac{5}{2}(\vec{S}_1\cdot\vec{n})^2\big(v_2^2 - 7\ \vec{v}_1\cdot\vec{n}\ \vec{v}_2\cdot\vec{n}\big) \\
& + \vec{S}_1\cdot\vec{v}_1\big(\vec{S}_1\cdot\vec{v}_1 - \vec{S}_1\cdot\vec{v}_2 - \vec{S}_1\cdot\vec{n}\ \ (4\ \vec{v}_1\cdot\vec{n} - 5\ \vec{v}_2\cdot\vec{n})\ \big) + 5\ \vec{S}_1\cdot\vec{v}_2\ \vec{S}_1\cdot\vec{n}\ \vec{v}_1\cdot\vec{n}\Big) \\
& + \vec{v}_1\cdot\vec{v}_2\times\vec{n}\Big(-\big(\vec{S}_1\cdot\vec{n}\big)^2\Big(\vec{S}_1\cdot\vec{v}_1 + \frac{5}{2}\ \vec{S}_1\cdot\vec{v}_2\Big) + \frac{1}{2}S_1^2\ \vec{S}_1\cdot\vec{v}_2\Big), \qquad (2.111)
\end{aligned}
$$

$$
L_{[4]} = \frac{1}{2}\big(\vec{S}_1\cdot\vec{v}_1\times\vec{n} - \vec{S}_1\cdot\vec{v}_2\times\vec{n}\big)\big(S_1^2 - 5\big(\vec{S}_1\cdot\vec{n}\big)^2\big), \qquad (2.112)
$$

$$
L_{[5]} = -4\ \big(\vec{S}_1\cdot\vec{v}_1\times\vec{n} - \vec{S}_1\cdot\vec{v}_2\times\vec{n}\big)\big(S_1^2 - 5\big(\vec{S}_1\cdot\vec{n}\big)^2\big), \qquad (2.113)
$$

$$
\begin{aligned}
L_{[6]} = {} & 3\Bigg[\Big(\vec{S}_1\cdot\vec{v}_1\times\vec{a}_1 - \vec{S}_1\cdot\vec{v}_2\times\vec{a}_1\Big)\Big(S_1^2 - 2\Big(\vec{S}_1\cdot\vec{n}\Big)^2\Big) \\
& + \vec{S}_1\cdot\vec{a}_1\times\vec{n}\Big(S_1^2\big(\vec{v}_1\cdot\vec{n} - \vec{v}_2\cdot\vec{n}\big) - 2\vec{S}_1\cdot\vec{n}\big(\vec{S}_1\cdot\vec{v}_1 - \vec{S}_1\cdot\vec{v}_2\big)\Big)\Bigg] \\
& - \frac{3}{2}\Bigg[\dot{\vec{S}}_1\cdot\vec{S}_1\times\vec{v}_1\Big(\vec{S}_1\cdot\vec{v}_1 - \vec{S}_1\cdot\vec{v}_2 - \vec{S}_1\cdot\vec{n}\,(\vec{v}_1\cdot\vec{n} - \vec{v}_2\cdot\vec{n})\Big) \\
& - \dot{\vec{S}}_1\cdot\vec{v}_1\times\vec{v}_2\Big(S_1^2 - 2\Big(\vec{S}_1\cdot\vec{n}\Big)^2\Big) \\
& - \dot{\vec{S}}_1\cdot\vec{v}_1\times\vec{n}\Big(S_1^2\big(\vec{v}_1\cdot\vec{n} - \vec{v}_2\cdot\vec{n}\big) - 2\vec{S}_1\cdot\vec{n}\big(\vec{S}_1\cdot\vec{v}_1 - \vec{S}_1\cdot\vec{v}_2\big)\Big)\Bigg], \qquad (2.114)
\end{aligned}
$$

$$
L_{[7]} = \ -3\ \dot{\vec{S}}_1\cdot\vec{S}_1\times\vec{n}\ \vec{S}_1\cdot\vec{n}, \qquad (2.115)
$$

$$
\begin{aligned}
L_{[8]} =& \frac{1}{6}\Big(2\ \vec{S}_1\cdot\vec{v}_1\times\vec{v}_2\big(\dot{\vec{S}}_1\cdot\vec{S}_1-3\ \dot{\vec{S}}_1\cdot\vec{n}\ \vec{S}_1\cdot\vec{n}\big)+\dot{\vec{S}}_1\cdot\vec{v}_1\times\vec{v}_2\big(S_1^2-3(\vec{S}_1\cdot\vec{n})^2\big)\\
&+\vec{S}_1\cdot\vec{a}_1\times\vec{v}_2\big(S_1^2-3(\vec{S}_1\cdot\vec{n})^2\big)+\vec{S}_1\cdot\vec{v}_1\times\vec{a}_2\big(S_1^2-3(\vec{S}_1\cdot\vec{n})^2\big)\\
&-6\ \vec{S}_1\cdot\vec{v}_1\times\vec{n}\ \Big(\vec{S}_1\cdot\vec{v}_1\ \dot{\vec{S}}_1\cdot\vec{n}+\dot{\vec{S}}_1\cdot\vec{v}_1\ \vec{S}_1\cdot\vec{n}+\vec{S}_1\cdot\vec{a}_1\ \vec{S}_1\cdot\vec{n}\\
&-\vec{v}_2\cdot\vec{n}\big(\dot{\vec{S}}_1\cdot\vec{S}_1-5\ \dot{\vec{S}}_1\cdot\vec{n}\ \vec{S}_1\cdot\vec{n}\big)\Big)\\
&-3\ \dot{\vec{S}}_1\cdot\vec{v}_1\times\vec{n}\ \Big(2\vec{S}_1\cdot\vec{v}_1\ \vec{S}_1\cdot\vec{n}-\vec{v}_2\cdot\vec{n}\big(S_1^2-5(\vec{S}_1\cdot\vec{n})^2\big)\Big)\\
&-3\ \vec{S}_1\cdot\vec{a}_1\times\vec{n}\ \Big(2\vec{S}_1\cdot\vec{v}_1\ \vec{S}_1\cdot\vec{n}-\vec{v}_2\cdot\vec{n}\big(S_1^2-5(\vec{S}_1\cdot\vec{n})^2\big)\Big)\\
&+6\ \vec{S}_1\cdot\vec{v}_2\times\vec{n}\Big(\vec{S}_1\cdot\vec{v}_1\ \dot{\vec{S}}_1\cdot\vec{n}+\dot{\vec{S}}_1\cdot\vec{v}_1\ \vec{S}_1\cdot\vec{n}+\vec{S}_1\cdot\vec{a}_1\ \vec{S}_1\cdot\vec{n}\\
&-\vec{v}_2\cdot\vec{n}\big(\dot{\vec{S}}_1\cdot\vec{S}_1-5\ \dot{\vec{S}}_1\cdot\vec{n}\ \vec{S}_1\cdot\vec{n}\big)\Big)\\
&+3\ \dot{\vec{S}}_1\cdot\vec{v}_2\times\vec{n}\Big(2\vec{S}_1\cdot\vec{v}_1\ \vec{S}_1\cdot\vec{n}-\vec{v}_2\cdot\vec{n}\big(S_1^2-5(\vec{S}_1\cdot\vec{n})^2\big)\Big)\\
&+3\ \vec{S}_1\cdot\vec{a}_2\times\vec{n}\Big(2\vec{S}_1\cdot\vec{v}_1\ \vec{S}_1\cdot\vec{n}+\vec{v}_1\cdot\vec{n}\big(S_1^2-5(\vec{S}_1\cdot\vec{n})^2\big)\Big)\Big),
\end{aligned}
\tag{2.116}
$$

$$
L_{[9]} = -\frac{1}{3}\ \vec{S}_1\cdot\vec{a}_2\times\vec{n}\big(\dot{\vec{S}}_1\cdot\vec{S}_1-3\ \dot{\vec{S}}_1\cdot\vec{n}\ \vec{S}_1\cdot\vec{n}\big)-\frac{1}{6}\ \dot{\vec{S}}_1\cdot\vec{a}_2\times\vec{n}\big(S_1^2-3\big(\vec{S}_1\cdot\vec{n}\big)^2\big).
\tag{2.117}
$$

As can be seen in the result above we have grouped together terms according to their mass ratios and Wilson coefficients, and the total number/order of their higher-order time derivatives. At this stage this result is rather bulky, but it is easy to see that after the reduction of the higher-order action to an ordinary action by the removal of higher-order time derivative terms, we will only be left with such pieces as the first 4 ones in $L^{\rm NLO}_{S_1^2S_2}$ and the first 5 ones in $L^{\rm NLO}_{S_1^3}$, which becomes significantly more compact. The EOMs can also be derived directly from this higher-order action, and then reduced at the level of the EOMs, as was pointed out in [136].

However, before we will proceed in future work to handle via redefinitions the higher-order time derivatives appearing in the cubic-in-spin sector at this order, we will need to also take into account all the contributions to the action in this sector at this order, which originate from lower-order redefinitions of the variables made at lower-order sectors in order to remove higher-order time derivatives there, as was shown in detail in section 6 of [136]. First, for example, we recall that we have kinematic contributions as noted in eq. (5.28) of [136], that are linear in the spin, but have no field coupling. Those are required here

to NLO as follows:

$$L_{\rm kin} = -\vec{S}\cdot\vec{\Omega} - \frac{1}{2}\left(1+\frac{3}{4}v^2\right)\epsilon_{ijk}S_k v^j a^i, \tag{2.118}$$

where $S_{ij} = \epsilon_{ijk}S_k$, and $\Omega_{ij} = \epsilon_{ijk}\Omega_k$. At LO, e.g., we define the following shift of the positions, $\Delta\vec{y}_I$, according to

$$\vec{y}_1 \to \vec{y}_1 + \frac{1}{2m_1}\vec{S}_1 \times \vec{v}_1, \tag{2.119}$$

and similarly for particle 2 with $1 \leftrightarrow 2$, to remove the leading accelerations. Note that as of the NLO linear-in-spin level higher-order time derivatives of spin also appear, where it was shown how to generically treat these in section 5 of [159]. Yet, since the leading spin redefinition is of higher PN order, terms quadratic in the leading redefinition contribute only at the next-to-NNLO (NNNLO) level. Therefore, here it is sufficient to consider the redefinition of the spins to linear order.

To recap, let us list the additional contributions coming from lower-order variable redefinitions that we will have from other sectors. From position shifts in lower-order sectors we will have:

1. The LO (1.5PN) position shift in eq. (2.119) implemented to linear order on the NLO quadratic-in-spin (spin1-spin2 + spin-squared) sectors.

2. The above LO position shift implemented to quadratic order on the Newtonian and LO spin-orbit sectors.

3. The above LO position shift to cubic order implemented on the Newtonian sector.

4. The NLO position shift at 2.5PN order in eq. (6.20) of [136] implemented to linear order on the LO quadratic-in-spin sectors.

5. The NLO position shifts at 3PN order in eqs. (6.30), (6.43) of [136] implemented to linear order on the *shifted* LO spin-orbit sector.

The leading redefinition of spin (of 2PN order) in eq. (6.21) of [136] will not contribute to our sector. From spin redefinitions, i.e. rotations of the spin, we will have then:

1. The spin redefinitions at 2.5PN order in eqs. (6.31), (6.44) of [136] implemented to linear order on the LO quadratic-in-spin sectors.

2. The spin redefinitions at 3PN order, which were required at the LO cubic-in-spin sector [135], implemented to linear order on the LO spin-orbit sector.

In a future publication we will present the full details of these redefinitions and the contributions from lower-order sectors, which add up to the reduced effective action in this sector.

2.2.6 Discussion

In this work we derived for the first time the complete NLO cubic-in-spin PN effective action for the interaction of generic compact binaries via the self-contained EFT formulation for gravitating spinning objects in [136], and its extension in this work to the leading sector, where gravitational non-linearities are considered at an order in the spins that is beyond quadratic. This sector, which enters at the 4.5PN order for rapidly-rotating compact objects, completes finite-size effects up to this PN order, and is the first sector completed beyond the current state of the art for generic compact binary dynamics at the 4PN order. Once again the EFT of gravitating spinning objects has enabled a push in the state of the art in PN Gravity. Yet the analysis in this work indicates that going beyond this sector into the intriguing gray area of table 2.1 may become extremely intricate.

We have seen that at this order in spins with nonlinearities in gravity we have to take into account additional terms, which arise from a new type of worldline couplings, due to the fact that at this order the Tulczyjew gauge, which involves the linear momentum, can no longer be approximated only in terms of the four-velocity, as the latter approximation differs from the linear momentum by a spin-dependent part of an order $\mathcal{O}(RS^2)$. The spin-dependent correction gives rise to new "composite" couplings from the gauge of rotational DOFs. It is interesting to consider whether these new couplings have an insightful physical interpretation.

As we noted in section 2.2.1 one of the main motivations for us to tackle this sector was also to see what happens when we go to a sector at order higher than quadratic in the spins and nonlinear in gravity, which corresponds to a gravitational Compton scattering with quantum spins of $s \geq 3/2$, and to possibly also get an insight on the non-uniqueness of fixing its amplitude from factorization when spins of $s \geq 5/2$ are involved [89]. From [136] and the analysis in section 2.2.4, we can see that going to an order quintic in the spins, or in the quantum case to $s = 5/2$, exactly corresponds to where the

spin-dependent correction to p_μ in eq. (2.84) has to be taken into account at quadratic order. We will discuss this interesting connection between the classical and the quantum levels at a future publication. A general observation that we can clearly make already is that even-parity sectors in l, see table 2.1, are easier to handle than odd ones. In the quantum context this corresponds to the greater ease of dealing with bosons compared to fermions.

Unless all the additional terms from section 2.2.4 conspire to cancel out eventually, we would obtain an effective action that differs from that with the gauge used in lower-spin sectors, involving only the four-velocity. Even still, it could be that when computing the consequent observable quantities, such as the binding energy, or the EOMs, one finds that this difference does not matter, and the two gauges are physically equivalent. In a forthcoming publication we will present the resulting Hamiltonian, EOMs, and gauge-invariant quantities, such as the binding energy, and get an answer to these questions, including self-consistency checks of the method.

At the moment it is not clear whether computations carried out within a scattering amplitudes framework can capture all the classical effects derived in this paper. The generic results in this work can serve to streamline such a framework, as that which was initiated in [90, 93], or provide crosschecks for the conjectured result for the scattering angle at one-loop level in the restricted case of black holes with aligned spins in [92].

Chapter 3

Quantum Amplitudes for Classical Gravity

In this chapter, we derive the static Schwarzschild-Tangherlini metric by extracting the classical contributions from the multi-loop vertex functions of a graviton emitted from a massive scalar field [2]. At each loop orders the classical contribution is proportional to a unique master integral given by the massless sunset integral. By computing the scattering amplitudes up to three-loop order in general dimension, we explicitly derive the expansion of the metric up to the fourth post-Minkowskian order $O(G_N^4)$ in four, five and six dimensions. There are ultraviolet divergences that are cancelled with the introduction of higher-derivative non-minimal couplings. The standard Schwarzschild-Tangherlini is recovered by absorbing their effects by an appropriate coordinate transformation induced from the de Donder gauge condition.

3.1 Introduction

General relativity is a theory for the action of gravity in space and time. The dynamics of the gravitational field is constrained by the Einstein's classical field equations. They are tensorial non-linear equations, because of the self-interaction of the gravitational field, notoriously difficult to solve. It is therefore important to develop efficient methods for studying gravity in various regimes.

General relativity can be embedded in quantum theory where the gravitational force results from the exchange of a quantized massless spin-2 graviton field [6–10]. One can then consider the Einstein-Hilbert term as the first term of a low-energy effective action containing an infinite number of higher derivative operators [11].

The classical limit $\hbar \to 0$ has been studied by Duff in [164] where he showed how to reproduce the classical Schwarzschild metric in four dimensions from quantum tree graphs up to the second order $O(G_N^2)$ in Newton's constant.

The relation between the quantum theory of gravity and the classical Einstein's theory of general relativity has received a new interpretation with the understanding [23–28] that an appropriate (and subtle) $\hbar \to 0$ limit of quantum multi-loop scattering gravitational amplitudes lead to higher G_N-order classical gravity contributions. Considering the importance of such approach for the evaluation of the post-Minkowskian expansion for the gravitational two-body scattering [51, 73, 74, 76–78, 93], we use the procedure given in [27] for extracting the classical contributions from the multi-loop vertex function of a graviton emission from a massive scalar field to recover the Schwarzschild-Tangherlini metric in various dimensions. The scattering amplitude approach works in general dimensions [53, 165–167] and gives the opportunity to explore general relativity in higher-dimensions [168, 169]. At tree-level and one-loop our results agree with the general dimension results in [165, 167]. We show how to reconstruct the metric up to the fourth order $O(G_N^4)$ in Newton's constant by evaluating the scattering amplitudes up to three-loop orders.

Using the procedure designed in [27] we argue, in section 3.2.1, that the classical contribution at l-loop order is given by the two-point l-loop massless sunset graphs. We verify this explicitly evaluating the classical limit of the quantum scattering amplitudes up to three-loop order.

The scattering amplitudes develop ultraviolet divergences. In section 3.4, we show how to recover the finite static Schwarzschild-Tangherlini metric by the addition of non-minimal couplings given schematically by (see (3.88) for a precise expression)

$$\delta^{(n)} S^{\text{ct.}} \sim (G_N m)^{\frac{2n}{d-2}} \int d^{d+1}x \sqrt{-g}\, \nabla^{2(n-1)} \mathcal{R}_{\mu\nu} \partial^\mu \phi \partial^\nu \phi \,. \tag{3.1}$$

In four dimensions the non-minimal couplings $\delta^{(1)} S^{\text{ct.}}$ have been introduced in [34] for the analysis up to the third post-Minkowskian order in the context of the world-line formalism. The relation between the world-line formalism and the amplitude approach is detailed in [73]. Higher-derivative couplings with $n \geq 2$ would be needed in four dimensions from the fifth post-Minkowskian order, but they appear at lowest order in higher dimensions. Indeed, we show that in five dimensions one needs to consider higher dimensional of non-minimal couplings $\delta^{(2)} S^{\text{ct.}}$ at the third post-Minkowskian order and $\delta^{(3)} S^{\text{ct.}}$ at the fourth

post-Minkowskian. Interestingly, the metric components are finite in space-time dimensions greater or equal to six, although the stress-tensor develops ultraviolet divergences from one-loop order in odd dimensions and from two-loop order in even dimensions. These divergences are cancelled by the non-minimal couplings $\delta^{(n)}S^{\rm ct.}$. Actually, we expect that an all order computation in perturbation will require an infinite set of such non-minimal couplings.

We show that the effects of the non-minimal couplings can be reabsorbed by a coordinate transformation, and they do not affect the Schwarzschild-Tangherlini space-time geometry. Since we work in the fixed gauge de Donder gauge, we give the coordinate transformation for extracting the classical space-time metric from the scattering amplitudes in that gauge. Although general relativity is coordinate system invariant, our analysis shows that there is a preferred coordinate system when extracting the classical geometry from scattering amplitudes in the de Donder gauge. The lowest-order $n = 1$ non-minimal couplings have been shown to arise from the gauge fixing in [73, 167, 170]. We will not address the question of the gauge dependence, but we remark that the choice of coordinate system (or gauge) can be critical for finding solution to Einstein's equations [171].

Since "black hole formation is a robust prediction of the general theory of relativity" [172], it is satisfying to be able to embed such classical solutions in the new understanding of the relation between general relativity and the quantum theory of gravity.

The rest of the chapter is organised as follows. In section 3.2 we setup the connection between the perturbation expansion vertex function for the emission a graviton from a massive scalar field and the post-Minkowskian expansion of the static metric in $d+1$ dimensions. In section 3.2.1 we show that the classical contribution from the multi-loop amplitudes is given by the massless sunset multi-loop integrals in d dimensions. In section 3.2.2 we evaluate the master integrals. In section 3.3 we derive the metric component up to the order $O(G_N^4)$ by computing the relevant amplitudes up to three-loop order in $d+1$ dimensions. In section 3.4 we compute the non-minimal couplings required for cancelling the ultraviolet divergences in the amplitude computation. In section 3.5 we solve the Einstein's equations in four ($d = 3$), five ($d = 4$) and six ($d = 5$) dimensions in the de Donder gauge, and we show in section 3.6 how these results match the results derived from the amplitude computations. In section 3.7 we give an interpretation of the results in this paper. The appendix A.1 contains formulæ for the Fourier transforms used in the text, and appendix A.2 the vertices for the scattering amplitude computations.

3.2 The Schwarzschild-Tangherlini metric from scalar field amplitudes

The Schwarzschild metric is obtained by the gravitational scattering of a scalar field of mass m

$$\mathcal{S} = \int d^{d+1}x\sqrt{-g}\left(\frac{R}{16\pi G_N} + \frac{1}{2}g^{\mu\nu}\partial_\mu\phi\partial_\nu\phi - \frac{1}{2}m^2\phi^2\right). \tag{3.2}$$

For further reference Newton's constant has length dimensions $[G_N] = (length)^{d-1}$, the scalar field has dimension $[\phi] = (length)^{1-d}$ and the mass $[m] = (length)^{-1}$. We work with the mostly negative signature $(+,-,\cdots,-)$ metric.

The graviton emission from a scalar particle of mass $p_1^2 = p_2^2 = m^2$ is given by the three-point vertex function

$\mathcal{M}_3(p_1,q) =$ 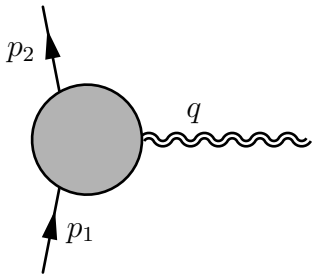

. (3.3)

At each loop order we extract the l-loop contribution to the transition density of the stress-energy tensor $\langle T_{\mu\nu}(q^2)\rangle = \sum_{l\geq 0}\langle T^{(l)}_{\mu\nu}(q^2)\rangle$

$$i\mathcal{M}_3^{(l)}(p_1,q) = -\frac{i\sqrt{32\pi G_N}}{2}\langle T^{(l)\,\mu\nu}(q^2)\rangle\epsilon_{\mu\nu} \tag{3.4}$$

where $\epsilon^{\mu\nu}$ is the polarisation of the graviton with momentum $q = p_1 - p_2$ is the momentum transfer.

The scattering amplitude computation is not done in the harmonic gauge coordinates $g^{\mu\nu}\Gamma^\lambda_{\mu\nu}(g) = 0$ but in the *de Donder gauge* coordinate system [7, 34, 78, 165, 167]

$$\eta^{\mu\nu}\Gamma^\lambda_{\mu\nu}(g) = \eta^{\mu\nu}g^{\lambda\rho}\left(\frac{\partial g_{\rho\mu}}{\partial x^\nu} + \frac{\partial g_{\rho\nu}}{\partial x^\mu} - \frac{\partial g_{\mu\nu}}{\partial x^\rho}\right) = 0\,, \tag{3.5}$$

the metric perturbations $g_{\mu\nu} = \eta_{\mu\nu} + \sum_{n\geq 1} h^{(n)}_{\mu\nu}$ satisfy*

$$\frac{\partial}{\partial x^\lambda}h^{\lambda(n)}_\nu - \frac{1}{2}\frac{\partial}{\partial x^\nu}h^{(n)} = 0\,. \tag{3.6}$$

*The harmonic gauge linearized at the first order in perturbation gives (3.6) with $n = 1$. The higher-order expansions of the harmonic gauge differ from these conditions.

The de Donder gauge relation between the metric perturbation and the stress-energy tensor reads

$$h_{\mu\nu}^{(l+1)}(\vec{x}) = -16\pi G_N \int \frac{d^d\vec{q}}{(2\pi)^d} e^{i\vec{q}\cdot\vec{x}} \frac{1}{\vec{q}^2} \left(\langle T_{\mu\nu}^{(l)} \rangle^{\text{class.}}(q^2) - \frac{1}{d-1}\eta_{\mu\nu}\langle T^{(l)} \rangle^{\text{class.}}(q^2) \right) . \tag{3.7}$$

In this relation enters the classical contribution at l loop order $\langle T_{\mu\nu}^{(l)} \rangle^{\text{class.}}(q^2)$ defined by the classical limit of the quantum scattering amplitude [25, 27, 28]. From now, we are dropping the super-script class and just use the notation $\langle T_{\mu\nu}^{(l)} \rangle(q^2)$ for the classical contribution.

3.2.1 The classical contribution of the amplitude

In this section we derive the generic form of the classical contribution of the gravity amplitudes (3.3) in the static limit where $q = (0, \vec{q})$ and $\vec{q}^2 \ll m^2$. The classical limit is obtained by taking $\hbar \to 0$ with the momentum transfer $q/\hbar$ held fixed [28].

At the l-loop order we have to consider the graphs

$\mathcal{M}_3^{(l)}(p_1, q) =$ 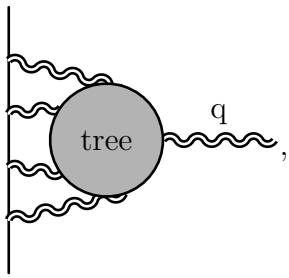

, (3.8)

The classical contribution emerges as a particular $\hbar \to 0$ limit of the amplitude in [23, 25–28]. The classical limit results in cutting the massive lines, projecting on the contribution from localised sources at different positions in space [27, 173, 174], pictorially represented by shaded blobs

$\mathcal{M}_3^{(l)\ \text{class.}}(p_1, q) =$ 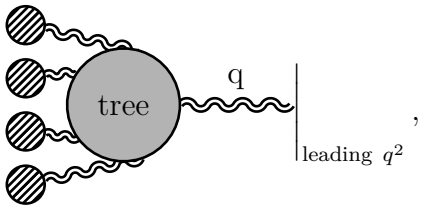

, (3.9)

In this process one keeps only the leading q^2 contribution from the multi-graviton tree-level amplitudes. The quantum tree-level graphs that were considered in [164] arise from the classical limit of the scattering amplitude up to

two-loop order. In the rest of this section, we derive the generic features of the classical limit to all orders in perturbation. We then explicitly evaluate the classical limit up to three-loop order in perturbation.

The quantum amplitude in (3.8) is an $l+2$ gravitons amplitude with $l+1$ gravitons attached to the massive scalar line

$\mathcal{L}_{\mu_1\nu_1,\ldots,\mu_{l+1}\nu_{l+1}}(p_1,p_2,\ell_1,\ldots,\ell_{l+1}) =$ 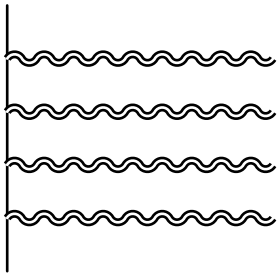 (3.10)

$$= \frac{(-i\sqrt{8\pi G_N})^{l+1}\tau_{\mu_1\nu_1}(p_1,p_1-\ell_1)\tau_{\mu_2\nu_2}(p_1\ell_1,p_1-\ell_1-\ell_2)\cdots\tau_{\mu_{l+1}\nu_{l+1}}(p_1-\ell_1-\cdots-\ell_{l+1},p_2)}{\prod_{i=1}^{l}\left((p_1-\sum_{j=1}^{i}\ell_j)^2-m^2+i\epsilon\right)}, \tag{3.11}$$

with the momentum conservation condition $\ell_1+\cdots+\ell_{l+1}=q=p_1-p_2$ and the vertex for emitting a graviton from a scalar field[†]

$$\tau^{\mu\nu}(p_1,p_2) = p_1^\mu p_2^\nu + p_1^\nu p_2^\mu + \frac{1}{2}\eta^{\mu\nu}\,(p_1-p_2)^2\,. \tag{3.12}$$

This line is attached to an $l+2$ tree-level graviton amplitude

$\mathcal{M}^{\mu_1\nu_1,\ldots,\mu_{l+1}\nu_{l+1}}(\ell_1,\ldots,\ell_{l+1},q) =$ 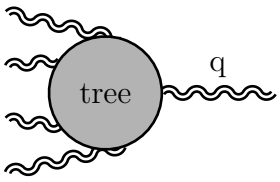

. (3.13)

We have to sum over all the permutation of the graviton lines attached to the scalar lines. Because the gravity amplitude is invariant under the action of the

[†]The vertices are given in appendix A.2. We have stripped of a factor $i\sqrt{8\pi G_N}$ from their normalisation.

permutation of the graviton lines we have

$$i\mathcal{M}_3^{(l)}(p_1,q)=\frac{1}{\sqrt{4E_1E_2}}\int\prod_{n=1}^{l}\frac{d^{d+1}\ell_n}{(2\pi)^D}\left(\sum_{\sigma\in\mathfrak{S}_{l+1}}\mathcal{L}_{\mu_1\nu_1,\ldots,\mu_{l+1}\nu_{l+1}}(p_1,p_2,\ell_{\sigma(1)},\ldots,\ell_{\sigma(l+1)})\right)\\ \times\prod_{i=1}^{l+1}\frac{i\mathcal{P}^{\mu_i\nu_i,\rho_i\sigma_i}}{\ell_i^2+i\epsilon}\mathcal{M}_{\rho_1\sigma_1,\ldots,\rho_{l+1}\sigma_{l+1}}(\ell_1,\ldots,\ell_{l+1},q) \quad (3.14)$$

where $\mathfrak{S}_{l+1}$ is the group of permutation of $l+1$ elements. In the static limit the vertex (3.12) becomes

$$\tau_{\mu\nu}(p_1,p_1-\ell)\simeq -2m^2\delta^0_\mu\delta^0_\nu\,, \quad (3.15)$$

therefore the scalar line approximates to

$$\mathcal{L}(p_1,p_2,\ell_1,\ldots,\ell_{l+1})\simeq\frac{\prod_{i=1}^{l+1}i\sqrt{32\pi G_N}m^2\delta^0_{\mu_i}\delta^0_{\nu_i}}{\prod_{i=1}^{l}\left((p_1-\sum_{j=1}^{i}\ell_j)^2-m^2+i\epsilon\right)}\,. \quad (3.16)$$

In the static limit $(p_1-L)^2-m^2+i\epsilon=L^2-2p_1\cdot L+i\epsilon\simeq L_0^2-\vec{L}^2-2mL_0+i\epsilon$. In the limit where the mass m is large compared to the graviton loop momenta $|L|\ll m$ we have

$$L_0^2-\vec{L}^2-2mL_0+i\epsilon=\left(L_0-m-\sqrt{\vec{L}^2+m^2-i\epsilon}\right)\left(L_0-m+\sqrt{\vec{L}^2+m^2-i\epsilon}\right)\\ \simeq\left(L_0-2m-\frac{\vec{L}^2}{2m}+i\epsilon\right)\left(L_0+\frac{\vec{L}^2}{2m}-i\epsilon\right)\simeq-2m\left(L_0-i\epsilon\right)\,. \quad (3.17)$$

Therefore we have

$$\mathcal{L}(p_1,p_2,\ell_1,\ldots,\ell_{l+1})\simeq i\sqrt{32\pi G_N}m^2\delta^0_{\mu_{l+1}}\delta^0_{\nu_{l+1}}\prod_{i=1}^{l}\frac{-i2\sqrt{2\pi G_N}m\delta^0_{\mu_i}\delta^0_{\nu_i}}{\sum_{j=1}^{i}\ell_j^0-i\epsilon}\,. \quad (3.18)$$

Using momentum conservation $\ell_1+\cdots+\ell_{l+1}=p_1-p_2$ and that in the static limit $p_1^0-p_2^0\simeq 0$ we have

$$\mathcal{L}(p_1,p_2,\ell_1,\ldots,\ell_{l+1})\simeq 2mi\epsilon\prod_{i=1}^{l+1}\frac{-i2\sqrt{2\pi G_N}m\delta^0_{\mu_i}\delta^0_{\nu_i}}{\sum_{j=1}^{i}\ell_j^0-i\epsilon}\,. \quad (3.19)$$

Using the identity[‡]

$$\sum_{\sigma\in\mathfrak{S}_{l+1}}\prod_{i=1}^{l+1}\frac{1}{\sum_{j=1}^{i}x_{\sigma(j)}}=\prod_{i=1}^{l+1}\frac{1}{x_i}\,. \tag{3.22}$$

In the limit $\epsilon\to 0$ the expression vanishes unless some of the ℓ_j^0 vanish at the same time. This means that one needs to pick the residues at $\ell_j^0=i\epsilon$ for $j=1,\dots,l$ to have a non vanishing answer. This implies that the amplitude (3.14) reduces to

$$\begin{aligned}i\mathcal{M}_3^{(l)}(p_1,q)\simeq&-i^l\left(2\sqrt{2\pi G_N}m\right)^{l+1}\\&\times\int\prod_{n=1}^{l}\frac{d^d\vec{\ell}_n}{(2\pi)^d}\prod_{i=1}^{l+1}\frac{\mathcal{P}^{00,\rho_i\sigma_i}}{\prod_{i=1}^{l+1}(\ell_i^2+i\epsilon)}\mathcal{M}_{\rho_1\sigma_1,\dots,\rho_{l+1}\sigma_{l+1}}(\ell_1,\dots,\ell_{l+1},q)\Big|_{\ell_i^0=0}\end{aligned} \tag{3.23}$$

with $\ell_1+\cdots+\ell_{l+1}=q$. We recall that

$$\mathcal{P}^{00,\rho\sigma}=\delta_0^\rho\delta_0^\sigma-\frac{\eta^{\rho\sigma}}{D-2}\,. \tag{3.24}$$

The amplitude (3.23) corresponds to the graph where the scalar line has been collapsed to a point

$\mathcal{M}_3^{(l)}(p_1,q)\simeq$ 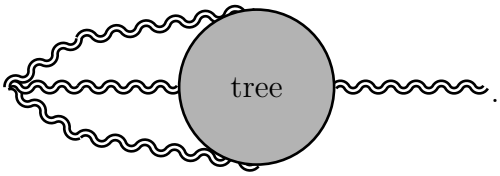

. (3.25)

[‡]This was proven in the appendix of [175]. We give here an alternative proof using recursion. For $l=1$ we have $\Sigma(2)=\frac{1}{x_1(x_1+x_2)}+\frac{1}{x_2(x_1+x_2)}=\frac{1}{x_1x_2}$. Assuming that (3.22) is true at the order l, then at the order $l+1$ we have

$$\Sigma(l+1)=\sum_{\sigma\in\mathfrak{S}_{l+1}}\prod_{i=1}^{l+1}\frac{1}{\sum_{j=1}^{i}x_{\sigma(j)}}=\frac{1}{x_1+\cdots+x_{l+1}}\sum_{i=1}^{l+1}\sum_{\sigma\in\mathfrak{S}_l}\prod_{i=1}^{l}\frac{1}{\sum_{j=1}^{i}\hat{x}_{\sigma(j)}} \tag{3.20}$$

where $\sigma(n+1)=i$ and the $\{\hat{x}_1,\dots,\hat{x}_l\}=\{x_1,\dots,x_{l+1}\}\backslash\{x_i\}$. By recursion hypothesis we can use the expression for $\Sigma(l)$

$$\Sigma(l+1)=\frac{1}{x_1+\cdots+x_{l+1}}\sum_{i=1}^{l+1}\prod_{i=1}^{l}\frac{1}{\hat{x}_i}=\frac{1}{x_1+\cdots+x_{l+1}}\sum_{i=1}^{l+1}x_i\prod_{i=1}^{l+1}\frac{1}{x_i}=\prod_{i=1}^{l+1}\frac{1}{x_i}\,. \tag{3.21}$$

In the static with $q = (0, \vec{q})$, $|q| \ll m$, the $l+2$-tree level gravitons amplitude has the leading behaviour

$$\prod_{n=1}^{l+1} \mathcal{P}^{00,\rho_i\sigma_i} \mathcal{M}_{\rho_i\sigma_i,\cdots,\rho_{l+1}\sigma_{l+1}}(\ell_1,\ldots,\ell_{l+1},q) \propto {G_N}^{l/2} q^2\,, \tag{3.26}$$

and higher powers of $\vec{q}^2$ contribute to higher powers of $\hbar$ and are sub-leading quantum corrections (see section 3.3.1 for more about this).

Therefore, the classical contribution to the stress-tensor in (3.4) is given by[§]

$$\langle T^{(l)}_{\mu\nu}\rangle = \pi^l (G_N m)^l m \Big(c_1^{(l)}(d)\delta^0_\mu\delta^0_\nu + c_2^{(l)}(d)\big(\frac{q_\mu q_\nu}{q^2} - \eta_{\mu\nu}\big)\Big)\, J_{(l)}(q^2)\,, \tag{3.27}$$

where $c_1^{(l)}(d)$ and $c_2^{(l)}(d)$ are rational functions of the dimension d and $J_{(n)}(q^2)$ is the massless n-loop sunset graph

$J_{(n)}(\vec{q}^2) =$ 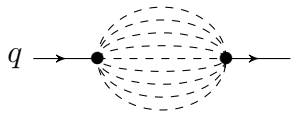 $= \displaystyle\int \frac{\vec{q}^2}{\prod_{i=1}^n \vec{l}_i^2\,(\vec{l}_1+\cdots+\vec{l}_n+\vec{q})^2} \prod_{i=1}^n \frac{d^d\vec{l}_i}{(2\pi)^d}\,.$ (3.28)

3.2.2 The master integrals for the classical limit

The master integrals (3.28) can be evaluated straightforwardly with the parametric representation of the n-loop sunset in D dimensions (see [178])

$$J_{(n)}(\vec{q}^2) = \frac{(\vec{q}^2)^{\frac{n(d-2)}{2}}}{(4\pi)^{\frac{nd}{2}}}\Gamma\left(n+1-\frac{nd}{2}\right)\int_{x_i\geq 0}\left(\frac{1}{x_1}+\cdots+\frac{1}{x_n}+1\right)^{\frac{(n+1)(2-d)}{2}}\prod_{i=1}^n \frac{dx_i}{x_i^{\frac{d}{2}}} \tag{3.29}$$

since the first Symanzik polynomial is $U_{n+1} = \left(\sum_{i=1}^{n+1}\frac{1}{x_i}\right)\left(\prod_{i=1}^{n+1} x_i\right)$ and the second Symanzik polynomial is $F_{n+1} = -q^2 x_1\cdots x_{n+1} = \vec{q}^2 x_1\cdots x_{n+1}$. Changing variables to $y_i = 1/x_i$ we have

$$J_{(n)}(\vec{q}^2) = \frac{(\vec{q}^2)^{\frac{n(d-2)}{2}}}{(4\pi)^{\frac{nd}{2}}}\Gamma\left(n+1-\frac{nd}{2}\right)\int_{y_i\geq 0}(y_1+\cdots+y_n+1)^{\frac{(n+1)(2-d)}{2}}\prod_{i=1}^n \frac{dy_i}{y_i^{\frac{4-d}{2}}}\,. \tag{3.30}$$

Using the expression for Euler's beta-function

$$\int_0^\infty (x+a)^\alpha \frac{dx}{x^{1-\beta}} = a^{\alpha+\beta}\frac{\Gamma(-\beta-\alpha)\Gamma(\beta)}{\Gamma(-\alpha)}, \tag{3.31}$$

[§]We have checked this explicitly to three-loop order using the `LiteRed` code [176, 177].

the master integral is readily evaluated to be

$$J_{(n)}(\vec{q}^2) = \frac{(\vec{q}^2)^{\frac{n(d-2)}{2}}}{(4\pi)^{\frac{nd}{2}}} \frac{\Gamma\left(n+1-\frac{nd}{2}\right)\Gamma\left(\frac{d-2}{2}\right)^{n+1}}{\Gamma\left(\frac{(n+1)(d-2)}{2}\right)} . \tag{3.32}$$

The master integrals develop ultraviolet poles at loop orders, inducing divergences in the stress-energy tensor. We will show in section 3.4 how to renormalise these divergences with the introduction of higher-derivative couplings.

3.3 The metric perturbation from graviton emission

Using the relation (3.7) between the metric perturbation and using the expression (3.27) for the stress-energy tensor in d-dimension in the static limit we have

$$h^{(l+1)}_{\mu\nu}(\vec{q}) = -8\left(c_1^{(l)}(d)(2\delta^0_\mu\delta^0_\nu - \eta_{\mu\nu}) + c_2^{(l)}(d)\left(2\frac{q_\mu q_\nu}{q^2} + (d-2)\eta_{\mu\nu}\right)\right) \times \frac{(\pi G_N m)^{l+1} J_{(l)}(\vec{q}^2)}{\vec{q}^2} . \tag{3.33}$$

The static space-time components are obtained by computing the Fourier transform in d dimensions

$$h^{(l+1)}_{\mu\nu}(\vec{x}) = \int_{\mathbb{R}^d} h^{(l+1)}_{\mu\nu}(\vec{q}) e^{i\vec{q}\cdot\vec{x}} \frac{d^d\vec{q}}{(2\pi)^d} . \tag{3.34}$$

Using the Fourier transformations given in appendix A.1, and setting $r = |\vec{x}|$, the Fourier transform of the master integrals are given by

$$\int_{\mathbb{R}^d} \frac{J_{(l)}(\vec{q}^2)}{\vec{q}^2} e^{i\vec{q}\cdot\vec{x}} \frac{d^d\vec{q}}{(2\pi)^d} = \left(\frac{\Gamma\left(\frac{d-2}{2}\right)}{4\pi^{\frac{d}{2}}} \frac{1}{r^{d-2}}\right)^{l+1} \tag{3.35}$$

which is finite to all loop orders. The infrared divergences in the momentum space representation in (3.32) have been cancelled by the Fourier transform.[¶]

The tensorial Fourier transform

$$\int_{\mathbb{R}^d} \frac{q_i q_j}{\vec{q}^2} \frac{J_{(l)}(\vec{q}^2)}{\vec{q}^2} e^{i\vec{q}\cdot\vec{x}} \frac{d^d\vec{q}}{(2\pi)^d} = \left(\frac{\Gamma\left(\frac{d-2}{2}\right)}{4\pi^{\frac{d}{2}}} \frac{1}{r^{d-2}}\right)^{l+1} \frac{1}{2-l(d-2)} \left(-\delta_{ij} + (l+1)(d-2)\frac{x_i x_j}{r}\right) . \tag{3.36}$$

[¶]This fact had been noticed by L. Planté in his PhD thesis [173].

diverges for $l = 1$ and $d = 4$ and for $l = 2$ and $d = 3$, and are otherwise finite.

By spherical symmetry we parameterise the metric in $d + 1$ dimensions

$$ds^2 = h_0(r,d)dt^2 - h_1(r,d)d\vec{x}^2 - h_2(r,d)\frac{(\vec{x}\cdot d\vec{x})^2}{\vec{x}^2}\,, \tag{3.37}$$

so that

$$h_i(\vec{x}) = h_i^{(0)} + \sum_{l\geq 1} h_i^{(l)}(\vec{x})\,, \tag{3.38}$$

with $h_i^{(0)} = 1, 1, 0$ for $i = 0, 1, 2$, the post-Minkowskian expansion of the metric components

$$\begin{aligned}
h_0^{(l+1)}(r,d) &= -\frac{16}{d-1}\left((d-2)c_1^{(l)}(d) + c_2^{(l)}(d)\right)\left(\frac{\rho(r,d)}{4}\right)^{l+1}, \\
h_1^{(l+1)}(r,d) &= \frac{16}{d-1}\left(c_1^{(l)}(d) - \left(1 + \frac{d-1}{2-l(d-2)}\right)c_2^{(l)}(d)\right)\left(\frac{\rho(r,d)}{4}\right)^{l+1}, \\
h_2^{(l+1)}(r,d) &= 16\frac{(d-2)(l+1)}{2-l(d-2)}c_2^{(l)}(d)\left(\frac{\rho(r,d)}{4}\right)^{l+1}.
\end{aligned} \tag{3.39}$$

We have introduced the radial parameter

$$\rho(r,d) = \frac{\Gamma\left(\frac{d-2}{2}\right)}{\pi^{\frac{d-2}{2}}}\frac{G_N m}{r^{d-2}}\,, \tag{3.40}$$

which is our post-Minkowskian expansion parameter. Recall that in $d+1$ dimensions the length dimension of $[G_N m] = (length)^{d-2}$ and $\rho(r,d)$ is dimensionless.

The metric component present poles in four dimensions ($d = 3$) from two-loop order and in five dimensions ($d = 4$) from one-loop order. Such divergences will be removed by the contribution from the non-minimal coupling contributions in section 3.4.

3.3.1 Tree-level amplitude

At tree-level, the only contributing diagram is

$\mathcal{M}_3^{(0)}(p_1,q) =$ 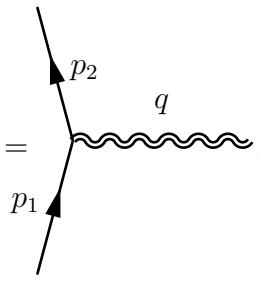

, (3.41)

is the emission of a graviton from the scattering of two massive scalars of momenta p_1 and p_2 and $p_1^2 = p_2^2 = m^2$ with momentum transfert $q = p_1 - p_2$. The scattering amplitude is given by the 2-scalar-1-graviton vertex $\tau^{\mu\nu}(p_1, p_2)$ in (A.6)

$$i\mathcal{M}_3^{(0)}(p_1, q) = -\frac{i\sqrt{32\pi G_N}}{2\sqrt{4E_1E_2}}\epsilon^{\mu\nu}\tau_{\mu\nu} = -\frac{i\sqrt{32\pi G_N}}{2}\epsilon^{\mu\nu}\left(p_{1\mu}p_{2\nu}+p_{2\mu}p_{1\nu}-\eta_{\mu\nu}(p_1\cdot p_2-m^2)\right). \tag{3.42}$$

Using that $P = (p_1 + p_2)/2$ and $q = p_1 - p_2$ we have that

$$i\mathcal{M}_3^{(0)}(p_1, q) = -\frac{i\sqrt{32\pi G_N}}{2\sqrt{4E_1E_2}}\epsilon^{\mu\nu}\left(2P_\mu P_\nu - \frac{1}{2}(q_\mu q_\nu - \eta_{\mu\nu}q^2)\right). \tag{3.43}$$

In the static limit $q = p_1 - p_2 \simeq (0, \vec{q})$, $E_1 \simeq E_2 \simeq m$ and $|\vec{q}| \ll m$ we have

$$\langle T_{\mu\nu}^{(0)}(q^2)\rangle \simeq m\delta_\mu^0\delta_\nu^0 + \left(\frac{q_iq_j}{\vec{2}q^2}\eta_\mu^i\eta_\nu^j + \frac{1}{2}\eta_{\mu\nu}\right)\vec{q}^2\,. \tag{3.44}$$

The $\vec{q}^2$ term in this expression is the contact term which has a higher power of $\hbar$ and does not contribute to the classical limit [27, 52]. The coefficients of the classical contribution to the stress-tensor at tree-level are given by

$$\begin{aligned} c_1^{(0)}(d) &= 1, \\ c_2^{(0)}(d) &= 0\,. \end{aligned} \tag{3.45}$$

From this we deduce the metric components in $d+1$ dimensions using (3.39)

$$\begin{aligned} h_0^{(1)}(r, d) &= -4\frac{d-2}{d-1}\rho(r, d), \\ h_1^{(1)}(r, d) &= \frac{4}{d-1}\rho(r, d), \\ h_2^{(1)}(r, d) &= 0\,, \end{aligned} \tag{3.46}$$

where $\rho(r, d)$ is defined in (3.40). This reproduces the expression given in [165, 167].

3.3.2 One-loop amplitude

At one-loop the only contributing diagram to the classical limit is

$$i\mathcal{M}_3^{(1)}(p_1,q) = \quad = -\frac{i\sqrt{32\pi G_N}}{2}\epsilon_{\mu\nu}T^{(1)\ \mu\nu}(q^2)\,, \tag{3.47}$$

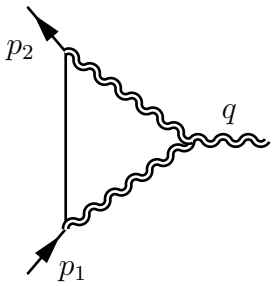

from which we extract the one-loop contribution to the stress-energy tensor in $d+1$ dimensions

$$T^{(1)\ \mu\nu}(q^2) = \frac{i8\pi G_N}{\sqrt{4E_1E_2}}\int\frac{d^{d+1}l}{(2\pi)^D}\frac{\tau^{\sigma\rho}(p_1,l+p_1)\tau^{\mu\nu}_{(3)\sigma\rho,\kappa\delta}(l,q)\tau^{\kappa\delta}(p_2,l+p_1)}{(l^2+i\epsilon)((l+q)^2+i\epsilon)((l+p_1)^2-m^2+i\epsilon)}, \tag{3.48}$$

where $\tau^{\mu\nu}_{(3)\ \pi\rho,\sigma\tau}(p_1,p_2)$ is the three graviton vertex and $\tau^{\mu\nu}(p_1,p_2)$ the vertex for the emission of a graviton from two scalars with momenta p_1 and p_2. We refer to appendix A.2 for definitions and normalisation of our vertices.

In the static limit, $\vec{q}^2 \ll m^2$, the classical contribution coming from the two scalars to one-graviton vertex is

$$\tau_{\alpha\beta} \approx 2m^2\delta^0_\alpha\delta^0_\beta, \tag{3.49}$$

using that $p_1^2 = p_2^2 = m^2$. This gives for the stress-energy tensor

$$T^{(1)\ \mu\nu}(q^2) = i16\pi G_N m^3\int\frac{d^{d+1}l}{(2\pi)^D}\frac{\tau^{\mu\nu}_{(3)00,00}(l,q)}{(l^2+i\epsilon)((l+q)^2+i\epsilon)((l+p_1)^2-m^2+i\epsilon)}. \tag{3.50}$$

At this point, we want to focus on the computation of the classical contribution at the static limit. Thus, we will employ a trick, which will prove useful for higher loops. We symmetrize the diagram

$$T^{(1)\ \mu\nu}(q^2) = i8\pi G_N m^3\int\frac{d^{d+1}l}{(2\pi)^D}\frac{\tau^{\mu\nu}_{(3)00,00}(l,q)}{(l^2+i\epsilon)((l+q)^2+i\epsilon)} \times\left[\frac{1}{(l+p_1)^2-m^2+i\epsilon}+\frac{1}{(l-p_2)^2-m^2+i\epsilon}\right]. \tag{3.51}$$

In the approximation $l^2 \ll m^2$ we have $(l+p_i)^2 - m^2 = l^2 + 2l\cdot p_1 = l^2 + 2l_0 E - \vec{l}\cdot\vec{q} \simeq l_0^2 + 2ml_0$ and the amplitude reduces at leading order

$$T^{(1)\ \mu\nu}(q^2) \simeq i8\pi G_N m^3 \int \frac{d^{d+1}l}{(2\pi)^D} \frac{\tau^{\mu\nu}_{(3)00,00}(l,q)}{(l^2+i\epsilon)((l+q)^2+i\epsilon)} \times \left[\frac{1}{l_0^2+2ml_0+i\epsilon} + \frac{1}{l_0^2-2ml_0+i\epsilon}\right]. \quad (3.52)$$

It is obvious that at $\mathcal{O}(\epsilon^0)$ order we get a zero contribution at leading order in $1/m$, since $l_0 \ll m$. Thus, we can compute the leading contribution of the integral over l_0 via *Cauchy's theorem*, by taking the residue $2ml_0 = i\epsilon$ and closing the contour of integration in the upper half-plane[‖]

$$T^{(1)\ \mu\nu}(q^2) = 4\pi G_N m^2 \int \frac{d^d\vec{l}}{(2\pi)^d} \frac{\tau^{\mu\nu}_{(3)00,00}(l,q)}{(\vec{l}^2-i\epsilon)((\vec{l}+\vec{q})^2-i\epsilon)}\bigg|_{l_0=0}, \quad (3.53)$$

with

$$\tau^{\mu\nu}_{(3)00,00}(l,q) = \frac{1}{d-1}\bigg((d-2)\big(l^\mu l^\nu + (l+q)^\mu(l+q)^\nu + q^\mu q^\nu + \frac{3}{2}\eta^{\mu\nu}\vec{q}^2\big) - 2(d-2)\big(\vec{l_1}^2 + (\vec{l_1}+\vec{q})^2\big)(\delta^\mu_0\delta^\mu_0 - \frac{\eta^{\mu\nu}}{4}) - 2(d-3)\vec{q}^2\delta^\mu_0\delta^\mu_0\bigg). \quad (3.54)$$

The component of the stress-tensor are proportional to the one-loop master integral $J_{(1)}(\vec{q}^2)$ as expected from the general discussion of section 3.2.2

$$\langle T^{(1)}_{\mu\nu}\rangle = \pi G_N m^2 \left(c_1^{(1)}(d)\delta^0_\mu\delta^0_\nu + c_2^{(1)}(d)\left(\frac{q_\mu q_\nu}{q^2} - \eta_{\mu\nu}\right)\right) J_{(1)}(q^2), \quad (3.55)$$

with the master integral

$$J_{(1)}(q^2) = \frac{\Gamma\left(\frac{4-d}{2}\right)\Gamma\left(\frac{d-2}{2}\right)^2}{2^d\pi^{\frac{d}{2}}\Gamma(d-2)}\left(\vec{q}^2\right)^{\frac{d-2}{2}}, \quad (3.56)$$

[‖] One could have taken the residue at $2ml_0 = -i\epsilon$ and closing the contour in the lower half-plane with the same result.

and the coefficients

$$c_1^{(1)}(d) = -\frac{2(4d^2-15d+10)}{(d-1)^2},$$
$$c_2^{(1)}(d) = -\frac{2(d-2)(3d-2)}{(d-1)^2}. \tag{3.57}$$

3.3.2.1 The one-loop contribution to the metric components

Using (3.39) we get for the metric components in $d+1$ dimensions

$$h_0^{(2)}(r,d) = \frac{8(d-2)^2}{(d-1)^2}\rho(r,d)^2,$$
$$h_1^{(2)}(r,d) = -\frac{4(2d^2-9d+14)}{(d-4)(d-1)^2}\rho(r,d)^2,$$
$$h_2^{(2)}(r,d) = \frac{4(d-2)^2(3d-2)}{(d-4)(d-1)^2}\rho(r,d)^2, \tag{3.58}$$

where $\rho(r,d)$ is defined in (3.40).

This reproduces the expression given in [165] and the expression in [167, eq. (22)] for $\alpha = 0$.

3.3.3 Two-loop amplitude

The diagrams contributing to the classical corrections at third post-Minkowskian order of the metric at the two-loop graphs

$$i\mathcal{M}_3^{(2)}(p_1,q) = -\sqrt{32\pi G_N}T^{(2)\,\mu\nu}\epsilon_{\mu\nu}, \tag{3.59}$$

there are four contributions

$T^{(2)\mu\nu}_{(a)} =$ 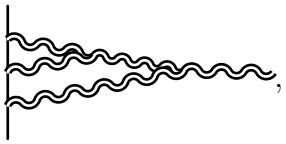 , $T^{(2)\mu\nu}_{(b)} =$ 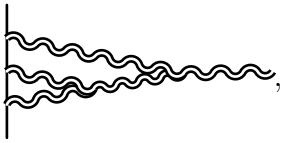 ,

$T^{(2)\mu\nu}_{(c)} =$ 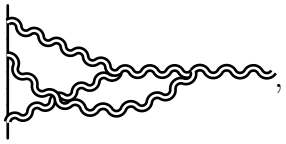 , $T^{(2)\mu\nu}_{(d)} =$ 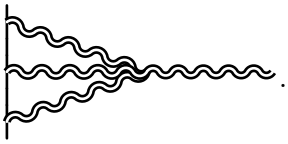 .

3.3.3.1 The diagrams (a), (b), (c)

The sum of the contributions from the diagrams (a), (b), (c) after appropriate labelling of the momenta, can be expressed as

$$\sum_{i=a}^{c} T^{(2)\,\mu\nu}_{(i)} = -\frac{16G_N^2\pi^2}{m}\int\prod_{n=1}^{3}\frac{d^{d+1}l_n}{(2\pi)^{2d}}\delta(l_1+l_2+l_3+q)$$
$$\times\frac{\tau^{\gamma\delta}(p_1,l_1+p_1)\tau^{\sigma\tau}(l_1+p_1,-l_2+p_1)\tau^{\iota\theta}(l_2-p_2,-p_2)\tau^{\phi\chi}_{(3)\iota\theta,\sigma\tau}(-l_2,l_1+q)\cdot\mathcal{P}^{\alpha\beta}_{\phi\chi}\cdot\tau^{\mu\nu}_{(3)\alpha\beta,\gamma\delta}(l_1+q,q}{l_1^2l_2^2l_3^2(l_1+q)^2}$$
$$\times\left(\frac{1}{(l_1+p_1)^2-m^2}\frac{1}{(l_2-p_2)^2-m^2}+\frac{1}{(l_3+p_1)^2-m^2}\frac{1}{(l_1-p_2)^2-m^2}\right.$$
$$\left.+\frac{1}{(l_3+p_1)^2-m^2}\frac{1}{(l_2-p_2)^2-m^2}\right). \quad (3.60)$$

Using the approximate form of the two scalars one graviton vertex in (3.49) and $(l_1+p_1)^2-m^2\approx 2ml_1^0$ and taking the residue $2ml_i^0=i\epsilon$, since for the rest of the residues we get a zero contribution at order $\mathcal{O}(\epsilon^0)$, we get

$$\sum_{i=a}^{c} T^{(2)\,\mu\nu}_{(i)} = 32\pi^2G_N^2m^3\int\prod_{n=1}^{2}\frac{d^{d+1}l_n}{(2\pi)^{2d}}\frac{\tau^{\mu\nu}_{(3)\alpha\beta,00}(l_1+q,q)\cdot\mathcal{P}^{\alpha\beta}_{\phi\chi}\cdot\tau^{\phi\chi}_{(3)\,00,00}(-l_2,l_1+q)}{(\vec{l_1})^2(\vec{l_2})^2(\vec{l_3})^2(\vec{l_1}+\vec{q})^2}\Bigg|_{l_1^0=l_2^0=0}, \quad (3.61)$$

with

$$\eta_{\mu\nu}\tau^{\mu\nu}_{(3)\phi\chi,00}(l_1+q,q) = \big(l^\mu l^\nu-(l+q)^\mu(l+q)^\nu-q^\mu q^\nu\big)-\frac{3}{2}\eta^{\mu\nu}\vec{q}^2\big(\eta^{\mu\nu}-(d-1)\delta_0^\mu\delta_0^\nu\big)$$
$$+\frac{\eta^{\mu\nu}}{2}\big(\vec{l_1}^2-(\vec{l_1}+\vec{q})^2\big)-\frac{5-d}{2}\delta_0^\mu\delta_0^\nu\big(\vec{l_1}^2+(\vec{l_1}+\vec{q})^2\big), \quad (3.62)$$

and

$$\delta^0_\mu\delta^0_\nu\tau^{\mu\nu}_{(3)\phi\chi,00}(l_1+q,q) = \frac{1}{d-1}\Big((d-3)\big((l+q)^\mu(l+q)^\nu+q^\mu q^\nu\big)+(d-1)\big(l_1^\mu l_1^\nu-\frac{\vec{l_1}^2}{2}(3\delta_0^\mu\delta_0^\nu-\eta^{\mu\nu})\big)$$
$$+\frac{\eta^{\mu\nu}-\delta_0^\mu\delta_0^\nu}{2}\big(\vec{q}^2(d-5)+(3d-7)(\vec{l_1}+\vec{q})^2\big)\Big), \quad (3.63)$$

and

$$\tau^{\mu\nu}_{(3)00,00}(l,q) = \frac{1}{d-1}\Big((d-2)\big(l^\mu l^\nu+(l+q)^\mu(l+q)^\nu+q^\mu q^\nu+\frac{3}{2}\eta^{\mu\nu}\vec{q}^2\big)$$
$$-2(d-2)\big(\vec{l_1}^2+(\vec{l_1}+\vec{q})^2\big)(\delta_0^\mu\delta_0^\mu-\frac{\eta^{\mu\nu}}{4})-2(d-3)\vec{q}^2\delta_0^\mu\delta_0^\mu\Big). \quad (3.64)$$

Using the `LiteRed` code [176, 177] in d dimensions, we find that all the contributions are proportional to the master integral as expected from the general discussion of section 3.2.2

$$\begin{aligned} J_{(2)}(\vec{q}) &= \int \prod_{i=1}^{2} \frac{d^d \vec{l}_i}{(2\pi)^d} \frac{\vec{q}^2}{\prod_{i=1}^{2} \vec{l}_i^2 (\vec{l}_1 + \vec{l}_2 + \vec{q})^2} \\ &= -\frac{\vec{q}^2}{32\pi^2(d-3)} - \left(-3 + \gamma_E - \log(4\pi) + \log(\vec{q}^2)\right) \vec{q}^2 + O(d-3) \end{aligned} \tag{3.65}$$

where $\gamma_E = 0.57721\cdots$ is the Euler-Mascheroni constant [179].

We find for the 00-component

$$\sum_{i=a}^{c} T_{(i)}^{(2)\,00} = \frac{32\pi^2 G_N^2 m^3}{3} \frac{6d^3 - 45d^2 + 134d - 160}{(d-4)(d-1)^2} J_{(2)}(\vec{q}^2)\,, \tag{3.66}$$

and for the trace part

$$\sum_{i=a}^{c} T_{(i)}^{(2)\,\mu\nu} \eta_{\mu\nu} = -\frac{32\pi^2 G_N^2 m^3}{3} \frac{10d^3 - 63d^2 + 123d - 86}{(d-1)^2} J_{(2)}(\vec{q}^2)\,. \tag{3.67}$$

3.3.3.2 The diagrams (d)

The diagram (d) after symmetrisation over the massive scalar legs reads

$$\begin{aligned} T_{(d)}^{(2)\,\mu\nu} = -\frac{32 G_N^2 \pi^2}{3m} \int \prod_{n=1}^{3} \frac{d^{d+1} l_n}{(2\pi)^{2d}} \frac{\delta(l_1 + l_2 + l_3 + q)}{l_1^2 l_2^2 l_3^2} \Bigg(& \frac{1}{(l_1 + p_1)^2 - m^2 + i\epsilon} \frac{1}{(l_2 - p_2)^2 - m^2 + i\epsilon} \\ + \frac{1}{(l_3 + p_1)^2 - m^2 + i\epsilon} \frac{1}{(l_1 - p_2)^2 - m^2 + i\epsilon} & + \frac{1}{(l_3 + p_1)^2 - m^2 + i\epsilon} \frac{1}{(l_2 - p_2)^2 - m^2 + i\epsilon} \Bigg) \\ \times \tau^{\gamma\delta}(p_1, l_1 + p_1) \tau^{\sigma\tau}(l_1 + p_1, -l_2 + p_1) \tau^{\iota\theta}(l_2 - p_2, -p_2) & \tau^{\mu\nu}_{(4)\gamma\delta,\sigma\tau,\iota\theta}(q, l_1, l_2, l_3), \end{aligned} \tag{3.68}$$

and leads to the contribution

$$T_{(d)}^{(2)\,\mu\nu} = -\frac{64\pi^2 G_N^2 m^3}{3} \int \prod_{n=1}^{2} \frac{d^{d+1} l_n}{(2\pi)^d} \frac{\tau^{\mu\nu}_{(4)\,00,00,00}(q, l_1, l_2, -l_1 - l_2 - q)}{(\vec{l}_1)^2 (\vec{l}_2)^2 (\vec{l}_1 + \vec{l}_2 + \vec{q})^2} \Bigg|_{l_1^0 = l_2^0 = 0} \tag{3.69}$$

with the vertex

$$\tau^{\mu\nu}_{(4)\,00,00,00}(q,l_1,l_2,l_3) = \frac{1}{(d-1)^2}\Bigg(\vec{q}^{\,2}\frac{\delta^\mu_0\delta^\nu_0}{2}(7d^2-45d+70)-\vec{q}^{\,2}\frac{\eta^{\mu\nu}}{2}(d-2)(6d-23) + (d-2)\Big((9-2d)q^\mu q^\nu + (7-2d)\big(l_1^\mu l_1^\nu + l_2^\mu l_2^\nu + l_3^\mu l_3^\nu\big)\Big) + \frac{d-2}{2}\big(\vec{l_1}^{\,2}+\vec{l_2}^{\,2}+\vec{l_3}^{\,2}\big)\big(\delta^\mu_0\delta^\nu_0(7d-23)-\eta^{\mu\nu}(2d-9)\big)\Bigg)\,. \quad (3.70)$$

Evaluating these integral we find, for the 00-component

$$T^{(2)\,00}_{(d)} = -\frac{32\pi^2 G_N^2 m^3}{3}\frac{(4-d)(6-d)}{(d-1)^2}J_{(2)}(\vec{q}^{\,2})\,, \quad (3.71)$$

and for the trace part

$$T^{(2)\,\mu\nu}_{(d)}\eta_{\mu\nu} = \frac{64\pi^2 G_N^2 m^3}{3}\frac{3d^3-20d^2+41d-30}{(d-1)^2}J_{(2)}(\vec{q}^{\,2})\,. \quad (3.72)$$

3.3.3.3 The two-loop contribution to the metric components

Summing up all the contributions the two-loop stress-tensor is given by

$$\langle T^{(2)}_{\mu\nu}\rangle = \pi^2 G_N^2 m^3\Big(c_1^{(2)}(d)\delta^0_\mu\delta^0_\nu + c_2^{(2)}(d)\big(\frac{q_\mu q_\nu}{q^2}-\eta_{\mu\nu}\big)\Big)\,J_{(2)}(q^2)\,, \quad (3.73)$$

with the coefficients given by

$$c_1^{(2)}(d) = \frac{32}{3(d-4)(d-1)^3}\left(9d^4-70d^3+203d^2-254d+104\right),$$
$$c_2^{(2)}(d) = \frac{64(d-2)}{3(d-4)(d-1)^3}\left(2d^3-13d^2+25d-10\right), \quad (3.74)$$

and the expression for the master integral

$$J_{(2)}(\vec{q}^{\,2}) = \frac{\Gamma(3-d)\Gamma\left(\frac{d-2}{2}\right)^3}{(4\pi)^d\Gamma\left(\frac{3(d-2)}{2}\right)}\left(\vec{q}^{\,2}\right)^{d-2}\,. \quad (3.75)$$

From which we extract the metric components using the relations (3.39) (using the definition of $\rho(r,d)$ in (3.40))

$$\begin{aligned} h_0^{(3)}(r,d) &= -\frac{8(3d-7)(d-2)^3}{(d-4)(d-1)^3}\rho(r,d)^3, \\ h_1^{(3)}(r,d) &= \frac{8(7d^4-63d^3+214d^2-334d+212)}{3(d-3)(d-4)(d-1)^3}\rho(r,d)^3, \\ h_2^{(3)}(r,d) &= -\frac{8(d-2)^2(2d^3-13d^2+25d-10)}{(d-3)(d-4)(d-1)^3}\rho(r,d)^3\,. \end{aligned} \tag{3.76}$$

3.3.4 Three-loop amplitude

The diagrams contributing to the classical corrections at third post-Minkowskian order of the metric at the two-loop graphs

$$i\mathcal{M}_3^{(3)}(p_1,q) = -\sqrt{32\pi G_N}T^{(3)\,\mu\nu}\epsilon_{\mu\nu}, \tag{3.77}$$

where the three-loop stress-tensor is given by five distinct diagrams

$T^{(3)\mu\nu}_{(a)} =$ 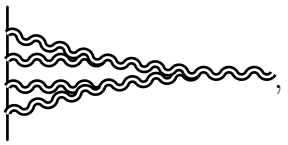 ,
$T^{(3)\mu\nu}_{(b)} =$ 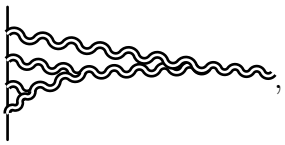 ,
$T^{(3)\mu\nu}_{(c)} =$ 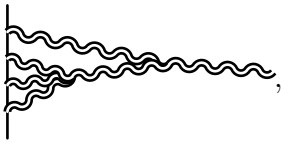 ,
$T^{(3)\mu\nu}_{(d)} =$ 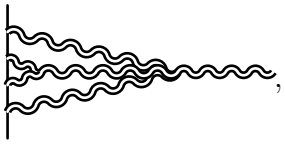 ,
$T^{(3)\mu\nu}_{(e)} =$ 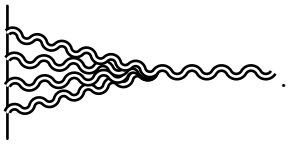 .

As before, we permute the internal momenta such that by taking the residue at $2ml_i^0 = i\epsilon$ from the massive propagators, we extract the non-analytic terms which contribute to the classical metric in the static limit. After taking the residues and including the symmetry factors

$$
\begin{aligned}
T^{(3)\,\mu\nu}_{(a)} &= 64\pi^3 G_N^3 m^4 \int \prod_{n=1}^{3} \frac{d^d\vec{l}_n}{(2\pi)^d} \frac{\tau^{\mu\nu}_{(3)\pi\rho,\sigma\tau}(l_1+l_2,q)\tau^{\pi\rho}_{(3)}(-l_1,l_1+l_2)\tau^{\sigma\tau}_{(3)}(-l_3,l_3+l_4)}{(\vec{l}_1)^2(\vec{l}_2)^2(\vec{l}_3)^2(\vec{l}_4)^2(\vec{l}_1+\vec{l}_2)^2(\vec{l}_3+\vec{l}_4)^2}\Bigg|_{l_1^0=l_2^0=l_3^0=0}\,,\\
T^{(3)\,\mu\nu}_{(b)} &= 256\pi^3 G_N^3 m^4 \int \prod_{n=1}^{3} \frac{d^d\vec{l}_n}{(2\pi)^d} \frac{\tau^{\mu\nu}_{(3)\sigma\tau,00}(l_1+q,q)\tau^{\pi\rho}_{(3)}(-l_3,l_3+l_4)\tau^{\sigma\tau}_{(3)00,\pi\rho}(-l_2,l_1+q)}{(\vec{l}_1)^2(\vec{l}_2)^2(\vec{l}_3)^2(\vec{l}_4)^2(\vec{l}_1+\vec{q})^2(\vec{l}_3+\vec{l}_4)^2}\Bigg|_{l_1^0=l_2^0=l_3^0=0}\,,\\
T^{(3)\,\mu\nu}_{(c)} &= -\frac{512\pi^3 G_N^3 m^4}{3} \int \prod_{n=1}^{3} \frac{d^d\vec{l}_n}{(2\pi)^d} \frac{\tau^{\mu\nu}_{(3)\alpha\beta,00}(l_1+q,q)\tau^{\alpha\beta}_{(4)00,00,00}(l_1+q,l_2,l_3,l_4)}{(\vec{l}_1)^2(\vec{l}_2)^2(\vec{l}_3)^2(\vec{l}_4)^2(\vec{l}_1+\vec{q})^2}\Bigg|_{l_1^0=l_2^0=l_3^0=0}\,,\\
T^{(3)\,\mu\nu}_{(d)} &= -256\pi^3 G_N^3 m^4 \int \prod_{n=1}^{3} \frac{d^d\vec{l}_n}{(2\pi)^d} \frac{\tau^{\gamma\delta}_{(3)}(-l_3,l_3+l_4)\tau^{\mu\nu}_{(4)\gamma\delta,00,00}(q,l_1,l_2,l_3+l_4)}{(\vec{l}_1)^2(\vec{l}_2)^2(\vec{l}_3)^2(\vec{l}_4)^2(\vec{l}_3+\vec{l}_4)^2}\Bigg|_{l_1^0=l_2^0=l_3^0=0}\,,\\
T^{(3)\,\mu\nu}_{(e)} &= \frac{256\pi^3 G_N^3 m^4}{3} \int \prod_{n=1}^{3} \frac{d^d\vec{l}_n}{(2\pi)^d} \frac{\tau^{\mu\nu}_{(5)00,00,00,00}(q,l_1,l_2,l_3,l_4)}{(\vec{l}_1)^2(\vec{l}_2)^2(\vec{l}_3)^2(\vec{l}_4)^2}\Bigg|_{l_1^0=l_2^0=l_3^0=0}\,,
\end{aligned}
\tag{3.78}
$$

with the five-graviton vertex contribution

$$
\begin{aligned}
&\tau^{\mu\nu}_{(5)\,00,00,00,00}(k_1,k_2,k_3,k_4,k_5) := \tilde{\tau}^{\mu\nu}_{(5)\,\alpha\beta,\gamma\delta,\epsilon\eta,\kappa\lambda}(k_1,k_2,k_3,k_4,k_5)\mathcal{P}^{\alpha\beta}_{00}\mathcal{P}^{\gamma\delta}_{00}\mathcal{P}^{\epsilon\eta}_{00}P^{\kappa\lambda}_{00}\\
&= \frac{1}{4(d-1)^3}\Bigg(4\delta^0_\mu\delta^0_\nu\Bigg(4(2d^3-18d^2+57d-61)k_1^2+(d-2)(8d^2-47d+79)\sum_{i=2}^{5}k_i^2\Bigg)\\
&-(d-2)\eta_{\mu\nu}\Bigg((29d^2-191d+362)k_1^2+(7d^2-61d+142)\sum_{i=2}^{5}k_i^2\Bigg)\\
&+2(d-2)\Bigg((11d^2-73d+150)k_{1\mu}k_{1\nu}+(7d^2-53d+102)(k_{2\mu}k_{2\nu}+k_{3\mu}k_{3\nu}+k_{4\mu}k_{4\nu}+k_{5\mu}k_{5\nu})\Bigg)\Bigg)
\end{aligned}
\tag{3.79}
$$

where the vertex $\tau^{\mu\nu}_{(5)\,\alpha\beta,\gamma\delta,\epsilon\eta,\kappa\lambda}(k_1,k_2,k_3,k_4,k_5)$ has been derived using the results of [180].

The integral reduction is done using the `LiteRed` code [176,177] in d dimensions. In agreement with the general analysis of section 3.2.2, we find that the classical contribution is proportional to the single master integral

$$
J_{(3)}(\vec{q}^2) = \int \frac{d^d\vec{l}_1 d^d\vec{l}_2 d^d\vec{l}_3}{(2\pi)^{3d}} \frac{\vec{q}^2}{\vec{l}_1^{\,2}\vec{l}_2^{\,2}\vec{l}_3^{\,2}(\vec{l}_1+\vec{l}_2+\vec{l}_3+\vec{q})^2}\,. \tag{3.80}
$$

3.3.4.1 The $\mu = \nu = 0$ component

$$
\begin{aligned}
T^{(3)\,00}_{(a)} &= -\frac{32\pi^3 G_N^3 m^4}{3}\frac{3d^5-169d^4+1378d^3-4592d^2+7256d-4752}{(d-4)^2(d-1)^3}J_{(3)}(\vec{q}^2),\\
T^{(3)\,00}_{(b)} &= -\frac{128\pi^3 G_N^3 m^4}{3}\frac{68d^6-1003d^5+6211d^4-20820d^3+40020d^2-41584d+17824}{(d-4)(d-3)(3d-4)(d-1)^3}J_{(3)}(\vec{q}^2),\\
T^{(3)\,00}_{(c)} &= \frac{64\pi^3 G_N^3 m^4}{3}\frac{37d^5-502d^4+2731d^3-7486d^2+10164d-5256}{(d-3)(3d-4)(d-1)^3}J_{(3)}(\vec{q}^2),\\
T^{(3)\,00}_{(d)} &= \frac{32\pi^3 G_N^3 m^4}{3}\frac{53d^4-615d^3+2690d^2-5572d+4840}{(d-4)(d-1)^3}J_{(3)}(\vec{q}^2),\\
T^{(3)\,00}_{(e)} &= 64\pi^3 G_N^3 m^4\frac{(6-d)(d^2-7d+14)}{(d-1)^3}J_{(3)}(\vec{q}^2).
\end{aligned}
\tag{3.81}
$$

3.3.4.2 Contraction with $\eta_{\mu\nu}$

$$
\begin{aligned}
T^{(3)\,\mu\nu}_{(a)}\eta_{\mu\nu} &= \frac{32\pi^3 G_N^3 m^4}{3}\frac{85d^6-1126d^5+6307d^4-19114d^3+32944d^2-30472d+11952}{(d-4)^2(d-1)^3}J_{(3)}(\vec{q}^2),\\
T^{(3)\,\mu\nu}_{(b)}\eta_{\mu\nu} &= \frac{128\pi^3 G_N^3 m^4}{3}\frac{168d^6-2231d^5+12319d^4-35796d^3+57396d^2-48304d+16736}{(d-4)(3d-4)(d-1)^3}J_{(3)}(\vec{q}^2),\\
T^{(3)\,\mu\nu}_{(c)}\eta_{\mu\nu} &= -\frac{64\pi^3 G_N^3 m^4}{3}\frac{147d^6-1801d^5+8727d^4-21555d^3+28942d^2-20148d+5688}{(3d-4)(d-1)^4}J_{(3)}(\vec{q}^2),\\
T^{(3)\,\mu\nu}_{(d)}\eta_{\mu\nu} &= -\frac{32\pi^3 G_N^3 m^4}{3}\frac{179d^5-2146d^4+10305d^3-24614d^2+28972d-13704}{(d-4)(d-1)^3}J_{(3)}(\vec{q}^2),\\
T^{(3)\,\mu\nu}_{(e)}\eta_{\mu\nu} &= \frac{64\pi^3 G_N^3 m^4}{3}\frac{29d^4-274d^3+973d^2-1484d+852}{(d-1)^3}J_{(3)}(\vec{q}^2).
\end{aligned}
\tag{3.82}
$$

3.3.4.3 The classical three-loop contribution to the stress-tensor

Summing up all the contributions we get for the three-loop stress-tensor

$$
\langle T^{(3)}_{\mu\nu}\rangle = \pi^3 G_N^3 m^4\Big(c_1^{(3)}(d)\delta^0_\mu\delta^0_\nu + c_2^{(3)}(d)\big(\frac{q_\mu q_\nu}{q^2}-\eta_{\mu\nu}\big)\Big)\,J_{(3)}(q^2)\,, \tag{3.83}
$$

with the master integral

$$
J_{(3)}(q^2) = \frac{\Gamma\left(\frac{8-3d}{2}\right)\Gamma\left(\frac{d-2}{2}\right)^4}{8^d\pi^{\frac{3d}{2}}\Gamma(2(d-2))}\,|\vec{q}|^{3(d-2)}\,, \tag{3.84}
$$

and the three-loop coefficients are given by

$$c_1^{(3)}(d) = -\frac{64}{3(d-3)(d-4)^2(d-1)^4} \times \Big(56d^7 - 889d^6 + 5868d^5 - 20907d^4 + 43434d^3 - 52498d^2 + 33888d - 8760\Big),$$
$$c_2^{(3)}(d) = -\frac{64}{3(d-3)(d-4)^2(d-1)^4} \times \Big(45d^7 - 670d^6 + 4167d^5 - 14016d^4 + 27430d^3 - 30916d^2 + 18104d - 3952\Big). \tag{3.85}$$

Using the relations (3.39) we obtained the three-loop contribution to the metric from the classical stress-tensor in (3.126) (using the notation for ρ in (3.40))

$$h_0^{(4)}(r,d) = \frac{16(d-2)^3(14d^3 - 85d^2 + 165d - 106)}{3(d-3)(d-4)(d-1)^4}\rho(r,d)^4,$$
$$h_1^{(4)}(r,d) = -\frac{8(39d^7 - 691d^6 + 5155d^5 - 21077d^4 + 51216d^3 - 74346d^2 + 60168d - 21208)}{3(d-3)(d-4)^2(d-1)^4(3d-8)}\rho(r,d)$$
$$h_2^{(4)}(r,d) = \frac{16(d-2)^2(45d^6 - 580d^5 + 3007d^4 - 8002d^3 + 11426d^2 - 8064d + 1976)}{3(d-3)(d-4)^2(d-1)^4(3d-8)}\rho(r,d)^4. \tag{3.86}$$

3.4 Non-minimal couplings and renormalised metric

The stress-tensor and the metric components have ultraviolet divergences. These divergences can be removed by the addition of the non-minimal couplings made from the powers of the covariant derivative ∇_μ acting on a single power of the Riemann tensor and its contractions. The Bianchi identity on the Riemann tensor $\nabla_\mu R_{\nu\rho\sigma\lambda} + \nabla_\nu R_{\rho\mu\sigma\lambda} + \nabla_\rho R_{\mu\nu\sigma\lambda} = 0$, implies that

$$\nabla_\mu R^\mu{}_{\rho\sigma\lambda} = \nabla_\sigma R_{\rho\lambda} - \nabla_\lambda R_{\rho\sigma}, \qquad \nabla_\mu R^\mu{}_\nu = \frac{1}{2}\nabla_\nu R\,. \tag{3.87}$$

The counter-terms are powers of covariant derivative acting on a single power of the Ricci tensor and Ricci scalar. Therefore the counter-terms are given by the following non-minimal couplings

$$\delta^{(n)}S^{\rm ct.} = (G_N m)^{\frac{2n}{d-2}} \int d^{d+1}x\sqrt{-g}\Big(\alpha^{(n)}(d)(\nabla^2)^{n-1}R\partial_\mu\phi\partial^\mu\phi + \Big(\beta_0^{(n)}(d)\nabla_\mu\nabla_\nu(\nabla^2)^{n-2}R + \beta_1^{(n)}(d)(\nabla^2)^{n-1}R_{\mu\nu}\Big)\partial^\mu\phi\partial^\nu\phi\Big). \tag{3.88}$$

where $\alpha^{(n)}(d)$, $\beta_0^{(n)}(d)$ and $\beta_1^{(n)}(d)$ are dimensionless coefficients depending on the space-time dimension. The power of $G_N m$ is determined by dimensional analysis, and give the correct order of G_N in all dimensions. The first non-minimal coupling with $n = 1$ is given by

$$\delta^{(1)} S^{\text{ct.}} = (G_N m)^{\frac{2}{d-2}} \int d^{d+1}x\sqrt{-g}\, \left(\alpha^{(1)}(d) R\partial_\mu\phi\partial^\mu\phi + \beta^{(1)}(d) R^{\mu\nu}\partial_\mu\phi\partial_\nu\phi\right) . \tag{3.89}$$

This non-minimal coupling has been introduced in [34] in four dimensions and [167] in five dimensions. We will see that up to three-loop order the renormalisation of the static metric component only require the counter-term $\alpha^{(1)}(d) R\partial_\mu\phi\partial^\mu\phi$, whereas both couplings are needed for the cancellation of the stress-tensor divergences. This coupling is induced by harmonic gauge condition [73, 167] and the value of its coefficient depends on the choice of gauge. In our gauge, the de Donder gauge, this corresponds to $\alpha = 0$ in the work of [167] and $\xi = \frac{1}{4}$ in the work of [73]. Since we are working in fixed gauge we will not discuss further the gauge dependence of the higher-order non-minimal coupling coefficients, but we expect that the gauge dependence of these coefficients will be an extension of the discussion in [167, app. B].

The power of the Newton constant in (3.89) is an integer only in four dimensions with $d = 3$ and five dimensions $d = 4$. Therefore this counter-term will not appear in dimensions $D \geq 6$.

In four dimensions, from five-loop order, or the sixth post-Minkowskian order $O(G_N^6)$, one expects that higher derivative non-minimal couplings will be needed to get finite stress-tensor components. In dimensions five and six, the higher-derivative non-minimal couplings arise at lower loop order.

In five dimensions one needs to consider higher-derivative non-minimal couplings $\delta^{(n)} S^{\text{ct.}}$ with $n \geq 2$ for removing the divergences in the stress-tensor. The non-minimal coupling at this order is then given by

$$\begin{aligned}\delta^{(2)} S^{ct.} = (G_N m)^{\frac{4}{d-2}} \int d^{d+1}x\sqrt{-g}\Big(&\alpha^{(2)}(d)\Box R\partial_\mu\phi\partial^\mu\phi \\ &+ \left(\beta_0^{(2)}(d)\nabla_\mu\nabla_\nu R + \beta_1^{(2)}(d)\Box R_{\mu\nu}\right)\partial^\mu\phi\partial^\nu\phi\Big) .\end{aligned} \tag{3.90}$$

We will need the non-minimal coupling

$$\begin{aligned}\delta^{(3)} S^{ct.} = (G_N m)^{\frac{6}{d-2}} \int d^{d+1}x\sqrt{-g}\Big(&\alpha^{(3)}(d)(\nabla^2)^2 R\partial_\mu\phi\partial^\mu\phi \\ &+ \left(\beta_0^{(3)}(d)\nabla_\mu\nabla_\nu\nabla^2 R + \beta_1^{(3)}(d)(\nabla^2)^2 R_{\mu\nu}\right)\partial^\mu\phi\partial^\nu\phi\Big) ,\end{aligned} \tag{3.91}$$

for removing the two-loop divergence in the stress-tensor in six ($d = 5$) dimensions and the three-loop divergence in five ($d = 4$) dimensions. In five dimensions ($d = 4$) the metric, up to G_N^4, is renormalised using only the $n = 1$ and the metric is finite to all order in six dimensions ($d = 5$).

The higher-order non-minimal couplings $\delta^{(n)}S^{\text{ct.}}$ with $n \geq 2$ will not contribute to the classical limit when inserted into graphs with loops, because they contribute to higher powers in the momentum transfer $\vec{q}$, and are sub-leading with respect to the classical contributions. Their tree-level insertions will contribute to the renormalisation of the stress-tensor but thanks to the properties of the Fourier transform they will not contribute to the metric components.

3.4.1 Tree-level insertions

We give the contribution of the insertions of the non-minimal counter-terms with $n = 1$ in (3.89), with $n = 2$ in (3.90) and with $n = 3$ in (3.91) in the tree-level graph.

3.4.1.1 Insertion of $\delta^{(1)}S^{\text{ct.}}$

The insertion of the non-minimal couplings $\delta^{(1)}S^{\text{ct.}}$ in (3.89) into the tree-level diagram

$\delta^{(1)}\mathcal{M}^{(0)}(p_1, q) =$ 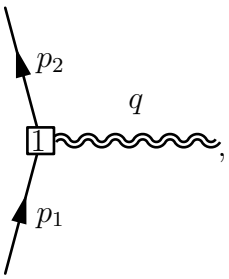

, (3.92)

leads to the stress-tensor contribution in $d + 1$ dimensions

$$\delta^{(1)}\langle T^{(0)}_{\mu\nu}\rangle = -\vec{q}^{\,2}(G_N m)^{\frac{2}{d-2}} m \left(-\beta^{(1)}(d)\delta^0_\mu\delta^0_\nu + 2\alpha^{(1)}(d)\left(\frac{q_\mu q_\nu}{q^2} - \eta_{\mu\nu}\right)\right), \tag{3.93}$$

and using (3.7) this contributes to the metric components

$$\delta^{(1)}h^{(1)}_0(r, d) = 0, \tag{3.94}$$

$$\delta^{(1)}h^{(1)}_1(r, d) = \frac{16\alpha^{(1)}(d)\Gamma\left(\frac{d}{2}\right)}{\pi^{\frac{d-2}{2}}}\left(\frac{(G_N m)^{\frac{1}{d-2}}}{r}\right)^d,$$

$$\delta^{(1)}h^{(1)}_2(r, d) = -\frac{32\alpha^{(1)}(d)\Gamma\left(\frac{d+2}{2}\right)}{\pi^{\frac{d-2}{2}}}\left(\frac{(G_N m)^{\frac{1}{d-2}}}{r}\right)^d. \tag{3.95}$$

Thanks to the properties of the Fourier transformation (see appendix A.1) only the coefficient $\alpha(d)$ contributes to static metric perturbation.

3.4.1.2 Insertion of $\delta^{(2)}S^{\text{ct.}}$

The insertion of the non-minimal couplings $\delta^{(2)}S^{\text{ct.}}$ in (3.90) into the tree-level diagram

$$\delta^{(2)}\mathcal{M}^{(0)}(p_1,q) = \tag{3.96}$$

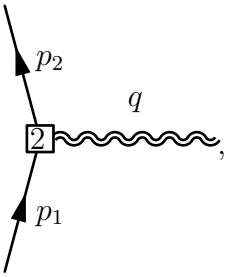

leads to the stress-tensor condition in $d+1$ dimensions

$$\delta^{(2)}\langle T^{(0)}_{\mu\nu}\rangle = |\vec{q}|^4 (G_N m)^{\frac{4}{d-2}} m \left(-\beta_1^{(2)}(d)\delta^0_\mu\delta^0_\nu + 2\left(\alpha^{(2)}(d) + \frac{1}{2}\beta_0^{(2)}(d)\right)\left(\frac{q_\mu q_\nu}{q^2} - \eta_{\mu\nu}\right)\right). \tag{3.97}$$

Because of the vanishing of the Fourier transforms

$$\int_{\mathbb{R}^d} |\vec{q}|^2 e^{i\vec{q}\cdot\vec{x}} \frac{d^d\vec{q}}{(2\pi)^d} = 0, \qquad \int_{\mathbb{R}^d} \frac{q_i q_j}{|\vec{q}|^2} |\vec{q}|^2 e^{i\vec{q}\cdot\vec{x}} \frac{d^d\vec{q}}{(2\pi)^d} = 0\,, \tag{3.98}$$

this extra contribution to the stress-tensor does not affect the metric components

$$\delta^{(2)}h_0^{(1)}(r,d) = 0, \tag{3.99}$$

$$\delta^{(2)}h_1^{(1)}(r,d) = 0,$$

$$\delta^{(2)}h_2^{(1)}(r,d) = 0\,. \tag{3.100}$$

3.4.1.3 Insertion of $\delta^{(3)}S^{\text{ct.}}$

The insertion of the non-minimal couplings $\delta^{(3)}S^{\text{ct.}}$ in (3.91) into the tree-level diagram

$$\delta^{(3)}\mathcal{M}^{(0)}(p_1,q) = \tag{3.101}$$

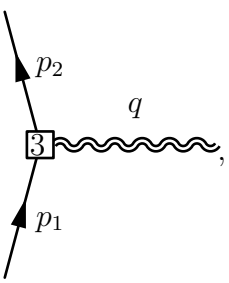

leads to the stress-tensor condition in six dimensions ($d = 5$)

$$\delta^{(3)}\langle T^{(0)}_{\mu\nu}\rangle = -|\vec{q}|^6 (G_N m)^{\frac{6}{d-2}} m \left(-\beta_1^{(3)}(d)\delta^0_\mu\delta^0_\nu + 2\left(\alpha^{(3)}(d) + \frac{1}{4}\beta_0^{(3)}(d)\right)\left(\frac{q_\mu q_\nu}{q^2} - \eta_{\mu\nu}\right)\right) . \tag{3.102}$$

Because of the vanishing of the Fourier transforms

$$\int_{\mathbb{R}^d} |\vec{q}|^4 e^{i\vec{q}\cdot\vec{x}} \frac{d^d\vec{q}}{(2\pi)^d} = 0, \qquad \int_{\mathbb{R}^d} \frac{q_i q_j}{|\vec{q}|^2} |\vec{q}|^4 e^{i\vec{q}\cdot\vec{x}} \frac{d^d\vec{q}}{(2\pi)^d} = 0\,, \tag{3.103}$$

this extra contribution to the stress-tensor does not affect the metric components

$$\delta^{(2)} h_0^{(1)}(r,d) = 0, \tag{3.104}$$
$$\delta^{(2)} h_1^{(1)}(r,d) = 0,$$
$$\delta^{(2)} h_2^{(1)}(r,d) = 0\,. \tag{3.105}$$

3.4.2 One-loop insertions

We give the contribution of the insertions of the counter-terms (3.88) with $n = 1$ in (3.89) in the one-loop graph.

3.4.2.1 Insertion of $\delta^{(1)} S^{\text{ct.}}$

The insertion of the non-minimal coupling in (3.89) in the one-loop graph

$\delta^{(1)}\mathcal{M}^{(1)}(p_1,q) =$ 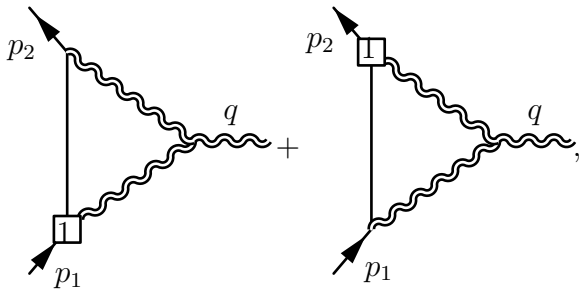

, (3.106)

leads to the stress-tensor contribution

$$\begin{aligned}\delta^{(1)}\langle T^{(1)}_{\mu\nu}\rangle &= 32i\alpha^{(1)}(d)\pi(G_N m)^{\frac{d}{d-2}} m^2 \\ &\times \int \frac{d^d\vec{l}}{(2\pi)^d} \frac{\tau^{\mu\nu}_{10\ \alpha\beta,\gamma\delta}(l,q)\mathcal{P}^{\alpha\beta}_{00} l^\gamma l^\delta}{l^2(l+q)^2}\left[\frac{1}{(l+p_1)^2 - m^2 + i\epsilon} + \frac{1}{(l-p_2)^2 - m^2 + i\epsilon}\right] \\ &= 8\pi\alpha^{(1)}(d)(G_N m)^{\frac{d}{d-2}} m\vec{q}^2 \frac{d-2}{(d-1)^2}\left(d\delta^0_\mu\delta^0_\nu + \frac{q_\mu q_\nu}{q^2} - \eta_{\mu\nu}\right) J_{(1)}(\vec{q}^2)\end{aligned} \tag{3.107}$$

where we used that

$$\eta_{\mu\nu}\tau^{\mu\nu}_{10\ 00,\gamma\delta}(l,q)l^\gamma l^\delta = \frac{\vec{l_1}^2}{2}\left(\vec{q}^2+(\vec{l_1}+\vec{q})^2-\vec{l_1}^2\right), \tag{3.108}$$

and

$$\delta^0_\mu\delta^0_\nu\tau^{\mu\nu}_{10\ 00,\gamma\delta}(l,q)l^\gamma l^\delta = \frac{1}{2(d-1)}\Big((d-2)\vec{q}^4+(d-2)(\vec{l_1}+\vec{q})^2\big((\vec{l_1}+\vec{q})^2-2\vec{q}^2\big)-\vec{l_1}^4 - (d-3)\vec{l_1}^2\big((\vec{l_1}+\vec{q})^2+\vec{q}^2\big)\Big). \tag{3.109}$$

Using the Fourier transforms

$$\begin{aligned}\int_{\mathbb{R}^d} J_{(1)}(\vec{q}^2)e^{i\vec{q}\cdot\vec{x}}\frac{d^d\vec{q}}{(2\pi)^d} &= -\frac{\Gamma\left(\frac{d}{2}\right)^2}{2\pi^d r^{2(d-1)}},\\ \int_{\mathbb{R}^d}\frac{q_iq_j}{\vec{q}^2}J_{(1)}(\vec{q}^2)e^{i\vec{q}\cdot\vec{x}}\frac{d^d\vec{q}}{(2\pi)^d} &= \frac{\Gamma\left(\frac{d-2}{2}\right)\Gamma\left(\frac{d}{2}\right)}{4\pi^d r^{2(d-1)}}\left(\delta_{ij}-2(d-1)\frac{x_ix_j}{r}\right).\end{aligned} \tag{3.110}$$

and the relation between the stress-tensor and the metric components in (3.7) we obtain the following contribution to the metric components

$$\begin{aligned}\delta^{(1)}h^{(2)}_0(r,d) &= 64\alpha^{(1)}(d)\frac{(d-2)\Gamma(\frac{d}{2})^2}{(d-1)\pi^{d-2}}\left(\frac{(G_Nm)^{\frac{1}{d-2}}}{r}\right)^{2(d-1)},\\ \delta^{(1)}h^{(2)}_1(r,d) &= -64\alpha^{(1)}(d)\frac{\Gamma(\frac{d}{2})^2}{(d-1)\pi^{d-2}}\left(\frac{(G_Nm)^{\frac{1}{d-2}}}{r}\right)^{2(d-1)},\\ \delta^{(1)}h^{(2)}_2(r,d) &= 128\alpha^{(1)}(d)\frac{\Gamma(\frac{d}{2})^2}{(d-1)\pi^{d-2}}\left(\frac{(G_Nm)^{\frac{1}{d-2}}}{r}\right)^{2(d-1)}.\end{aligned} \tag{3.111}$$

3.4.2.2 Two insertions of $\delta^{(1)}S^{\text{ct.}}$

Two insertions of the non-minimal coupling $\delta^{(1)}S^{\text{ct.}}$ in (3.89) in the one-loop graph

$(\delta^{(1)})^2\mathcal{M}^{(1)}(p_1,q) =$ 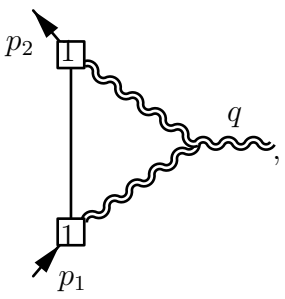

, (3.112)

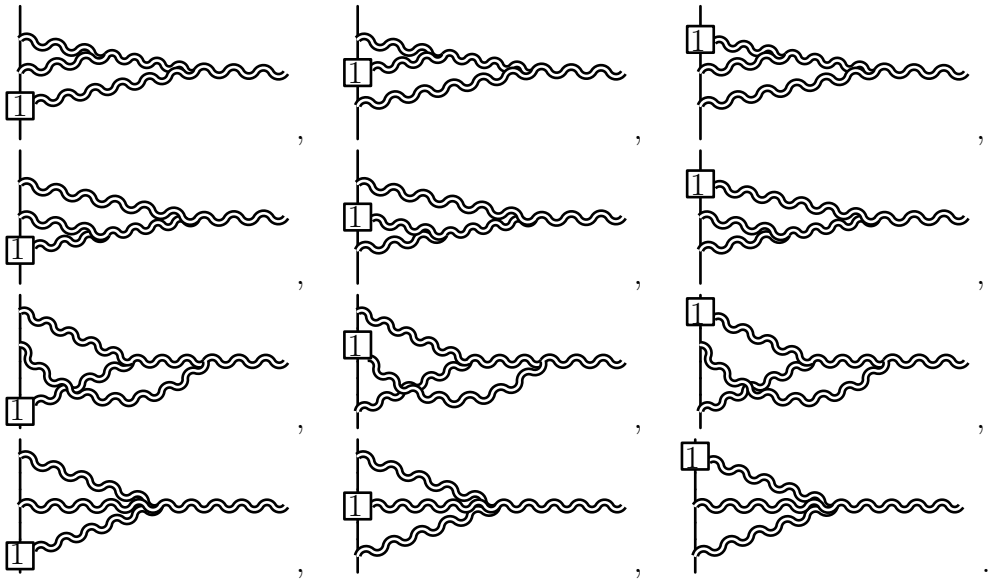

TABLE 3.1: Insertion of the non-minimal coupling in the two-loop graph

leads to the stress-tensor contribution

$$(\delta^1)^2\langle T^{(1)}_{\mu\nu}\rangle = \frac{2(\alpha^{(1)}(d))^2(G_N m)^{\frac{d+2}{d-2}}\pi m\vec{q}^4}{d-1}\left(\delta^0_\mu\delta^0_\nu - (d-2)\big(\frac{q_\mu q_\nu}{q^2}-\eta_{\mu\nu}\big)\right)J_{(1)}(\vec{q}^2), \tag{3.113}$$

and the metric contributions

$$\begin{aligned}
(\delta^1)^2 h^{(2)}_0(r,d) &= 0,\\
(\delta^1)^2 h^{(2)}_1(r,d) &= \frac{64(\alpha^{(1)}(d))^2}{\pi^{d-2}}\Gamma\left(\frac{d}{2}\right)^2\left(\frac{(G_N m)^{\frac{1}{d-2}}}{r}\right)^{2d},\\
(\delta^1)^2 h^{(2)}_2 &= \frac{64d(d-2)(\alpha^{(1)}(d))^2}{\pi^{d-2}}\Gamma\left(\frac{d}{2}\right)^2\left(\frac{(G_N m)^{\frac{1}{d-2}}}{r}\right)^{2d}.
\end{aligned} \tag{3.114}$$

3.4.3 Two-loop insertions

For the insertion of the non-minimal coupling $\delta^{(1)}S^{\text{ct.}}$ in (3.89) in the two-loop graph one needs to sum over all the contributions in table 3.1. The classical limit of the sum of all these graphs lead to the following contribution to the

stress-tensor

$$\delta^{(1)}\langle T^{(2)}_{\mu\nu}\rangle = -\frac{128\pi^2(d-2)\alpha^{(1)}(d)}{3(d-4)(3d-4)(d-1)^2}(G_N m)^{\frac{2(d-1)}{d-2}} m\vec{q}^2\Bigg((3d^3-19d^2+28d-10)\delta^0_\mu\delta^0_\nu + (3d^3-15d^2+18d-4)\Big(\frac{q_\mu q_\nu}{q^2}-\eta_{\mu\nu}\Big)\Bigg)J_{(2)}(\vec{q}^2), \quad (3.115)$$

which leads to the following contributions to the metric components

$$\delta^{(1)}h^{(3)}_0(r,d) = -\frac{512\alpha^{(1)}(d)}{d-1}\frac{\Gamma(\frac{d}{2})^3}{\pi^{\frac{3}{2}(d-2)}}\left(\frac{(G_N m)^{\frac{1}{d-2}}}{r}\right)^{3d-4}, \quad (3.116)$$

$$\delta^{(1)}h^{(3)}_1(r,d) = \frac{256\alpha^{(1)}(d)\,(3d^3-23d^2+46d-28)}{(d-4)(d-2)(d-1)^2(3d-4)}\frac{\Gamma(\frac{d}{2})^3}{\pi^{\frac{3}{2}(d-2)}}\left(\frac{(G_N m)^{\frac{1}{d-2}}}{r}\right)^{3d-4},$$

$$\delta^{(1)}h^{(3)}_2(r,d) = -\frac{256\alpha^{(1)}(d)\,(3d^3-15d^2+18d-4)}{(d-4)(d-2)(d-1)^2}\frac{\Gamma(\frac{d}{2})^3}{\pi^{\frac{3}{2}(d-2)}}\left(\frac{(G_N m)^{\frac{1}{d-2}}}{r}\right)^{3d-4}.$$

3.4.4 The renormalised metric in four dimensions

The metric components have ultraviolet poles in four dimensions from two-loop order. We show how the addition of the non-minimal couplings leads to finite renormalised metric components.

3.4.4.1 The two-loop renormalisation

The two-loop metric components in (3.76) have a divergence in four dimensions ($d=3$)

$$\begin{aligned} h^{(3)}_0(r,d) &= O(1),\\ h^{(3)}_1(r,d) &= -\frac{2}{3(d-3)}\left(\frac{G_N m}{r}\right)^3 + O(1),\\ h^{(3)}_2(r,d) &= \frac{2}{d-3}\left(\frac{G_N m}{r}\right)^3 + O(1)\,. \end{aligned} \quad (3.117)$$

This divergence is cancelled by adding the metric contribution from the non-minimal coupling in (3.94)

$$h_i^{\text{renor. }(3)}(r,d) := h^{(3)}_i(r,d) + \delta^{(1)}h^{(1)}_i(r,d), \qquad i=0,1,2 \quad (3.118)$$

and setting the $\alpha^{(1)}(d)$ coefficient to be

$$\alpha^{(1)}(d) = \frac{1}{12(d-3)} + a^{(1)}(3) - \frac{\log(2)}{6} + O(d-3)\,. \tag{3.119}$$

The resulting renormalised two-loop metric reads

$$\begin{aligned}
h_0^{\text{renor. }(3)}(r,d) &= 2\left(\frac{G_N m}{r}\right)^3 + O(d-3),\\
h_1^{\text{renor. }(3)}(r,d) &= \frac{4}{3}\left(-\frac{1}{2} + 6a^{(1)}(3) + \log\left(\frac{rC_E}{G_N m}\right)\right)\left(\frac{G_N m}{r}\right)^3 + O(d-3),\\
h_2^{\text{renor. }(3)}(r,d) &= 4\left(\frac{1}{3} - 6a^{(1)}(3) - \log\left(\frac{rC_E}{G_N m}\right)\right)\left(\frac{G_N m}{r}\right)^3 + O(d-3),
\end{aligned} \tag{3.120}$$

where we have introduced the following combination of the Euler-Mascheroni constant [179] and π

$$C_E := \sqrt{\pi} e^{\frac{\gamma_E}{2}}\,. \tag{3.121}$$

The divergence in the two-loop stress-tensor in (3.73)

$$\langle T^{(2)}_{\mu\nu}\rangle = \frac{G_N^2 \vec{q}^2 m^3}{6(d-3)}\left(2\delta^0_\mu\delta^0_\nu + \left(\frac{q_\mu q_\nu}{q^2} - \eta_{\mu\nu}\right)\right) + O(1)\,, \tag{3.122}$$

is cancelled by adding the contribution in (3.93) from the non-minimal coupling with the following choice of $\beta^{(1)}(d)$ coefficient

$$\beta^{(1)}(d) = -\frac{1}{3(d-3)} + O(1)\,. \tag{3.123}$$

Notice that this computation does not determine the finite part of the $\alpha^{(1)}(d)$ and $\beta^{(1)}(d)$. They are free scales in the logarithms. We will show in section 3.6 that this freedom is totally reabsorbed in the change of coordinate and the Schwarzschild-Tangherlini metric does not have any ambiguity.

3.4.4.2 The three-loop renormalisation

The three-loop metric components in (3.86) have a divergence in four dimensions ($d = 3$) given by

$$\begin{aligned} h_0^{(4)}(r,d) &= -\frac{2}{3(d-3)}\left(\frac{G_N m}{r}\right)^4 + O(1), \\ h_1^{(4)}(r,d) &= \frac{2}{3(d-3)}\left(\frac{G_N m}{r}\right)^4 + O(1), \\ h_2^{(4)}(r,d) &= -\frac{4}{3(d-3)}\left(\frac{G_N m}{r}\right)^4 + O(1), \,. \end{aligned} \tag{3.124}$$

Adding to this contribution the (3.111) from the insertion of the non-minimal couplings at one-loop, and using the value of $\alpha^{(1)}(d)$ determined in (3.119), we obtain the renormalised three-loop metric

$$\begin{aligned} h_0^{\text{renorm.}(4)}(r) &= \left(-\frac{32}{3} + 8a^{(1)}(3) + \frac{4}{3}\log\left(\frac{rC_E}{G_N m}\right)\right)\left(\frac{G_N m}{r}\right)^4 + O(d-3), \\ h_1^{\text{renorm.}(4)}(r) &= \left(10 - 8a^{(1)}(3) - \frac{4}{3}\log\left(\frac{rC_E}{G_N m}\right)\right)\left(\frac{G_N m}{r}\right)^4 + O(d-3), \\ h_2^{\text{renorm.}(4)}(r) &= \left(-\frac{86}{3} + 16a^{(1)}(3) + \frac{8}{3}\log\left(\frac{rC_E}{G_N m}\right)\right)\left(\frac{G_N m}{r}\right)^4 + O(d-3)\,. \end{aligned} \tag{3.125}$$

The classical three-loop contribution to the stress-tensor has an ultraviolet divergence

$$\langle T_{\mu\nu}^{(3)}(\vec{q})\rangle = -\frac{\pi G_N^3 m^4 |\vec{q}|^{\frac{3}{2}}}{48(d-3)}\left(3\delta_\mu^0\delta_\nu^0 + \left(\frac{q_\mu q_\nu}{q^2} - \eta_{\mu\nu}\right)\right) + O(1)\,, \tag{3.126}$$

this divergence is cancelled by the addition of the contribution in (3.107) from the non-minimal coupling and the choice of $\alpha^{(1)}(d)$ in (3.119).

3.4.5 The renormalised metric in five dimensions

The metric components have ultraviolet divergences in five dimensions from one-loop order. We show how the addition of the non-minimal couplings leads to finite renormalised metric components.

3.4.5.1 The one-loop renormalisation

The metric components in (3.58) have a divergence in five dimension ($d = 4$) given by

$$\begin{aligned} h_0^{(2)}(r,d) &= O(1), \\ h_1^{(2)}(r,d) &= -\frac{40}{9(d-4)}\left(\frac{G_N m}{\pi r^2}\right)^2 + O(1), \\ h_2^{(2)}(r,d) &= \frac{160}{9(d-4)}\left(\frac{G_N m}{\pi r^2}\right)^2 + O(1)\,. \end{aligned} \tag{3.127}$$

The divergences in the metric components (3.127) are cancelled for the choice

$$\alpha^{(1)}(d) = \frac{5}{18\pi(d-4)} + a^{(1)}(5) + O(d-4)\,, \tag{3.128}$$

so that the renormalised metric components

$$h_i^{\text{renor. }(2)}(r,d) := h_i^{(2)}(r,d) + \delta^{(1)} h_i^{(1)}(r,d), \qquad i = 0,1,2\,, \tag{3.129}$$

have a finite expansion near $d = 4$

$$h_0^{\text{renor. }(2)}(r,d) = \frac{32}{9}\left(\frac{G_N m}{\pi r^2}\right)^2 + O(d-4), \tag{3.130}$$

$$h_1^{\text{renor. }(2)}(r,d) = \frac{20}{9}\left(\frac{14}{15} + \frac{36a^{(1)}(5)\pi}{5} + \log\left(\frac{r^2 C_E^2}{G_N m}\right)\right)\left(\frac{G_N m}{\pi r^2}\right)^2 + O(d-4),$$

$$h_2^{\text{renor}(2)}(r,d) = -\frac{80}{9}\left(\frac{7}{30} + \frac{36a^{(1)}(5)\pi}{5} + \log\left(\frac{r^2 C_E^2}{G_N m}\right)\right)\left(\frac{G_N m}{\pi r^2}\right)^2 + O(d-4)\,.$$

where C_E is defined in (3.121).

Thanks to the properties of the Fourier transform, only the coefficient $\alpha^{(1)}(d)$ enters the counter-term contribution to the metric component. To determine as well the coefficient $\beta^{(1)}(d)$ in (3.89) one needs to look at the divergences of the stress-tensor

$$\langle T_{\mu\nu}^{(1)} \rangle = \frac{G_N m^2 \vec{q}^2}{18\pi(d-4)}\left(7\delta_\mu^0\delta_\nu^0 + 10\left(\frac{q_\mu q_\nu}{q^2} - \eta_{\mu\nu}\right)\right) + O(1) \tag{3.131}$$

The cancellation of the pole fixes the pole part of $\beta^{(1)}(d)$ near five dimensions

$$\beta^{(1)}(d) = -\frac{7}{18\pi(d-4)} + O(1)\,. \tag{3.132}$$

3.4.5.2 The two-loop renormalisation

The two-loop metric components in (3.76) have a divergence in five dimensions ($d = 4$)

$$\begin{aligned} h_0^{(3)}(r,d) &= -\frac{320}{27(d-4)}\left(\frac{G_N m}{\pi r^2}\right)^3 + O(1), \\ h_1^{(3)}(r,d) &= \frac{160}{27(d-4)}\left(\frac{G_N m}{\pi r^2}\right)^3 + O(1), \\ h_2^{(3)}(r,d) &= -\frac{320}{27(d-4)}\left(\frac{G_N m}{\pi r^2}\right)^3 + O(1)\,. \end{aligned} \tag{3.133}$$

The divergences in the metric components (3.76) are cancelled for the choice made at one-loop in (3.128), so that the renormalised metric components

$$h_i^{\text{renor. }(3)}(r,d) := h_i^{(3)}(r,d) + \delta^{(1)} h_i^{(2)}(r,d), \qquad i = 0,1,2\,, \tag{3.134}$$

have a finite expansion near $d = 4$

$$\begin{aligned} h_0^{\text{renor. }(3)}(r,d) &= \frac{160}{27}\left(\frac{2}{15} + \frac{36a^{(1)}(5)\pi}{5} + \log\left(\frac{r^2 C_E^2}{G_N m}\right)\right)\left(\frac{G_N m}{\pi r^2}\right)^3 + O(d-4), \\ h_1^{\text{renor. }(3)}(r,d) &= -\frac{80}{27}\left(\frac{7}{15} + \frac{36a^{(1)}(5)\pi}{5} + \log\left(\frac{r^2 C_E^2}{G_N m}\right)\right)\left(\frac{G_N m}{\pi r^2}\right)^3 + O(d-4), \\ h_2^{\text{renor}(3)}(r,d) &= \frac{160}{27}\left(-\frac{1}{15} + \frac{36a^{(1)}(5)\pi}{5} + \log\left(\frac{r^2 C_E^2}{G_N m}\right)\right)\left(\frac{G_N m}{\pi r^2}\right)^3 + O(d-4)\,. \end{aligned} \tag{3.135}$$

The two-loop stress-tensor in (3.73) is not finite in $d = 4$ as it diverges like

$$\begin{aligned} \langle T_{\mu\nu}^{(2)} \rangle = {} & \frac{5G_N^2 m^3 |\vec{q}|^4}{162\pi^2(d-4)^2}\left(4\delta_\mu^0\delta_\nu^0 + \frac{q_\mu q_\nu}{q^2} - \eta_{\mu\nu}\right) \\ & + \frac{5G^2 m^3 |\vec{q}|^4}{162\pi^2(d-4)}\Bigg(\left(4\log\left(\frac{\vec{q}^2}{4\pi}\right) + 4\gamma_E - \frac{183}{20}\right)\delta_\mu^0\delta_\nu^0 \\ & + \left(\log\left(\frac{\vec{q}^2}{4\pi}\right) + \gamma_E - \frac{41}{20}\right)\left(\frac{q_\mu q_\nu}{q^2} - \eta_{\mu\nu}\right)\Bigg) + O(1)\,. \end{aligned} \tag{3.136}$$

The addition of the counter-term in (3.107) from the non-minimal couplings in (3.89) is not enough for making the stress-tensor finite in $d = 4$

$$\begin{aligned}\langle T^{(2)}_{\mu\nu}\rangle + \delta^{(1)}\langle T^{(1)}_{\mu\nu}\rangle = &-\frac{5G_N^2 m^3|\vec{q}|^4}{162\pi^2(d-4)^2}\left(4\delta^0_\mu\delta^0_\nu + \frac{q_\mu q_\nu}{q^2} - \eta_{\mu\nu}\right)\\ &+\frac{5G^2 m^3|\vec{q}|^4}{162\pi^2(d-4)}\left(\left(4\log\left(G_N m\right) - \frac{144\pi a^{(1)}(5)}{5} - \frac{109}{60}\right)\delta^0_\mu\delta^0_\nu\right.\\ &\left.+\left(\left(\log\left(G_N m\right) + \frac{17}{60} - \frac{36}{5}\pi a^{(1)}(5)\right)\left(\frac{q_\mu q_\nu}{q^2} - \eta_{\mu\nu}\right)\right)\right) + O(1)\,. \end{aligned} \tag{3.137}$$

We need to consider the addition of the counter-term from the insertion of $\delta^{(2)}S^{\text{ct.}}$ evaluated in section 3.4.1.2 with the values of the coefficient near $d = 4$

$$\begin{aligned}\beta_1^{(2)}(d) &= \frac{1}{\pi^2}\left(\frac{10}{81(d-4)^2} + \frac{109 + 1728\pi a^{(1)}(5)}{1944(d-4)} + a^{(2)}(5) + O(d-4)\right),\\ \alpha^{(2)}(d) + \frac{1}{2}\beta_0^{(2)}(d) &= -\frac{1}{2\pi^2}\left(\frac{5}{162(d-4)^2} + \frac{432\pi a^{(1)}(5) - 17}{1944(d-4)} + b^{(2)}(5) + O(d-4)\right),\end{aligned} \tag{3.138}$$

plugged in (3.97) cancel the divergences in (3.137)

$$\langle T^{(2)}_{\mu\nu}\rangle + \delta^{(1)}\langle T^{(1)}_{\mu\nu}\rangle + \delta^{(2)}\langle T^{(0)}_{\mu\nu}\rangle = O(1)\,. \tag{3.139}$$

3.4.5.3 The three-loop renormalisation

The three-loop metric components in (3.86) have a divergence in five dimensions ($d = 4$)

$$\begin{aligned}h_0^{(4)}(r,d) &= \frac{1280}{27(d-4)}\left(\frac{G_N m}{\pi r^2}\right)^4 + O(1),\\ h_1^{(4)}(r,d) &= \left(\frac{400}{81(d-4)^2} - \frac{20\left(101 + 120\log\left(r^2 C_E^2\right)\right)}{243(d-4)}\right)\left(\frac{G_N m}{\pi r^2}\right)^4 + O(1),\\ h_2^{(4)}(r,d) &= \left(\frac{3200}{81(d-4)^2} + \frac{160\left(187 - 120\log\left(r^2 C_E^2\right)\right)}{243}\right)\left(\frac{G_N m}{\pi r^2}\right)^4 + O(1).\end{aligned} \tag{3.140}$$

The divergences in the metric components (3.86) are cancelled for the choice made at one-loop in (3.128), so that the renormalised metric components

$$h_i^{\text{renor. }(4)}(r,d) := h_i^{(4)}(r,d) + \delta^{(1)}h_i^{(3)}(r,d) + (\delta^1)^2 h_i^{(2)}(r,d), \qquad i = 0,1,2\,, \tag{3.141}$$

have a finite expansion near $d = 4$

$$
\begin{aligned}
h_0^{\text{renor. }(4)}(r,d) =& -\frac{128}{243}\left(23+324a^{(1)}(5)\pi+45\log\left(\frac{r^2C_E^2}{G_Nm}\right)\right)\left(\frac{G_Nm}{\pi r^2}\right)^4+O(d-4),\\
h_1^{\text{renor. }(4)}(r,d) =& \frac{100}{81}\Bigg(\left(\frac{36a^{(1)}(5)\pi}{5}+\log\left(\frac{r^2C_E^2}{G_Nm}\right)\right)\left(\frac{161}{30}+\frac{36}{5}a^{(1)}(5)\pi+\log\left(\frac{r^2C_E^2}{G_Nm}\right)\right)+\\
&+\frac{7085}{1800}\Bigg)\times\left(\frac{G_Nm}{\pi r^2}\right)^4+O(d-4),\\
h_2^{\text{renor}(4)}(r,d) =& -\frac{800}{81}\Bigg(\left(\frac{36a^{(1)}(5)\pi}{5}+\log\left(\frac{r^2C_E^2}{G_Nm}\right)\right)\left(\frac{41}{15}-\frac{36}{5}a^{(1)}(5)\pi-\log\left(\frac{r^2C_E^2}{G_Nm}\right)\right)+\\
&+\frac{2381}{900}\Bigg)\times\left(\frac{G_Nm}{\pi r^2}\right)^4+O(d-4).
\end{aligned}
\tag{3.142}
$$

The three-loop stress-tensor in (3.83) is not finite in $d = 4$ as it diverges like

$$
\begin{aligned}
\langle T^{(3)}_{\mu\nu}\rangle =& \frac{25G_N^3m^4|\vec{q}|^6}{5832\pi^3(d-4)^3}\left(-\frac{1}{2}\delta^0_\mu\delta^0_\nu+\frac{q_\mu q_\nu}{q^2}-\eta_{\mu\nu}\right)\\
&+\frac{25G_N^3m^4|\vec{q}|^6}{3888\pi^3(d-4)^2}\Bigg(-\frac{1}{2}\left(\log\left(\frac{\vec{q}^2}{4\pi}\right)+\gamma_E-\frac{41}{6}\right)\delta^0_\mu\delta^0_\nu\\
&+\left(\log\left(\frac{\vec{q}^2}{4\pi}\right)+\gamma_E-\frac{17}{10}\right)\left(\frac{q_\mu q_\nu}{q^2}-\eta_{\mu\nu}\right)\Bigg)\\
&+\frac{225G_N^3m^4|\vec{q}|^6}{839808\pi^3(d-4)}\Bigg(\frac{1}{2}\left(\frac{70939}{450}+\pi^2-18\left(\log\left(\frac{\vec{q}^2}{4\pi}\right)+\gamma_E-\frac{41}{6}\right)^2\right)\delta^0_\mu\delta^0_\nu\\
&+\left(\frac{4769}{450}-\pi^2+18\left(\log\left(\frac{\vec{q}^2}{4\pi}\right)+\gamma_E-\frac{17}{10}\right)^2\right)\left(\frac{q_\mu q_\nu}{q^2}-\eta_{\mu\nu}\right)\Bigg)+O(1)\,.
\end{aligned}
\tag{3.143}
$$

The addition of the counter-terms in $(\delta^1)^2\langle T^{(1)}_{\mu\nu}\rangle$ in (3.113), and $\delta^{(1)}\langle T^{(2)}_{\mu\nu}\rangle$ in (3.115)

from the non-minimal couplings in (3.89) is not enough for making the stress-tensor finite in $d = 4$

$$\begin{aligned}\langle T^{(3)}_{\mu\nu}\rangle + (\delta^1)^2\langle T^{(1)}_{\mu\nu}\rangle + \delta^{(1)}\langle T^{(2)}_{\mu\nu}\rangle &= \frac{25G_N^3m^4|\vec{q}|^6}{5832\pi^3(d-4)^3}\left(-\frac{1}{2}\delta^0_\mu\delta^0_\nu + \frac{q_\mu q_\nu}{q^2} - \eta_{\mu\nu}\right)\\ &+ \frac{25G_N^3m^4|\vec{q}|^6}{3888\pi^3(d-4)^2}\Bigg(-\frac{1}{2}\left(\frac{25}{12}+\frac{36}{5}a^{(1)}(5)\pi - \log(G_Nm)\right)\delta^0_\mu\delta^0_\nu\\ &+ \left(\frac{1}{60}+\frac{36}{5}a^{(1)}(5)\pi - \log(G_Nm)\right)\left(\frac{q_\mu q_\nu}{q^2}-\eta_{\mu\nu}\right)\Bigg)\\ &- \frac{25G_N^3m^4|\vec{q}|^6}{5184\pi^3(d-4)}\times\\ \times\Bigg(&\left(\frac{27487}{48600}+a^{(1)}(5)\pi\left(1+\frac{288}{25}a^{(1)}(5)\pi\right)-\frac{\log(G_Nm)}{3}\left(\frac{7}{2}+\log(G_Nm)+\frac{72}{5}a^{(1)}(5)\pi\right)\right)\delta^0_\mu\delta^0_\nu\\ +&\left(\frac{6749}{16200}-\frac{6a^{(1)}(5)\pi}{25}\left(1+144a^{(1)}(5)\pi\right)-\log(G_Nm)\left(\frac{19}{30}+\log(G_Nm)-\frac{72}{5}a^{(1)}(5)\pi\right)\right)\left(\frac{q_\mu q_\nu}{q^2}\right.\\ &+O(1)\,. \end{aligned} \tag{3.144}$$

We need to consider the addition of the counter-term from the insertion of $\delta^{(3)}S^{\text{ct.}}$ evaluated in section 3.4.1.3 with the values of the coefficient near $d = 4$

$$\begin{aligned}\beta_1^{(3)}(d) &= \frac{25}{11664\pi^3(d-4)^3}+\frac{5(432\pi a^{(1)}(5)+125)}{93312\pi^3(d-4)^2}\\ &+\frac{559872(\pi a^{(1)}(5))^2+486000\pi a^{(1)}(5)+27487}{6718464\pi^3(d-4)}+O(1),\\ \alpha^{(3)}(d)+\frac{1}{4}\beta_0^{(3)}(d) &= \frac{25}{11664\pi^3(d-4)^3}+\frac{2160\pi a^{(1)}(5)+5}{93312\pi^3(d-4)^2}\\ &+\frac{559872(\pi a^{(1)}(5))^2+3888\pi a^{(1)}(5)-6749}{6718464\pi^3(d-4)}+O(1)\end{aligned} \tag{3.145}$$

plugged in (3.97) cancel the divergences in (3.137)

$$\langle T^{(2)}_{\mu\nu}\rangle + \delta^{(1)}\langle T^{(2)}_{\mu\nu}\rangle + (\delta^{(1)}\langle T^{(2)}_{\mu\nu}\rangle + \delta^{(3)}\langle T^{(0)}_{\mu\nu}\rangle = O(1)\,. \tag{3.146}$$

3.4.6 The renormalised stress-tensor in six dimensions

In six dimensions, the metric component are finite to all order in perturbation but the two-loop stress-tensor in (3.73) presents an ultraviolet divergence in six dimensions ($d = 5$)

$$\langle T^{(2)}_{\mu\nu}\rangle = -\frac{G_N^2m^3|\vec{q}|^6}{40320\pi^2(d-5)}\left(49\delta^0_\mu\delta^0_\nu+15\left(\frac{q_\mu q_\nu}{q^2}-\eta_{\mu\nu}\right)\right)+O(1)\,, \tag{3.147}$$

which is cancelled by the addition of the insertion of the non-minimal coupling $\delta^{(3)}S^{\text{ct.}}$ at tree-level in (3.102) with the choice of the coefficients

$$\begin{aligned}\alpha^{(3)}(d)+\frac{1}{4}\beta_0^{(3)}(d) &= -\frac{15}{80640\pi^2(d-5)}+O(1),\\ \beta_1^{(3)}(d) &= -\frac{49}{40320\pi^2(d-5)}+O(1)\,.\end{aligned} \tag{3.148}$$

3.5 The Schwarzschild-Tangherlini metric in de Donder gauge in four, five and six dimensions

The Schwarzschild-Tangherlini [181] space-time metric in $d+1$ dimensions is given by the Tangherlini solution, using $\rho(r,d)$ defined in (3.40),**

$$ds^2_{\text{Schw}}=\left(1-4\frac{d-2}{d-1}\rho(r,d)\right)dt^2-d\vec{x}^2-\frac{4\frac{d-2}{d-1}\rho(r,d)}{1-4\frac{d-2}{d-1}\rho(r,d)}\frac{(\vec{x}\cdot d\vec{x})^2}{r^2}\,. \tag{3.150}$$

As explained in section 3.2 the amplitude computation selects the de Donder gauge in (3.5). We make the coordinate transformation $(t,\vec{x})\to(t,f(r)\vec{x})$ so that the Schwarzschild metric reads

$$ds^2=h_0(r)dt^2-h_1(r)d\vec{x}^2-h_2(r)\frac{(\vec{x}\cdot d\vec{x})^2}{r^2}, \tag{3.151}$$

with $r=|\vec{x}|$ and

$$\begin{aligned}h_0(r) &:= 1-4\frac{d-2}{d-1}\frac{\rho(r,d)}{f(r)^{d-2}},\\ h_1(r) &:= f(r)^2,\\ h_2(r) &:= -f(r)^2-f(r)^{d-2}\frac{(f(r)+r\frac{df(r)}{dr})^2}{f(r)^{d-2}-4\frac{d-2}{d-1}\rho(r,d)}\,.\end{aligned} \tag{3.152}$$

The de Donder gauge condition (3.5) then reads

$$2(d-1)h_2(r)=r\frac{d}{dr}\left(h_0(r)+(d-2)h_1(r)-h_2(r)\right)\,. \tag{3.153}$$

**In spherical coordinate the metric reads

$$ds^2=\left(1-\frac{\mu}{r^{d-2}}\right)dt^2-\frac{dr^2}{1-\frac{\mu}{r^{d-1}}}-r^2d\Omega_{d-1} \tag{3.149}$$

with $\mu=\frac{16\pi G_N m}{(d-1)\Omega_{d-1}}$ and $\Omega_{d-1}=\frac{2\pi^{\frac{d}{2}}}{\Gamma\left(\frac{d}{2}\right)}$ is the area of the unit $(d-1)$-sphere.

We will be solving the de Donder gauge condition (3.5) in four dimensions ($d = 3$), five dimensions ($d = 4$) and six dimensions ($d = 5$), using the post-Minkowskian expansion

$$f(r) = 1 + \sum_{n\geq 1} f_n(r)\rho(r,d)^n \tag{3.154}$$

with the condition at each order that

$$\lim_{r\to+\infty} f_n(r)/r^n = 0\,. \tag{3.155}$$

3.5.1 The metric in the de Donder gauge in four dimensions

The de Donder gauge condition (3.5) in $d = 3$ reads

$$4h_2(r) = r\frac{d}{dr}\left(h_0(r) + h_1(r) - h_2(r)\right)\,, \tag{3.156}$$

supplemented with the asymptotic boundary condition

$$\lim_{r\to\infty} f(r) = 1\,. \tag{3.157}$$

This differential equation implies either that $f(r) = C/r$, which does not satisfy the boundary condition (3.157), or $f(r)$ satisfies the differential equation, with $x = G_N m/r$

$$\begin{aligned} &xf(x)^3(2x - f(x))\frac{d^2f(x)}{dx^2} + (xf\,(x))^2\left(\frac{df(x)}{dx}\right)^2 \\ &+2\,f\,(x)^3\,(f(x)-3x)\frac{df(x)}{dx} - 3\,(f\,(x))^4 + 8\,(f\,(x))^3\,x + (f\,(x))^2 - 4\,f\,(x)\,x + 4\,x^2 = 0. \end{aligned} \tag{3.158}$$

We solve the equation (3.158) using a series expansion in $G_N m$ using (3.154) and the boundary condition (3.155). The result to the order $(G_N m)^7$ is given

by

$$f(r) = 1 + \frac{G_N m}{r} + 2\left(\frac{G_N m}{r}\right)^2 + \frac{2}{3}\log\left(\frac{rC_3}{G_N m}\right)\left(\frac{G_N m}{r}\right)^3 + \left(\frac{2}{3} - \frac{4}{3}\log\left(\frac{rC_3}{G_N m}\right)\right)\left(\frac{G_N m}{r}\right)^4 + \left(-\frac{21}{25} + \frac{32}{15}\log\left(\frac{rC_3}{G_N m}\right)\right)\left(\frac{G_N m}{r}\right)^5 + \left(\frac{112}{75} - \frac{28}{15}\log\left(\frac{rC_3}{G_N m}\right)\right)\left(\frac{G_N m}{r}\right)^6 + \left(\frac{50023}{34300} + \frac{1139}{2205}\log\left(\frac{rC_3}{G_N m}\right) + \frac{2}{7}\log\left(\frac{rC_3}{G_N m}\right)^2\right)\left(\frac{G_N m}{r}\right)^7 + O(G_N^8)\,. \tag{3.159}$$

This solution is finite and has $\log(r)$ terms from the order G_N^3. The solution has a single constant of integration C_3 associated with the scale of the logarithm.

3.5.1.1 The metric perturbation

In $d = 3$ we derive components of the metric in perturbation by plugging the expression for $f(r)$ in (3.159) in (3.152).

We obtain for the time component

$$h_0^{\rm dD}(r) = 1 - 2\frac{G_N m}{r} + 2\left(\frac{G_N m}{r}\right)^2 + 2\left(\frac{G_N m}{r}\right)^3 + \left(\frac{4}{3}\log\left(\frac{rC_3}{G_N m}\right) - 6\right)\left(\frac{G_N m}{r}\right)^4 + \left(-\frac{16}{3}\log\left(\frac{rC_3}{G_N m}\right) + \frac{10}{3}\right)\left(\frac{G_N m}{r}\right)^5 + \left(\frac{124}{15}\log\left(\frac{rC_3}{G_N m}\right) + \frac{424}{75}\right)\left(\frac{G_N m}{r}\right)^6 + \left(-\frac{8}{9}\log\left(\frac{rC_3}{G_N m}\right)^2 + \frac{16}{15}\log\left(\frac{rC_3}{G_N m}\right) - \frac{674}{75}\right)\left(\frac{G_N m}{r}\right)^7 + O(G_N^8), \tag{3.160}$$

and for the spatial components

$$h_1^{\rm dD}(r) = 1 + 2\frac{G_N m}{r} + 5\left(\frac{G_N m}{r}\right)^2 + \left(\frac{4}{3}\log\left(\frac{rC_3}{G_N m}\right) + 4\right)\left(\frac{G_N m}{r}\right)^3 + \left(-\frac{4}{3}\log\left(\frac{rC_3}{G_N m}\right) + \frac{16}{3}\right)\left(\frac{G_N m}{r}\right)^4 + \left(\frac{64}{15}\log\left(\frac{rC_3}{G_N m}\right) - \frac{26}{75}\right)\left(\frac{G_N m}{r}\right)^5 + \left(\frac{4}{9}\log\left(\frac{rC_3}{G_N m}\right)^2 - \frac{24}{5}\log\left(\frac{rC_3}{G_N m}\right) + \frac{298}{75}\right)\left(\frac{G_N m}{r}\right)^6 + O(G_N^7), \tag{3.161}$$

and

$$h_2^{\rm dD}(r) = -7\left(\frac{G_N m}{r}\right)^2 - \left(4\log\left(\frac{rC_3}{G_N m}\right) + \frac{38}{3}\right)\left(\frac{G_N m}{r}\right)^3 + \left(\frac{8}{3}\log\left(\frac{rC_3}{G_N m}\right) - \frac{58}{3}\right)\left(\frac{G_N m}{r}\right)^4 - \left(\frac{16}{3}\log\left(\frac{rC_3}{G_N m}\right) - \frac{32}{3}\right)\left(\frac{G_N m}{r}\right)^5 + \left(\frac{4}{3}\log\left(\frac{rC_3}{G_N m}\right)^2 + \frac{508}{45}\log\left(\frac{rC_3}{G_N m}\right) + \frac{7378}{225}\right)\left(\frac{G_N m}{r}\right)^6 + O(G_N^7). \tag{3.162}$$

Notice the appearance of the $\log(r)^2$ at the sixth post-Minkowskian order, G_N^6, in the spatial components of the metric. This is one order less than the appearance in the time component. The same phenomenon happens for the $\log(r)$ contribution which appears one order earlier in the spatial component than in the time component.

3.5.2 The metric in the de Donder gauge in five dimensions

The de Donder gauge condition (3.5) in $d = 4$ reads

$$6h_2(r) = r\frac{d}{dr}\left(h_0(r) + 2h_1(r) - h_2(r)\right)\,, \tag{3.163}$$

supplemented with the asymptotic boundary condition

$$\lim_{r\to\infty} f(r) = 1\,. \tag{3.164}$$

This differential equation implies either that $f(r) = C/r$, which does not satisfy the boundary condition (3.164), or $f(r)$ satisfies the differential equation, setting $x = G_N m/(\pi r^2)$

$$x f(x)^5\left(8x - 3f(x)^2\right)\frac{d^2 f(x)}{dx^2} + 8f(x)^4 x^2\left(\frac{df(x)}{dx}\right)^2 + f(x)^5\left(3f(x)^2 - 16x\right)\frac{df(x)}{dx} - 4f(x)^6 + (16x+2)f(x)^4 - \frac{32}{3}x f(x)^2 + \frac{128x^2}{9} = 0\,. \tag{3.165}$$

We solve the equation (3.165) using a series expansion in $G_N m$ using (3.154) and the boundary condition (3.155). The result to the order $(G_N m)^7$ is given

by

$$f(r) = 1+\frac{2}{3}\frac{G_N m}{\pi r^2}+\frac{10}{9}\log\left(\frac{r^2C_2}{G_N m}\right)\left(\frac{G_N m}{\pi r^2}\right)^2-\frac{4}{81}\left(-8+45\log\left(\frac{r^2C_2}{G_N m}\right)\right)\left(\frac{G_N m}{\pi r^2}\right)^3$$
$$+\frac{67+3780\log\left(\frac{r^2C_2}{G_N m}\right)}{972}\left(\frac{G_N m}{\pi r^2}\right)^4-\frac{32963+156420\log\left(\frac{r^2C_2}{G_N m}\right)-43200\log\left(\frac{r^2C_2}{G_N m}\right)^2}{21870}\left(\frac{G_N m}{\pi r^2}\right)^5$$
$$+\frac{409303+1620270\log\left(\frac{r^2C_2}{G_N m}\right)-1087200\log\left(\frac{r^2C_2}{G_N m}\right)^2}{131220}\left(\frac{G_N m}{\pi r^2}\right)^6$$
$$-\frac{11148022313+37508666370\log\left(\frac{r^2C_2}{G_N m}\right)-64367301600\log\left(\frac{r^2C_2}{G_N m}\right)^2}{2362944150}\left(\frac{G_N m}{\pi r^2}\right)^7$$
$$-\frac{4939200000}{2362944150}\log\left(\frac{r^2C_2}{G_N m}\right)^3\left(\frac{G_N m}{\pi r^2}\right)^7+O(G_N^8). \quad (3.166)$$

Again there is a single constant of integration C_2 arising as the scale of the $\log(r)$ arising from the G_N^2 order.

3.5.2.1 The metric perturbation

In $d = 4$ we derive components of the metric in perturbation by plugging the expression for $f(r)$ in (3.166) in (3.152).

We obtain for the time component

$$h_0^{\rm dD}(r) = 1-\frac{8}{3}\frac{G_N m}{\pi r^2}+\frac{32}{9}\left(\frac{G_N m}{\pi r^2}\right)^2+\frac{32\left(-3+5\log\left(\frac{r^2C_2}{G_N m}\right)\right)}{27}\left(\frac{G_N m}{\pi r^2}\right)^3$$
$$-\frac{640\left(-2+9\log\left(\frac{r^2C_2}{G_N m}\right)\right)}{243}\left(\frac{G_N m}{\pi r^2}\right)^4+O(G_N^5), \quad (3.167)$$

and for the spatial components

$$h_1^{\rm dD}(r) = 1+\frac{4}{3}\frac{G_N m}{\pi r^2}+\frac{4\left(1+5\log\left(\frac{r^2C_2}{G_N m}\right)\right)}{9}\left(\frac{G_N m}{\pi r^2}\right)^2+\frac{\left(64-240\log\left(\frac{r^2C_2}{G_N m}\right)\right)}{81}\left(\frac{G_N m}{\pi r^2}\right)^3$$
$$+\frac{\left(323+2340\log\left(\frac{r^2C_2}{G_N m}\right)+600\log^2\left(\frac{r^2C_2}{G_N m}\right)\right)}{486}\left(\frac{G_N m}{\pi r^2}\right)^4+O(G_N^5), \quad (3.168)$$

and

$$h_2^{\mathrm{dD}}(r) = \frac{40\left(1-2\log\left(\frac{r^2C_2}{G_N m}\right)\right)}{9}\left(\frac{G_N m}{\pi r^2}\right)^2 + \frac{32\left(-4+5\log\left(\frac{r^2C_2}{G_N m}\right)\right)}{27}\left(\frac{G_N m}{\pi r^2}\right)^3 + \frac{8\left(-31-1260\log\left(\frac{r^2C_2}{G_N m}\right)+300\log\left(\frac{r^2C_2}{G_N m}\right)^2\right)}{243}\left(\frac{G_N m}{\pi r^2}\right)^4 + O(G_N^5)\,. \tag{3.169}$$

3.5.3 The metric in the de Donder gauge in six dimensions

The de Donder gauge condition (3.5) in $d = 5$ reads

$$8h_2(r) = r\frac{d}{dr}\left(h_0(r) + 3h_1(r) - h_2(r)\right)\,, \tag{3.170}$$

supplemented with the asymptotic boundary condition

$$\lim_{r\to\infty} f(r) = 1\,. \tag{3.171}$$

This differential equation implies either that $f(r) = C/r$, which does not satisfy the boundary condition (3.171), or $f(r)$ satisfies the differential equation with $x = G_N m/(\pi r^3)$

$$x f(x)^7\left(6x - 4f(x)^3\right)\frac{d^2f(x)}{dx^2} + 9f(x)^6x^2\left(\frac{df(x)}{dx}\right)^2 + f(x)^7\left(\frac{8}{3}f(x)^3 - 10x\right)\frac{df(x)}{dx} - \frac{5}{3}f(x)^8 + f(x)^6 + 4xf(x)^5 - 3xf(x)^3 + \frac{9x^2}{4} = 0\,. \tag{3.172}$$

We solve the equation (3.172) using a series expansion in G_N using (3.154) and the boundary condition (3.155). Asking for an expression with only integer powers of G_N, the result to the order G_N^7 is given by

$$f(r) = 1 + \frac{G_N m}{4\pi r^3} - \frac{5}{8}\left(\frac{G_N m}{\pi r^3}\right)^2 + \frac{2}{3}\left(\frac{G_N m}{\pi r^3}\right)^3 - \frac{775}{1344}\left(\frac{G_N m}{\pi r^3}\right)^4 + \frac{545977}{537600}\left(\frac{G_N m}{\pi r^3}\right)^5 - \frac{15194099}{10483200}\left(\frac{G_N m}{\pi r^3}\right)^6 + \frac{4421000509}{1878589440}\left(\frac{G_N m}{\pi r^3}\right)^7 + O(G_N^8)\,. \tag{3.173}$$

The expression is uniquely determined and finite.

3.5.3.1 The metric perturbation

In $d = 5$ we derive components of the metric in perturbation by plugging the expression for $f(r)$ in (3.173) in (3.152).

We obtain for the metric components

$$\begin{aligned}
h_0^{\rm dD}(r) &= 1 - \frac{3G_N m}{2\pi r^3} + \frac{9}{8}\left(\frac{G_N m}{\pi r^3}\right)^2 - \frac{27}{8}\left(\frac{G_N m}{\pi r^3}\right)^3 + \frac{387}{64}\left(\frac{G_N m}{\pi r^3}\right)^4 + O(G_N^5)\,,\\
h_1^{\rm dD}(r) &= 1 + \frac{G_N m}{2\pi r^3} - \frac{19}{16}\left(\frac{G_N m}{\pi r^3}\right)^2 + \frac{49}{48}\left(\frac{G_N m}{\pi r^3}\right)^3 - \frac{577}{1344}\left(\frac{G_N m}{\pi r^3}\right)^4 + O(G_N^5)\,,\\
h_2^{\rm dD}(r) &= \frac{117}{16}\left(\frac{G_N m}{\pi r^3}\right)^2 - \frac{45}{16}\left(\frac{G_N m}{\pi r^3}\right)^3 + \frac{1599}{112}\left(\frac{G_N m}{\pi r^3}\right)^4 + O(G_N^5)\,.
\end{aligned} \tag{3.174}$$

3.6 Recovering the Schwarzschild-Tangherlini metric from the amplitude computations

In this section we show how the amplitude computations match the Schwarzschild-Tangherlini metric in four, five and six dimensions in the de Donder gauge of the previous section.

3.6.1 The Schwarzschild metric in four dimensions

3.6.1.1 The first post-Minkowskian contribution $O(G_N)$

Setting $d = 3$ in the expressions for the metric perturbation from the tree-level amplitude in (3.46) matches the de Donder gauge first post-Minkowskian order in four dimension ($d = 3$) in (3.160)–(3.162).

3.6.1.2 The second post-Minkowskian contribution $O(G_N^2)$

At the order G_N^2, setting $d = 3$ in the metric perturbation from the one-loop amplitude in (3.58) matches the metric in the de Donder gauge in four dimensions ($d = 3$) in (3.160)–(3.162).

3.6.1.3 The third post-Minkowskian contributions $O(G_N^3)$

At this order the components of the metric in the de Donder gauge in four dimensions ($d = 3$) from (3.160)—(3.162) match the metric components from the renormalised two-loop amplitude computation in (3.120) for the value of

the constant of integration

$$\log C_3 = \log C_E - \frac{7}{2} + 6a^{(1)}(3)\,, \tag{3.175}$$

where C_E is given in (3.121).

With this identification we recover the results of [34] for the renormalisation of the metric divergences and the coordinate change from the de Donder gauge to the harmonic gauge from the world-line approach.

Substituting this value of C_3 in the solution (3.159) completely determines the solution to the de Donder gauge in four dimensions and the coordinate change in (3.159) to the Schwarzschild metric in (3.151) in four dimensions. The parameter $a^{(1)}(3)$ is a free parameter, which corresponds to the running coupling in [34].

3.6.1.4 The fourth post-Minkowskian contribution $O(G_N^4)$

At the fourth post-Minkowskian order, we get again a diverging metric from the amplitude computation. This finite component metric in the de Donder gauge in four dimensions ($d = 3$) in (3.160)—(3.162) using the value of the constant of integration C_3 determined in (3.175) give

$$\begin{aligned}
h_0^{\mathrm{dD}(4)} &= \left(-\frac{32}{3} + 8a^{(1)}(3) + \frac{4}{3}\log\left(\frac{rC_E}{G_N m}\right)\right)\left(\frac{G_N m}{r}\right)^4, \\
h_1^{\mathrm{dD}(4)} &= \left(10 - 8a^{(1)}(3) - \frac{4}{3}\log\left(\frac{rC_E}{G_N m}\right)\right)\left(\frac{G_N m}{r}\right)^4, \\
h_2^{\mathrm{dD}(4)} &= \left(-\frac{86}{3} + 16a^{(1)}(3) + \frac{8}{3}\log\left(\frac{rC_E}{G_N m}\right)\right)\left(\frac{G_N m}{r}\right)^4.
\end{aligned} \tag{3.176}$$

This matches exactly the renormalised metric components from the three-loop amplitude computation obtained in (3.125) with $d = 3$.

3.6.2 The Schwarzschild-Tangherlini metric in five dimensions

3.6.2.1 The first post-Minkowskian contribution $O(G_N)$

Setting $d = 4$ in the expressions for the metric perturbation from the tree-level amplitude in (3.46) matches the de Donder gauge first post-Minkowskian order in five dimensions ($d = 4$) in (3.167)–(3.169).

3.6.2.2 The second post-Minkowskian contribution $O(G_N^2)$

The renormalised one-loop computation in (3.130) matches the expression at order $O(G_N^2)$ from the de Donder gauge in (3.167)—(3.169) for the choice of the constant of integration

$$\log C_2 = \frac{11}{15} + 2\log C_E + \frac{36\pi}{5} a^{(1)}(5)\,. \tag{3.177}$$

Again there is a free parameter $a^{(1)}(5)$ which can be associated with a running coupling constant.

3.6.2.3 The third post-Minkowskian contributions $O(G_N^3)$

At this order in perturbation, the two-loop amplitude computation had divergences that had to be renormalized to give (3.135). This matches exactly the finite component metric in the de Donder gauge in five dimensions ($d = 4$) in (3.167)—(3.169), using the value of the constant of integration C_2 determined in (3.177), given by

$$\begin{aligned}
h_0^{\mathrm{dD}(3)} &= \frac{160}{27}\left(\frac{2}{15} + \frac{36a^{(1)}(5)\pi}{5} + \log\left(\frac{r^2C_E^2}{G_N m}\right)\right)\left(\frac{G_N m}{\pi r^2}\right)^3 + O(d-4), \\
h_1^{\mathrm{dD}(3)} &= -\frac{80}{27}\left(\frac{7}{15} + \frac{36a^{(1)}(5)\pi}{5} + \log\left(\frac{r^2C_E^2}{G_N m}\right)\right)\left(\frac{G_N m}{\pi r^2}\right)^3 + O(d-4), \\
h_2^{\mathrm{dD}(3)} &= \frac{160}{27}\left(-\frac{1}{15} + \frac{36a^{(1)}(5)\pi}{5} + \log\left(\frac{r^2C_E^2}{G_N m}\right)\right)\left(\frac{G_N m}{\pi r^2}\right)^3 + O(d-4)\,.
\end{aligned} \tag{3.178}$$

3.6.2.4 The fourth post-Minkowskian contribution $O(G_N^4)$

The three-loop amplitude computation diverges and the finite metric component at the fourth post-Minkowskian order was obtained after normalisation in (3.142). This matches exactly, the finite component metric in the de Donder gauge in five dimensions ($d = 4$) in (3.167)—(3.169), using the value of the

constant of integration C_2 determined in (3.177), given by

$$
\begin{aligned}
h_0^{\mathrm{dD}(4)} &= -\frac{128}{243}\left(23+324a^{(1)}(5)\pi+45\log\left(\frac{r^2C_E^2}{G_Nm}\right)\right)\left(\frac{G_Nm}{\pi r^2}\right)^4+O(d-4),\\
h_1^{\mathrm{dD}(4)} &= \left(\frac{7085+69552\pi a^{(1)}(5)+93312(\pi a^{(1)}(5))^2}{1458}+\frac{10}{243}(161+432\pi a^{(1)}(5))\log\left(\frac{r^2C_E^2}{G_Nm}\right)\right.\\
&\quad\left.+\frac{100}{81}\log\left(\frac{r^2C_E^2}{G_Nm}\right)^2\right)\left(\frac{G_Nm}{\pi r^2}\right)^4+O(d-4),\\
h_2^{\mathrm{dD}(4)} &= \left(\frac{-19048-141696\pi a^{(1)}(5)373248(\pi a^{(1)}(5))^2}{729}+\frac{160}{243}(-41+216\pi a^{(1)}(5))\log\left(\frac{r^2C_E^2}{G_Nm}\right)\right.\\
&\quad\left.+\frac{800}{81}\log\left(\frac{r^2C_E^2}{G_Nm}\right)^2\right)\left(\frac{G_Nm}{\pi r^2}\right)^4+O(d-4)\,.
\end{aligned}
\tag{3.179}
$$

3.6.3 The Schwarzschild-Tangherlini metric in six dimensions

The metric components in six dimensions ($d=5$) are finite. They are given up to the order $O(G_N^4)$ in (3.174) and are reproduced by the sum of the contributions of the tree-level amplitude in (3.46), one-loop amplitude in (3.58), two-loop amplitude in (3.76) and three-loop amplitude in (3.86) and setting $d=5$ in these expressions.

3.7 Discussion

General relativity can be considered in space-times of various dimensions. It is therefore important to validate our current understanding of the connection between scattering amplitudes and classical general relativity in general dimensions [53, 166]

We have shown how to reconstruct the classical Schwarzschild-Tangherlini metric from scattering amplitudes in four, five and six dimensions. We have extracted the classical contribution as defined in [27] from the vertex function for the emission of a graviton from a massive scalar field. For such a static metric, the classical contribution is obtained by taking appropriate residues on the time components of the loop momenta. These residues project the quantum scattering amplitude on contribution similar to the quantum tree graphs considered in [164], by cutting the massive propagators.

The amplitudes develop ultraviolet divergences which are renormalised by introducing higher-derivative non-minimal couplings in (3.88). The non-minimal coupling removes the ultraviolet divergences in the stress-tensor and the metric components. For the static solution the higher $n \geq 2$ non-minimal coupling only contribute from insertions in tree-level graphs. Interestingly, in six dimensions the metric components are finite but the stress-tensor has ultraviolet divergences. These divergences are removed by adding counter-terms from non-minimal couplings. These counter-terms do not induce any contribution to the metric components. From the presence of ultraviolet poles in the master integrals $J_{(l)}(\vec{q}^2)$ in (3.32), we conclude that in all dimensions one needs to introduce an infinite set of higher-derivative non-minimal operators for removing the ultraviolet divergences from the scattering amplitude. These counter-terms do not affect the space-time geometry because their effect is reabsorbed by the change of coordinate from the de Donder coordinate system to the Schwarzschild-Tangherlini coordinate system.

The scattering amplitude approach presented in this work can be applied to any effective field theory of gravity coupled to matter fields. The amplitudes computations, being performed in general dimensions, lead to results that have an analytic dependence on the space-time dimensions. As black-hole solutions develop non trivial properties in general dimensions [168,169], it is interesting to apply the method of this paper to other black-hole metrics. The Kerr-Newman and Reissner-Nordström metric in four dimensions have been obtained in [24, 90, 92, 182–186] by considering tree-level and one-loop vertex function of the emission of the graviton from a massive particle of spin s. The higher order post-Minkowskian contributions should be obtained from higher-loop amplitudes in a direct application of the methods used in this work.

Chapter 4

Post-Minkowskian Effective Field Theory

In this chapter, we will discuss the Post-Minkowskian Effective Field Theory (PMEFT) [71] formalism to solve for the dynamics of binary systems in gravity. Firstly, we will introduce the formalism and report the state of the art results for the conservative sector [79,81,82,97], which for the spinless case has reached the 4PM order. Then, we will focus on some recent results based on [3] for the radiation sector. Specifically, we derive the conserved stress-energy tensor linearly coupled to gravity and the classical probability amplitude of graviton emission at leading and next-to-leading order in the Newton's constant G. The amplitude can be expressed in compact form as one-dimensional integrals over a Feynman parameter involving Bessel functions. We use it to recover the leading-order radiated angular momentum expression. Upon expanding it in the relative velocity between the two bodies v, we compute the total four-momentum radiated into gravitational waves at leading-order in G and up to order v^8, finding agreement with what recently computed using scattering amplitude methods. Our results also allow to investigate the zero frequency limit of the emitted energy spectrum.

4.1 Introduction

The application of the on-shell methods for Scattering Amplitudes and the strong motivation due to the observational data we are getting, has fuelled immensely the attempts for analytic solutions to the gravitational 2-body problem. The culminating product of the scattering amplitude program is the recent derivation of the 4PM two-body Hamiltonian [80,81]. At this order, a tail effect is present [187–189] and manifests an infrared divergence proportional

to the leading-order (G^3) energy of the radiated Bremsstrahlung, the gravitational waves emitted during the scattering of two masses approaching each other from infinity. Studies on the leading-order gravitational Bremsstrahlung include [42, 190–195]. The full leading-order energy spectrum found in [80] was independently obtained in [102] using the formalism of [28], which derives classical observables from scattering amplitudes and their unitarity cuts. Recently, it was rederived independently in [104] using the eikonal approximation and in the Worldline QFT formalism in [105]. It is well known from PN approximation that radiation effects backreact on the conservative dynamics, therefore is becomes very important to study these effects in detail and develop appropriate techniques. In addition, the gravitational waveform being a crucial ingredient for the gravitational wave templates can only be derived in such formulations making their importance even more apparent. In this chapter we study the gravitational Bremsstrahlung using a worldline approach inspired by Non-Relativistic-General-Relativity (NRGR) [34] (see [111, 112, 196–198] for reviews) and recently applied to the PM expansion [69–71, 79, 199].

The rest of the chapter is organized as follows. In Section 4.2, we will briefly review the basics of the PMEFT formalism needed for the rest of the sections. In Section 4.3, we include radiation in the PMEFT setup and define the Feynman rules that allow us to derive, in Section 4.4 the leading and next-to-leading order stress-energy tensor linearly coupled to gravity. In Section 4.5, we compute the classical probability amplitude of graviton emission, which is directly related to the waveform in Fourier space. The amplitude is the basic ingredient for the computation of observables such as the radiated four-momentum, computed in Section 4.6, and angular momentum in Section 4.7, which we discuss in various limit and compare to the literature. In Section 4.8, we provide a discussion of our results and future investigations. In appendix B.1 we give the explicit expression for the polarization tensors in the tranverse-traceless gauge and the expression for the angular momentum operator in polar coordinates. In appendix B.2, we provide the details of the master integrals involved in our computation and in appendix B.3, the values of several coefficients we are using in our expressions. In appendix B.4 we give the explicit expression for the waveform in direct space and in appendix B.5 the spectral and angular dependence of the radiated four-momentum in momentum space.

4.2 PMEFT setup

Following the EFT "spirit" in [34] and the extension to the PM framework in [71], we construct a worldline action to describe the bodies as point particles

$$S_{pp} = -\sum_a m_a \int d\sigma_a \sqrt{g_{\mu\nu}(x_a^\alpha(\sigma))\mathcal{U}_a^\mu(\sigma_a)\mathcal{U}_a^\nu(\sigma_a)} + \dots \,, \tag{4.1}$$

where $\mathcal{U}_a^\mu \equiv \frac{dx^\mu}{d\sigma}$ and the ellipses account for finite size effects and possible counterterms (as we saw in the previous chapter). For example, using the proper time τ, the ellipses takes the form

$$\dots = \int d\tau_a \big(c_R^{(a)} R(x_a) + c_V^{(a)} R_{\mu\nu}(x_a)\mathcal{U}_a^\mu \mathcal{U}_a^\nu + c_{E^2}^{(a)} E_{\mu\nu}(x_a)E^{\mu\nu}(x_a) + c_{B^2}^{(a)} B_{\mu\nu}(x_a)B^{\mu\nu}(x_a) + \dots\big) \,, \tag{4.2}$$

and additional operators to include spin effects and higher order finite size effects. Importantly, as observed in the previous chapter, the c_R, c_V coefficients fo not contribute to physical quantities since they can be removed by field redefinitions. However, they may be needed to properly renormalize the theory removing intermediate UV poles. The c_{E^2}, c_{B^2} operators represent tidal Love numbers. In the following, we will not consider these higher order operators since they do not contribute to the order we are interested.

In the PM formalism, it is convenient to work with a Polyakov-like parametrization of the action

$$S_{pp} = -\sum_a \frac{m_a}{2} \int d\sigma_a e_a \Big[\frac{1}{e_a^2} g_{\mu\nu}(x_a^\alpha(\sigma))\mathcal{U}_a^\mu(\sigma_a)\mathcal{U}_a^\nu(\sigma_a) + 1\Big] \,, \tag{4.3}$$

such that variations with respect to e_a give $e_a = \sqrt{g_{\mu\nu}\mathcal{U}_a^\mu\mathcal{U}_a^\nu}$, recovering 4.1. Therefore, we can choose the gauge where $e_a = 1$, giving $\sigma_a = \tau_a$. In the weak field approximation, expanding the metric as

$$g_{\mu\nu} = \eta_{\mu\nu} + \frac{h_{\mu\nu}}{m_{\rm Pl}} \,, \tag{4.4}$$

we notice that the action 4.3 generates only a one-point function. Therefore, all the non-linearity is encoded in the bulk action. This fact will prove very useful for practical purposes.

From now on, we will work in Einstein's gravity, described by the Einstein-Hilbert action

$$S_{EH} = -2m_{\rm Pl}^2 \int d^4x\sqrt{-g}R \ . \tag{4.5}$$

In order to work perturbatively, we need to use a gauge fixing term. In [71], it was considered a generalized gauge fixing condition as well as total derivatives which simplifiy the graviton vertices. In addition, one can consider also field redefinitions which would further simplify the graviton vertices, but in turn they would modify the worldline vertices, spoiling the apparent simplicity when working with the Polyakov-like point particle action. Even though, considering a generalized gauge fixing term is advantegeous for higher order computations, in the order that we are considering for the radiation contribution, it is equivalent to work in the usual de Donder gauge.

$$S_{\rm gf} = \int d^4x \left[\frac{1}{2}\partial_\rho h_{\mu\nu}\partial^\rho h^{\mu\nu} - \frac{1}{4}\partial_\rho h \partial^\rho h\right] \ , \tag{4.6}$$

where $h \equiv h^\alpha_\alpha$ is the trace of the metric perturbation. Using the above PMEFT formalism, results for the conservative scattering angle have been derived up to 4PM order for the spinless case [81] finding complete agreement with previously derived results in [80], as well as results including conservative tidal effects [82] and spin effects [97]. Our purpose in the following is to complement the above results with the radiated momentum and angular momentum derived within the PMEFT formalism at leading order.

4.3 Radiation in PMEFT

We consider the scattering of two gravitationally interacting spinless bodies with mass m_1 and m_2 approaching each other from infinity. The gravitational dynamics is described by the usual Einstein-Hilbert action. Neglecting finite size effects, which would contribute at higher order in G (see e.g. [71, 82]), the bodies are treated as external sources described by point-particle actions. We use the Polyakov-like parametrization of the action and fix the vielbein to unity. This has the advantage of simplifying the gravitational coupling to the matter sources [71, 200, 201]. Therefore, using the mostly minus metric signature, setting $\hbar = c = 1$ and defining the Planck mass as $m_{\rm Pl} \equiv 1/\sqrt{32\pi G}$, we have

$$\begin{aligned} S = &-2m_{\rm Pl}^2 \int d^4x\sqrt{-g}R \\ &- \sum_{a=1,2} \frac{m_a}{2} \int d\tau_a \left[g_{\mu\nu}(x_a)\mathcal{U}_a^\mu(\tau_a)\mathcal{U}_a^\nu(\tau_a) + 1\right] \ , \end{aligned} \tag{4.7}$$

where, for each body a, τ_a is its proper time and $\mathcal{U}_a^\mu \equiv dx_a^\mu/d\tau_a$ is its four-velocity.

To compute the waveform we need the (pseudo) stress-energy tensor $T^{\mu\nu}$, defined as the linear term sourcing the gravitational field in the effective action [9, 34, 202], i.e.,

$$\Gamma[x_a, h_{\mu\nu}] = -\frac{1}{2m_{\rm Pl}} \int d^4x T^{\mu\nu}(x) h_{\mu\nu}(x) \ . \tag{4.8}$$

In this equation $h_{\mu\nu} \equiv m_{\rm Pl}(g_{\mu\nu} - \eta_{\mu\nu})$ denotes a radiated field propagating on-shell, while $T^{\mu\nu}$ must include the contribution of both potential modes, i.e. off-shell modes responsible for the conservative forces in the two-body system, and radiation modes. (We will come back to this split below.)

From the Fourier transform of $T^{\mu\nu}$, defined by $\tilde{T}^{\mu\nu}(k) = \int d^4x\, T^{\mu\nu}(x) e^{ik\cdot x}$, one can compute the (classical) probability amplitude of one graviton emission with momentum $\mathbf{k}$ and helicity $\lambda = \pm 2$ [34],

$$i\mathcal{A}_\lambda(k) = -\frac{i}{2m_{\rm Pl}} \epsilon^{*\lambda}_{\mu\nu}(\mathbf{k}) \tilde{T}^{\mu\nu}(k) \ , \tag{4.9}$$

where $\epsilon^\lambda_{\mu\nu}(\mathbf{k})$ is the transverse-traceless helicity-2 polarization tensor, with normalization $\epsilon^{*\lambda}_{\mu\nu}(\mathbf{k})\epsilon^{\mu\nu}_{\lambda'}(\mathbf{k}) = \delta^\lambda_{\lambda'}$ (see definition in App. B.1). At distances r much larger than the interaction region, the waveform is given in terms of the amplitude as (see e.g. [203])

$$h_{\mu\nu}(x) = -\frac{1}{4\pi r} \sum_{\lambda=\pm 2} \int \frac{dk^0}{2\pi} e^{-ik^0 u} \epsilon^\lambda_{\mu\nu}(\mathbf{k}) \mathcal{A}_\lambda(k)|_{k^\mu = k^0 n^\mu} \ , \tag{4.10}$$

where $u \equiv t - r$. The amplitude is evaluated on-shell, i.e. $k^\mu = k^0 n^\mu$, with $n^\mu \equiv (1, \mathbf{n})$ and $\mathbf{n}$ the unitary vector pointing along the graviton trajectory.

We can obtain the stress-energy tensor defined above by matching eq. (4.8) to the effective action computed order by order in G using Feynman diagrams. Let us now introduce the Feynman rules. Adding the usual de Donder gauge-fixing term to eq. (4.7),

$$S_{\rm gf} = \int d^4x \left[\frac{1}{2} \partial_\rho h_{\mu\nu} \partial^\rho h^{\mu\nu} - \frac{1}{4} \partial_\rho h \partial^\rho h \right] \ , \tag{4.11}$$

where $h \equiv \eta^{\mu\nu} h_{\mu\nu}$, from the quadratic part of the gravitational action one can extract the graviton propagator,

$$\mu\nu \quad \overset{k}{\bullet\!\!\sim\!\!\sim\!\!\sim\!\!\bullet} \quad \rho\sigma = \frac{i}{k^2} P_{\mu\nu;\rho\sigma} \ , \tag{4.12}$$

where $P_{\mu\nu;\rho\sigma} \equiv \frac{1}{2}(\eta_{\mu\rho}\eta_{\nu\sigma} + \eta_{\mu\sigma}\eta_{\nu\rho} - \eta_{\mu\nu}\eta_{\rho\sigma})$. As usual, we must specify the contour of integration in the complex k^0 plane by suitable boundary conditions. This is customary done by splitting the gravitons into potential and radiation modes (see e.g. [34, 71]). Potential modes never hit the pole $k^2 = 0$, so the choice of boundary conditions does not affect the calculations. For radiation modes one must impose retarded boundary conditions, i.e. $[(k^0+i\epsilon)^2-|\mathbf{k}|^2]^{-1}$, to account only for outgoing gravitons. Even though not relevant at the order in G at which we work here, in general one must treat with care the pole of radiation modes since they play a key role for hereditary effects at higher orders [123].

Finally, from the gravitational action one can derive the cubic interaction vertex, which is the only one relevant for this paper. In de Donder gauge it can be found, for instance, in [9, 204].

Thanks to the Polyakov-like form, the point-particle action contains only a linear interaction vertex. However, in order to isolate the powers of G, we parametrize the worldline by expanding around straight trajectories [71, 79], i.e.,

$$x_a^\mu(\tau_a) = b_a^\mu + u_a^\mu \tau_a + \delta^{(1)} x_a^\mu(\tau_a) + \dots \,, \tag{4.13}$$

$$\mathcal{U}_a^\mu(\tau_a) = u_a^\mu + \delta^{(1)} u_a^\mu(\tau_a) + \dots \,. \tag{4.14}$$

Here u_a is the (constant) asymptotic incoming velocity and b_a is the body displacement orthogonal to it, $b_a \cdot u_a = 0$, while $\delta^{(1)} x_a^\mu$ and $\delta^{(1)} u_a^\mu$ are respectively the deviation from the straight trajectory and constant velocity of body a at order G, induced by the gravitational interaction. Moreover, we define the impact parameter as $b^\mu \equiv b_1^\mu - b_2^\mu$ and the relative Lorentz factor as

$$\gamma \equiv u_1 \cdot u_2 = \frac{1}{\sqrt{1-v^2}} \,, \tag{4.15}$$

where v is the relativistic relative velocity between the two bodies.

The expansion of the worldline action in the second line of eq. (4.7) generates two Feynman interaction rules that differ by their order in G. At zeroth order, we have (with $\int_q \equiv \int \frac{d^4q}{(2\pi)^4}$)

$$\tau_a \bullet\!\!\sim\!\!\sim = -\frac{i m_a}{2 m_{\rm Pl}} u_a^\mu u_a^\nu \int d\tau_a \int_q e^{-iq\cdot(b_a + u_a \tau_a)} \,, \tag{4.16}$$

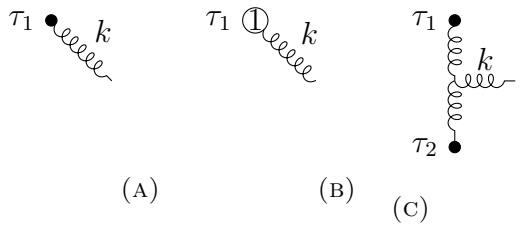

FIGURE 4.1: The three Feynman diagrams needed for the computation of the stress-energy tensor up to NLO order in G. To compute the symmetric one, it is enough to exchange $1 \leftrightarrow 2$.

where a filled dot denotes the point particle evaluated using the straight worldline. At first order in G we have

$$\begin{aligned} \overset{\tau_a}{\textcircled{1}\!\!\sim\!\!\sim} &= -\frac{im_a}{2m_{\rm Pl}} \int d\tau_a \int_q e^{-iq\cdot(b_a+u_a\tau_a)} \\ &\quad \times \left(2\delta^{(1)}u_a^{(\mu}(\tau_a)u_a^{\nu)} - i(q\cdot\delta^{(1)}x_a(\tau_a))u_a^\mu u_a^\nu\right) \ , \end{aligned} \tag{4.17}$$

where the correction $\mathcal{O}(G^n)$ to the trajectory is denoted by the order n inside the circle. Following [71], the $\mathcal{O}(G)$ correction to the velocity and the trajectory can be computed by solving the geodesic equation obtained from the effective Lagrangian at order G. In de Donder gauge it reads, for particle 1,

$$\delta^{(1)}u_1^\mu(\tau) = \frac{m_2}{4m_{\rm Pl}^2}\int_q \bar{\delta}(q\cdot u_2)\frac{e^{-iq\cdot b - iq\cdot u_1\tau}}{q^2}B_1^\mu \ , \tag{4.18}$$

$$\delta^{(1)}x_1^\mu(\tau) = \frac{im_2}{4m_{\rm Pl}^2}\int_q \bar{\delta}(q\cdot u_2)\frac{e^{-iq\cdot b - iq\cdot u_1\tau}}{q^2(q\cdot u_1+i\varepsilon)}B_1^\mu \ , \tag{4.19}$$

where $B_1^\mu \equiv \frac{2\gamma^2-1}{2}\frac{q^\mu}{q\cdot u_1+i\varepsilon} - 2\gamma u_2^\mu + u_1^\mu$. (An analogous expression holds for particle 2.) The $+i\epsilon$ in the above equations ensures to recover straight motion in the asymptotic past, i.e. $\delta^{(1)}u_1^\mu(-\infty) = 0$ and $\delta^{(1)}x_1^\mu(-\infty) = 0$. At our order in G, the deflected trajectories are completely determined by potential gravitons but in general one must take into account also radiation modes with appropriate boundary conditions. Note also that at higher order it can be convenient to use different gauge-fixing conditions to simplify the graviton vertices [71].

4.4 Stress-energy tensor

The radiated field can be computed in powers of G in terms of the diagrams shown in Fig. 4.1. The leading stress-energy tensor is obtained from Fig. 4.1a

and corresponds to the one of free point-particles, i.e.,

$$\tilde{T}^{\mu\nu}_{\text{Fig. 4.1a}}(k) = \sum_a m_a u_a^\mu u_a^\nu e^{ik\cdot b_a} \bar{\delta}(\omega_a) \,, \tag{4.20}$$

where we use the notation $\bar{\delta}^{(n)}(x) \equiv (2\pi)^n \delta^{(n)}(x)$ and for convenience we define

$$\omega_a \equiv k \cdot u_a \,, \qquad a = 1, 2 \,. \tag{4.21}$$

This generates a static and non-radiating contribution to the amplitude, proportional to $\bar{\delta}(\omega_a)$. While this contribution can be neglected when computing the radiated momentum, it must be crucially included for the computation of the angular momentum, as shown below.

At the next order we find

$$\begin{aligned}\tilde{T}^{\mu\nu}_{\text{Fig. 4.1b}}(k) = \frac{m_1 m_2}{4m_{\text{Pl}}^2} \int_{q_1,q_2} \mu_{1,2}(k) \frac{1}{q_2^2} \Bigg[& \frac{2\gamma^2-1}{\omega_1 + i\epsilon} q_2^{(\mu} u_1^{\nu)} - 4\gamma u_2^{(\mu} u_1^{\nu)} \\ & - \left(\frac{2\gamma^2-1}{2} \frac{k\cdot q_2}{(\omega_1+i\epsilon)^2} - \frac{2\gamma\omega_2}{\omega_1+i\epsilon} - 1 \right) u_1^\mu u_1^\nu \Bigg] \,, \end{aligned} \tag{4.22}$$

$$\begin{aligned}\tilde{T}^{\mu\nu}_{\text{Fig. 4.1c}}(k) = \frac{m_1 m_2}{4m_{\text{Pl}}^2} \int_{q_1,q_2} \mu_{1,2}(k) \frac{1}{q_1^2 q_2^2} \Bigg[& \frac{2\gamma^2-1}{2} q_2^\mu q_2^\nu + \left(2\omega_2^2 - q_1^2\right) u_1^\mu u_1^\nu + 4\gamma\omega_2 q_2^{(\mu} u_1^{\nu)} \\ & - \eta^{\mu\nu} \left(\gamma\omega_1\omega_2 + \frac{2\gamma^2-1}{4} q_2^2 \right) + 2\left(\gamma q_1^2 - \omega_1\omega_2\right) u_1^{(\mu} u_2^{\nu)} \Bigg] \,, \end{aligned} \tag{4.23}$$

where

$$\mu_{1,2}(k) \equiv e^{i(q_1\cdot b_1 + q_2\cdot b_2)} \bar{\delta}^{(4)}(k - q_1 - q_2) \bar{\delta}(q_1\cdot u_1) \bar{\delta}(q_2 \cdot u_2) \,, \tag{4.24}$$

and we have used momentum conservation, on-shell and harmonic-gauge conditions to simplify the final expression. Of course, we must also include the analogous diagrams with bodies 1 and 2 exchanged. The contribution in Fig. 4.1b comes from evaluating the worldline along deflected trajectories while the one in Fig. 4.1c comes from the gravitational cubic interaction (see Appendix A.2). We have checked that the sum of these two contributions is transverse for on-shell momenta, i.e. $k_\mu \tilde{T}^{\mu\nu} = 0$ for $k^2 = 0$, as expected for radiated gravitons. We have also verified that the finite part of the stress-energy tensor agrees with that computed in [69] once the contribution from the dilaton is removed.

4.5 Amplitudes and waveforms

We expand the amplitude defined in eq. (4.9) in powers of G, $\mathcal{A}_\lambda = \mathcal{A}_\lambda^{(1)} + \mathcal{A}_\lambda^{(2)} + \dots$. Given the definition (4.9) and the stress-energy tensor (4.20), the leading order reads

$$\mathcal{A}_\lambda^{(1)}(k) = -\frac{1}{2m_{\rm Pl}} \sum_a m_a \, \epsilon^{*\lambda}_{\mu\nu}(\mathbf{n}) u_a^\mu u_a^\nu \, e^{ik\cdot b_a} \bar{\delta}(\omega_a) \, . \tag{4.25}$$

The NLO can be obtained by summing eqs. (4.22) and (4.23) and inserting the result in eq. (4.9). Integrating over one of the internal momenta,

$$\begin{aligned}\mathcal{A}_\lambda^{(2)}(k) = -\frac{m_1 m_2}{8 m_{\rm Pl}^3} \epsilon^{*\lambda}_{\mu\nu}(\mathbf{n}) \Bigg\{ e^{ik\cdot b_1} \Bigg[\left(-\frac{2\gamma^2-1}{2} \frac{k\cdot I_{(1)}}{(\omega_1 + i\epsilon)^2} + \frac{2\gamma\omega_2}{\omega_1 + i\epsilon} I_{(0)} + 2\omega_2^2 J_{(0)} \right) u_1^\mu u_1^\nu \\ + \left(\frac{2\gamma^2-1}{\omega_1 + i\epsilon} I^\mu_{(1)} + 4\gamma\omega_2 J^\mu_{(1)} \right) u_1^\nu - 2\left(\gamma I_{(0)} + \omega_1\omega_2 J_{(0)} \right) u_1^\mu u_2^\nu + \frac{2\gamma^2-1}{2} J^{\mu\nu}_{(2)} \Bigg] \Bigg\} + (1 \leftrightarrow 2) \, ,\end{aligned} \tag{4.26}$$

where we have defined the following integrals,

$$I^{\mu_1\dots\mu_n}_{(n)} \equiv \int_q \bar{\delta}(q\cdot u_1 - \omega_1) \, \bar{\delta}(q\cdot u_2) \, \frac{e^{-iq\cdot b}}{q^2} q^{\mu_1} \dots q^{\mu_n} \, , \tag{4.27}$$

$$J^{\mu_1\dots\mu_n}_{(n)} \equiv \int_q \bar{\delta}(q\cdot u_1 - \omega_1) \, \bar{\delta}(q\cdot u_2) \, \frac{e^{-iq\cdot b}}{q^2 (k-q)^2} q^{\mu_1} \dots q^{\mu_n} \, . \tag{4.28}$$

(The indices inside these integrals must be changed when evaluating the symmetric contribution $(1 \leftrightarrow 2)$.) As detailed in App. B.2, the first set of integrals in eq. (4.27) can be solved in terms of Bessel functions. The second set of integrals in eq. (4.28) comes exclusively from the gravitational cubic interaction in Fig. 4.1c. Unfortunately we were not able to come up with an explicitly solution to these integrals. However, we can express them as one- dimensional integrals over a Feynman parameter, involving Bessel functions.

To simplify the treatment, from now on we choose a frame in which one of the two bodies, say 2, is at rest. Moreover, for convenience we can set $b_2^\mu = 0$ and $b_1^\mu = b^\mu$ and define the unit spatial vectors in the direction of $\mathbf{v}$ and of the impact parameter $\mathbf{b}$, respectively $\mathbf{e}_v \equiv \mathbf{v}/v$ and $\mathbf{e}_b = \mathbf{b}/|\mathbf{b}|$, with $\mathbf{e}_v \cdot \mathbf{e}_b = 0$. We also define $v^\mu \equiv (1, v\mathbf{e}_v)$ so that

$$u_2^\mu = \delta_0^\mu \, , \qquad u_1^\mu = \gamma v^\mu = \gamma(1, v\mathbf{e}_v) \, . \tag{4.29}$$

The energies of the radiated gravitons measured by the two bodies become, respectively, $\omega_2 = k^0 \equiv \omega$ and $\omega_1 = \gamma\omega \, n\cdot v$. The amplitude simplifies to the

following compact forms

$$\mathcal{A}^{(1)}_{\lambda}(k) = -\frac{m_1}{2m_{\rm Pl}}\,\frac{\gamma v^2}{n\cdot v}\epsilon^{*\lambda}_{ij}\mathbf{e}^i_v\mathbf{e}^j_v\,\bar{\delta}(\omega)e^{ik\cdot b}\,, \tag{4.30}$$

$$\mathcal{A}^{(2)}_{\lambda}(k) = -\frac{Gm_1m_2}{m_{\rm Pl}\gamma v}\epsilon^{*\lambda}_{ij}\mathbf{e}^i_I\mathbf{e}^j_J A_{IJ}(k)e^{ik\cdot b}\,, \tag{4.31}$$

where the functions A_{IJ} can be obtained after solving the integrals (4.27) and (4.28). We find

$$\begin{aligned} A_{vv} &= c_1K_0\big(z(n\cdot v)\big) + ic_2\Big[K_1\big(z(n\cdot v)\big) - i\pi\delta\big(z(n\cdot v)\big)\Big] \\ &\quad + \int_0^1 dy\, e^{iyzv\mathbf{n}\cdot\mathbf{e}_b}\Big[d_1(y)zK_1\big(zf(y)\big) + c_0K_0\big(zf(y)\big)\Big]\,, \end{aligned} \tag{4.32}$$

$$\begin{aligned} A_{vb} &= ic_0\Big[K_1\big(z(n\cdot v)\big) - i\pi\delta\big(z(n\cdot v)\big)\Big] \\ &\quad + i\int_0^1 dy\, e^{iyzv\mathbf{n}\cdot\mathbf{e}_b}d_2(y)zK_0\big(zf(y)\big)\,, \end{aligned} \tag{4.33}$$

$$A_{bb} = \int_0^1 dy\, e^{iyzv\mathbf{n}\cdot\mathbf{e}_b}d_0(y)zK_1\big(zf(y)\big)\,, \tag{4.34}$$

where K_0 and K_1 are modified Bessel functions of the second kind and we have introduced

$$z \equiv \frac{|\mathbf{b}|\omega}{v}\,, \tag{4.35}$$

and

$$f(y) \equiv \sqrt{(1-y)^2(n\cdot v)^2 + 2y(1-y)(n\cdot v) + y^2/\gamma^2}\,. \tag{4.36}$$

The coefficients c_0, c_1 and c_2 depend on v and on the relative angles between the graviton direction and the basis $(\mathbf{e}_v, \mathbf{e}_b)$. Moreover, d_0, d_1 and d_2 depend also on the integration parameter y. Their explicit form is given in App. B.3. In eqs. (4.32) and (4.33) we have also included the non-radiating contribution proportional to a delta function,* which may become relevant, for instance, when computing the radiated angular momentum at NLO.

For small-velocities we find agreement between our amplitude and the waveform in Fourier space of [194]. In this limit $f(y) \to 1$, $e^{iyzv\mathbf{n}\cdot\mathbf{e}_b} \to 1$, $\gamma \to 1$, and

*To compute this contribution we have used this integral:

$$\int_q \delta(q\cdot u_1)\delta(q\cdot u_2)\frac{e^{-iq\cdot b}q^\mu}{q^2} = \frac{b^\mu}{2\pi\gamma v|\mathbf{b}|^2}\,. \tag{4.37}$$

thus[†]

$$A_{vv} \xrightarrow[v\to 0]{} zK_1(z) + K_0(z) \,, \tag{4.38}$$

$$A_{vb} \xrightarrow[v\to 0]{} -i\left[K_1(z) + zK_0(z) - i\pi\delta(z)\right] \,, \tag{4.39}$$

$$A_{bb} \xrightarrow[v\to 0]{} -zK_1(z) \,. \tag{4.40}$$

We have also checked that we recover their amplitude in the forward and backward limit (i.e. $\mathbf{n}$ along the direction of $\mathbf{e}_v$), for which $\mathbf{n}\cdot\mathbf{e}_b \to 0$ and the integral in y can be solved exactly. The waveform can be computed by replacing the amplitude in eq. (4.10) and integrating in k^0. We discuss this calculation in App. B.4.

4.6 Radiated four-momentum

In terms of the asymptotic waveform, the radiated four-momentum at infinity ($r \to \infty$) is given by [101, 194][‡]

$$P^\mu_{\rm rad} = \int d\Omega\, du\, r^2\, n^\mu\, \dot{h}_{ij}\dot{h}_{ij} \,, \tag{4.41}$$

where a dot denotes the derivative with respect to the retarded time u and $d\Omega$ is the integration surface element.

Using eq. (4.10) for the waveform, this can be expressed in a manifestly Lorentz-invariant way in terms of the amplitude (4.9) as [69]

$$P^\mu_{\rm rad} = \sum_\lambda \int_k \bar{\delta}(k^2)\theta(k^0)k^\mu \left|\mathcal{A}_\lambda(k)_{\rm finite}\right|^2 \,, \tag{4.42}$$

where θ is the Heaviside step function and on the right-hand side we take only the finite part of the amplitude, excluding the terms proportional to a delta function that do not contribute to $\dot{h}_{ij}$. Thus, at leading order $|\mathcal{A}_\lambda(k)_{\rm finite}|^2 = |\mathcal{A}^{(2)}_\lambda(k)_{\rm finite}|^2 + \dots$ and hence the radiated four-momentum starts at order G^3

Since the modulo squared of the amplitude is symmetric under $\mathbf{k} \to -\mathbf{k}$ the four-momentum cannot depend on the spatial direction b^μ. Moreover, the energy measured in the frame of one body is the same as the one measured in the frame of the other one, hence the final result must be proportional to

[†]The signs in front of K_0 and K_1 of the last term of eqs. (2.9b) and (2.9c) of [194] are incorrect.

[‡]We are using a different normalization of $h_{\mu\nu}$ with respect to these references, which explains the absence of the prefactor $(32\pi G)^{-1}$.

$u_1^\mu + u_2^\mu$. Using eq. (4.31), we can write it as

$$P^\mu_{\rm rad} = \frac{G^3 m_1^2 m_2^2}{|\mathbf{b}|^3} \frac{u_1^\mu + u_2^\mu}{\gamma+1} \mathcal{E}(\gamma) + \mathcal{O}(G^4) \,, \tag{4.43}$$

which confirms that at this order the result has homogeneous mass dependence and is thus fixed by the probe limit [102, 188, 194]. The function $\mathcal{E}(\gamma)$ can be found by integrating over the phase space the modulo squared of the amplitude,

$$\mathcal{E}(\gamma) = \int d\Omega \int_0^\infty dz \frac{d\mathcal{E}}{dz d\Omega}(z, \Omega; \gamma) \tag{4.44}$$

with

$$\frac{d\mathcal{E}}{dz d\Omega} \equiv \frac{2vz^2}{\pi^2 \gamma^2} \sum_\lambda \left| \epsilon^{*\lambda}_{ij} \mathbf{e}^i_I \mathbf{e}^j_J A_{IJ}(z, \Omega) \right|^2 . \tag{4.45}$$

A more explicit but long expression of this function is reported in App. B.5, see eq. (B.46).

Due to the involved structure of the y integrals in eq. (4.31), we were unable to compute $\mathcal{E}$ explicitly. Nevertheless, we can first compute the integrals in y in the $v \ll 1$ regime at any order. Then we can perform the phase-space integral expressing the angular dependence in a particular coordinate system. We have computed the energy up to order $\mathcal{O}(v^8)$, obtaining

$$\frac{\mathcal{E}}{\pi} = \frac{37}{15} v + \frac{2393}{840} v^3 + \frac{61703}{10080} v^5 + \frac{3131839}{354816} v^7 + \mathcal{O}(v^9) \,. \tag{4.46}$$

The radiated energy in center-of-mass frame, $P_{\rm rad} \cdot u_{\rm CoM}$, where

$$u^\mu_{\rm CoM} = \frac{m_1 u_1^\mu + m_2 u_2^\mu}{\sqrt{m_1^2 + m_2^2 + 2 m_1 m_2 \gamma}} \,, \tag{4.47}$$

agrees with the 2PN results [188, 194, 205] while eq. (4.46) matches the expansion of the fully relativistic result recently found in [102]. This is a non-trivial check of our NLO amplitude (4.31).

As an extra check, we can compute the leading-order energy spectrum in the soft limit, which is obtained by considering only wavelengths of the emitted gravitons much larger than the interaction region, i.e. $|\mathbf{b}|\omega/v \ll 1$. For $E_{\rm rad} \equiv P^0_{\rm rad}$ this is given by

$$\frac{dE_{\rm rad}}{d\omega}\Big|_{\omega\to 0} = \frac{1}{2(2\pi)^3} \sum_\lambda \int d\Omega |\omega \mathcal{A}_\lambda(k)_{\omega\to 0}|^2 \,. \tag{4.48}$$

In this limit the amplitude at order G^2 receives contributions exclusively from

the diagram in Fig. 4.1b, so it is not affected by the gravitational self-interactions. From eqs. (4.31)–(4.34), it reads

$$i\mathcal{A}^{(2)}_{\lambda}(k)_{\omega\to 0} = \frac{Gm_1m_2}{m_{\rm Pl}|\mathbf{b}|}\frac{1}{\gamma\omega n\cdot v}\epsilon^{*\lambda}_{ij}(c_2\mathbf{e}^i_v\mathbf{e}^j_v + 2c_0\mathbf{e}^i_v\mathbf{e}^i_b)\ . \tag{4.49}$$

Integrating eq. (4.48) over the angles by fixing some angular coordinate system and introducing the function $\mathcal{I}(v) \equiv -\frac{16}{3} + \frac{2}{v^2} + \frac{2(3v^2-1)}{v^3}\text{arctanh}(v)$ [101], we obtain

$$\left.\frac{dE_{\rm rad}}{d\omega}\right|_{\omega\to 0} = \frac{4}{\pi}\frac{(2\gamma^2-1)^2}{\gamma^2v^2}\frac{G^3m_1^2m_2^2}{|\mathbf{b}|^2}\mathcal{I}(v) + \mathcal{O}(G^4)\ , \tag{4.50}$$

which agrees with [68, 206]. We will come back to this result below.

4.7 Radiated angular momentum

The angular momentum lost by the system is another interesting observable as it can be related to the correction to the scattering angle due to radiation reaction [101]. In terms of the asymptotic waveform this is given by [101, 207]

$$J^i_{\rm rad} = \epsilon^{ijk}\int d\Omega\, du\, r^2\left(2h_{jl}\dot{h}_{lk} - x^j\partial_k h_{lm}\dot{h}_{lm}\right)\ . \tag{4.51}$$

As pointed out in [101], the waveform at order G is static and can be pulled out of the time integration leaving with the computation of the gravitational wave memory $\Delta h_{ij} \equiv \int_{-\infty}^{+\infty} du\, \dot{h}_{ij}$. This can be related to the classical amplitude by eq. (4.10),

$$\Delta h_{ij} = \frac{i}{4\pi r}\sum_{\lambda}\int\frac{d\omega}{2\pi}\epsilon^{\lambda}_{ij}\bar{\delta}(\omega)\omega\mathcal{A}_{\lambda}(k)_{\omega\to 0}\ , \tag{4.52}$$

where from the right-hand side it is clear that only the soft limit contributes to the gravitational wave memory. Moreover, since at this order the soft limit is uniquely determined by the diagram in Fig. 4.1b, the radiated angular momentum does not depend on the gravitational self-interaction, confirming [101].

To compute the radiated angular momentum, it is convenient to introduce a system of polar coordinates where $\mathbf{n} = (\sin\theta\cos\phi, \sin\theta\sin\phi, \cos\theta)$ and an orthonormal frame tangent to the sphere, with $\mathbf{e}_\theta = (\cos\theta\cos\phi, \cos\theta\sin\phi, -\sin\theta)$ and $\mathbf{e}_\phi = (-\sin\phi, \cos\phi, 0)$. To express eq. (4.51) in terms of the amplitudes, we can rewrite the angular dependence in the polarization tensors of the first term inside the parenthesis using $2\varepsilon^{ijk}\epsilon^{\lambda}_{jl}\epsilon^{*\lambda'}_{lk} = -i\lambda n^i\delta^{\lambda\lambda'}$. The second term can be rewritten by noticing that $\epsilon^{ijk}x^j\partial_k = i\hat{L}^i$, where $\hat{L}^i$ is the usual orbital angular

momentum operator, expressed in terms of the angles and their derivatives (see App. B.1). Using $\epsilon^{*\lambda'}_{lm}\hat{\mathbf{L}}\epsilon^{\lambda}_{lm} = \lambda\cot\theta\mathbf{e}_\theta\delta^{\lambda\lambda'}$, we obtain

$$\mathbf{J}_{\rm rad} = \sum_\lambda \int \frac{d\Omega}{(4\pi)^2}\,\omega\mathcal{A}^{(2)*}_\lambda(k)_{\omega\to 0}\,\hat{\mathbf{J}}\bar{\mathcal{A}}^{(1)}_\lambda + \mathcal{O}(G^3)\,, \tag{4.53}$$

where $\hat{\mathbf{J}} \equiv \lambda(\mathbf{n} + \cot\theta\mathbf{e}_\theta) + \hat{\mathbf{L}}$ and we have introduced $\bar{\mathcal{A}}^{(1)}_\lambda$ as the leading-order amplitude striped off of the delta function, i.e. defined by

$$\mathcal{A}^{(1)}_\lambda(k) = \bar{\mathcal{A}}^{(1)}_\lambda\bar{\delta}(\omega)e^{ik\cdot b}\,. \tag{4.54}$$

One can perform the angular integral in eq. (4.53) by aligning $\mathbf{e}_v$ and $\mathbf{e}_b$ along any (mutually orthogonal) directions and eventually obtains

$$\mathbf{J}_{\rm rad} = \frac{2(2\gamma^2-1)}{\gamma v}\frac{G^2m_1m_2J}{|\mathbf{b}|^2}\mathcal{I}(v)(\mathbf{e}_b\times\mathbf{e}_v)\,, \tag{4.55}$$

where $J = m_1\gamma v|\mathbf{b}|$ is the angular momentum at infinity. This result agrees with [101].

As noticed in [68], from eqs. (4.50) and (4.53) we observe an intriguing proportionality between the energy spectrum in the soft limit and the total emitted angular momentum. We leave a more thorough exploration of this result for the future.

4.8 Discussion

We have studied the gravitational Bremsstrahlung using a worldline approach. In particular, we have computed through the use of Feynman diagrams, expanding perturbatively in G, the leading and next-to-leading order classical probability amplitude of graviton emission and consequently the waveform in Fourier space. The next-to-leading order amplitude receives two contributions: one from the deviation from straight orbits, which can be expressed in terms of modified Bessel functions of the second kind; another from the cubic gravitational self-interaction, which we could rewrite as one-dimensional integrals over a Feynman parameter of modified Bessel functions. When comparison was possible, we found agreement with earlier calculations of the waveforms [190, 193] in different limits.

We have used the amplitude to compute the leading-order radiated angular momentum, recovering the result of [101]. Moreover, we have computed the total emitted four-momentum expanded in small velocities up to order v^8 and

we found agreement with the recent results of [80, 102]. Unfortunately we were not able to reproduce their fully relativistic result, which we leave for the future. The bottleneck of going to higher orders seems to be the integrals of the form 4.28 which were also encountered in [104]. Nevertheless, we have built the foundations for an alternative derivation of the recent results obtained with amplitude techniques.

Another interesting limit is for small gravitational wave frequencies, where the amplitude does not receive contributions from the gravitational interaction. We have computed the soft energy spectrum recovering an intriguing relation with the emitted angular momentum [68]. Future directions include the study of spin and finite-size effects and a more thorough investigation of the relations between differential observables. In addition, going to higher order in the angular momentum loss and the radiated momentum is crucial for the completion of the conservative sector.

Chapter 5

Conclusions

The gravitational waves era has just began. The theoretical understanding and precise modelling of the gravitational dissipative binary problem is essential to investigate the plethora of the forthcoming observational data. In this thesis, we focused on the analytical treatment of the inspiral phase of the binary coalescence. This phase can be treated in different perturbative approximations using several different frameworks. High precision is required in order to probe new physics and therefore it is essential to obtain a good analytic control of the inspiral phase.

Recent advances in the field of Scattering Amplitudes, Effective Field Theory treatment and traditional General Relativity has offered new insights and results regarding the gravitational dynamics of the two-body problem. It is clear that gravity admits a QFT description when viewed as an EFT. Thus, exploiting the toolbox of QFT is a promising avenue both of theoretical and phenomenological interest. In addition, PN and PM approximations, viewed as complementary approximations schemes, along with the connection between scattering and bound systems offers a remarkable opportunity to improve the precision of the perturbative analysis.

In this context, the main body of the thesis comprises of different approaches on the binary problem. Specifically, in Chapter 2 we focused on the NRGR framework for the PN study of the binary problem. We provided a self-contained introduction of the formalism which offers a clean conceptual outline of the several different effects entering the dynamics of the two-body problem. NRGR has resulted in high precision results offering insights of the conceptual and practical bottlenecks that one faces when working in high-precision. Thus, it is an important framework that can teach us a lot when considering alternative approaches. Using NRGR, we computed explicitly the S^3 conservative action at NLO, entering at 4.5 PN order for rapidly rotating compact objects providing

a novel result to the literature.

In Chapter 3, we considered an EFT description of gravity and derived explicitly the Schwarzschild-Tangherlini metric of a spherically symmetric static object from Quantum Scattering Amplitudes. We addressed and resolved several conceptual issues arising in the computation of off-shell gauge dependent quantities from Scattering Amplitudes. Furthermore, we were able to prescribe a general and simple procedure to extract the classical contributions from a Quantum Scattering Amplitude which can be used for the two-body dynamics. Classical limit of Quantum Scattering Amplitudes, in the light of the recent advances in on-shell methods for Scattering Amplitudes, is an essential step to exploit this toolbox to get information for the classical, and the quantum, contributions to the binary problem.

Finally, in Chapter 4 we considered a more recent formalism for PM approximation. Inspired from the NRGR formalism, PMEFT is a classical worldline framework that deals effectively with the PM dynamics of the problem. We extended the formalism to include radiation emission effects and computed explicitly several observables. In addition, we addressed the radiation reaction contribution to the scattering angle of the two-body scattering, providing a crosscheck of previous results. We exhibited the simplicity of this framework and at the same time we faced a technical difficulty regarding the computation of a master integral.

The future of gravitational physics is extremely promising. In order to acquire higher precision, we need to understand and resolve both the conceptual and technical difficulties that arise. An important lesson is that different approaches have different advantages and therefore they should all be pushed to higher orders in order to probe new physics. An important, and common, issue is the integration techniques used in higher-loop computations. In addition, spin and finite size effects are an integral part of the analysis going to higher orders, since they are essential features of astrophysical compact objects. Furthermore, hereditary effects entering both the conservative and dissipative dynamics of the system are of paramount importance. Finally, one should look for GR modifications and quantum signatures in the gravitational wave signal which will be important to investigate the incompleteness of General Relativity.

Appendices

Appendix A

The Schwarzschild-Tangherlini metric from scattering amplitudes in various dimensions

A.1 Fourier transforms

Here we collect the Fourier integrals used to calculate the long range corrections to the energy momentum tensor and the metric.

The Fourier transform form momentum space to direct space

$$\mathcal{F}(\alpha,d)=\int_{\mathbb{R}^d}\frac{1}{|q|^\alpha}e^{i\vec{q}\cdot\vec{x}}\frac{d^d\vec{q}}{(2\pi)^d}=\frac{1}{(4\pi)^{\frac{d}{2}}}\frac{\Gamma\left(\frac{d-\alpha}{2}\right)}{\Gamma\left(\frac{\alpha}{2}\right)}\left(\frac{2}{|\vec{x}|}\right)^{d-\alpha}. \tag{A.1}$$

Using that

$$\partial_{x^i}\partial_{x^j}(\vec{x}^2)^\alpha=2\alpha(\vec{x}^2)^{\alpha-1}\left(\delta_{ij}+2(\alpha-1)\frac{x_ix_j}{\vec{x}^2}\right), \tag{A.2}$$

we have that

$$\mathcal{F}_{ij}(\alpha,d):=\int_{\mathbb{R}^d}\frac{q_iq_j}{|\vec{q}|^{\alpha+2}}e^{i\vec{q}\cdot\vec{x}}\frac{d^d\vec{q}}{(2\pi)^d}=\mathcal{F}(\alpha,d)\left(\frac{1}{\alpha}\delta_{ij}+\frac{\alpha-d}{\alpha}\frac{x_ix_j}{\vec{x}^2}\right). \tag{A.3}$$

We have in particular that

$$\mathcal{F}(0,d)=0,\qquad \mathcal{F}_{ij}(0,d)=\frac{\Gamma\left(\frac{d}{2}\right)}{2\pi^{\frac{d}{2}}|\vec{x}|^d}\left(\delta_{ij}-d\frac{x_ix_j}{\vec{x}^2}\right). \tag{A.4}$$

A.2 Vertices and Propagators

We will here list the Feynman rules which are employed in our calculation. For the derivation of these forms, see [8–10, 24, 49, 208, 209]. Our convention differs from these work by having all incoming momenta. We have stripped off factors of $i\sqrt{8\pi G_N}$ from the vertices and made them explicit in the amplitudes.

- The massive scalar propagator is $\dfrac{i}{q^2 - m^2 + i\varepsilon}$.
- The graviton propagator in de Donder gauge can be written in the form $\dfrac{i\mathcal{P}^{\alpha\beta,\gamma\delta}}{q^2 + i\varepsilon}$ where $\mathcal{P}^{\alpha\beta,\gamma\delta}$ is defined by

$$\mathcal{P}^{\mu\nu,\rho\sigma} = \frac{1}{2}\left(\eta^{\mu\rho}\eta^{\nu\sigma} + \eta^{\mu\sigma}\eta^{\nu\rho} - \frac{2}{D-2}\eta^{\mu\nu}\eta^{\rho\sigma}\right) \tag{A.5}$$

- The 2-scalar-1-graviton vertex $\tau_1^{\mu\nu}(p_1, p_2)$ is

$$\tau^{\mu\nu}(p_1, p_2) = p_1^\mu p_2^\nu + p_1^\nu p_2^\mu + \frac{1}{2}\eta^{\mu\nu}\left(p_1 - p_2\right)^2. \tag{A.6}$$

- The three-graviton vertex has been derived in [208], where $k + q + \pi = 0$,

$$\begin{aligned}
\tau_{(3)}{}^{\mu\nu}_{\alpha\beta,\gamma\delta}(k,q) = -\Bigg(&\mathcal{P}_{\alpha\beta\gamma\delta}\left[k^\mu k^\nu + \pi^\mu\pi^\nu + q^\mu q^\nu - \frac{3}{2}\eta^{\mu\nu}q^2\right] \\
&+ 2q_\lambda q_\sigma\left[I_{\alpha\beta}{}^{\sigma\lambda}I_{\gamma\delta}{}^{\mu\nu} + I_{\gamma\delta}{}^{\sigma\lambda}I_{\alpha\beta}{}^{\mu\nu} - I_{\alpha\beta}{}^{\mu\sigma}I_{\gamma\delta}{}^{\nu\lambda} - I_{\gamma\delta}{}^{\mu\sigma}I_{\alpha\beta}{}^{\nu\lambda}\right] \\
&+ \Big[q_\lambda q^\mu\left(\eta_{\alpha\beta}I_{\gamma\delta}{}^{\nu\lambda} + \eta_{\gamma\delta}I_{\alpha\beta}{}^{\nu\lambda}\right) + q_\lambda q^\nu\left(\eta_{\alpha\beta}I_{\gamma\delta}{}^{\mu\lambda} + \eta_{\gamma\delta}I_{\alpha\beta}{}^{\mu\lambda}\right) \\
&- q^2\left(\eta_{\alpha\beta}I_{\gamma\delta}{}^{\mu\nu} + \eta_{\gamma\delta}I_{\alpha\beta}{}^{\mu\nu}\right) - \eta^{\mu\nu}q_\sigma q_\lambda\left(\eta_{\alpha\beta}I_{\gamma\delta}{}^{\sigma\lambda} + \eta_{\gamma\delta}I_{\alpha\beta}{}^{\sigma\lambda}\right)\Big] \\
&+ \Big[2q_\lambda\big(I_{\alpha\beta}{}^{\lambda\sigma}I_{\gamma\delta\sigma}{}^{\nu}\pi^\mu + I_{\alpha\beta}{}^{\lambda\sigma}I_{\gamma\delta\sigma}{}^{\mu}\pi^\nu + I_{\gamma\delta}{}^{\lambda\sigma}I_{\alpha\beta\sigma}{}^{\nu}k^\mu + I_{\gamma\delta}{}^{\lambda\sigma}I_{\alpha\beta\sigma}{}^{\mu}k^\nu\big) \\
&+ q^2\left(I_{\alpha\beta\sigma}{}^{\mu}I_{\gamma\delta}{}^{\nu\sigma} + I_{\alpha\beta}{}^{\nu\sigma}I_{\gamma\delta\sigma}{}^{\mu}\right) + \eta^{\mu\nu}q_\sigma q_\lambda\left(I_{\alpha\beta}{}^{\lambda\rho}I_{\gamma\delta\rho}{}^{\sigma} + I_{\gamma\delta}{}^{\lambda\rho}I_{\alpha\beta\rho}{}^{\sigma}\right)\Big] \\
&+ \Big\{(k^2 + \pi^2)\big[\mathcal{P}_{\alpha\beta}{}^{\mu\sigma}\mathcal{P}_{\gamma\delta,\sigma}{}^{\nu} + \mathcal{P}_{\gamma\delta}{}^{\mu\sigma}\mathcal{P}_{\alpha\beta,\sigma}{}^{\nu} - \frac{1}{2}\eta^{\mu\nu}(\mathcal{P}_{\alpha\beta,\gamma\delta} - \eta_{\alpha\beta}\eta_{\gamma\delta})\big] \\
&+ \left(\mathcal{P}_{\gamma\delta}{}^{\mu\nu}\eta_{\alpha\beta}\pi^2 + \mathcal{P}_{\alpha\beta}{}^{\mu\nu}\eta_{\gamma\delta}k^2\right)\Big\}\Bigg),
\end{aligned} \tag{A.7}$$

where $I_{\alpha\beta,\gamma\delta} := \mathcal{P}_{\alpha\beta,\gamma\delta} + \frac{1}{2}\,\eta_{\alpha\beta}\eta_{\gamma\delta}$. These vertices are equivalent to the ones computed with the vertices given by De Witt [8–10] and Sannan [209]. We remark that the expression for τ_3 is simpler than the three-graviton vertex in these references.

We notice that the three-graviton vertex satisfies the identity

$$\tau_{(3)}{}^{\mu\nu}_{\ \ \pi\rho,\sigma\tau}(l,q)\mathcal{P}^{\pi\rho}_{\alpha\beta}\mathcal{P}^{\sigma\tau}_{\gamma\delta} = \tau_{(3)}{}^{\mu\nu}_{\ \ \alpha\beta,\gamma\delta}(l,q) \tag{A.8}$$

that will be used to simplify the expression of the amplitude.

- The four-graviton vertex with $k_1 + k_2 + k_3 + k_4 = 0$ is given in [173, 209]

$$\begin{aligned}
\tilde{\tau}^{\rho\lambda}_{(4)\,\mu\nu,\sigma\tau,\iota\kappa}(k_1,k_2,k_3,k_4) = &-\frac{1}{32}(k_1\cdot k_2\eta^{\mu\nu}\eta^{\sigma\tau}\eta^{\rho\lambda}\eta_{\iota\kappa}) - \frac{1}{16}(k_1^\sigma k_1^\tau\eta^{\mu\nu}\eta^{\rho\lambda}\eta_{\iota\kappa}) \\
&- \frac{1}{16}(k_1^\sigma k_2^\mu\eta^{\nu\tau}\eta^{\rho\lambda}\eta_{\iota\kappa}) + \frac{1}{32}(k_1\cdot k_2\eta^{\mu\sigma}\eta^{\nu\tau}\eta^{\rho\lambda}\eta_{\iota\kappa}) + \frac{1}{16}(k_1\cdot k_2\eta^{\mu\nu}\eta^{\sigma\tau}\eta_\iota^\rho\eta_\kappa^\lambda) \\
&+ \frac{1}{8}(k_1^\sigma k_1^\tau\eta^{\mu\nu}\eta_\iota^\rho\eta_\kappa^\lambda) + \frac{1}{8}(k_1^\sigma k_2^\mu\eta^{\nu\tau}\eta_\iota^\rho\eta_\kappa^\lambda) - \frac{1}{16}(k_1\cdot k_2\eta^{\mu\sigma}\eta^{\nu\tau}\eta_\iota^\rho\eta_\kappa^\lambda) \\
&+ \frac{1}{4}(k_1\cdot k_2\eta^{\mu\nu}\eta^{\sigma\rho}\eta\tau\lambda\eta_{\iota\kappa}) + \frac{1}{4}(k_1^\sigma k_1^\tau\eta^{\mu\rho}\eta^{\nu\lambda}\eta_{\iota\kappa}) + \frac{1}{8}(k_1^\rho k_2^\lambda\eta^{\mu\sigma}\eta^{\nu\tau}\eta_{\iota\kappa}) \\
&+ \frac{1}{2}(k_1^\sigma k_2^\rho\eta^{\tau\mu}\eta^{\nu\lambda}\eta_{\iota\kappa}) - \frac{1}{4}(k_1\cdot k_2\eta^{\nu\sigma}\eta^{\tau\rho}\eta^{\lambda\mu}\eta_{\iota\kappa}) + \frac{1}{4}(k_1^\sigma k_2^\mu\eta^{\tau\rho}\eta^{\lambda\nu}\eta_{\iota\kappa}) \\
&+ \frac{1}{4}(k_1^\sigma k_1^\rho\eta^{\tau\lambda}\eta^{\mu\nu}\eta_{\iota\kappa}) - \frac{1}{2}(k_1\cdot k_2\eta^{\mu\nu}\eta^{\tau\rho}\eta_\iota^\lambda\eta_\kappa^\sigma) - \frac{1}{2}(k_1^\sigma k_1^\tau\eta^{\nu\rho}\eta_\iota^\lambda\eta_\kappa^\mu) \\
&- \frac{1}{2}(k_1^\rho k_2^\lambda\eta_\iota^\nu\eta_\kappa^\sigma\eta^{\tau\mu}) - (k_1^\sigma k_2^\rho\eta_\iota^\tau\eta_\kappa^\mu\eta^{\nu\lambda}) - \frac{1}{2}(k_1^\rho k_{2\,\iota}\eta^{\lambda\sigma}\eta^{\tau\mu}\eta_\kappa^\nu) \\
&+ \frac{1}{4}(k_1\cdot k_2\eta^{\nu\rho}\eta^{\lambda\sigma}\eta_\iota^\tau\eta_\kappa^\mu) - \frac{1}{2}(k_1^\sigma k_1^\rho\eta^{\mu\nu}\eta_\iota^\tau\eta_\kappa^\lambda) - \frac{1}{4}(k_1\cdot k_2\eta^{\mu\rho}\eta^{\nu\lambda}\eta_\iota^\sigma\eta_\kappa^\tau) \\
&- \frac{1}{2}(k_1^\sigma k_1^\rho\eta^{\tau\lambda}\eta_\iota^\mu\eta_\kappa^\nu) - \frac{1}{4}(k_1^\rho k_{2\,\iota}\eta_\kappa^\lambda\eta^{\mu\sigma}\eta^{\nu\tau}) - (k_1^\sigma k_2^\rho\eta^{\tau\mu}\eta_\iota^\nu\eta_\kappa^\lambda) \\
&- \frac{1}{2}(k_1^\sigma k_2^\mu\eta^{\tau\rho}\eta_\iota^\lambda\eta_\kappa^\nu) + \frac{1}{2}(k_1\cdot k_2\eta^{\nu\sigma}\eta^{\tau\rho}\eta_\iota^\lambda\eta_\kappa^\mu) + Sym(k_1,k_2,k_3,k_4)
\end{aligned} \tag{A.9}$$

we introduce the short hand notation

$$\tau^{\mu\nu}_{(4)\,\gamma\delta,\sigma\tau,\iota\theta}(k_1,k_2,k_3,k_4) := \tilde{\tau}^{\mu\nu}_{(4)\,\alpha\beta,\gamma\delta,\epsilon\eta}(k_1,k_2,k_3,k_4)\mathcal{P}^{\alpha\beta}_{\gamma\delta}\mathcal{P}^{\gamma\delta}_{\sigma\tau}\mathcal{P}^{\epsilon\eta}_{\iota\theta}\,. \tag{A.10}$$

Appendix B

Gravitational Bremsstrahlung in the Post-Minkowskian Effective Field Theory

B.1 Angular dependence

We can introduce the transverse-traceless helicity-2 tensors, normalized to unity, in terms of the orthonormal frame tangent to the sphere, $\mathbf{e}_\theta = (\cos\theta\cos\phi, \cos\theta\sin\phi, -\sin\theta)$ and $\mathbf{e}_\phi = (-\sin\phi, \cos\phi, 0)$, used in the main text. We define

$$\epsilon_i^\pm \equiv \frac{1}{\sqrt{2}}(\pm\mathbf{e}_\theta^i + i\mathbf{e}_\phi^i) \,, \qquad \epsilon_{ij}^{\pm 2} = \epsilon_i^\pm \epsilon_j^\pm \,. \tag{B.1}$$

We can relate these tensors to the (real) plus and cross parametrization often used in the literature by

$$\epsilon_{ij}^{\rm plus} = \epsilon_{ij}^+ + \epsilon_{ij}^- \,, \qquad\qquad \epsilon_{ij}^{\rm cross} = -i\left(\epsilon_{ij}^+ - \epsilon_{ij}^-\right) \,. \tag{B.2}$$

For convenience, here we also explicitly report the expression of the (orbital) angular momentum operator in terms of the same polar coordinates,

$$\hat{L}^x = i(\sin\phi\partial_\theta + \cot\theta\cos\phi\partial_\phi) \,, \tag{B.3}$$

$$\hat{L}^y = -i(\cos\phi\partial_\theta - \cot\theta\sin\phi\partial_\phi) \,, \tag{B.4}$$

$$\hat{L}^z = -i\partial_\phi \,. \tag{B.5}$$

B.2 Integrals $I_{(n)}$ and $J_{(n)}$

In this section, we are going to solve the set of integrals defined in eqs. (4.27) and (4.28). In particular, we show how the $I_{(n)}$ set can be solved exactly, while for $J_{(n)}$, we can rewrite them as integrals over a one dimensional Feynman parameter.

Since the final result will be in terms of Lorentz invariants, we can solve this integral in a particular frame, and it is convenient to pick the one defined in (4.29). Solving the two delta functions, we reduce $I_{(0)}$ to a two dimensional integral over the components $\mathbf{q}_\perp$ that lie on the plane perpendicular to the direction of the scattering bodies. Hence

$$\begin{aligned} I_{(0)} &= -\frac{1}{\sqrt{\gamma^2-1}}\int \frac{d^2\mathbf{q}_\perp}{(2\pi)^2}\frac{e^{i\mathbf{q}_\perp\cdot\mathbf{b}}}{\mathbf{q}_\perp^2+\frac{(k\cdot u_1)^2}{\gamma^2-1}} \\ &= -\frac{1}{\sqrt{\gamma^2-1}}\int_0^\infty dt\int \frac{d^2\mathbf{q}_\perp}{(2\pi)^2}\exp\left[-t\mathbf{q}_\perp^2+i\mathbf{q}_\perp\cdot\mathbf{b}-t\frac{(k\cdot u_1)^2}{\gamma^2-1}\right], \end{aligned} \tag{B.6}$$

where in the second step we introduced a Schwinger parameter t. Solving the Gaussian integral in $\mathbf{q}_\perp$ eventually gives us the final result

$$I_{(0)} = -\frac{1}{4\pi\sqrt{\gamma^2-1}}\int_0^\infty \frac{dt}{t}\exp\left[-\frac{|\mathbf{b}|^2}{4t}-t\frac{(k\cdot u_1)^2}{\gamma^2-1}\right] = -\frac{K_0(z_1)}{2\pi\sqrt{\gamma^2-1}}, \tag{B.7}$$

where K_n are the modified Bessel functions of the second kind and we defined for simplicity

$$z_a \equiv \frac{\sqrt{-b^2}(k\cdot u_a)}{\sqrt{\gamma^2-1}} \qquad a=1,2\,. \tag{B.8}$$

Once solved the scalar integral, the vectorial $I^\mu_{(1)}$ can be computed decomposing it on a complete basis, i.e.

$$I^\mu_{(1)} = A_b b^\mu + A_u(u_1^\mu-\gamma u_2^\mu)\,, \tag{B.9}$$

where the dependence on the combination $u_1^\mu-\gamma u_2^\mu$ comes from the fact that $u_2\cdot I_{(1)}=0$. Contracting both sides with b^μ and u_1^μ, one eventually gets

$$A_b = \frac{ib^\mu}{b^2}\frac{\partial I_{(0)}}{\partial b^\mu} = -\frac{i}{2\pi\sqrt{\gamma^2-1}}\frac{z_1\,K_1(z_1)}{|b^2|}\,, \tag{B.10}$$

$$A_u = -\frac{k\cdot u_1}{\gamma^2-1}I_{(0)} = \frac{k\cdot u_1}{2\pi(\gamma^2-1)^{3/2}}K_0(z_1)\,, \tag{B.11}$$

Due to the presence of two massless propagator, the second set of integrals

defined in eq. (4.28) is a bit more involved. Considering again the scalar integral $J_{(0)}$ first, we can use Feynman parametrization to rewrite it in terms of just one massless propagator

$$J_{(0)} = \int_0^1 dy \int_q \bar{\delta}(q\cdot u_1 - k\cdot u_1)\bar{\delta}(q\cdot u_2)\frac{e^{-iq\cdot b}}{(q-yk)^4} \tag{B.12}$$

$$= \int_0^1 dy e^{-iyk\cdot b}\int_q \bar{\delta}(q\cdot u_1 - (1-y)k\cdot u_1)\bar{\delta}(q\cdot u_2 + yk\cdot u_2)\frac{e^{-iq\cdot b}}{q^4}\,, \tag{B.13}$$

where to get to the second line, we performed the shift $q \to q + yk$. Recall that, since this amplitude must eventually be evaluated on-shell, we are imposing that $k^2 = 0$. At this point, we can follow a procedure analogous to the one we used for $I_{(0)}$. Choosing again the frame defined in eq. (4.29), we use the two delta functions to reduce the computation to a two dimensional integration over $\mathbf{q}_\perp$, that we can solve using Schwinger parametrization, hence

$$J_{(0)} = \frac{1}{\sqrt{\gamma^2-1}}\int_0^1 dy e^{-iyk\cdot b}\int_0^\infty dt\; t\int\frac{d^2\mathbf{q}_\perp}{(2\pi)^2}\exp\left[-t\mathbf{q}_\perp^2 + i\mathbf{q}_\perp\cdot b - t\frac{s^2(y)}{\gamma^2-1}\right]. \tag{B.14}$$

Here we have defined for convenience

$$s(y) \equiv \sqrt{(1-y)^2(k\cdot u_1)^2 + 2\gamma y(1-y)(k\cdot u_1)(k\cdot u_2) + y^2(k\cdot u_2)^2}\,. \tag{B.15}$$

Notice that $s(y)$ changes when computing the symmetric contribution $1 \leftrightarrow 2$. At this point, the integral over $\mathbf{q}_\perp$ in eq (B.14) is Gaussian and can be easily solved. One eventually gets

$$J_{(0)} = \frac{\sqrt{-b^2}}{4\pi}\int_0^1 dy e^{-iyk\cdot b}\frac{1}{s(y)}K_1\left(\frac{\sqrt{-b^2}s(y)}{\sqrt{\gamma^2-1}}\right). \tag{B.16}$$

The procedure to solve $J^\mu_{(1)}$ and $J^{\mu\nu}_{(2)}$ is then similar to the one we used for $I^\mu_{(1)}$. The only difference is that, before decomposing on a complete basis as in eq. (B.9), we find it convenient to use again Feynman parametrization, e.g. $J^\mu_{(1)}$ becomes

$$J^\mu_{(1)} = \int_0^1 dy e^{-iyk\cdot b}\int_q \bar{\delta}(q\cdot u_1 - (1-y)k\cdot u_1)\bar{\delta}(q\cdot u_2 + yk\cdot u_2)\frac{e^{-iq\cdot b}}{q^4}(q^\mu + yk^\mu)\,, \tag{B.17}$$

where we performed again the shift $q \to q + yk$. The contribution proportional to k^μ can be computed using the result of $J_{(0)}$, while the one proportional to

q^μ must be decomposed on a complete basis. The very same procedure can be carried out for $J^{\mu\nu}_{(2)}$ yielding to

$$J^\mu_{(1)} = \int_0^1 dy e^{-iyk\cdot b}\left[B_b b^\mu + B_1 u_1^\mu + B_2 u_2^\mu + \cdots\right], \tag{B.18}$$

$$J^{\mu\nu}_{(2)} = \int_0^1 dy e^{-iyk\cdot b}\left[C_\eta \eta^{\mu\nu} + C_b^\mu b^\nu + C_1 b^{(\mu}u_1^{\nu)} C_2 b^{(\mu}u_2^{\nu)} + C_3 u_1^{(\mu}u_2^{\nu)} + C_4 u_1^\mu u_1^\nu + C_5 u_2^\mu u_2^\nu + \cdots\right], \tag{B.19}$$

where we omitted the terms proportional to k^μ.

In order to find the coefficients B of eq. (B.18) one must solve the following system

$$B_b = \frac{ib^\mu}{b^2}\frac{\partial J_{(0)}}{\partial b^\mu}, \tag{B.20}$$

$$B_1 = \frac{(y-1)k\cdot u_1 - y\gamma k\cdot u_2}{\gamma^2-1} J_{(0)}, \tag{B.21}$$

$$B_2 = \frac{yk\cdot u_2 - (y-1)\gamma k\cdot u_1}{\gamma^2-1} J_{(0)}. \tag{B.22}$$

Using the result of eq. (B.16) one gets

$$B_b = \frac{i}{4\pi\sqrt{\gamma^2-1}} K_0\left(\frac{\sqrt{-b^2}s(y)}{\sqrt{\gamma^2-1}}\right), \tag{B.23}$$

$$B_1 = \frac{\sqrt{-b^2}}{4\pi(\gamma^2-1)}\frac{(y-1)k\cdot u_1 - y\gamma k\cdot u_2}{s(y)} K_1\left(\frac{\sqrt{-b^2}s(y)}{\sqrt{\gamma^2-1}}\right), \tag{B.24}$$

$$B_2 = \frac{\sqrt{-b^2}}{4\pi(\gamma^2-1)}\frac{yk\cdot u_2 - (y-1)\gamma k\cdot u_1}{s(y)} K_1\left(\frac{\sqrt{-b^2}s(y)}{\sqrt{\gamma^2-1}}\right). \tag{B.25}$$

Contracting eq. (B.19) with all the tensors structures one has on the right hand side, it is not too hard to get the following system for the C coefficients

$$b^2\left(C_\eta + C_b b^2\right) = -b^\mu b^\nu \frac{\partial^2 J_{(0}}{\partial b^\mu \partial b^\nu} \,, \tag{B.26}$$

$$\frac{b^2}{2}\left(C_1 + \gamma C_2\right) = -b^2(y-1)k\cdot u_1 B_b \,, \tag{B.27}$$

$$\frac{b^2}{2}\left(\gamma C_1 + C_2\right) = -b^2 y k\cdot u_2 B_b \,, \tag{B.28}$$

$$C_\eta + \gamma C_3 + C_4 + \gamma^2 C_5 = (y-1)^2 (k\cdot u_1)^2 J_{(0)} \,, \tag{B.29}$$

$$C_\eta + \gamma C_3 + \gamma^2 C_4 + C_5 = y^2 (k\cdot u_2)^2 J_{(0)} \,, \tag{B.30}$$

$$\gamma C_\eta + \frac{C_3}{2}(\gamma^2+1) + \gamma(C_4 + C_5) = (y-1)y(k\cdot u_1)(k\cdot u_2) J_{(0)} \,, \tag{B.31}$$

$$4C_\eta + b^2 C_b + \gamma C_3 + C_4 + C_5 = \int_q \bar{\delta}(q\cdot u_1 - (1-y)k\cdot u_1)\bar{\delta}(q\cdot u_2 + yk\cdot u_2)\frac{e^{-iq\cdot b}}{q^2} \,. \tag{B.32}$$

Here the only object we have still not computed is the right hand side of the last equation. Performing the same steps we implemented to solve $J_{(0)}$, one eventually finds

$$\int_q \bar{\delta}(q\cdot u_1 - (1-y)k\cdot u_1)\bar{\delta}(q\cdot u_2 + yk\cdot u_2)\frac{e^{-iq\cdot b}}{q^2} = -\frac{1}{2\pi\sqrt{\gamma^2-1}} K_0\left(\frac{\sqrt{-b^2}s(y)}{\sqrt{\gamma^2-1}}\right) \,. \tag{B.33}$$

Solving the previous system, we finally get

$$C_\eta = -\frac{1}{4\pi\sqrt{\gamma^2-1}} K_0\left(\frac{\sqrt{-b^2}s(y)}{\sqrt{\gamma^2-1}}\right) , \tag{B.34}$$

$$C_b = -\frac{1}{4\pi(\gamma^2-1)} \frac{s(y)}{\sqrt{-b^2}} K_1\left(\frac{\sqrt{-b^2}s(y)}{\sqrt{\gamma^2-1}}\right) , \tag{B.35}$$

$$C_1 = \frac{i}{2\pi(\gamma^2-1)} \frac{(y-1)k\cdot u_1 - y\gamma k\cdot u_2}{\sqrt{\gamma^2-1}} K_0\left(\frac{\sqrt{-b^2}s(y)}{\sqrt{\gamma^2-1}}\right) , \tag{B.36}$$

$$C_2 = \frac{i}{2\pi(\gamma^2-1)} \frac{yk\cdot u_2 - (y-1)\gamma k\cdot u_1}{\sqrt{\gamma^2-1}} K_0\left(\frac{\sqrt{-b^2}s(y)}{\sqrt{\gamma^2-1}}\right) , \tag{B.37}$$

$$\begin{aligned} C_3 = \frac{1}{2\pi(\gamma^2-1)^{3/2}} \Bigg\{ & \gamma K_0\left(\frac{\sqrt{-b^2}s(y)}{\sqrt{\gamma^2-1}}\right) \\ & - \frac{\sqrt{-b^2}s(y)}{\sqrt{\gamma^2-1}} K_1\left(\frac{\sqrt{-b^2}s(y)}{\sqrt{\gamma^2-1}}\right) \left[\gamma + \frac{(\gamma^2-1)}{s^2(y)} y(y-1)k\cdot u_1 k\cdot u_2\right] \Bigg\} , \end{aligned} \tag{B.38}$$

$$\begin{aligned} C_4 = \frac{1}{4\pi(\gamma^2-1)^{3/2}} \Bigg\{ & - K_0\left(\frac{\sqrt{-b^2}s(y)}{\sqrt{\gamma^2-1}}\right) \\ & + \frac{\sqrt{-b^2}s(y)}{\sqrt{\gamma^2-1}} K_1\left(\frac{\sqrt{-b^2}s(y)}{\sqrt{\gamma^2-1}}\right) \left[1 + \frac{(\gamma^2-1)}{s^2(y)} y^2 (k\cdot u_2)^2\right] \Bigg\} , \end{aligned} \tag{B.39}$$

$$\begin{aligned} C_5 = \frac{1}{4\pi(\gamma^2-1)^{3/2}} \Bigg\{ & - K_0\left(\frac{\sqrt{-b^2}s(y)}{\sqrt{\gamma^2-1}}\right) \\ & + \frac{\sqrt{-b^2}s(y)}{\sqrt{\gamma^2-1}} K_1\left(\frac{\sqrt{-b^2}s(y)}{\sqrt{\gamma^2-1}}\right) \left[1 + \frac{(\gamma^2-1)}{s^2(y)} (y-1)^2 (k\cdot u_1)^2\right] \Bigg\} . \end{aligned} \tag{B.40}$$

B.3 Coefficients

The coefficients in eqs. (4.32), (4.33) and (4.34) are

$$\begin{aligned} & c_0 = 1 - 2\gamma^2 , \quad c_1 = -c_0 + \frac{3-2\gamma^2}{n\cdot v} , \quad c_2 = v c_0 \frac{\mathbf{n}\cdot\mathbf{e}_b}{n\cdot v} , \\ & d_0(y) = f(y) c_0 , \\ & d_1(y) = v^2 \frac{4\gamma^2(y-1)(n\cdot v) - c_0(y-1)^2 - 2y - 1}{f(y)} - d_0(y) , \\ & d_2(y) = -1 + (1-y) c_0 (n\cdot v - 1) . \end{aligned} \tag{B.41}$$

B.4 Waveform in direct space

In this paper we focus on computing the emitted energy and angular momentum, obtained from the waveform in *Fourier space* or, equivalently, the amplitude of graviton emission. In this appendix, which was added in v2 of the paper to address one of the reviewer's comments, we show how to find the waveform in *direct space* from the expression of our amplitude.

First we replace the NLO amplitude (4.31) in eq. (4.10), we go in the rest frame of particle 2 and integrate over q^0, removing $\bar{\delta}(q\cdot u_2)$. Then we can get rid of the other delta function by integrating over k^0, which leads to a three-dimensional integral over $\mathbf{q}$. More explicitly, at order G^2 one can find (with $h_\lambda \equiv \epsilon^{*\mu\nu}_\lambda h_{\mu\nu}$)

$$h^{(2)}_{\pm 2} = \frac{m_1 m_2 G}{8 m_{\rm Pl} r}\int_{\mathbf{q}} e^{i\mathbf{q}\cdot\tilde{\mathbf{b}}}\left[\frac{q^i \mathcal{N}^i_\pm}{\mathbf{q}^2\,(\mathbf{q}\cdot\mathbf{e}_v - i\epsilon)} + \frac{q^i q^j \mathcal{M}^{ij}_\pm}{\mathbf{q}^2\,(\mathbf{q}^2 + \mathbf{q}\cdot L\cdot\mathbf{q})}\right], \tag{B.42}$$

where [105]*

$$\mathcal{N}^i_\pm \equiv 4\frac{\gamma v}{(n\cdot v)^2}(\boldsymbol{\epsilon}^\pm\cdot\mathbf{e}_v)^2\left[(1+v^2)\,n^i - 4v\,e^i_v\right] + 8\frac{\gamma(1+v^2)}{n\cdot v}(\boldsymbol{\epsilon}^\pm\cdot\mathbf{e}_v)\epsilon^i_\pm\,, \tag{B.43}$$

$$\mathcal{M}^{ij}_\pm \equiv 16\frac{\gamma v^4}{(n\cdot v)^3}(\boldsymbol{\epsilon}^\pm\cdot\mathbf{e}_v)^2\,e^i_v e^j_v + 8\frac{\gamma(1+v^2)}{n\cdot v}\,\epsilon^i_\pm\epsilon^j_\pm - 32\frac{\gamma v^2}{(n\cdot v)}(\boldsymbol{\epsilon}^\pm\cdot\mathbf{e}_v)\,e^{(i}_v\epsilon^{j)}_\pm\,, \tag{B.44}$$

and we have introduced

$$\tilde{\mathbf{b}} \equiv \mathbf{b} + \frac{v}{n\cdot v}(u + \mathbf{b}\cdot\mathbf{n})\,, \qquad L^{ij} \equiv 2\frac{v}{n\cdot v}\mathbf{e}^{(i}_v\mathbf{n}^{j)}\,. \tag{B.45}$$

The integrations in $\mathbf{q}$ can be performed following [105]. Eventually one finds an expression of the waveform equivalent to that of this reference, which agrees with [194].

*To compare these expressions with those in [105] one must replace $\mathbf{e}_v \to \hat{\mathbf{e}}_1$, $\mathbf{e}_b \to \hat{\mathbf{e}}_2$, $\mathbf{e}_\theta \to \hat{\boldsymbol{\theta}}$, $\mathbf{e}_\phi \to \hat{\boldsymbol{\phi}}$, $n^\mu \to \rho^\mu$, $v^\mu \to v_2^\mu/\gamma$ and use eq. (B.1).

B.5 Energy and spectral dependence

The spectral and angular dependence of the radiated four-momentum is given by eq. (4.45). Using the expressions for the functions A_{IJ} in eqs. (4.32)–(4.34) and summing over the helicities, we find

$$\begin{aligned}\frac{\pi^2\gamma^2}{2vz^2}\frac{d\mathcal{E}}{dzd\Omega} &= 2a_{vv}^2c_1^2K_0^2\left(z(n\cdot v)\right)+2a_{vv}\left[4a_{bb}c_0^2+c_2(4a_{vb}c_0+a_{vv}c_2)\right]K_1^2\left(z(n\cdot v)\right)\\ &+4c_1K_0\left(z(n\cdot v)\right)\left[(2a_{vb}^2-a_{vv}a_{bb})I_0^{(c)}+a_{vv}^2I_1^{(c)}-2a_{vv}a_{vb}I_2^{(s)}\right]\\ &+4K_1\left(z(n\cdot v)\right)\Big[\left(2a_{bb}a_{vb}c_0+(2a_{vb}^2-a_{vv}a_{bb})c_2\right)I_0^{(s)}+(2a_{vv}a_{vb}c_0+a_{vv}^2c_2)I_1^{(s)}+2a_{vv}(2a_{bb}c_0\\ &+2a_{bb}^2\Big[\left(I_0^{(c)}\right)^2+\left(I_0^{(s)}\right)^2\Big]+2a_{vv}^2\Big[\left(I_1^{(c)}\right)^2+\left(I_1^{(s)}\right)^2\Big]+8a_{vv}a_{bb}\Big[\left(I_2^{(c)}\right)^2+\left(I_2^{(s)}\right)^2\Big]\\ &+4(2a_{vb}^2-a_{vv}a_{bb})\left(I_0^{(c)}I_1^{(c)}+I_0^{(s)}I_1^{(s)}\right)+8a_{vb}I_2^{(c)}\left(a_{bb}I_0^{(s)}+a_{vv}I_1^{(s)}\right)-8a_{vb}I_2^{(s)}\left(a_{bb}I_0^{(c)}+a_{vv}I_1^{(c)}\right.\end{aligned} \tag{B.46}$$

where we have defined $a_{IJ}\equiv[(\mathbf{e}_\theta\cdot\mathbf{e}_I)(\mathbf{e}_\theta\cdot\mathbf{e}_J)+(\mathbf{e}_\phi\cdot\mathbf{e}_I)(\mathbf{e}_\phi\cdot\mathbf{e}_J)]/2$,[†], and the two sets of integrals,

$$\begin{aligned}I_i^{(s)}(z,\Omega)&\equiv\int_0^1 dy\,\sin(yzv\mathbf{n}\cdot\mathbf{e}_b)g_i(z,\Omega;y)\ ,\\ I_i^{(c)}(z,\Omega)&\equiv\int_0^1 dy\,\cos(yzv\mathbf{n}\cdot\mathbf{e}_b)g_i(z,\Omega;y)\ ,\end{aligned} \tag{B.47}$$

with

$$\begin{aligned}g_0(z,\Omega;y)&\equiv d_0(y)zK_1\left(zf(y)\right)\ ,\\ g_1(z,\Omega;y)&\equiv c_0K_0\left(zf(y)\right)+d_1(y)zK_1\left(zf(y)\right)\ ,\\ g_2(z,\Omega;y)&\equiv d_2(y)zK_0\left(zf(y)\right)\ .\end{aligned} \tag{B.48}$$

It is straightforward to integrate analytically over the polar angle, while we were not able to integrate over the azimutal one. Because of its length, we prefer not to report the integrated expression here.

[†]Choosing $\mathbf{e}_v$ along z and $\mathbf{e}_b$ along x we have $a_{vv}=\sin^2\theta/2$, $a_{vb}=-\sin\theta\cos\theta\cos\phi/2$, $a_{bb}=[\cos^2\theta\cos^2\phi+\sin^2\phi]/2$.

Bibliography

[1] Michèle Levi, Stavros Mougiakakos, and Mariana Vieira. Gravitational cubic-in-spin interaction at the next-to-leading post-Newtonian order. *JHEP*, 01:036, 2021. arXiv:1912.06276, doi:10.1007/JHEP01(2021)036.

[2] Stavros Mougiakakos and Pierre Vanhove. Schwarzschild-Tangherlini metric from scattering amplitudes in various dimensions. *Phys. Rev. D*, 103(2):026001, 2021. arXiv:2010.08882, doi:10.1103/PhysRevD.103.026001.

[3] Stavros Mougiakakos, Massimiliano Maria Riva, and Filippo Vernizzi. Gravitational Bremsstrahlung in the post-Minkowskian effective field theory. *Phys. Rev. D*, 104(2):024041, 2021. arXiv:2102.08339, doi:10.1103/PhysRevD.104.024041.

[4] Juan Maldacena and Leonard Susskind. Cool horizons for entangled black holes. *Fortsch. Phys.*, 61:781–811, 2013. arXiv:1306.0533, doi:10.1002/prop.201300020.

[5] Juan Martin Maldacena. The Large N limit of superconformal field theories and supergravity. *Adv. Theor. Math. Phys.*, 2:231–252, 1998. arXiv:hep-th/9711200, doi:10.1023/A:1026654312961.

[6] Gerard 't Hooft and M. J. G. Veltman. One loop divergencies in the theory of gravitation. *Ann. Inst. H. Poincare Phys. Theor. A*, 20:69–94, 1974.

[7] M. J. G. Veltman. Quantum Theory of Gravitation. *Conf. Proc. C*, 7507281:265–327, 1975.

[8] Bryce S. DeWitt. Quantum Theory of Gravity. 1. The Canonical Theory. *Phys. Rev.*, 160:1113–1148, 1967. doi:10.1103/PhysRev.160.1113.

[9] Bryce S. DeWitt. Quantum Theory of Gravity. 2. The Manifestly Covariant Theory. *Phys. Rev.*, 162:1195–1239, 1967. doi:10.1103/PhysRev.162.1195.

[10] Bryce S. DeWitt. Quantum Theory of Gravity. 3. Applications of the Covariant Theory. *Phys. Rev.*, 162:1239–1256, 1967. doi:10.1103/PhysRev.162.1239.

[11] John F. Donoghue. General relativity as an effective field theory: The leading quantum corrections. *Phys. Rev. D*, 50:3874–3888, 1994. arXiv:gr-qc/9405057, doi:10.1103/PhysRevD.50.3874.

[12] Lance J. Dixon. A brief introduction to modern amplitude methods. In *Theoretical Advanced Study Institute in Elementary Particle Physics: Particle Physics: The Higgs Boson and Beyond*, pages 31–67, 2014. arXiv:1310.5353, doi:10.5170/CERN-2014-008.31.

[13] Clifford Cheung. *TASI Lectures on Scattering Amplitudes*, pages 571–623. 2018. arXiv:1708.03872, doi:10.1142/9789813233348_0008.

[14] Henriette Elvang and Yu-tin Huang. *Scattering Amplitudes in Gauge Theory and Gravity*. Cambridge University Press, 4 2015.

[15] Zvi Bern, Lance J. Dixon, David C. Dunbar, and David A. Kosower. One loop n point gauge theory amplitudes, unitarity and collinear limits. *Nucl. Phys. B*, 425:217–260, 1994. arXiv:hep-ph/9403226, doi:10.1016/0550-3213(94)90179-1.

[16] Zvi Bern, Lance J. Dixon, David C. Dunbar, and David A. Kosower. Fusing gauge theory tree amplitudes into loop amplitudes. *Nucl. Phys. B*, 435:59–101, 1995. arXiv:hep-ph/9409265, doi:10.1016/0550-3213(94)00488-Z.

[17] Ruth Britto, Freddy Cachazo, and Bo Feng. Generalized unitarity and one-loop amplitudes in N=4 super-Yang-Mills. *Nucl. Phys. B*, 725:275–305, 2005. arXiv:hep-th/0412103, doi:10.1016/j.nuclphysb.2005.07.014.

[18] Z. Bern, J. J. M. Carrasco, and Henrik Johansson. New Relations for Gauge-Theory Amplitudes. *Phys. Rev.*, D78:085011, 2008. arXiv:0805.3993, doi:10.1103/PhysRevD.78.085011.

[19] Zvi Bern, John Joseph M. Carrasco, and Henrik Johansson. Perturbative Quantum Gravity as a Double Copy of Gauge Theory. *Phys. Rev. Lett.*, 105:061602, 2010. arXiv:1004.0476, doi:10.1103/PhysRevLett.105.061602.

[20] Zvi Bern, John Joseph Carrasco, Marco Chiodaroli, Henrik Johansson, and Radu Roiban. The Duality Between Color and Kinematics and its Applications. 9 2019. arXiv:1909.01358.

[21] H. Kawai, D. C. Lewellen, and S. H. H. Tye. A Relation Between Tree Amplitudes of Closed and Open Strings. *Nucl. Phys. B*, 269:1–23, 1986. doi:10.1016/0550-3213(86)90362-7.

[22] Albert Einstein. The Foundation of the General Theory of Relativity. *Annalen Phys.*, 49(7):769–822, 1916. doi:10.1002/andp.200590044.

[23] Y. Iwasaki. Quantum theory of gravitation vs. classical theory. - fourth-order potential. *Prog. Theor. Phys.*, 46:1587–1609, 1971. doi:10.1143/PTP.46.1587.

[24] Niels Emil Jannik Bjerrum-Bohr, John F. Donoghue, and Barry R. Holstein. Quantum corrections to the Schwarzschild and Kerr metrics. *Phys. Rev. D*, 68:084005, 2003. [Erratum: Phys.Rev.D 71, 069904 (2005)]. arXiv:hep-th/0211071, doi:10.1103/PhysRevD.68.084005.

[25] Barry R. Holstein and John F. Donoghue. Classical physics and quantum loops. *Phys. Rev. Lett.*, 93:201602, 2004. arXiv:hep-th/0405239, doi:10.1103/PhysRevLett.93.201602.

[26] John F. Donoghue and Tibor Torma. On the power counting of loop diagrams in general relativity. *Phys. Rev. D*, 54:4963–4972, 1996. arXiv:hep-th/9602121, doi:10.1103/PhysRevD.54.4963.

[27] N. E. J. Bjerrum-Bohr, Poul H. Damgaard, Guido Festuccia, Ludovic Planté, and Pierre Vanhove. General Relativity from Scattering Amplitudes. *Phys. Rev. Lett.*, 121:171601, 2018. arXiv:1806.04920, doi:10.1103/PhysRevLett.121.171601.

[28] David A. Kosower, Ben Maybee, and Donal O'Connell. Amplitudes, Observables, and Classical Scattering. *JHEP*, 02:137, 2019. arXiv:1811.10950, doi:10.1007/JHEP02(2019)137.

[29] N. E. J. Bjerrum-Bohr, Ludovic Plante, and P. Vanhove. Post-Minkowskian Radial Action from Soft Limits and Velocity Cuts. 11 2021. arXiv:2111.02976.

[30] B. P. and others Abbott. Observation of Gravitational Waves from a Binary Black Hole Merger. *Phys. Rev. Lett.*, 116:061102, 2016. arXiv:1602.03837, doi:10.1103/PhysRevLett.116.061102.

[31] B.P. Abbott et al. GW170817: Observation of Gravitational Waves from a Binary Neutron Star Inspiral. *Phys. Rev. Lett.*, 119:161101, 2017. arXiv:1710.05832, doi:10.1103/PhysRevLett.119.161101.

[32] Luc Blanchet. Gravitational Radiation from Post-Newtonian Sources and Inspiralling Compact Binaries. *Living Rev. Rel.*, 17:2, 2014. arXiv:1310.1528, doi:10.12942/lrr-2014-2.

[33] Luc Blanchet. Analytic Approximations in GR and Gravitational Waves. *Int. J. Mod. Phys. D*, 28(06):1930011, 2019. arXiv:1812.07490, doi:10.1142/S0218271819300118.

[34] Walter D. Goldberger and Ira Z. Rothstein. An Effective field theory of gravity for extended objects. *Phys.Rev.*, D73:104029, 2006. arXiv:hep-th/0409156, doi:10.1103/PhysRevD.73.104029.

[35] Rafael A. Porto. The tune of love and thenature(ness)of spacetime. *Fortschritte der Physik*, 64(10):723–729, Sep 2016. URL: http://dx.doi.org/10.1002/prop.201600064, doi:10.1002/prop.201600064.

[36] B. Bertotti. On gravitational motion. *Nuovo Cim.*, 4(4):898–906, 1956. doi:10.1007/bf02746175.

[37] B. Bertotti and J. Plebanski. Theory of gravitational perturbations in the fast motion approximation. *Annals Phys.*, 11(2):169–200, 1960. doi:10.1016/0003-4916(60)90132-9.

[38] Peter Havas and Joshua N. Goldberg. Lorentz-Invariant Equations of Motion of Point Masses in the General Theory of Relativity. *Phys. Rev.*, 128:398–414, 1962. doi:10.1103/PhysRev.128.398.

[39] K. Westpfahl and M. Goller. GRAVITATIONAL SCATTERING OF TWO RELATIVISTIC PARTICLES IN POSTLINEAR APPROXIMATION. *Lett. Nuovo Cim.*, 26:573–576, 1979. doi:10.1007/BF02817047.

[40] M. Portilla. SCATTERING OF TWO GRAVITATING PARTICLES: CLASSICAL APPROACH. *J. Phys. A*, 13:3677–3683, 1980. doi:10.1088/0305-4470/13/12/017.

[41] LLuis Bel, T. Damour, N. Deruelle, J. Ibanez, and J. Martin. Poincaré-invariant gravitational field and equations of motion of two pointlike objects: The postlinear approximation of general relativity. *Gen. Rel. Grav.*, 13:963–1004, 1981. doi:10.1007/BF00756073.

[42] Konradin Westpfahl. High-Speed Scattering of Charged and Uncharged Particles in General Relativity. *Fortsch. Phys.*, 33(8):417–493, 1985. doi:10.1002/prop.2190330802.

[43] Thibault Damour. Gravitational scattering, post-Minkowskian approximation and Effective One-Body theory. *Phys. Rev.*, D94:104015, 2016. arXiv:1609.00354, doi:10.1103/PhysRevD.94.104015.

[44] Thibault Damour. High-energy gravitational scattering and the general relativistic two-body problem. *Phys. Rev. D*, 97:044038, Feb 2018. URL: https://link.aps.org/doi/10.1103/PhysRevD.97.044038, doi:10.1103/PhysRevD.97.044038.

[45] Luc Blanchet and Athanassios S. Fokas. Equations of motion of self-gravitating N-body systems in the first post-Minkowskian approximation. *Phys. Rev. D*, 98(8):084005, 2018. arXiv:1806.08347, doi:10.1103/PhysRevD.98.084005.

[46] Andrea Antonelli, Alessandra Buonanno, Jan Steinhoff, Maarten van de Meent, and Justin Vines. Energetics of two-body Hamiltonians in post-Minkowskian gravity. *Phys. Rev. D*, 99(10):104004, 2019. arXiv:1901.07102, doi:10.1103/PhysRevD.99.104004.

[47] Thibault Damour. Classical and quantum scattering in post-Minkowskian gravity. *Phys. Rev. D*, 102(2):024060, 2020. arXiv:1912.02139, doi:10.1103/PhysRevD.102.024060.

[48] Duff Neill and Ira Z. Rothstein. Classical Space-Times from the S Matrix. *Nucl. Phys.*, B877:177–189, 2013. arXiv:1304.7263, doi:10.1016/j.nuclphysb.2013.09.007.

[49] N. E. J. Bjerrum-Bohr, John F. Donoghue, and Pierre Vanhove. On-shell Techniques and Universal Results in Quantum Gravity. *JHEP*, 02:111, 2014. arXiv:1309.0804, doi:10.1007/JHEP02(2014)111.

[50] Andrés Luna, Isobel Nicholson, Donal O'Connell, and Chris D. White. Inelastic Black Hole Scattering from Charged Scalar Amplitudes. *JHEP*, 03:044, 2018. arXiv:1711.03901, doi:10.1007/JHEP03(2018)044.

[51] Clifford Cheung, Ira Z. Rothstein, and Mikhail P. Solon. From Scattering Amplitudes to Classical Potentials in the Post-Minkowskian Expansion. *Phys. Rev. Lett.*, 121:251101, 2018. arXiv:1808.02489, doi:10.1103/PhysRevLett.121.251101.

[52] Andrea Cristofoli, N. E. J. Bjerrum-Bohr, Poul H. Damgaard, and Pierre Vanhove. Post-Minkowskian Hamiltonians in general relativity. *Phys. Rev. D*, 100(8):084040, 2019. arXiv:1906.01579, doi:10.1103/PhysRevD.100.084040.

[53] Andrea Cristofoli, Poul H. Damgaard, Paolo Di Vecchia, and Carlo Heissenberg. Second-order Post-Minkowskian scattering in arbitrary dimensions. *JHEP*, 07:122, 2020. arXiv:2003.10274, doi:10.1007/JHEP07(2020)122.

[54] N. Emil J. Bjerrum-Bohr, Poul H. Damgaard, Ludovic Planté, and Pierre Vanhove. Classical gravity from loop amplitudes. *Phys. Rev. D*, 104(2):026009, 2021. arXiv:2104.04510, doi:10.1103/PhysRevD.104.026009.

[55] N. E. J. Bjerrum-Bohr, P. H. Damgaard, L. Planté, and P. Vanhove. The Amplitude for Classical Gravitational Scattering at Third Post-Minkowskian Order. 5 2021. arXiv:2105.05218.

[56] John F. Donoghue. General relativity as an effective field theory: The leading quantum corrections. *Phys. Rev. D*, 50:3874–3888, Sep 1994. URL: https://link.aps.org/doi/10.1103/PhysRevD.50.3874, doi:10.1103/PhysRevD.50.3874.

[57] N. E. J. Bjerrum-Bohr, John F. Donoghue, and Barry R. Holstein. Quantum gravitational corrections to the nonrelativistic scattering potential of two masses. *Phys. Rev. D*, 67:084033, Apr 2003. URL: https://link.aps.org/doi/10.1103/PhysRevD.67.084033, doi:10.1103/PhysRevD.67.084033.

[58] Y. Iwasaki. Fourth-order gravitational potential based on quantum field theory. *Lett. Nuovo Cim.*, 1S2:783–786, 1971. doi:10.1007/BF02770190.

[59] D. Amati, M. Ciafaloni, and G. Veneziano. Classical and Quantum Gravity Effects from Planckian Energy Superstring Collisions. *Int. J. Mod. Phys. A*, 3:1615–1661, 1988. doi:10.1142/S0217751X88000710.

[60] D. Amati, M. Ciafaloni, and G. Veneziano. Planckian scattering beyond the semiclassical approximation. *Phys. Lett. B*, 289:87–91, 1992. doi:10.1016/0370-2693(92)91366-H.

[61] D. Amati, M. Ciafaloni, and G. Veneziano. Effective action and all order gravitational eikonal at Planckian energies. *Nucl. Phys. B*, 403:707–724, 1993. doi:10.1016/0550-3213(93)90367-X.

[62] Daniel Kabat and Miguel Ortiz. Eikonal quantum gravity and planckian scattering. *Nuclear Physics B*, 388(2):570–592, Dec 1992. URL: http://dx.doi.org/10.1016/0550-3213(92)90627-N, doi:10.1016/0550-3213(92)90627-n.

[63] Arnau Koemans Collado, Paolo Di Vecchia, Rodolfo Russo, and Steven Thomas. The subleading eikonal in supergravity theories. *Journal of High Energy Physics*, 2018(10), Oct 2018. URL: http://dx.doi.org/10.1007/JHEP10(2018)038, doi:10.1007/jhep10(2018)038.

[64] Arnau Koemans Collado, Paolo Di Vecchia, and Rodolfo Russo. Revisiting the second post-minkowskian eikonal and the dynamics of binary black holes. *Physical Review D*, 100(6), Sep 2019. URL: http://dx.doi.org/10.1103/PhysRevD.100.066028, doi:10.1103/physrevd.100.066028.

[65] Paolo Di Vecchia, Andrés Luna, Stephen G. Naculich, Rodolfo Russo, Gabriele Veneziano, and Chris D. White. A tale of two exponentiations in $\mathcal{N} = 8$ supergravity. *Phys. Lett. B*, 798:134927, 2019. arXiv:1908.05603, doi:10.1016/j.physletb.2019.134927.

[66] Paolo Di Vecchia, Stephen G. Naculich, Rodolfo Russo, Gabriele Veneziano, and Chris D. White. A tale of two exponentiations in $\mathcal{N} = 8$ supergravity at subleading level. *JHEP*, 03:173, 2020. arXiv:1911.11716, doi:10.1007/JHEP03(2020)173.

[67] Paolo Di Vecchia, Carlo Heissenberg, Rodolfo Russo, and Gabriele Veneziano. Universality of ultra-relativistic gravitational scattering. *Phys. Lett. B*, 811:135924, 2020. arXiv:2008.12743, doi:10.1016/j.physletb.2020.135924.

[68] Paolo Di Vecchia, Carlo Heissenberg, Rodolfo Russo, and Gabriele Veneziano. Radiation Reaction from Soft Theorems. 1 2021. arXiv:2101.05772.

[69] Walter D. Goldberger and Alexander K. Ridgway. Radiation and the classical double copy for color charges. *Phys. Rev.*, D95:125010, 2017. arXiv:1611.03493, doi:10.1103/PhysRevD.95.125010.

[70] Walter D. Goldberger and Alexander K. Ridgway. Bound states and the classical double copy. *Phys. Rev.*, D97:085019, 2018. arXiv:1711.09493, doi:10.1103/PhysRevD.97.085019.

[71] Gregor Kälin and Rafael A. Porto. Post-Minkowskian Effective Field Theory for Conservative Binary Dynamics. 6 2020. arXiv:2006.01184.

[72] Florian Loebbert, Jan Plefka, Canxin Shi, and Tianheng Wang. Three-Body Effective Potential in General Relativity at 2PM and Resulting PN Contributions. 12 2020. arXiv:2012.14224.

[73] Gustav Mogull, Jan Plefka, and Jan Steinhoff. Classical black hole scattering from a worldline quantum field theory. 10 2020. arXiv:2010.02865.

[74] Gregor Kälin and Rafael A. Porto. From Boundary Data to Bound States. *JHEP*, 01:072, 2020. arXiv:1910.03008, doi:10.1007/JHEP01(2020)072.

[75] Gregor Kälin and Rafael A. Porto. From boundary data to bound states. Part II. Scattering angle to dynamical invariants (with twist). *JHEP*, 02:120, 2020. arXiv:1911.09130, doi:10.1007/JHEP02(2020)120.

[76] Zvi Bern, Clifford Cheung, Radu Roiban, Chia-Hsien Shen, Mikhail P. Solon, and Mao Zeng. Scattering Amplitudes and the Conservative Hamiltonian for Binary Systems at Third Post-Minkowskian Order. *Phys. Rev. Lett.*, 122(20):201603, 2019. arXiv:1901.04424, doi:10.1103/PhysRevLett.122.201603.

[77] Zvi Bern, Clifford Cheung, Radu Roiban, Chia-Hsien Shen, Mikhail P. Solon, and Mao Zeng. Black Hole Binary Dynamics from the Double Copy and Effective Theory. *JHEP*, 10:206, 2019. arXiv:1908.01493, doi:10.1007/JHEP10(2019)206.

[78] Clifford Cheung and Mikhail P. Solon. Classical gravitational scattering at $\mathcal{O}(G^3)$ from Feynman diagrams. *JHEP*, 06:144, 2020. arXiv:2003.08351, doi:10.1007/JHEP06(2020)144.

[79] Gregor Kälin, Zhengwen Liu, and Rafael A. Porto. Conservative Dynamics of Binary Systems to Third Post-Minkowskian Order from the

Effective Field Theory Approach. *Phys. Rev. Lett.*, 125(26):261103, 2020. arXiv:2007.04977, doi:10.1103/PhysRevLett.125.261103.

[80] Zvi Bern, Julio Parra-Martinez, Radu Roiban, Michael S. Ruf, Chia-Hsien Shen, Mikhail P. Solon, and Mao Zeng. Scattering Amplitudes and Conservative Binary Dynamics at $\mathcal{O}(G^4)$. 1 2021. arXiv:2101.07254.

[81] Christoph Dlapa, Gregor Kälin, Zhengwen Liu, and Rafael A. Porto. Dynamics of Binary Systems to Fourth Post-Minkowskian Order from the Effective Field Theory Approach. 6 2021. arXiv:2106.08276.

[82] Gregor Kälin, Zhengwen Liu, and Rafael A. Porto. Conservative Tidal Effects in Compact Binary Systems to Next-to-Leading Post-Minkowskian Order. *Phys. Rev. D*, 102:124025, 2020. arXiv:2008.06047, doi:10.1103/PhysRevD.102.124025.

[83] Zvi Bern, Julio Parra-Martinez, Radu Roiban, Eric Sawyer, and Chia-Hsien Shen. Leading Nonlinear Tidal Effects and Scattering Amplitudes. 10 2020. arXiv:2010.08559.

[84] Clifford Cheung and Mikhail P. Solon. Tidal Effects in the Post-Minkowskian Expansion. *Phys. Rev. Lett.*, 125(19):191601, 2020. arXiv:2006.06665, doi:10.1103/PhysRevLett.125.191601.

[85] Manuel Accettulli Huber, Andreas Brandhuber, Stefano De Angelis, and Gabriele Travaglini. Eikonal phase matrix, deflection angle and time delay in effective field theories of gravity. *Phys. Rev. D*, 102(4):046014, 2020. arXiv:2006.02375, doi:10.1103/PhysRevD.102.046014.

[86] Kays Haddad and Andreas Helset. Tidal effects in quantum field theory. *JHEP*, 12:024, 2020. arXiv:2008.04920, doi:10.1007/JHEP12(2020)024.

[87] Rafael Aoude, Kays Haddad, and Andreas Helset. On-shell heavy particle effective theories. *JHEP*, 05:051, 2020. arXiv:2001.09164, doi:10.1007/JHEP05(2020)051.

[88] Clifford Cheung, Nabha Shah, and Mikhail P. Solon. Mining the Geodesic Equation for Scattering Data. *Phys. Rev. D*, 103(2):024030, 2021. arXiv:2010.08568, doi:10.1103/PhysRevD.103.024030.

[89] Nima Arkani-Hamed, Tzu-Chen Huang, and Yu-tin Huang. Scattering Amplitudes For All Masses and Spins. 2017. arXiv:1709.04891.

[90] Ming-Zhi Chung, Yu-Tin Huang, Jung-Wook Kim, and Sangmin Lee. The simplest massive S-matrix: from minimal coupling to Black Holes. *JHEP*, 04:156, 2019. arXiv:1812.08752, doi:10.1007/JHEP04(2019)156.

[91] Justin Vines, Jan Steinhoff, and Alessandra Buonanno. Spinning-black-hole scattering and the test-black-hole limit at second post-Minkowskian order. *Phys. Rev. D*, 99(6):064054, 2019. arXiv:1812.00956, doi:10.1103/PhysRevD.99.064054.

[92] Alfredo Guevara, Alexander Ochirov, and Justin Vines. Scattering of Spinning Black Holes from Exponentiated Soft Factors. *JHEP*, 09:056, 2019. arXiv:1812.06895, doi:10.1007/JHEP09(2019)056.

[93] Ming-Zhi Chung, Yu-Tin Huang, and Jung-Wook Kim. Classical potential for general spinning bodies. *JHEP*, 09:074, 2020. arXiv:1908.08463, doi:10.1007/JHEP09(2020)074.

[94] Ming-Zhi Chung, Yu-tin Huang, Jung-Wook Kim, and Sangmin Lee. Complete Hamiltonian for spinning binary systems at first post-Minkowskian order. *JHEP*, 05:105, 2020. arXiv:2003.06600, doi:10.1007/JHEP05(2020)105.

[95] Zvi Bern, Andres Luna, Radu Roiban, Chia-Hsien Shen, and Mao Zeng. Spinning Black Hole Binary Dynamics, Scattering Amplitudes and Effective Field Theory. 5 2020. arXiv:2005.03071.

[96] Dimitrios Kosmopoulos and Andres Luna. Quadratic-in-spin Hamiltonian at $\mathcal{O}(G^2)$ from scattering amplitudes. *JHEP*, 07:037, 2021. arXiv:2102.10137, doi:10.1007/JHEP07(2021)037.

[97] Zhengwen Liu, Rafael A. Porto, and Zixin Yang. Spin Effects in the Effective Field Theory Approach to Post-Minkowskian Conservative Dynamics. *JHEP*, 06:012, 2021. arXiv:2102.10059, doi:10.1007/JHEP06(2021)012.

[98] D. Amati, M. Ciafaloni, and G. Veneziano. Higher Order Gravitational Deflection and Soft Bremsstrahlung in Planckian Energy Superstring Collisions. *Nucl. Phys. B*, 347:550–580, 1990. doi:10.1016/0550-3213(90)90375-N.

[99] Zvi Bern, Harald Ita, Julio Parra-Martinez, and Michael S. Ruf. Universality in the classical limit of massless gravitational scattering. *Phys.*

Rev. Lett., 125(3):031601, 2020. arXiv:2002.02459, doi:10.1103/PhysRevLett.125.031601.

[100] Manuel Accettulli Huber, Andreas Brandhuber, Stefano De Angelis, and Gabriele Travaglini. From amplitudes to gravitational radiation with cubic interactions and tidal effects. 12 2020. arXiv:2012.06548.

[101] Thibault Damour. Radiative contribution to classical gravitational scattering at the third order in G. *Phys. Rev. D*, 102(12):124008, 2020. arXiv:2010.01641, doi:10.1103/PhysRevD.102.124008.

[102] Enrico Herrmann, Julio Parra-Martinez, Michael S. Ruf, and Mao Zeng. Gravitational Bremsstrahlung from Reverse Unitarity. 1 2021. arXiv:2101.07255.

[103] Donato Bini, Thibault Damour, and Andrea Geralico. Radiative contributions to gravitational scattering. 7 2021. arXiv:2107.08896.

[104] Paolo Di Vecchia, Carlo Heissenberg, Rodolfo Russo, and Gabriele Veneziano. The Eikonal Approach to Gravitational Scattering and Radiation at $\mathcal{O}(G^3)$. 4 2021. arXiv:2104.03256.

[105] Gustav Uhre Jakobsen, Gustav Mogull, Jan Plefka, and Jan Steinhoff. Classical Gravitational Bremsstrahlung from a Worldline Quantum Field Theory. *Phys. Rev. Lett.*, 126(20):201103, 2021. arXiv:2101.12688, doi:10.1103/PhysRevLett.126.201103.

[106] Stefano Foffa, Pierpaolo Mastrolia, Riccardo Sturani, Christian Sturm, and William J. Torres Bobadilla. Static two-body potential at fifth post-Newtonian order. *Phys. Rev. Lett.*, 122(24):241605, 2019. arXiv:1902.10571, doi:10.1103/PhysRevLett.122.241605.

[107] Donato Bini, Thibault Damour, Andrea Geralico, Stefano Laporta, and Pierpaolo Mastrolia. Gravitational dynamics at $O(G^6)$: perturbative gravitational scattering meets experimental mathematics. 8 2020. arXiv:2008.09389.

[108] Donato Bini, Thibault Damour, Andrea Geralico, Stefano Laporta, and Pierpaolo Mastrolia. Gravitational scattering at the seventh order in G: nonlocal contribution at the sixth post-Newtonian accuracy. 12 2020. arXiv:2012.12918.

[109] Andrea Cristofoli, Riccardo Gonzo, David A. Kosower, and Donal O'Connell. Waveforms from Amplitudes. 7 2021. arXiv:2107.10193.

[110] Mariana Carrillo-González, Claudia de Rham, and Andrew J. Tolley. Scattering Amplitudes for Binary Systems beyond GR. 7 2021. arXiv:2107.11384.

[111] Rafael A. Porto. The effective field theorist's approach to gravitational dynamics. *Phys. Rept.*, 633:1–104, 2016. arXiv:1601.04914, doi:10.1016/j.physrep.2016.04.003.

[112] Michele Levi. Effective Field Theories of Post-Newtonian Gravity: A comprehensive review. *Rept. Prog. Phys.*, 2019. arXiv:1807.01699, doi:10.1088/1361-6633/ab12bc.

[113] Kenneth G. Wilson. Renormalization group and critical phenomena. i. renormalization group and the kadanoff scaling picture. *Phys. Rev. B*, 4:3174–3183, Nov 1971. URL: https://link.aps.org/doi/10.1103/PhysRevB.4.3174, doi:10.1103/PhysRevB.4.3174.

[114] Kenneth G. Wilson and J. Kogut. The renormalization group and the expansion. *Physics Reports*, 12(2):75–199, 1974. URL: https://www.sciencedirect.com/science/article/pii/0370157374900234, doi:https://doi.org/10.1016/0370-1573(74)90023-4.

[115] Don N. Page. Particle emission rates from a black hole: Massless particles from an uncharged, nonrotating hole. *Phys. Rev. D*, 13:198–206, Jan 1976. URL: https://link.aps.org/doi/10.1103/PhysRevD.13.198, doi:10.1103/PhysRevD.13.198.

[116] Rafael A. Porto. Lamb shift and the gravitational binding energy for binary black holes. *Phys. Rev. D*, 96(2):024063, 2017. arXiv:1703.06434, doi:10.1103/PhysRevD.96.024063.

[117] Stefano Foffa, Rafael A. Porto, Ira Rothstein, and Riccardo Sturani. Conservative dynamics of binary systems to fourth Post-Newtonian order in the EFT approach II: Renormalized Lagrangian. *Phys. Rev. D*, 100(2):024048, 2019. arXiv:1903.05118, doi:10.1103/PhysRevD.100.024048.

[118] J. Blümlein, A. Maier, and P. Marquard. Five-Loop Static Contribution to the Gravitational Interaction Potential of Two Point Masses. 2019. arXiv:1902.11180.

[119] Michèle Levi, Andrew J. Mcleod, and Matthew Von Hippel. N^{3}LO gravitational spin-orbit coupling at order G^4. *JHEP*, 07:115, 2021. arXiv:2003.02827, doi:10.1007/JHEP07(2021)115.

[120] Michèle Levi, Andrew J. Mcleod, and Matthew Von Hippel. N^{3}LO gravitational quadratic-in-spin interactions at G^4. *JHEP*, 07:116, 2021. arXiv:2003.07890, doi:10.1007/JHEP07(2021)116.

[121] Michèle Levi and Fei Teng. NLO gravitational quartic-in-spin interaction. *JHEP*, 01:066, 2021. arXiv:2008.12280, doi:10.1007/JHEP01(2021)066.

[122] Aneesh V. Manohar and Iain W. Stewart. The zero-bin and mode factorization in quantum field theory. *Physical Review D*, 76(7), Oct 2007. URL: http://dx.doi.org/10.1103/PhysRevD.76.074002, doi:10.1103/physrevd.76.074002.

[123] Walter D. Goldberger and Andreas Ross. Gravitational radiative corrections from effective field theory. *Phys. Rev. D*, 81:124015, 2010. arXiv:0912.4254, doi:10.1103/PhysRevD.81.124015.

[124] Chad R. Galley and Adam K. Leibovich. Radiation reaction at 3.5 post-Newtonian order in effective field theory. *Phys. Rev. D*, 86:044029, 2012. arXiv:1205.3842, doi:10.1103/PhysRevD.86.044029.

[125] S. Foffa and Riccardo Sturani. Tail terms in gravitational radiation reaction via effective field theory. *Phys. Rev. D*, 87(4):044056, 2013. arXiv:1111.5488, doi:10.1103/PhysRevD.87.044056.

[126] Chad R. Galley, Adam K. Leibovich, Rafael A. Porto, and Andreas Ross. Tail effect in gravitational radiation reaction: Time nonlocality and renormalization group evolution. *Phys. Rev. D*, 93:124010, 2016. arXiv:1511.07379, doi:10.1103/PhysRevD.93.124010.

[127] Natalia T. Maia, Chad R. Galley, Adam K. Leibovich, and Rafael A. Porto. Radiation reaction for spinning bodies in effective field theory I: Spin-orbit effects. *Phys. Rev. D*, 96(8):084064, 2017. arXiv:1705.07934, doi:10.1103/PhysRevD.96.084064.

[128] Natalia T. Maia, Chad R. Galley, Adam K. Leibovich, and Rafael A. Porto. Radiation reaction for spinning bodies in effective field theory II: Spin-spin effects. *Phys. Rev. D*, 96(8):084065, 2017. arXiv:1705.07938, doi:10.1103/PhysRevD.96.084065.

[129] Barak Kol and Michael Smolkin. Non-Relativistic Gravitation: From Newton to Einstein and Back. *Class.Quant.Grav.*, 25:145011, 2008. arXiv:0712.4116, doi:10.1088/0264-9381/25/14/145011.

[130] Michele Levi. Next to Leading Order gravitational Spin1-Spin2 coupling with Kaluza-Klein reduction. *Phys.Rev.*, D82:064029, 2010. arXiv:0802.1508, doi:10.1103/PhysRevD.82.064029.

[131] James B. Gilmore and Andreas Ross. Effective field theory calculation of second post-Newtonian binary dynamics. *Phys.Rev.*, D78:124021, 2008. arXiv:0810.1328, doi:10.1103/PhysRevD.78.124021.

[132] Michele Levi. Next to Leading Order gravitational Spin-Orbit coupling in an Effective Field Theory approach. *Phys.Rev.*, D82:104004, 2010. arXiv:1006.4139, doi:10.1103/PhysRevD.82.104004.

[133] Stefano Foffa and Riccardo Sturani. Effective field theory calculation of conservative binary dynamics at third post-Newtonian order. *Phys.Rev.*, D84:044031, 2011. arXiv:1104.1122, doi:10.1103/PhysRevD.84.044031.

[134] Michele Levi. Binary dynamics from spin1-spin2 coupling at fourth post-Newtonian order. *Phys.Rev.*, D85:064043, 2012. arXiv:1107.4322, doi:10.1103/PhysRevD.85.064043.

[135] Michele Levi and Jan Steinhoff. Leading order finite size effects with spins for inspiralling compact binaries. *JHEP*, 06:059, 2015. arXiv:1410.2601, doi:10.1007/JHEP06(2015)059.

[136] Michele Levi and Jan Steinhoff. Spinning gravitating objects in the effective field theory in the post-Newtonian scheme. *JHEP*, 09:219, 2015. arXiv:1501.04956, doi:10.1007/JHEP09(2015)219.

[137] Michele Levi and Jan Steinhoff. Next-to-next-to-leading order gravitational spin-orbit coupling via the effective field theory for spinning objects in the post-Newtonian scheme. *JCAP*, 1601:011, 2016. arXiv:1506.05056, doi:10.1088/1475-7516/2016/01/011.

[138] Michele Levi and Jan Steinhoff. Next-to-next-to-leading order gravitational spin-squared potential via the effective field theory for spinning objects in the post-Newtonian scheme. *JCAP*, 1601:008, 2016. arXiv:1506.05794, doi:10.1088/1475-7516/2016/01/008.

[139] Stefano Foffa, Pierpaolo Mastrolia, Riccardo Sturani, and Christian Sturm. Effective field theory approach to the gravitational two-body dynamics, at fourth post-Newtonian order and quintic in the Newton constant. *Phys. Rev.*, D95:104009, 2017. arXiv:1612.00482, doi:10.1103/PhysRevD.95.104009.

[140] B.M. Barker and R.F. O'Connell. Gravitational Two-Body Problem with Arbitrary Masses, Spins, and Quadrupole Moments. *Phys.Rev.*, D12:329–335, 1975. doi:10.1103/PhysRevD.12.329.

[141] Rafael A. Porto. Post-Newtonian corrections to the motion of spinning bodies in NRGR. *Phys.Rev.*, D73:104031, 2006. arXiv:gr-qc/0511061, doi:10.1103/PhysRevD.73.104031.

[142] Eric Poisson. Gravitational waves from inspiraling compact binaries: The Quadrupole moment term. *Phys.Rev.*, D57:5287–5290, 1998. arXiv:gr-qc/9709032, doi:10.1103/PhysRevD.57.5287.

[143] Rafael A Porto and Ira Z. Rothstein. Next to Leading Order Spin(1)Spin(1) Effects in the Motion of Inspiralling Compact Binaries. *Phys.Rev.*, D78:044013, 2008. [*Erratum-ibid.* D**81** (2010) 029905]. arXiv:0804.0260, doi:10.1103/PhysRevD.78.044013.

[144] Jan Steinhoff, Steven Hergt, and Gerhard Schäfer. Spin-squared Hamiltonian of next-to-leading order gravitational interaction. *Phys.Rev.*, D78:101503, 2008. arXiv:0809.2200, doi:10.1103/PhysRevD.78.101503.

[145] Steven Hergt and Gerhard Schäfer. Higher-order-in-spin interaction Hamiltonians for binary black holes from Poincare invariance. *Phys.Rev.*, D78:124004, 2008. arXiv:0809.2208, doi:10.1103/PhysRevD.78.124004.

[146] Steven Hergt, Jan Steinhoff, and Gerhard Schäfer. Reduced Hamiltonian for next-to-leading order Spin-Squared Dynamics of General Compact Binaries. *Class.Quant.Grav.*, 27:135007, 2010. arXiv:1002.2093, doi:10.1088/0264-9381/27/13/135007.

[147] Steven Hergt and Gerhard Schäfer. Higher-order-in-spin interaction Hamiltonians for binary black holes from source terms of Kerr geometry in approximate ADM coordinates. *Phys.Rev.*, D77:104001, 2008. arXiv:0712.1515, doi:10.1103/PhysRevD.77.104001.

[148] Varun Vaidya. Gravitational spin Hamiltonians from the S matrix. *Phys. Rev.*, D91:024017, 2015. arXiv:1410.5348, doi:10.1103/PhysRevD.91.024017.

[149] Sylvain Marsat. Cubic order spin effects in the dynamics and gravitational wave energy flux of compact object binaries. 2014. arXiv:1411.4118.

[150] Justin Vines and Jan Steinhoff. Spin-multipole effects in binary black holes and the test-body limit. *Phys. Rev. D*, 97(6):064010, 2018. arXiv:1606.08832, doi:10.1103/PhysRevD.97.064010.

[151] Freddy Cachazo and Alfredo Guevara. Leading Singularities and Classical Gravitational Scattering. 2017. arXiv:1705.10262.

[152] Alfredo Guevara. Holomorphic Classical Limit for Spin Effects in Gravitational and Electromagnetic Scattering. *JHEP*, 04:033, 2019. arXiv:1706.02314, doi:10.1007/JHEP04(2019)033.

[153] Michele Levi and Jan Steinhoff. Complete conservative dynamics for inspiralling compact binaries with spins at fourth post-Newtonian order. 2016. arXiv:1607.04252.

[154] Barak Kol, Michele Levi, and Michael Smolkin. Comparing space+time decompositions in the post-Newtonian limit. *Class.Quant.Grav.*, 28:145021, 2011. arXiv:1011.6024, doi:10.1088/0264-9381/28/14/145021.

[155] D. Binosi and L. Theussl. JaxoDraw: A Graphical user interface for drawing Feynman diagrams. *Comput. Phys. Commun.*, 161:76–86, 2004. arXiv:hep-ph/0309015, doi:10.1016/j.cpc.2004.05.001.

[156] D. Binosi, J. Collins, C. Kaufhold, and L. Theussl. JaxoDraw: A Graphical user interface for drawing Feynman diagrams. Version 2.0 release notes. *Comput. Phys. Commun.*, 180:1709–1715, 2009. arXiv:0811.4113, doi:10.1016/j.cpc.2009.02.020.

[157] J. A. M. Vermaseren. Axodraw. *Comput. Phys. Commun.*, 83:45–58, 1994. doi:10.1016/0010-4655(94)90034-5.

[158] Michele Levi and Jan Steinhoff. EFTofPNG: A package for high precision computation with the Effective Field Theory of Post-Newtonian Gravity. *Class. Quant. Grav.*, 34:244001, 2017. arXiv:1705.06309, doi:10.1088/1361-6382/aa941e.

[159] Michele Levi and Jan Steinhoff. Equivalence of ADM Hamiltonian and Effective Field Theory approaches at next-to-next-to-leading order spin1-spin2 coupling of binary inspirals. *JCAP*, 1412:003, 2014. arXiv:1408.5762, doi:10.1088/1475-7516/2014/12/003.

[160] W Tulczyjew. Motion of multipole particles in general relativity theory. *Acta Phys.Polon.*, 18:393, 1959.

[161] W. G. Dixon. Dynamics of extended bodies in general relativity. I. Momentum and angular momentum. *Proc. Roy. Soc. Lond. A*, 314:499–527, 1970. doi:10.1098/rspa.1970.0020.

[162] R. Schattner. The uniqueness of the center-of-mass in general relativity. *Gen.Rel.Grav.*, 10:395–399, 1979. doi:10.1007/BF00760222.

[163] R. Schattner. The center-of-mass in general relativity. *Gen.Rel.Grav.*, 10:377–393, 1979. doi:10.1007/BF00760221.

[164] M. J. Duff. Quantum Tree Graphs and the Schwarzschild Solution. *Phys. Rev. D*, 7:2317–2326, 1973. doi:10.1103/PhysRevD.7.2317.

[165] Arnau Koemans Collado, Paolo Di Vecchia, Rodolfo Russo, and Steven Thomas. The subleading eikonal in supergravity theories. *JHEP*, 10:038, 2018. arXiv:1807.04588, doi:10.1007/JHEP10(2018)038.

[166] Arnau Koemans Collado, Paolo Di Vecchia, and Rodolfo Russo. Revisiting the second post-Minkowskian eikonal and the dynamics of binary black holes. *Phys. Rev. D*, 100(6):066028, 2019. arXiv:1904.02667, doi:10.1103/PhysRevD.100.066028.

[167] Gustav Uhre Jakobsen. Schwarzschild-Tangherlini Metric from Scattering Amplitudes. *Phys. Rev. D*, 102(10):104065, 2020. arXiv:2006.01734, doi:10.1103/PhysRevD.102.104065.

[168] Roberto Emparan and Harvey S. Reall. Black Holes in Higher Dimensions. *Living Rev. Rel.*, 11:6, 2008. arXiv:0801.3471, doi:10.12942/lrr-2008-6.

[169] Roberto Emparan, Ryotaku Suzuki, and Kentaro Tanabe. The large D limit of General Relativity. *JHEP*, 06:009, 2013. arXiv:1302.6382, doi:10.1007/JHEP06(2013)009.

[170] N. E. J. Bjerrum-Bohr, John F. Donoghue, and Barry R. Holstein. On the parameterization dependence of the energy momentum tensor and the metric. *Phys. Rev. D*, 75:108502, 2007. arXiv:gr-qc/0610096, doi:10.1103/PhysRevD.75.108502.

[171] Pierre Fromholz, Eric Poisson, and Clifford M. Will. The Schwarzschild metric: It's the coordinates, stupid! *Am. J. Phys.*, 82:295, 2014. arXiv:1308.0394, doi:10.1119/1.4850396.

[172] Citation for the 2020 nobel prize award to roger penrose. URL: https://www.nobelprize.org/prizes/physics/2020/press-release/.

[173] L. Planté. Some aspects on effective field theory of gravity. *Phd thesis, Université Paris-Saclay 2016.*

[174] J. Galusha. Investigations into the classical limit of quantum field theory. *Master thesis Niels Bohr International Academy 2018.*

[175] Maurice Lévy and Joseph Sucher. Eikonal approximation in quantum field theory. *Phys. Rev.*, 186:1656–1670, Oct 1969. URL: https://link.aps.org/doi/10.1103/PhysRev.186.1656, doi:10.1103/PhysRev.186.1656.

[176] R. N. Lee. Presenting LiteRed: a tool for the Loop InTEgrals REDuction. 12 2012. arXiv:1212.2685.

[177] Roman N. Lee. LiteRed 1.4: a powerful tool for reduction of multiloop integrals. *J. Phys. Conf. Ser.*, 523:012059, 2014. arXiv:1310.1145, doi:10.1088/1742-6596/523/1/012059.

[178] Pierre Vanhove. The physics and the mixed Hodge structure of Feynman integrals. *Proc. Symp. Pure Math.*, 88:161–194, 2014. arXiv:1401.6438, doi:10.1090/pspum/088/01455.

[179] J.C. Lagarias. Euler's constant: Euler's work and modern developments. *Bull. Amer. Math. Soc. (N.S.)*, 4:527–628, 2013.

[180] David Prinz. Gravity-Matter Feynman Rules for any Valence. 4 2020. arXiv:2004.09543.

[181] F. R. Tangherlini. Schwarzschild field in n dimensions and the dimensionality of space problem. *Nuovo Cim.*, 27:636–651, 1963. doi:10.1007/BF02784569.

[182] John F. Donoghue, Barry R. Holstein, Björn Garbrecht, and Thomas Konstandin. Quantum corrections to the Reissner-Nordström and Kerr-Newman metrics. *Phys. Lett. B*, 529:132–142, 2002. [Erratum: Phys.Lett.B 612, 311–312 (2005)]. arXiv:hep-th/0112237, doi:10.1016/S0370-2693(02)01246-7.

[183] Nathan Moynihan. Kerr-Newman from Minimal Coupling. *JHEP*, 01:014, 2020. arXiv:1909.05217, doi:10.1007/JHEP01(2020)014.

[184] Ming-Zhi Chung, Yu-Tin Huang, and Jung-Wook Kim. Kerr-Newman stress-tensor from minimal coupling. *JHEP*, 12:103, 2020. arXiv:1911.12775, doi:10.1007/JHEP12(2020)103.

[185] Alfredo Guevara, Alexander Ochirov, and Justin Vines. Black-hole scattering with general spin directions from minimal-coupling amplitudes. *Phys. Rev. D*, 100(10):104024, 2019. arXiv:1906.10071, doi:10.1103/PhysRevD.100.104024.

[186] Andrea Cristofoli. Gravitational shock waves and scattering amplitudes. *JHEP*, 11:160, 2020. arXiv:2006.08283, doi:10.1007/JHEP11(2020)160.

[187] Donato Bini and Thibault Damour. Gravitational scattering of two black holes at the fourth post-Newtonian approximation. *Phys. Rev. D*, 96(6):064021, 2017. arXiv:1706.06877, doi:10.1103/PhysRevD.96.064021.

[188] Donato Bini, Thibault Damour, and Andrea Geralico. Sixth post-Newtonian nonlocal-in-time dynamics of binary systems. *Phys. Rev. D*, 102(8):084047, 2020. arXiv:2007.11239, doi:10.1103/PhysRevD.102.084047.

[189] Luc Blanchet, Stefano Foffa, François Larrouturou, and Riccardo Sturani. Logarithmic tail contributions to the energy function of circular compact binaries. *Phys. Rev. D*, 101(8):084045, 2020. arXiv:1912.12359, doi:10.1103/PhysRevD.101.084045.

[190] P. C. Peters. Relativistic gravitational bremsstrahlung. *Phys. Rev. D*, 1:1559–1571, 1970. doi:10.1103/PhysRevD.1.1559.

[191] K. S. Thorne and S. J. Kovacs. The Generation of Gravitational Waves. 1. Weak-field sources. *Astrophys. J.*, 200:245–262, 1975. doi:10.1086/153783.

[192] R. J. Crowley and K. S. Thorne. The Generation of Gravitational Waves. 2. The Postlinear Formalism Revisited. *Astrophys. J.*, 215:624–635, 1977. doi:10.1086/155397.

[193] S.J. Kovacs and K.S. Thorne. The Generation of Gravitational Waves. 3. Derivation of Bremsstrahlung Formulas. *Astrophys. J.*, 217:252–280, 1977. doi:10.1086/155576.

[194] S.J. Kovacs and K.S. Thorne. The Generation of Gravitational Waves. 4. Bremsstrahlung. *Astrophys. J.*, 224:62–85, 1978. doi:10.1086/156350.

[195] Michael Turner and Clifford M. Will. Post-Newtonian gravitational bremsstrahlung. *Astrophys. J.*, 220:1107–1124, 1978. doi:10.1086/155996.

[196] Walter D. Goldberger. Les Houches lectures on effective field theories and gravitational radiation. In *Les Houches Summer School - Session 86: Particle Physics and Cosmology: The Fabric of Spacetime Les Houches, France, July 31-August 25, 2006*, 2007. arXiv:hep-ph/0701129.

[197] Stefano Foffa and Riccardo Sturani. Effective field theory methods to model compact binaries. *Classical and Quantum Gravity*, 31:043001, 2014. arXiv:1309.3474, doi:10.1088/0264-9381/31/4/043001.

[198] Ira Z. Rothstein. Progress in effective field theory approach to the binary inspiral problem. *Gen.Rel.Grav.*, 46:1726, 2014. doi:10.1007/s10714-014-1726-y.

[199] Stefano Foffa. Gravitating binaries at 5PN in the post-Minkowskian approximation. *Phys.Rev.*, D89:024019, 2014. arXiv:1309.3956, doi:10.1103/PhysRevD.89.024019.

[200] Chad R. Galley and Rafael A. Porto. Gravitational self-force in the ultra-relativistic limit: the "large-N" expansion. *JHEP*, 1311:096, 2013. arXiv:1302.4486, doi:10.1007/JHEP11(2013)096.

[201] Adrien Kuntz. Half-solution to the two-body problem in General Relativity. *Phys. Rev. D*, 102(6):064019, 2020. arXiv:2003.03366, doi:10.1103/PhysRevD.102.064019.

[202] L.F. Abbott. Introduction to the Background Field Method. *Acta Phys. Polon. B*, 13:33, 1982.

[203] Michele Maggiore. *Gravitational Waves. Vol. 1: Theory and Experiments*. Oxford Master Series in Physics. Oxford University Press, 2007. URL: http://www.oup.com/uk/catalogue/?ci=9780198570745.

[204] Ricardo Paszko and Antonio Accioly. Equivalence between the semiclassical and effective approaches to gravity. *Class. Quant. Grav.*, 27:145012, 2010. doi:10.1088/0264-9381/27/14/145012.

[205] Luc Blanchet and Gerhard Schaefer. Higher order gravitational radiation losses in binary systems. *Mon. Not. Roy. Astron. Soc.*, 239:845–867, 1989. [Erratum: Mon.Not.Roy.Astron.Soc. 242, 704 (1990)].

[206] L. Smarr. Gravitational Radiation from Distant Encounters and from Headon Collisions of Black Holes: The Zero Frequency Limit. *Phys. Rev. D*, 15:2069–2077, 1977. doi:10.1103/PhysRevD.15.2069.

[207] K. S. Thorne. Multipole Expansions of Gravitational Radiation. *Rev. Mod. Phys.*, 52:299–339, 1980. doi:10.1103/RevModPhys.52.299.

[208] John F. Donoghue. Introduction to the effective field theory description of gravity. In *Advanced School on Effective Theories*, 6 1995. arXiv:gr-qc/9512024.

[209] Sigurd Sannan. Gravity as the Limit of the Type II Superstring Theory. *Phys. Rev. D*, 34:1749, 1986. doi:10.1103/PhysRevD.34.1749.

université PARIS-SACLAY | ÉCOLE DOCTORALE Physique en l'Île-de-France (PIF)

Titre: Amplitudes de diffusion en théorie de gravité effective

Mots clés: gravité, Amplitudes de diffusion, théorie effective

Résumé: Dans cette thèse, nous étudions la dynamique gravitationnelle décrite via une théorie des champs effectifs exploitant les méthodes des amplitudes de diffusion. Dans le premier chapitre, nous proposons une discussion sur les différentes approches du problème binaire en gravité et donnons quelques-uns des derniers résultats dans le domaine. Dans le deuxième chapitre, nous discutons en détail du formalisme de la relativité générale non relativiste (NRGR) et dérivons l'action efficace de spin cubique gravitationnelle conservatrice complète à l'ordre supérieur dans le développement post-newtonien (PN) pour le interaction de binaires compacts génériques entrant au quatrième et demi ordre PN (4,5PN). Dans le troisième chapitre, nous dérivons la métrique statique de Schwarzschild-Tangherlini en extrayant les contributions classiques des fonctions vertex multi-boucles d'un graviton émis à partir d'un champ scalaire massif. En calculant les amplitudes de diffusion jusqu'à l'ordre des trois boucles en dimension générale, nous dérivons explicitement l'expansion de la métrique jusqu'au quatrième ordre post-Minkowskien en quatre, cinq et six dimensions. Les problèmes de jauge et les couplages non minimaux non physiques induits ainsi que leur traitement ultérieur sont discutés en détail. Dans le quatrième chapitre, nous étudions le rayonnement gravitationnel émis lors de la diffusion de deux corps sans spin dans l'approche post-minkowskienne de la théorie des champs effectifs. Nous dérivons le tenseur d'énergie de contrainte conservé couplé linéairement à la gravité et l'amplitude de probabilité classique d'émission de graviton à l'ordre avant et suivant dans G. Nous l'utilisons pour récupérer l'ordre principal dans G moment angulaire et total de quatre impulsions irradié en ondes gravitationnelles en accord avec ce qui a été récemment calculé en utilisant des méthodes d'amplitude de diffusion. Nos résultats nous permettent également d'étudier la limite de fréquence zéro du spectre d'énergie émise.

Title: Scattering Amplitudes in effective gravitational theories

Keywords: gravity, scattering amplitudes, effective theory

Abstract: In this thesis we study gravitational dynamics described via an Effective Field Theory exploiting Scattering Amplitudes methods. In the first chapter, we provide a discussion regarding the different approaches on the binary problem in gravity and give some of the latest results in the field. In the second chapter, we discuss in detail the Non-Relativistic General Relativity (NRGR) formalism and derive the complete conservative gravitational cubic-in spin effective action at the next-to-leading order in the post-Newtonian (PN) expansion for the interaction of generic compact binaries entering at the fourth and a half PN (4.5PN) order. In the third chapter, we derive the static Schwarzschild-Tangherlini metric by extracting the classical contributions from the multi-loop vertex functions of a graviton emitted from a massive scalar field. By computing the scattering amplitudes up to three-loop order in general dimension, we explicitly derive the expansion of the metric up to the fourth post-Minkowskian order in four, five and six dimensions. Gauge issues and induced non-physical non-minimal couplings as well as their subsequent treatment are discussed in detail. In the fourth chapter, we study the gravitational radiation emitted during the scattering of two spinless bodies in the post-Minkowskian Effective Field Theory approach. We derive the conserved stress-energy tensor linearly coupled to gravity and the classical probability amplitude of graviton emission at leading and next-to-leading order in G. We use it to recover the leading-order in G angular momentum and total four-momentum radiated into gravitational waves finding agreement with what was recently computed using scattering amplitude methods. Our results also allow us to investigate the zero frequency limit of the emitted energy spectrum.